ESA DUE DIVERSITY II

Supporting the Convention on Biological Diversity

Products User Handbook Drylands

Issue 2.6
21st October 2015

Table of Contents

Figures

Tables

Diversity II Products User Handbook - Drylands

1 Introduction

The Diversity II dryland product user handbook provides an introduction to the suite of GIS maps generated for the 22 dryland globally distributed test sites (Figure 1). Users primarily interested in a shorter overview of certain test sites with specific regional maps are referred to the booklets (see chapter 6). The booklets can be downloaded at http://www.diversity2.info/products/ .

With the Diversity II project ESA aims at contributing to the strategic goals of two UN conventions: the Convention on Biological Diversity (CBD), and the UN Convention to Combat Desertification (UNCCD). As unanimously confirmed in a user and expert Diversity II dryland workshop held in Bonn in July 2014 (link to web material), both conventions have a common denominator in terms of basic information needs: ***Vegetation productivity***.

EO based information about the status and trends of vegetation productivity in relation to driving factors relates in particular to supportive goal E: of the CBD: *Enhance implementation through participatory planning, knowledge management and capacity building*; where Aichi target 19 says: *By 2020, knowledge, the science base and technologies relating to biodiversity, its values, functioning, status and trends, and the consequences of its loss, are improved, widely shared and transferred, and applied*[1].

The products provided in this project, in combination with local and regional knowledge and cooperation with local people, are envisaged to support such goals.

On the UNCCD site, the most recent UNCCD impact indicators as suggested by the UNCCD CST AGTE 20132 are directly linked to vegetation productivity and phenology in Strategic objective 2: *to improve the conditions of ecosystems*:

Strategic UNCCD objective 2: To improve the condition of ecosystems			
Indicator	***Metrics/proxies***	***Description***	***Potential data source as suggested by CST***
Trends in land cover structure	**Vegetative land cover structure**	Intended as the distribution of land cover types of greatest concern for land degradation (excluding artificial surfaces) by characterizing the spatial structure of vegetative land cover; it should include and specify natural habitat classes	Sourced from products like GlobCover,[3] or finer-resolution products under development (Gong et al., 2013); and following established land cover classifications (e.g. FAO/ UNEP LCCS[4])

[1] http://www.cbd.int/sp/targets/

[2] UNCCD Conference of the Parties, Committee on Science and Technology 2013m, Refinement of the set of impact indicators on strategic objectives 1, 2 and 3. Recommendations of the ad hoc advisory group of technical experts. Windhoek, Namibia, 17–20 September 2013

[3] http://www.gofcgold.wur.nl/sites/gofcgold_refdataportal.php

[4] http://www.fao.org/docrep/003/X0596E/X0596e00.htm

Trends in land productivity or functioning of the land	**Land productivity dynamics**	Based on long-term fluctuations and current efficiency levels of phenology and productivity factors affecting standing biomass conditions	New World Atlas of Desertification methodology;[5] update foreseen every five years

The Diversity II projects is an endeavour to contribute to both conventions with EO products **on a regional scale**, based on a predominant ground resolution of 300m * 300m uniquely achieved by the MERIS sensor on board ENVISAT from June 2002 until April 2012.

As major indicator of vegetation productivity, the fAPAR (Fraction of Absorbed Photosynthetically Active Radiation) was derived from the MERIS data and processed to halfmonthly time series data using BEAM. Further, co-analysed data sets include TRMM (and other EO based) rainfall data and CCI Soil Moisture data. Phenological and productivity parameters were extracted from the fAPAR time series data using ERDAS based processing modules specifically developed in the project. The resulting processing chain was also applied to NDVI (Normalised Difference Vegetation Index) or fAPAR data of other sensors, and can be potentially used for any other vegetation indices or biophysical variables with seasonal and cyclic behaviour through time. It will thus be also applicable to the upcoming Sentinel-3 OLCI satellite sensor data, which will provide continuity to the 300m MERIS data, and to other sensors bridging the time gap between MERIS and Sentinel 3. The latter is an important aspect, as for drylands a continuous monitoring of the highly variable climatic and consequently vegetation conditions is indispensable.

The work resulted in so called first level and second level indicator maps showing average vegetation conditions of the observation period, trends, and epochal changes. The fAPAR data were integrated for the phenological vegetation cycles at every (pixel) location, being comprised of the growing period(s), the dry season(s), and the entire vegetation year. Special attention was given to these seasonal vegetation indices and their relation (status and trends), pointing to potential degradation and/or functional shifts of the vegetation type. The latter were expressed in second order indices, for which several first order indices were combined. First order indicators include seasonal and yearly (vegetation year) primary productivity indices (NPP proxies), as well as seasonally differentiated rain use efficiency indices for average conditions and yearly trends. In addition, “soil moisture use efficiency” indices were generated, where rainfall data have been replaced by soil moisture data.

A total of 43 first order, seven second order and three phenology products was generated per test site, amounting to 1166 map products overall. All 43 first order products are thematic maps with worldwide uniform discrete classes. Their underlying continuous data sets can be made available to users on request. In addition, yearly vegetation proxies can be provided to interested users. Further on, we looked beyond the time series of the MERIS data and present NOAA GIMMS NDVI based results derived with the same methodology for longer time periods reaching back as far as 1982.

The results were in some cases contrasted with faunal species abundance data derived from models and partly from in situ investigations. Their spatial distribution patterns and temporal variability were compared to the derived NPP proxies, to check if expected commonalities can be seen. While a generic interpretation of the derived indicators in terms of primary productivity, vegetation degradation and functional vegetation composition/diversity is presented and related to the overall developments in the test sites, the systematic and direct validation with in situ data remains a problem due to the lack of such data.

[5] http://wad.jrc.ec.europa.eu/

2 Products Description

2.1 Scope of the Dryland Products

This section presents the geographical distribution of the dryland test sites, their selection criteria, and an overview of the temporal coverage.

2.1.1 Overview of Dryland Demonstration Sites

A total of 22 dryland areas were selected ranging from 0.42 to 1.64 Mio km² and covering an overall area of 15.7 Mio km². The numbers in Figure 1 correspond to those in Table 1, where the sites are listed along with major characteristics.

Figure 1: Distribution of global Diversity II dryland sites

The dryland sites were selected among WWF ecoregions with an aridity index (ratio of mean annual precipitation to mean annual potential evapotranspiration) largely including the range from 0.05 to 0.65. Areas with an aridity index of < 0.03 are considered hyper arid, those with an index >0.65 humid (UNEP 1997). Further selection criteria were the size (minimum of 05 Mio km² in all but one case), global distribution and representativeness for major terrestrial dryland ecosystems, and the inclusion of several regions of primary biodiversity importance. The test areas were not cut to the extent of the selected ecoregions, as also the surrounding areas may be of interest to the users. The finally selected sites are listed in Table 1.

Table 1: List and short description of the dryland test areas

Nr	Name of the testsite Dryland geographical area (WWF ecoregion no.)	Size of Ecoregion Country	Aridity Index WWF Info	Diversity Hotspot (Global 2000)	Other criteria
1	Northern - Central Mexico: Sierra Madre Occidental pine-oak forestsv (NA0302), Sonoran-Sinaloan transition subtropical dry forest (NA0201), Meseta Central matorral (NA1307), Central Mexican matorral (NA1302)	422.165 km² Mexico	AI 0,09 - 0,86 Tropical and subtropical coniferous forests, tropical and subtropical dry broadleaf forests, deserts	Part of Sierra Madre Oriental and Occidental Pine-Oak Forests (G200_NUM 61), Southern Mexican Dry Forests (G200_NUM 56),	Area contains two Centres of Plant Diversity and partially an Endemic Bird Area WRI Major Watersheds: Parts of Yaqui, Rio Grande, Santiago-Lerma-Chapala, Panuco

			and xeric shrublands	part of Chihuahuan-Tehuacán Deserts (G200_NUM 131)	
2	Northern Australia: Kimberly tropical savannah (AA0706), Victoria Plains tropical savannah (AA0709)	573.953 km² Australia	AI 0,13 – 0,73 Tropical and subtropical grasslands, savannas, and shrublands	Part of Northern Australia and Trans-Fly Savannas (G200_NUM 90)	Area contains two Centres of Plant Diversity and partially an Endemic Bird Area
3	South-West- Iran Nubo-Sindian desert and semi-desert (PA1328), Zagros Mountains forest steppe (PA0446)	743.331 km² Iran, Iraq, Turkey, Georgia, Armenia	AI 0,04 – 0,95 Temperate grasslands, savannas, and shrublands, temperate broadleaf and mixed forests		Area contains a Centre of Plant Diversity WRI Major Watersheds: Parts of Dasht and Tigris-Euphrates
4	Northern Kazakhstan Kazakh steppe (PA0810)	806.307 km² Kazakhstan, Russia	AI 0,2 – 0,8 Temperate grasslands, savannas, and shrublands		WRI Major Watersheds: Parts of Ural, Void and Ob
5	Eastern Mongolia, Western Manchuria Mongolian-Manchurian grassland (PA0813)	889.317 km² Mongolia, China	AI 0,16 – 0,76 Temperate grasslands, savannas, and shrublands	Part of Daurian/Mongolian Steppe (G200_NUM 96)	Area contains Protected Areas, partially an Endemic Bird Area and Transboundary Protected Areas WRI Major Watersheds: Parts of Baikal, Amur and Liao
6	Central Tibetan Plateau Alpine steppe (PA1002)	613.987 km² China	AI 0,03 – 0,58 Montane grasslands and shrublands	Part of Tibetan Plateau Steppe (G200_NUM 110)	Area contains partially an Endemic Bird Area WRI Major Watersheds: Parts of Indus, Ganges-Brahmaputra and Yangtze
7	Southern India Deccan thorn scrub forests (IM1301), Central Deccan Plateau dry deciduous forests (IM0201)	578.950 km² India	AI 0,2 – 0,9 Deserts and xeric shrublands, Tropical and subtropical dry broadleaf forests		Area contains a Centre of Plant Diversity and Protected Areas WRI Major Watersheds: Parts of Tapti, Godavari, Mahanadi, Krishna, Penner and Cauvery
8	Pontic steppe (PA0814)	996.065 km² Romania, Ukraine, Moldova, Russia	AI 0,21 – 1,13 Temperate grasslands, savannas, and shrublands		Area contains a Centre of Plant Diversity and Protected Areas and a Transboundary Protected Area WRI Major Watersheds: Parts of Danube, Dniester, Dnieper, Don and Terek
9	Northern Africa Mediterranean woodlands and forests (PA1214), Mediterranean dry woodlands and steppe (PA1213)	553.811 km² Morocco, Algeria, Tunisia	AI 0,07 – 0,81 Mediterranean forests, woodlands, and shrub	Part of Mediterranean Forests, Woodlands and Scrub (G200_NUM 123)	Area contains a Centre of Plant Diversity WRI Major Watersheds: Parts of Dra, Tafna and Medjerda
10	Southern Europe Iberian conifer forests, Northeastern Spain and Southern France Mediterranean forests (PA1208), Iberian sclerophyllous and semi-deciduous forests (PA1209), Southwest Iberian Mediterranean sclerophyllous and	524.698 km² Portugal, Spain, France, Italy	AI 0,21 – 1,78 Mediterranean forests, woodlands, and shrub	Part of Mediterranean Forests, Woodlands and Scrub (G200_NUM 123)	Area contains two Centres of Plant Diversity and Transboundary Protected Areas WRI Major Watersheds: Parts of Rhone, Garonne, Ebro, Douro-Duero, Tagus, Guadiana and Guadalquivir

	mixed forests (PA1221), Northwest Iberian montane forests (PA1216), Tyrrhenian-Adriatic Sclerophyllous and mixed forests (PA1222), South Appenine mixed montane forests (PA1218), Southeastern Iberian shrubs and woodlands (PA1219)				
11	Eastern Africa Somali Acacia-Commiphora bushlands and thickets (AT0715)	1.054.389 km² Somalia, Ethiopia, Kenya	AI 0,03 – 0,89 Tropical and subtropical grasslands, savannas, and shrublands		Horn of Africa Acacia Savannas (G200_NUM 86)
12	Southern Africa West Namibian savanna woodlands (AT1316), Nama Karoo (AT1314)	576.085 km² Angola, Namibia, South Africa	AI 0,02 – 0,58 Deserts and xeric shrublands		Part of Namib-Karoo-Kaokoveld Deserts and Shrublands (G200_NUM 124)
13	Western Sahel West Sudanian savannah (AT0722)	1.641.911 km² Senegal, Mali, Guinea, Cote d'Ivoire, Ghana, Burkina Faso, Togo, Benin, Niger, Nigeria	AI 0,17 – 1,08 Tropical and subtropical grasslands, savannas, and shrublands		
14	Southern Argentinia Patagonian steppe (NT0805)	538.629 km² Argentinia	AI 0,04 – 1,34 Temperate grasslands, savannas, and shrublands		Patagonian steppe (G200_NUM 95)
15	Caatinga, Brazil Caatinga (NT1304)	718.135 km² Brazil	AI 0,2 – 1,03 Deserts and xeric shrublands		
16	Western Southamerica Central Andean dry puna (NT1001), Central Andean puna, High Monte (NT1002)	509.553 km² Chile, Bolivien, Argentinia	AI 0,03 – 0,65 Montane grasslands and shrublands	Central Andean Dry Puna (G200_NUM 109)	Area contains Protected Areas, partially an Endemic Bird Area and Transboundary Protected Areas WRI Major Watersheds: Parts of Titicaca, Lauca, Amazon, Parana and Rio Colorado
17	Southern Central USA Western short grasslands (NA0815), Central and Southern mixed grasslands (NA0803)	718.907 km² USA	AI 0,14 – 0,66 Temperate grasslands, savannas, and shrublands		WRI Major Watersheds: Parts of Mississippi, Brazos, Rio Grande and Colorado River
18	Northern USA – Southern Canada Northern short grassland (NA0811)	639.831 km² Canada, USA	AI 0,23 – 0,52 Temperate grasslands, savannas, and shrublands	Northern Prairies (G200_NUM 94)	Area contains Protected Areas WRI Major Watersheds: Parts of Saskatchewan-Nelson and Mississippi
19	South-West USA Snake-Columbia shrub steppe (NA1309), Great Basin shrub steppe (NA1305)	511.852 km² USA	AI 0,4 – 0,78 Deserts and xeric shrublands		Area contains Protected Areas WRI Major Watersheds: Parts of Columbia, Sacramento and Colorado
20	Southern Australia Tirari-Sturt stony desert (AA1309), Central Ranges xeric scrub (AA1302)	660.019 km² Australia	AI 0,06 – 0,24 Deserts and xeric shrublands	Part of Great Sandy-Tanami-Central Ranges Desert (G200_NUM 129)	Area contains a Centre of Plant Diversity and Protected Areas WRI Major Watersheds: Part of Murray-Darling
21	Southern Africa East Zimbabwe: Zambezian and	870.742 km² Zimbabwe,	AI 0,19 – 1,81 Tropical and	Part of Central and Eastern	Area contains Protected Areas and Transboundary Protected

	Mopane woodlands (AT0725), Southern Miombo woodlands (AT0719), Zambezian Baikiaea woodlands (AT0726), Southern Africa bushveld (AT0717)	Zambia, Mozambique, Botswana, South Africa, Malawi	subtropical grasslands, savannas, and shrublands	Miombo Woodlands (G200_NUM 88)	Areas WRI Major Watersheds: Parts of Zambezi, Okavango, Limpopo and Save
22	Eastern Mediterranean Countries Central Anatolian steppe (PA0803), Northern Anatolian conifer and deciduous forests (PA0515), Central Anatolian steppe and woodlands (PA0410), Eastern Anatolian deciduous forests (PA0420), Central Anatolian steppe (PA0803), Southern Anatolian montane conifer and deciduous forests (PA1220), Eastern Mediterranean conifer-sclerophyllous-broadleaf forests (PA1207), Euxine-Colchic broadleaf forests (PA0422)	556.143 km² Turkey, Syria, Georgia	AI 0,15 – 2,59 Temperate grasslands, savannas, and shrublands, Temperate coniferous forests, Temperate broadleaf and mixed forests, Mediterranean forests, woodlands, and shrub	Parts of Mediterranean Forests, Woodlands and Scrub (G200_NUM 123), Caucasus-Anatolian-Hyrcanian Temperate Forests (G200_NUM 78)	Area contains a Centre of Plant Diverity WRI Major Watersheds: Parts of Kizil, Kel kit, Coruh, Tigris-Euphrates, Asi (Orontes) and Jordan

2.1.2 Overview of Temporal Coverage of the MERIS FR Data

The period covered by the ENVISAT MERIS data spans from June 2002 to April 2012 and thus almost 10 years. Figure 2 shows the worldwide coverage of the FR (Full Resolution) MERIS data. The distribution of MERIS RR (Reduced Resolution) data follows a similar pattern, though a larger number of RR data than FR data is available.

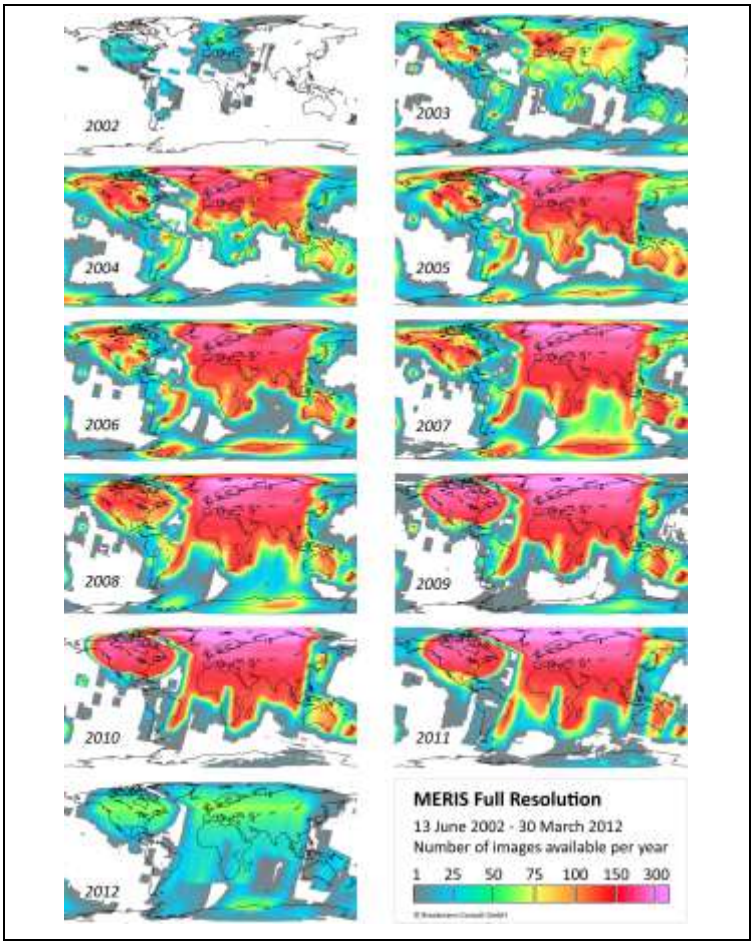

Figure 2: The global annual coverage of ENVISAT-MERIS, indicating the regional availability of MERIS based fAPAR products available from Diversity II. Cloud coverage is not taken into account

It can be seen that the FR coverage for the first year 2002 is rather sparse, partly also for 2003, and that the data availability is generally best in Europe, most of Asia and North America, and generally worse for the southern hemisphere, especially South America and parts of Australia. Where possible, missing MERIS FR based fAPAR data have been supplemented with RR based fAPAR data, but all derived fAPAR data were resampled to the 300m * 300m pixel size.

For the same reasons, when aggregating the fAPAR data in halfmonthly time series data, the minimum number of data takes considered to deliver a valid halfmonthly fAPAR estimate was one MERIS coverage.

As described in more detail in section 2.2.1 and chapter 3.6.11, the available temporal MERIS coverage allowed for the data integration over worldwide eight "vegetation years", starting in 2003(2002) at the **local begin** (per pixel) of the major vegetation season and ending in 2011(2012) at the end of the local dry season. Thus, globally, the entire full year period of MERIS data, 2003 – 2011, has been exploited, partly extending into 2002 and 2012, depending on the regional phenology.

The product naming nevertheless was referenced to the eight vegetation year starts from 2003 to 2010. The last vegetation year (2010) ends in 2011(2012), thus the start of the vegetation year 2011 was calculated for all test sites, but as the MERIS data end in April 2012, the vegetation parameters for the vegetation year 2011 could not be globally derived.

2.2 Product Contents

The dryland products are comprised of GIS ready, colour-coded maps with discrete classes. The underlying continuous data sets may be provided to the users on request. The products, along with metadata, and a product overview table can be downloaded at http://www.diversity2.info/products/ . The products have globally identical colour legends and class aggregations in the different dryland test sites, and are therfore globally comparable (only in some cases, the rainfall data have a larger class interval).

As major indicator of vegetation productivity, halfmonthly fAPAR (Fraction of Absorbed Photosynthetically Active Radiation) data, derived from MERIS data, were used. Further, co-analysed data sets include TRMM (and other EO based) rainfall data and CCI Soil Moisture data. Three groups of products have been generated:

1. First order order status and trend/change indicators (of vegetation productivity, Rain Use efficiency, Soil Moisture Use efficiency, rainfall and soil moisture)
2. Second order status and trend/change indicators (combinations of first order products)
3. Phenology maps (average conditions)

All products are either status (average, variability) or trend products covering the period from (2002)2003 to 2011(2012), with some epochal change products included. Hence, the Diversity II products reflect the condition, variability, trends and changes of the dryland vegetation during the MERIS period, both from a seasonal perspective and in relation to rainfall and soil moisture.

Before the products are presented in sections 2.2.2, 2.2.3, and 2.2.4, a short overview of the underlying concepts of vegetation phenology and productivty, as well as Rain Use Efficiency is given in section 2.2.1. in order to clarify the central concept and the essential terminology applied.

In section 3.1 an overview of the product organisation on the FTP server is provided.

2.2.1 Phenological and Productivity Parameters of the Vegetation as basis of the Diversity II products

The dryland products are based on a phenological analysis of the seasonal behaviour of the vegetation at the pixel level for every (vegetation) year. In chapter 4, section 4.3.3 and 4.3.4 the methodology is described in more detail. Figure 3shows a phenology diagram which explains the phenological and productivity parameters derived in Diversity II.

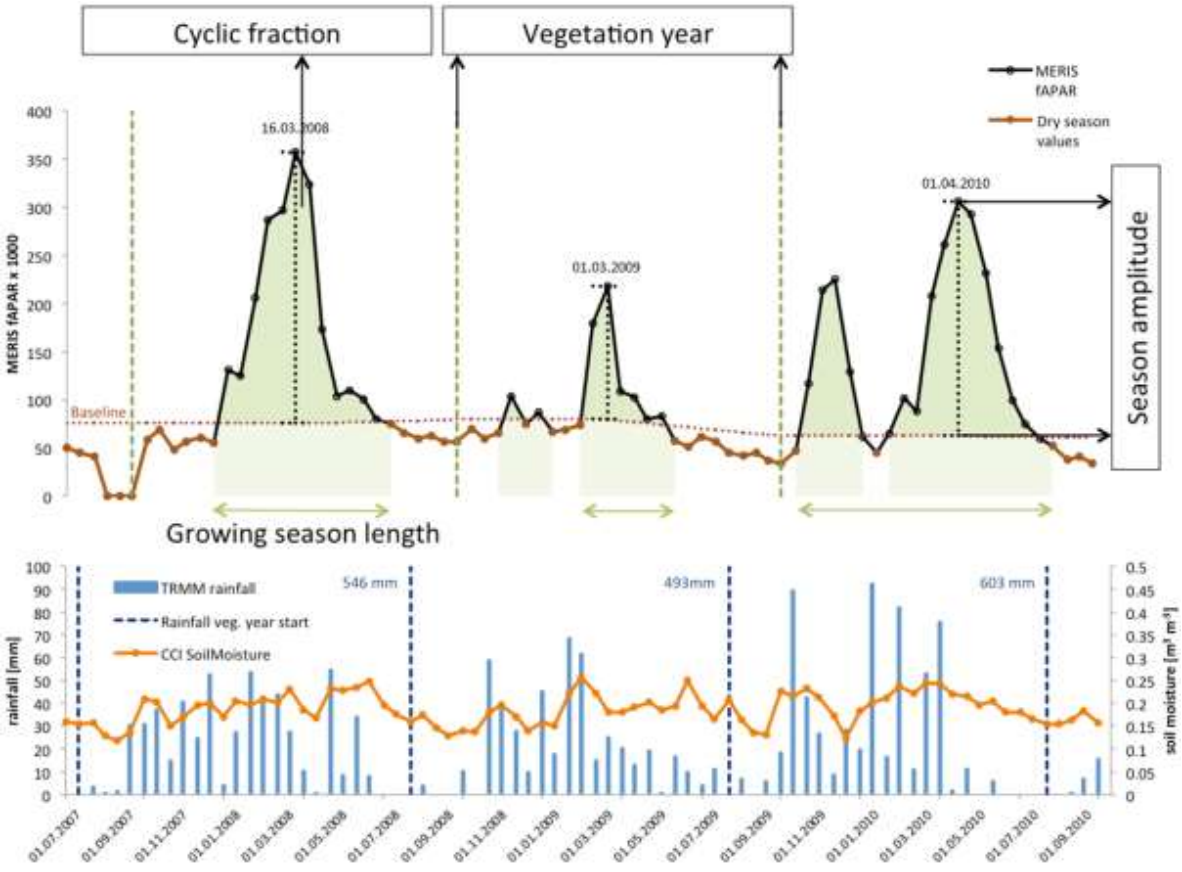

Figure 3: Scheme of the extracted phenological descriptors and periods, and corresponding rainfall and soil moisture data. Location: South Africa, Y: -29.896337, X: 25.7373764

The diagram displays the temporal course of the MERIS fAPAR data during a 3-year period and the subdivision into different seasonal periods. The ***vegetation year*** includes the full yearly vegetation cycle starting after the end of the preceding *dry season* (and/or cold season) and ending at the end of the following ***dry season*** (and/or cold season) – or in case of several green seasons during a year – at the begin of the dominant green season in the period from 2003 to 2010. The ***vegetation year length*** varies with possible shifts of the green season start time, which results from the high rainfall variability typical for drylands (see section 4.3.4 for further details).

The ***vegetation year*** can be subdivided into different periods, limited by defined starting and ending points in time. The ***growing season*** includes the major peak(s), i.e. ascending and descending parts of the time series and starts once a selected greenness threshold is surpassed on the way from the start of the vegetation year to the green peak. This threshold is depicted as brown dotted line and labeled with "***baseline***" in the phenology diagram. Hence, we explicitly make a difference between the start of the vegetation year and the start of the vegetation season. Map examples for both are presented in Figure 12 (median start of the vegetation year) and in Figure 13 (mean start of the vegetation season) for test site 10, Southern Europe.

The ***dry season*** (brown parts of the curve in Figure 3) starts once a defined lower fAPAR threshold, again represented by the baseline, is passed. The baseline values depend on the seasonal amplitude of the greenness and especially on the average level of the dry season values. The method for the baseline derivation is described in section 4.2.2. The ***growing season length*** is the time span between the start and the end of the growing season, marked with horizontal light green arrows in Figure 3.

In Figure 3, the second vegetation year has a very short growing season, which does not include the first small peak. To include such small peaks not into the growing season was deliberately decided in order to make the "length of the growing season" indicator sensitive to years with "shorter" main vegetation peaks.

The ***growing season amplitude*** is the span between the baseline and the ***greenness maximum*** of the vegetation year, as shown on the right hand site in Figure 3.

Table 2 describes how the above described phenological parameters relate to the different proxy parameters for vegetation productivity extracted from the time series.

Table 2: Relation between phenological and productivity parameters

Phenological parameters	Vegetation productivity parameter
Start of the vegetation year: first value of the vegetation year ***End of the vegetation year***: last value before the start of the following vegetation year	The fAPAR values from the start of the vegetation year until the end are averaged to build the ***Average vegetation year fAPAR:*** Mean value of all fAPAR values within one full vegetation cycle, constituting a proxy for the annual NPP, which however interferes with the standing green biomass depending on the vegetation structure and productivity.
Start of the growing season: first value above the baseline ***End of the growing season***: last value above the baseline	The fAPAR values from the start of the growing season until the end are summed up after subtracting from each value the corresponding baseline value, resulting in the ***Cyclic fraction fAPAR:*** The cyclic fraction fAPAR can be interpreted as the amount of NPP that is directly related to the annual cycle of the climatic vegetation growth factors, especially rainfall, but also heat and radiation
Dry season: spans the values after the growing season until the end of the vegetation year	The fAPAR values from the dry season are averaged to build the ***Average dry season fAPAR:*** The dry season greenness values reflect the portion of plants that remain green after senescence of the annual vegetation or grow new green leaves during the dry period. High dry season levels in general indicate the presence of shrubs, bushes and trees (neglecting the background reflectance of the soils of dead plant material)
Timing of the greenness maximum: timing of the absolute greenness maximum in the course of the vegetation year	The fAPAR value at the time of the greenness maximum is connected to two productivity values: • The absolute ***greenness maximum*** (often used as THE proxy for vegetation productivity) • The ***greenness amplitude***: the maximum minus the baseline value at the time of maximum Both parameters have been calculated in Diversity II, but are not provided as defined products.

Along with the fAPAR values, the respective halfmonthly rainfall and soil moisture values are shown in Figure 3. The dashed blue vertical lines are shifted by two months ahead of the fAPAR based vegetation year starts (dashed green lines), indicating that the temporal integration period of the rainfall data used to contrast the fAPAR data against, was shifted by two months ahead to account for the temporal delay observed between start of the rainy period and of start of major vegetation growth. The integration period for soil moisture was also shifted back, but only by one month, again based on empirical observations of the time delay between soil moisture and vegetation development. Figure 3 shows an obvious correspondence between the rainfall, the soil moisture data, and the vegetation data. However, the soil moisture have a much smaller relative amplitude when looking at their low values, which always stay relatively high compared to the maxima. It must be noted that the soil moisture and the rainfall data have a spatial resolution of 0.25°, which is very coarse compared to the 300m*300m vegetation data (see also 3.6.5, 4.2.4, and 4.2.5 for further information).

Why fAPAR and which are the most suited fAPAR derived NPP proxies?

fAPAR is the index "*most directly related to loss of plant productive capacity"* and it is the core variable used in models of primary production in terrestrial ecosystems (GEO BON, 2011). Hence fAPAR data are basically considered to be suited to represent vegetation productivity.

However, the question is which temporal integration of the EO based fAPAR is most suited to represent (above ground) net primary productivity. For yearly NPP, frequently the maximum of EO derived vegetation index values is taken in remote sensing studies, assuming that it represents the amount of plant material accumulated and produced during the yearly growing season. This may apply to crops or other plant communities with little species diversity. However, the maximum neglects the dry or cold season base level of greenness and the time span of the growing period, during which the plants may partly decay, may be partly consumed, and may partly start growing or keep being productive. Taking the Amplitude, i.e. the difference between the dry or cold season base level of greenness would consider the base value of perennially green vegetation. However, both the Maximum and the Amplitude are – as single values –prone to biases, especially due to cloud coverages during the growing period[6].

In theory, the "cyclic vegetation greenness" (see Figure 3) may be taken as proxy for the productivity during the (major) growing period, as it constitutes the sum of the incremental plant growth above the dry or cold season base level. The vegetation year sum or average on the other hand may be regarded as indicator for the yearly productivity, but especially in dense and high canopies (trees, bushes) the productivity estimation will interfere with standing biomass, depending on the structure and the productivity of the standing vegetation. The third major parameter used in Diversity II, the "dry season greenness", can be considered a proxy for the average standing (and partly active) green biomass during the dry and/or cold season.

This means that we do not derive NPP quantities from the MERIS data, but only use seasonally and yearly integrated fAPAR data as proxies for NPP (plus biomass depending on the indicator and on the type of standing vegetation). The estimation of NPP data would have required a great deal of additional input data and computational effort, and especially also calibration and validation data, which are not readily available for all these different land surface conditions and regions. Hence we preferred to produce only NPP and RUE proxies.

Rain Use Efficiency and Soil Moisture Use Efficiency

In addition to the NPP proxies, Rain Use Efficiency (RUE) and Soil Moisture Use Efficiency (SMUE) indicators were derived. While RUE is based on a widely applied, tested, discussed, and partly modified (with regard to the temporal integration periods) approach of Le Houérou (1984), SMUE is an analogue concept based on soil moisture data instead of rainfall as water availability parameter. Le Houérou defined RUE as *quotient of annual primary production by annual rainfall*. RUE thus expresses the amount of biomass growing per unit rainfall water. Theoretically, soil moisture is more directly related to plant water availability than rainfall, so SMUE is offered as a potentially useful additional indicator. RUE (and assumedly also SMUE) depends heavily on climate, soil, and soil and vegetation conditions. For instance, as Le Houérou states, it decreases with increasing aridity due to the decreasing rate of useful rainwater (increasing evaporation, heavy rains, soil crusting and consequently more runoff, etc.). As observable in the EO data as well, from a certain intermediate level of humidity (temporally and spatially variable) on, RUE decreases with increasing rainfall. This is especially obvious when taking the RUE status maps for the cyclic vegetation, where the perennially green vegetation is not included.

[6] The Maximum is nevertheless a very straight forward parameter and very easy to extract. We have extracted the Maxima values, also the timing of the Maxima, as well as the values and timing of multiple maxima, if they exist (which is less straight forward). However these results have not been developed as products, but may be provided on special requests.

It further depends on the way it is derived, especially the input parameters/data sources used for vegetation and rainfall. Since it is known to not necessarily normalize vegetation productivity based on rainfall variability, as RUE can be found to be correlated with rainfall over the years at a given place, its actual usefulness as an indicator for vegetation degradation (where RUE is supposed to decrease) is therefore limited and disputed (e.g., Fensholt et al. 2013). Nevertheless, we have included RUE and SMUE status and trend products in the Diversity II products, and the users may decide about its usefulness. Respective RUE and SMUE trend products are shown and discussed in section 3.5.6.

The function of RUE (or SMUE) as status indicator of ecosystem productivity and its usefulness for the comparison of the productivity of different ecosystems as proposed by Le Houérou (1984) is obvious and can be observed in the Diversity II results as well. Like the NPP proxy indicators, RUE and SMUE have been generated for the three phenological periods vegetation year, cyclic vegetation, and the dry season.

Beyond that, several authors have developed the idea of mapping RUE (or NPP) deviations from certain mean expectation levels derived for ecosystems or functional units or otherwise homogeneous regions, and interpret negative deviations as vegetation degradation. These approaches may lead to valuable results if they are applied based on comprehensive environmental and hydro-meteorological data and models for properly taking care of the major influencing factors of vegetation productivity at the scale of analysis. In the Diversity II project using 300*300 m² fAPAR data we could not go into that detail.

2.2.2 First Order Status and Trend/Change Products

The first order products include status and trend/change indicators for

- Seasonal and yearly (vegetation years) vegetation greenness
- Rainfall
- Soil moisture
- Rain Use Efficiency (RUE), and
- Soil Moisture Use Efficiency (SMUE)

They reflect the vegetation productivity – both standing biomass and the yearly increase during the wet seasons, vegetation decline/increase and potential degradation, and show the high variability and trends of vegetation greenness during the observed years. By differentiating between the green and the dry periods, they also highlight the relation and potential shifts of the seasonal vegetation growth. The latter may give hints to land cover changes and bush encroachment, a widespread dryland degradation process.

Figure 4 shows an example of the indicator for the average vegetation year greenness for test site 05, Eastern Mongolia – Western Manchuria, derived as the mean of the eight average vegetation year fAPAR values 2003 – 2010.

The organisation of first order products is explained in Figure 7: **Soil Moisture Use Efficiency trends of cyclic vegetation in site 18, Northern USA – Southern Canada**

Table 3. The left column contains the five parameters, for which indicators were derived. The second column shows the three temporal integration periods, for which these indicators were calculated. Column three and five list the derived status and trend/change parameters, followed by the product numbers.

Epochal changes were calculated for the rainfall and soil moisture data only. They are included as products in addition to the trend products, as they exhibit differences that are very often clearly related to the observed trends of vegetation productivity, although no significant rainfall trends may be present (because the rainfall-vegetation relationship goes beyond single vegetation years). This relation can be seen in Figure 5, which contrasts TRMM rainfall epochal changes, TRMM rainfall trends, fAPAR cyclic fraction and fAPAR dry season trends for test site 13, Western Sahel. The positive dry season greenness and cyclic fraction trends seen in northern Senegal or the dry season greenness trends in western and central Burkina Faso for instance, can be spatially (and probably causally) related to epochal rainfall increases, even though these locations do not exhibit significant rainfall trends at p=0.9.

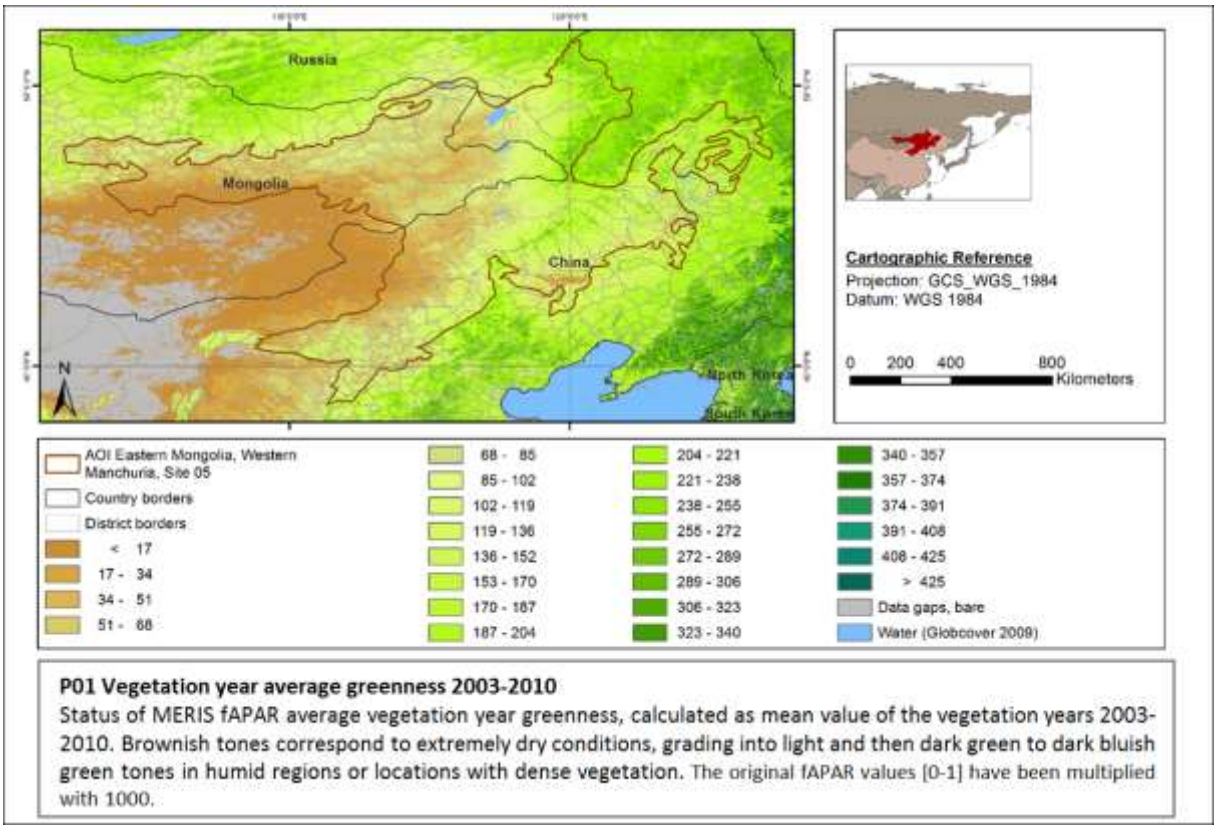

Figure 4: Vegetation year average greenness 2003-2010, site 05, Eastern Mongolia – Western Manchuria_

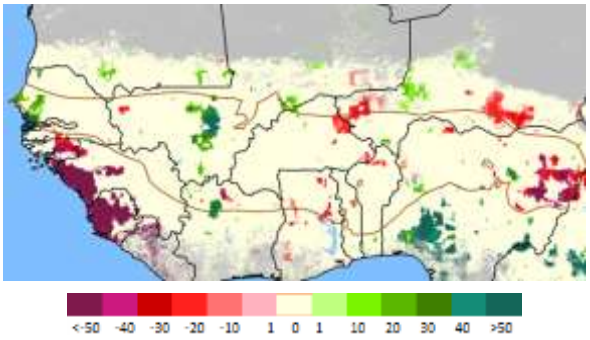

P42: Trend slope of TRMM rainfall aggregated to fAPAR vegetation years [mm]

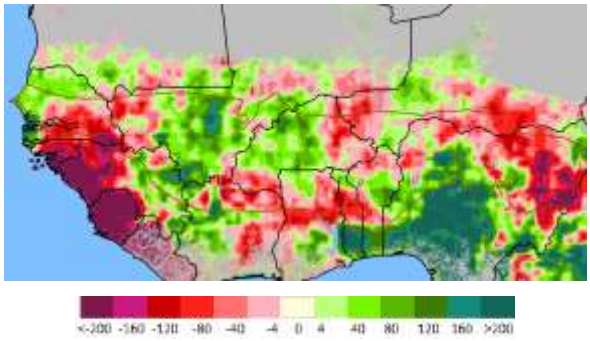

P46: Epochal differences of TRMM rainfall between the two epochs 2003-2006 and 2007-2010 [mm]

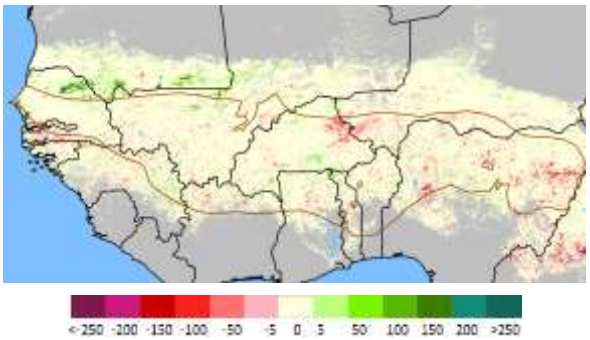

P34: Trend slope of cyclic fraction fAPAR sum (* 1000) 2003-2010

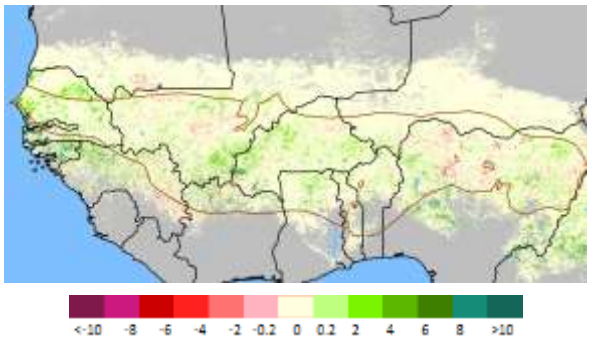

P35: Trend slope of dry season mean fAPAR (* 1000) 2003-2010

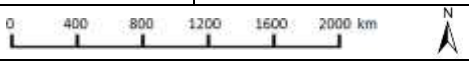

Figure 5: TRMM rainfall epochal changes (a) and trends (b) versus fAPAR cyclic fraction (c) and dry season(d) trends

Epochal differences for the NPP proxies in turn are not included as first order products, as they would exaggerate the impression of primary productivity changes, which might rather be “normal” variability.

Figure 5 and Figure 7 show two further examples of first order trend products, i.e., Rain Use Efficiency (RUE) and Soil Moisture Use Efficiency (SMUE) trends of the cyclic vegetation for test site 18, Northern USA – Southern Canada. In regions beyond 50° North and South, the TRMM rainfall data, which and at 50°, were substituted by GPCP rainfall data with a resolution of 2.5°. The product names refer nevertheless to TRMM rainfall, as this is the dominant rainfall data set used in the project. The two product examples display similar and partly strong, both positive and negative trends of RUE and SMUE, and within the actual test site AOIs positive trends dominate.

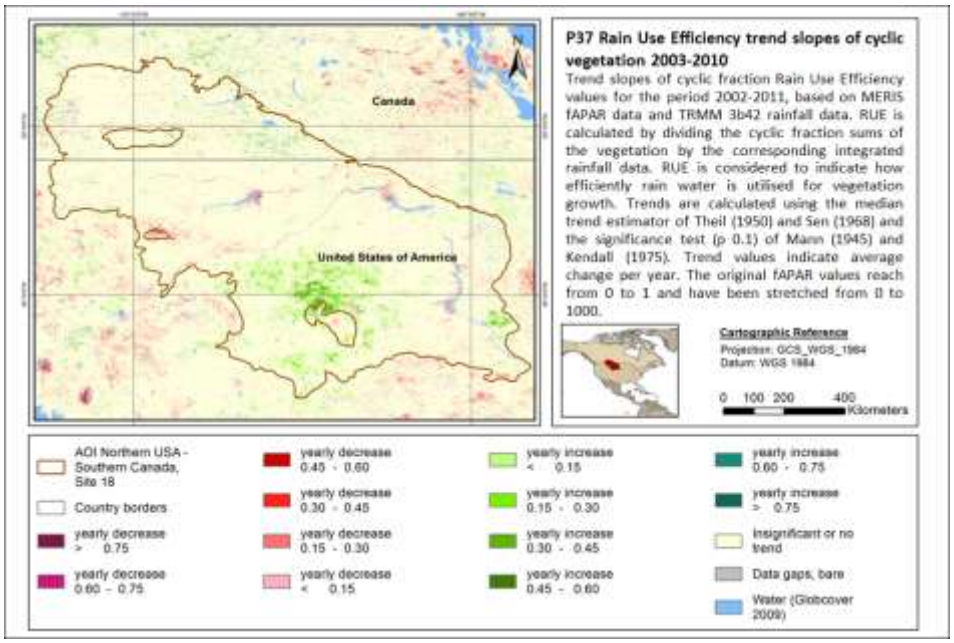

Figure 6: Rain Use Efficiency trends of cyclic vegetation in site 18, Northern USA – Southern Canada

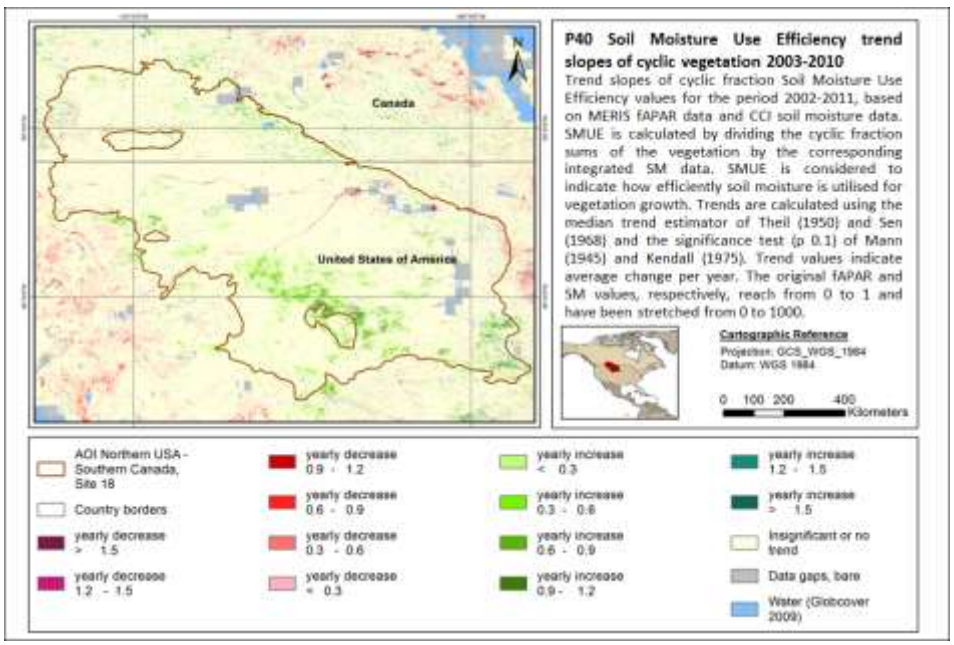

Figure 7: Soil Moisture Use Efficiency trends of cyclic vegetation in site 18, Northern USA – Southern Canada

Table 3: Overview of the organisation of the first order indicators and the related product numbers

Observed parameter	Phenological integration period	Status parameters	Prod. No.	Trend/Change parameter Prod. No.	Prod.No.
MERIS fAPAR	Vegetation year*	- Average 2003-2010 - Coefficient of variation [%] of the yearly averages	1 4	- Theil-Sen trend slope	33
	Cyclic Vegetation period**	- Average of the sums of the cyclic fractions 2003-2010 - Coefficient of variation [%] of the yearly averages	2 5	- Theil-Sen trend slope	34
	Dry season ***	- Average 2003-2010 - Coefficient of variation [%] of the yearly averages	3 6	- Theil-Sen trend slope	35
RUE (Rain Use Efficiency) Based on MERIS fAPAR and TRMM rainfall	Vegetation year*	- Overall vegetation year RUE 2003-2010 - Coefficient of variation [%] of the yearly RUE	8 9	- Theil-Sen trend slope	36
	Cyclic Vegetation period**	- Overall cyclic fraction RUE 2003-2010 - Coefficient of variation [%] of the yearly cyclic fraction RUE	10 11	- Theil-Sen trend slope	37
	Dry season***	- Overall dryseason RUE 2003-2010 - Coefficient of variation [%] of the yearly dryseason RUE	14 15	- Theil-Sen trend slope	38
SMUE (Soil moisture use efficiency) Based on MERIS fAPAR and CCI soil moisture	Vegetation year*	- Overall vegetation year SMUE 2003-2010 - Coefficient of variation [%] of the yearly SMUE	17 18	- Theil-Sen trend slope	39
	Cyclic Vegetation period**	- Overall cyclic fraction SMUE 2003-2010 - Coefficient of variation [%] of the yearly cyclic fraction SMUE	20 21	- Theil-Sen trend slope	40
	Dry season***	- Overall dryseason SMUE 2003-2010 - Coefficient of variation [%] of the yearly dryseason SMUE	23 24	- Theil-Sen trend slope	41
TRMM Rainfall	Vegetation year*	- Average rainfall sum 2003-2010 - Coefficient of variation [%] of the yearly averages	25 26	- Theil-Sen trend slope - Epochal change 2003-2006 vs 2007-2010	42 46
	Cyclic Vegetation period**	- Average rainfall sum 2003-2010 - Coefficient of variation [%] of the yearly averages	27 28	- Theil-Sen trend slope - Epochal change 2003-2006 vs 2007-2010	43 47
CCI Soil moisture	Vegetation year*	- Average soil moisture 2003-2010 - Coefficient of variation [%] of the yearly averages	29 30	- Theil-Sen trend slope - Epochal change 2003-2006 vs 2007-2010	44 48
	Cyclic Vegetation period**	- Average soil moisture 2003-2010 - Coefficient of variation [%] of the yearly averages	31 32	- Theil-Sen trend slope - Epochal change 2003-2006 vs 2007-2010	45 49

* Full vegetation cycle starting at the local Start of Season (SoS) and ending after the dry season

** The period of the green peaks of the vegetation cycles

*** Season between the rainy seasons, in drylands usually with little or no vegetation growth

2.2.3 Second Order Status and Trend/Change Products

Second order dryland indicators are based on the first order indicators and contain more complex and abstract information. They show status, changes and trends of the most essential first order indicators in various relations to each other. Table 4 provides an overview about the relation of the second order indicators to the first order indicators and their contents.

Table 4: Overview of the systematic of the second order indicators (colours reflect product types)

Input first order indicators	Second order indicator	Status / Trend / Change	Prod. No.
- Vegetation year average greenness 2003-2010 - Mean percent of cyclic vegetation of vegetation year greenness* 2003-2010	Functional classes Relation between vegetation year greenness classes and the classified percentage of the cyclic vegetation of the yearly vegetation 2003-2010	Status indicator 2003-2010	50
- Epochal Vegetation year average greenness 2003-2006 and 2007-2010 - Epochal percent of cyclic vegetation of vegetation year greenness 2003-2006 and 2007-2010	Functional differences Epochal (2003-2006/2007-2010) difference map of the relation between vegetation year greenness classes and the classified percentage of the cyclic vegetation of the yearly vegetation	Epochal difference indicator 2003-2006 vs 2007-2010	51
- Trendslope of vegetation year greeness 2003-2010 - Trendslope of cyclic fraction greenness 2003-2010 - Trendslope of dry season greenness 2003-2010	Seasonal Trend Relations Relation between vegetation year greenness trends and seasonal greenness trends 2003-2010	Combined trend indicator 2003-2010	52
- Trendslope of vegetation year greeness 2003-2010 - Trendslope of vegetation year TRMM rainfall 2003-2010	TRMM Rainfall versus MERIS fAPAR vegetation year greenness trend	Combined trend indicator 2003-2010	53
- Trendslope of cyclic fraction greenness 2003-2010 - Trendslope of cyclic fraction TRMM rainfall 2003-2010	TRMM Rainfall versus MERIS fAPAR cyclic fraction greenness trend	Combined trend indicator 2003-2010	54
- Trendslope of dry season greenness 2003-2010 - Trendslope of vegetation year TRMM rainfall 2003-2010	TRMM Rainfall versus MERIS fAPAR dry season greenness trend	Combined trend indicator2003-2010	55
- Trendslope of GIMMS NDVI 1981-2002** - Trendslope of GPCP rainfall 1981-2002**	GPCP Rainfall versus GIMMS NDVI vegetation year greenness trend	Combined trend indicator 1981-2002	56

* This parameter was not included in the product suite as a dedicated first order indicator

** These longer term trend maps were not included as separate indicators in the product suite

Basically three types of second order products were generated.

1. Functional Classes – Status (P50) and Change (P51)

This indicator combines yearly vegetation productivity (vegetation year greenness) and the quotient of cyclic vegetation and yearly vegetation in distinct classes. The status indicator (product no. 50) can be regarded as a functional classification of vegetation productivity and basic type: perennial versus annual/seasonal/ephemeral vegetation. The respective map is closely related to land use/cover patterns and also to soil type and terrain structures (see chapter 3, section 3.5.5 for interpretation). The change indicator (product no. 51) displays epochal (2003-2006 versus 2007-2010) changes between the aggregated classes of the two underlying first order indicators. Figure 8 and Figure 9 show product examples.

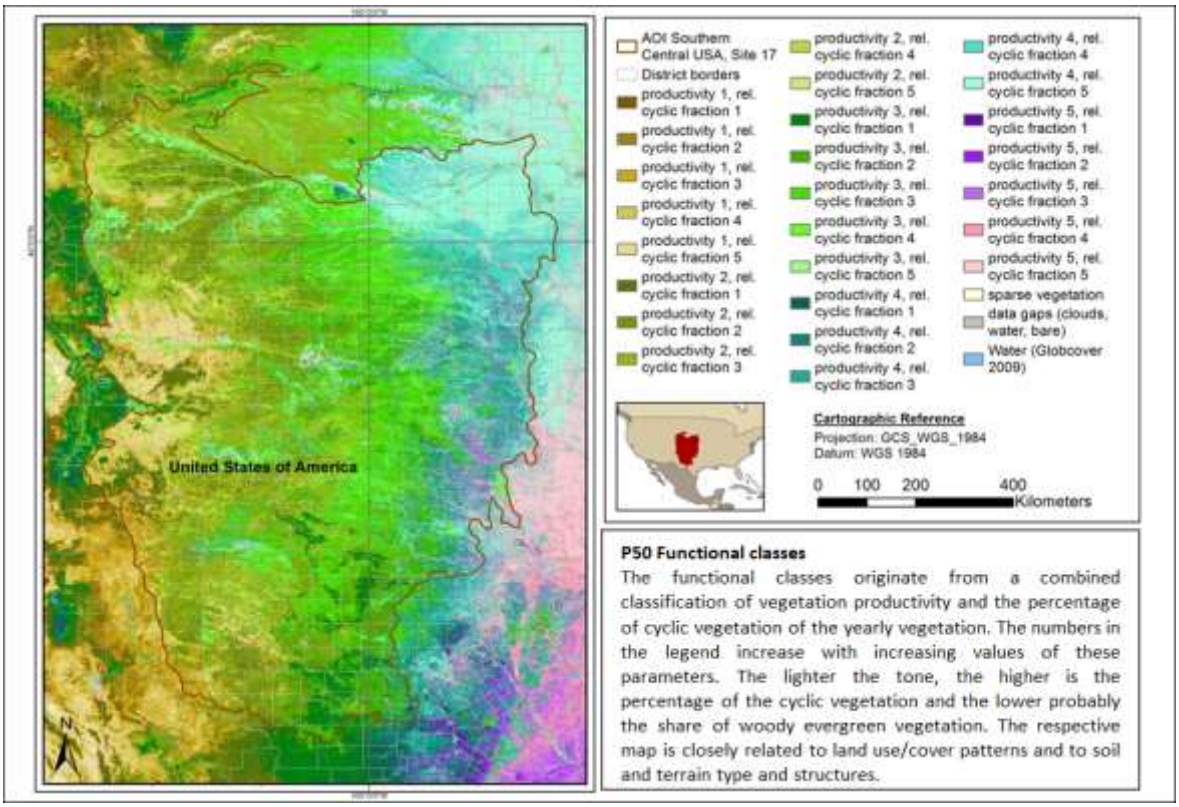

Figure 8: P50 Functional classes in test site 17, Southern Central USA

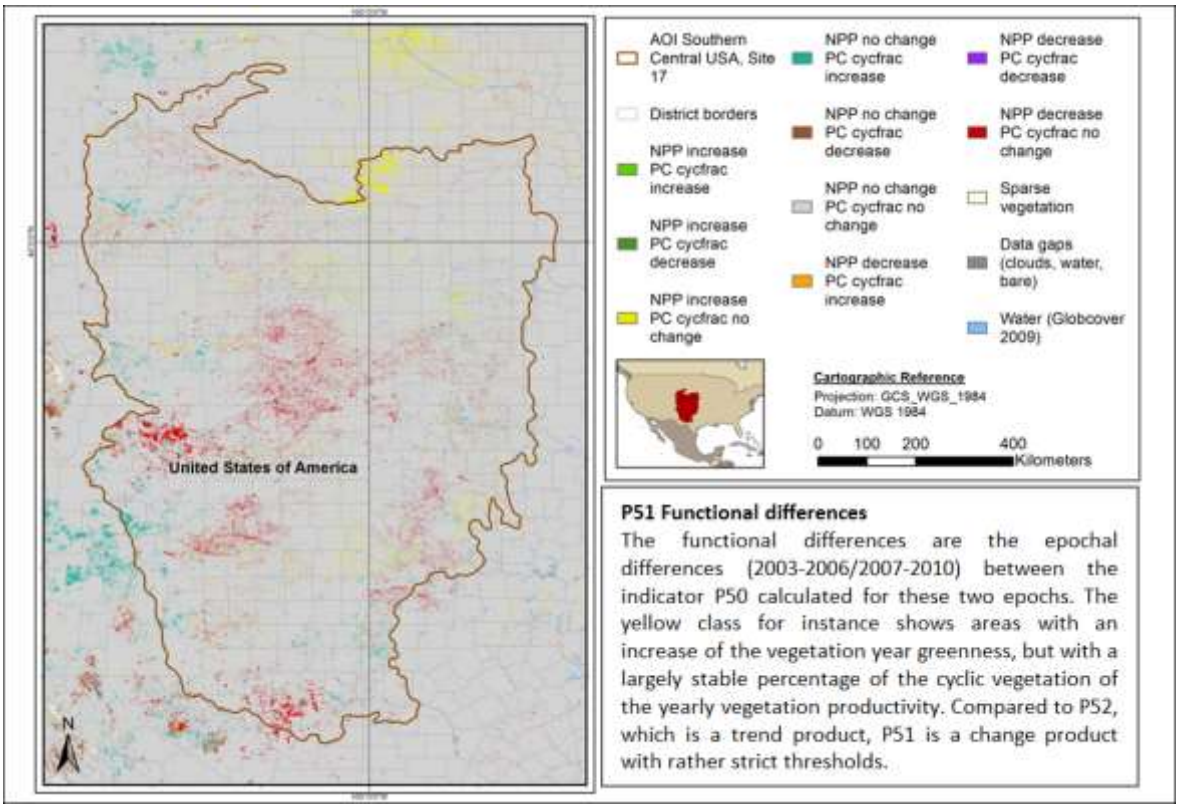

Figure 9: P51 Functional differences in test site 17, Southern Central USA

2. Trend relation between vegetation year greenness and seasonal greenness (P52)

This indicator (product no. 52) combines the yearly (vegetation year) greenness trends with those of the cyclic vegetation and the dry season greenness. It has commonalities with P51, but the trend patterns deviate partly from the change patterns. Essentially this indicator shows the dynamics of the different basic vegetation types in relation to each other in the observation period. Developments such as bush encroachment or the extension of crop area may be captured by this indicator, the first by a relative increase of the dry season greenness, the latter by a relative increase of the cyclic vegetation productivity in relation to that of the dry season.

The two indicators P51 and P52 often exhibit different developments and changes, even though they both relate to changes of the seasonal composition of the vegetation. Trends in P52 may be too weak to pop out as changes in P51, and vice versa, making the two indicators more complementary than redundant.

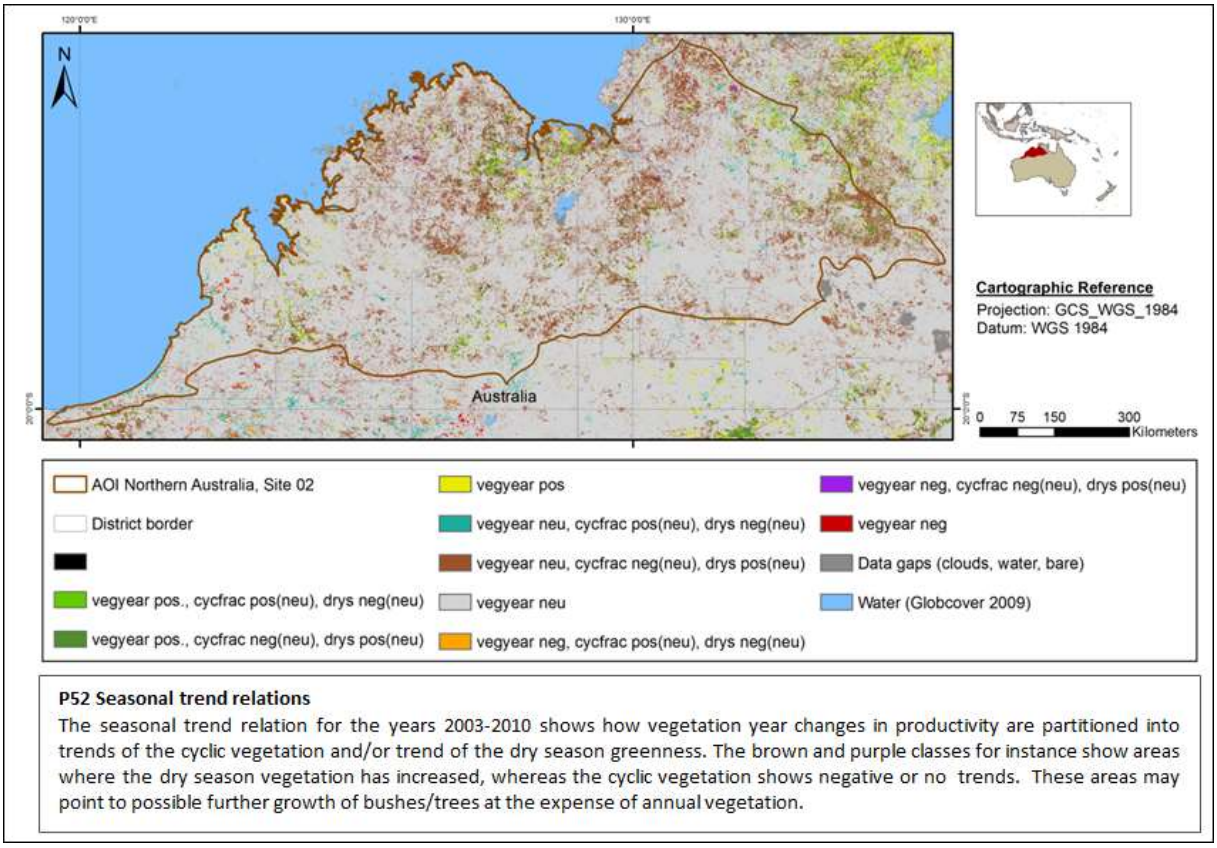

Figure 10: P52 Seasonal Trend Relation, test site 2, Northern Australia

3. Direct relation between Rainfall and Vegetation Productivity (P53, P54, P55)

As an alternative to RUE/SMUE trends contained in the first order products, as well as to the so called "RESTREND" approach (see for instance Wessels 2012), which assume linearity or even proportionality (RUE) between rainfall and NPP, assumption-free relation indicators between rainfall and NPP trends were generated. Indicators were prepared for the relation between rainfall and vegetation year greenness, cyclic vegetation, and dry season greenness, respectively (product no. 53, 54, 55). In addition, the same type of indicator was derived for a time span prior to the MERIS period (1981-2002), using GPCP rainfall data and NOAA GIMMS NDVI data (product no. 56, see for example Figure 61).

The second order indicators are explained in more detail and discussed in chapter 3, section 3.5.7. In Figure 11 we provide an example for product P55, showing that the trends towards a higher dry season greenness (a potential indicator for bush encroachment or growth of trees) seems not be related to a positive trend of the

yearly precipitation amount (as mentioned before, the increase in dry season productivity could still be related to epochal rainfall increases, which is indeed the case in parts of this test site).

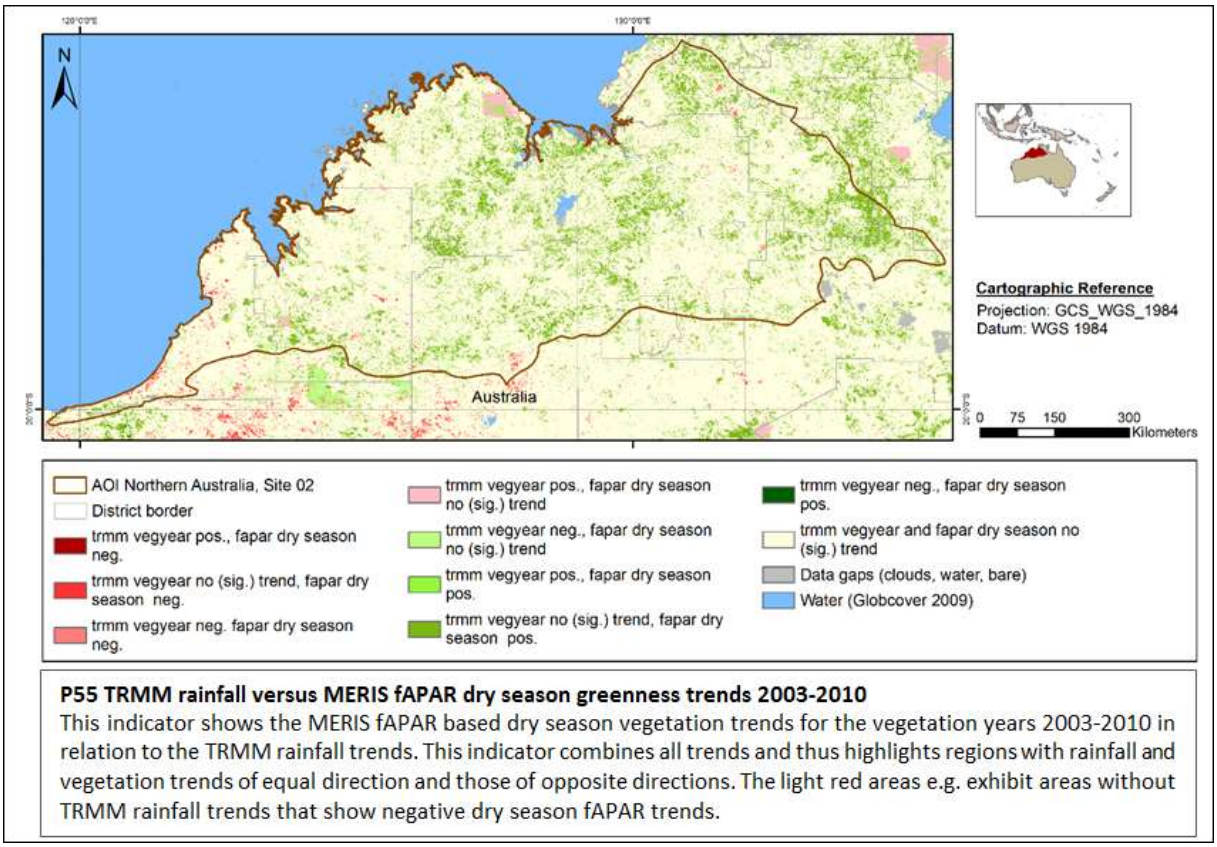

Figure 11: TRMM rainfall versus MERIS fAPAR dry season greenness trends 2003-2010, test site 02, Northern Australia

2.2.4 Phenology Products – Average Conditions

In addition to the first and second order products, which are all based on phenological and productivity parameters, explicit phenology products (maps) were generated in order to characterize the average conditions of major phenological properties of the test sites. Table 5 presents an overview of the map products.

Table 5: Phenology products

Phenology Product	Prod. No.
Median of the start times (half month number in the calendar year) of the vegetation year 2003-2010	57 (example in Figure 12)
Mean of the lengths of the vegetation seasons 2003-2010	58 (example in Figure 13)
Average start time (half month number in the calendar year) of the vegetation seasons (cyclic vegetation) 2003-2010	59 (example in Figure 14)

While the start of the vegetation year (P57) is situated at the very start of the vegetation signal rise at the end of the dry season (see Figure 1), the start time of the vegetation season is defined to be marked by the time when the vegetation rise has surpassed the baseline, i.e. the threshold between the (approximately) upper dry

season level and the cyclic vegetation (see section 2.2.1). Figure 12 shows an example for the median start time of the vegetation year, and Figure 13 for the start of the growing season for test site 10, Southern Europe.

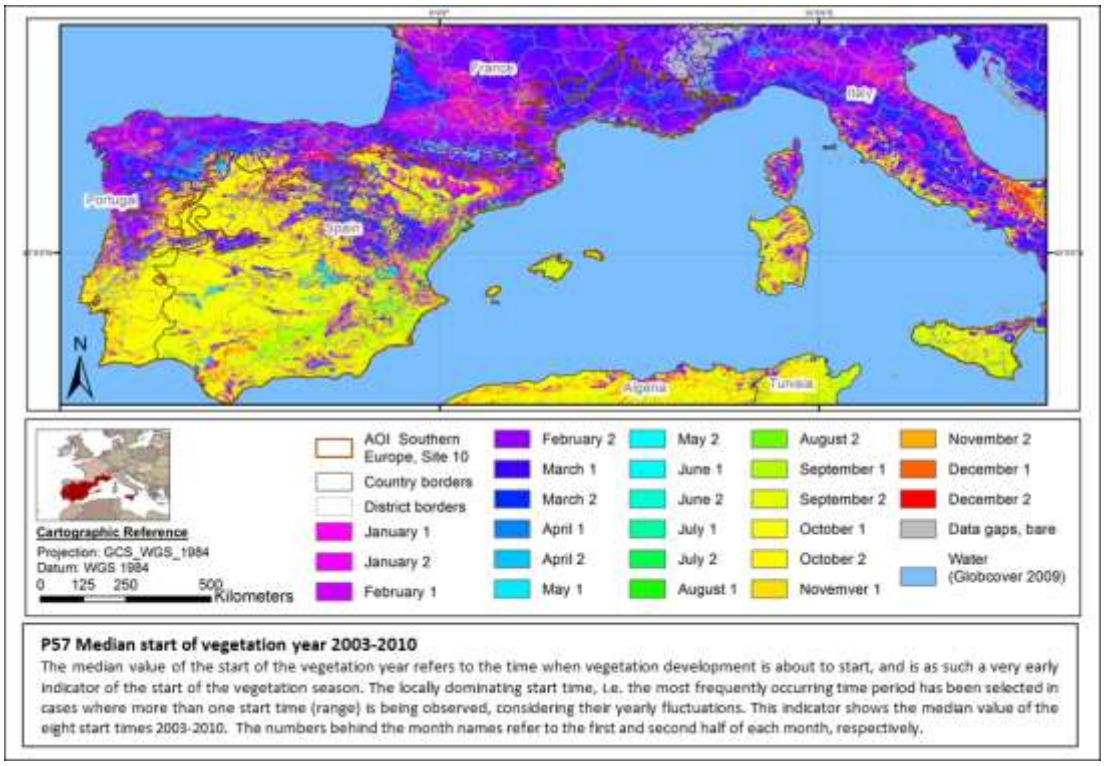

Figure 12: P57 Median start of vegetation year 2003-2010, site 10, Southern Europe

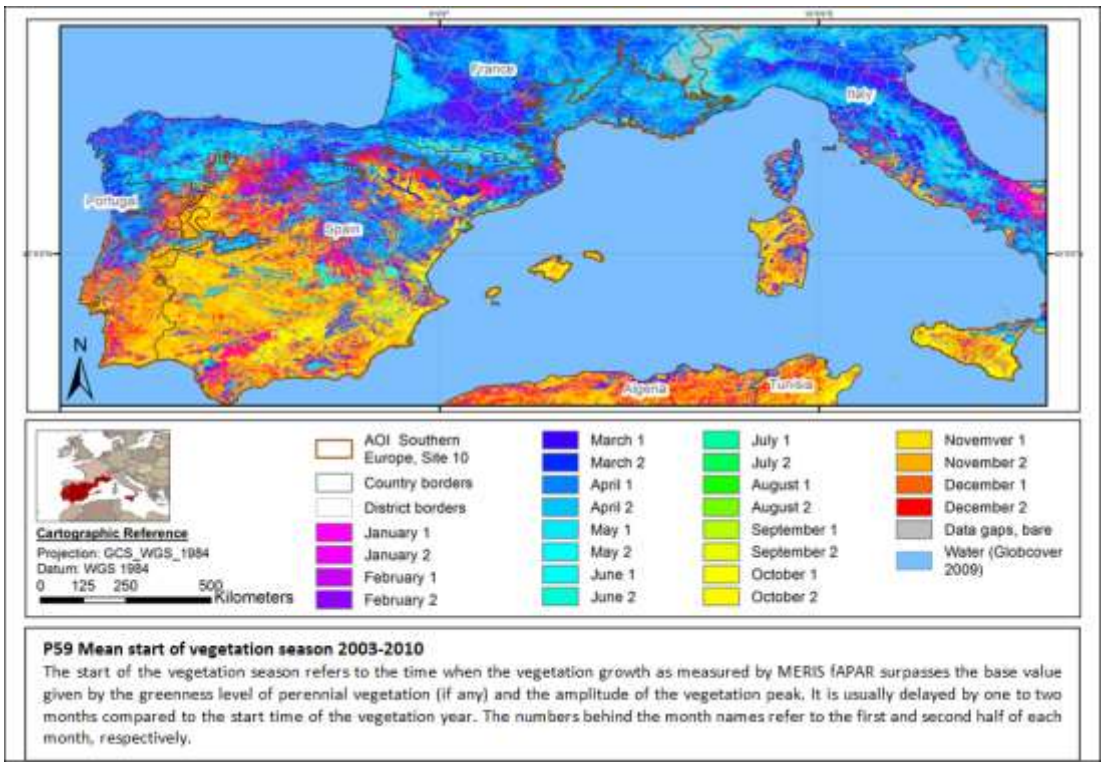

Figure 13: P59 Mean start of vegetation season 2003-2010, site 10, Southern Europe

The length of the vegetation season is given by the duration of the green peaks (or several green peaks within a vegetation year), without including very short and small peaks. The exact procedure is described in section 4.2.2.

A map example for the growing season length is shown in figure 14 for site 01, Northern – Central Mexico.

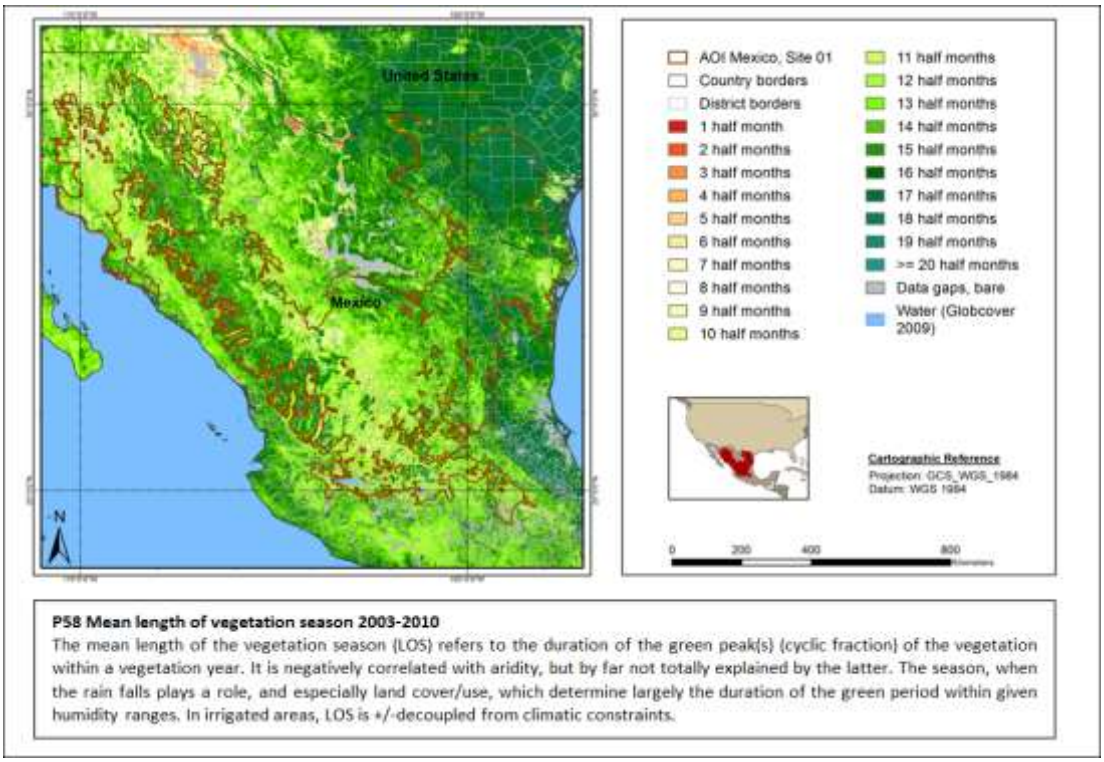

Figure 14: P58 Mean length of vegetation season 2003-2010, site 01, Northern – Central Mexico

2.2.5 NOAA GIMMS NDVI based analyses

As noted in section 2.2.3, with product P56 a GIMMS NDVI based product was added to the product suite, describing the relationship between rainfall and average vegetation greenness for the years prior to the MERIS period (see chapter 3, section 0). In addition to this product, GIMMS NDVI data (see 4.2.6) based analyses and comparisons to Diversity II products are presented in various sub-sections of chapter 3, section 3.5 Interpretation Guide and 3.6. Known Issues.

2.2.6 Overview table of all products

To summarize the complete product suite, in Table 6 a list of all provided products presented, with different colours marking the different product groups.

In chapter 3 all product types are discussed in more detail, showing the relationships among different indicators, and how they relate in particular to land cover maps. In essence it will be shown that none of the products can serve as THE indicator for all properties and developments in the analysed test sites. The indicators are rather complementary and are supposed to provide profiles of the characteristics and developments of the test sites with regard to vegetation productivity and functionality.

Thus, a multitude of different products has been generated; however we hope that this guide helps to structure and interpret these products and assist users in an assessment of the dryland processes going on in their region of interest.

Table 6: Overview of all Diversity II Dryland products (the missing product numbers are underlying products not contained in the regular deliveries)

Prod. No.	Product name	Product description
First order status products		
1	Vegetation year average greenness 2003-2010	26 greenness classes Mean of 8 vegetation years average values
2	Cyclic vegetation greenness 2003-2010	26 greenness classes Mean of 8 cyclic fraction sum values
3	Dry season greenness 2003-2010	26 greenness classes Mean of 8 dry season average values
4	Vegetation year greenness variability 2003-2010	26 greenness variability classes Variation coefficient of 8 vegetation year average values
5	Cyclic vegetation greenness variability 2003-2010	26 greenness variability classes Variation coefficient of 8 cyclic fraction average values
6	Dry season greenness variability 2003-2010	26 greenness variability classes Variation coefficient of 8 dry season average values
8	Vegetation year RUE mean 2003-2010	26 RUE classes Mean of 8 vegetation year RUE values
9	Vegetation year RUE variability 2003-2010	26 RUE variability classes Variation coefficient of 8 vegetation year RUE values
10	Cyclic fraction RUE mean 2003-2010	26 RUE classes Mean of 8 cyclic fraction RUE values
11	Cyclic fraction RUE variability 2003-2010	26 RUE variability classes Variation coefficient of 8 cyclic fraction RUE values
14	Dry season RUE mean 2003-2010	26 RUE classes Mean of 8 dry season RUE values
15	Dry season RUE variability 2003-2010	26 RUE classes Variation coefficient of 8 dry season RUE values
17	Vegetation year SMUE 2003-2010	26 SMUE classes Mean of 8 vegetation year SMUE values
18	Vegetation year SMUE variability 2003-2010	26 SMUE variability classes Variation coefficient of 8 vegetation year SMUE values
20	Cyclic fraction SMUE mean 2003-2010	26 SMUE classes Mean of 8 cyclic fraction SMUE values
21	Cyclic fraction SMUE variability 2003-2010	26 SMUE variability classes Variation coefficient of 8 cyclic fraction SMUE values
23	Dry season SMUE 2003-2010	26 SMUE classes Mean of 8 dry season SMUE values
24	Dry season RUE variability 2003-2010	26 RUE variability classes Variation coefficient of 8 dry season RUE values
25	Vegetation year trmm rainfall mean 2003-2010	26 trmm rainfall classes Mean of 8 vegetation year rainfall sum values
26	Vegetation year trmm rainfall variability 2003-2010	26 trmm rainfall variability classes Variation coefficient of 8 vegetation year rainfall sum values

27	Cyclic fraction trmm rainfall mean 2003-2010	26 trmm rainfall classes Mean of 8 cyclic fraction rainfall sum values
28	Cyclic fraction trmm rainfall variability 2003-2010	26 trmm rainfall variability classes Variation coefficient of 8 cyclic fraction rainfall sum values
29	Vegetation year CCI Soil Moisture mean 2003-2010	26 SM classes Mean of 8 vegetation year SM average values
30	Vegetation year CCI Soil Moisture variability 2003-2010	26 SM variability classes Variation coefficient of 8 vegetation year SM average values
31	Cyclic fraction CCI Soil Moisture mean 2003-2010	26 SM classes Mean of 8 cyclic fraction SM average values
32	Cyclic fraction CCI Soil Moisture variability 2003-2010	26 SM variability classes Variation coefficient of 8 cyclic fraction SM average values
First order trend/change products		
33	Trendslope of vegetation year greeness 2003-2010	12 slope classes Theil-Sen median trend, masked at 9 0.1
34	Trendslope of cyclic fraction greenness 2003-2010	12 slope classes Theil-Sen median trend, masked at 9 0.1
35	Trendslope of dry season greenness 2003-2010	12 slope classes Theil-Sen median trend, masked at 9 0.1
36	Trendslope of vegetation year RUE 2003-2010	12 slope classes Theil-Sen median trend, masked at 9 0.1
37	Trendslope of cyclic fraction RUE 2003-2010	12 slope classes Theil-Sen median trend, masked at 9 0.1
38	Trendslope of dry season RUE 2003-2010	12 slope classes Theil-Sen median trend, masked at 9 0.1
39	Trendslope of vegetation year SMUE 2003-2010	12 slope classes Theil-Sen median trend, masked at 9 0.1
40	Trendslope of cyclic fraction SMUE 2003-2010	12 slope classes Theil-Sen median trend, masked at 9 0.1
41	Trendslope of dry season SMUE 2003-2010	12 slope classes Theil-Sen median trend, masked at 9 0.1
42	Trendslope of vegetation year TRMM rainfall 2003-2010	12 slope classes Theil-Sen median trend, masked at 9 0.1
43	Trendslope of cyclic fraction TRMM rainfall 2003-2010	12 slope classes Theil-Sen median trend, masked at 9 0.1
44	Trendslope of vegetation year CCI Soil Moisture 2003-2010	12 slope classes Theil-Sen median trend, masked at 9 0.1
45	Trendslope of cyclic fraction CCI Soil Moisture 2003-2010	12 slope classes Theil-Sen median trend, masked at 9 0.1
46	Epochal difference of vegetation year TRMM rainfall 2003-2006 and 2007-2010	12 difference classes

47	Epochal difference of cyclic fraction TRMM rainfall 2003-2006 and 2007-2010	12 difference classes
48	Epochal difference of vegetation year CCI Soil Moisture 2003-2006 and 2007-2010	12 difference classes
49	Epochal difference of cyclic fraction CCI Soil Moisture 2003-2006 and 2007-2010	12 difference classes
Second order products		
50	Functional Classes	Relation between vegetation year greenness classes and the classified percentage of the cyclic vegetation of the yearly vegetation 2003-2010
51	Functional Differences	Epochal (2003-2006/2007-2010) difference map of the relation between vegetation year greenness classes and the classified percentage of the cyclic vegetation of the yearly vegetation
52	Seasonal Trend Relations	Relation between vegetation year greenness trends and seasonal greenness trends 2003-2010
53	TRMM Rainfall versus MERIS fAPAR vegetation year greenness trend	Relation between vegetation year rainfall trends and vegetation year greenness trends 2003-2010
54	TRMM Rainfall versus MERIS fAPAR cyclic fraction greenness trend	Relation between cyclic fraction rainfall trends and cyclic fraction greenness trends 2003-2010
55	TRMM Rainfall versus MERIS fAPAR dry season greenness trend	Relation between vegetation year rainfall trends and dry season greenness trends 2003-2010
56	GPCP Rainfall versus GIMMS NDVI vegetation year greenness trend	Relation between vegetation year GPCP rainfall trends and vegetation year greenness (GIMMS NDVI) trends 1981-2002
Phenology products		
57	Median start of vegetation year 2003-2010	Median of the start times (half month number in the calendar year) of the vegetation year 2003-2010
58	Mean length of vegetation season 2003-2010	Mean of the lenghts of the vegetation seasons 2003-2010
59	Mean start time of vegetation season 2003-2010	Average start time (half month number in the calendar year) of the vegetation seasons 2003-2010

2.3 Metadata

The metadata are raster files with the following number of layers per year:

2002: 14 (June to Dec.)

2003 - 2011: 24 layers (Jan. to Dec.)

2012: 7 layers (Jan. to mid Apr.)

Each layer contains a code from 1 to 4 for the respective halfmonth of the year:

1. Regular fAPAR value of MERIS FR data, where necessary and available, substituted by MERIS RR fAPAR values
2. Filled gaps
3. Remaining gaps
4. Snow or winter clouds: i.e., halfmonthly values, which due to their temporal distribution were considered snow or winter clouds, and not treated as gaps. The way they have been processed is described in section 4.2.2.

Figure 15 shows an example of the metadata of test site 18, Northern USA – Southern Canada, here northern Wyoming for year 2004, where the layers 4/10/18 (corresponding to the second half of February, May, and September, respectively) are depicted as RGB image. The red areas are all snow covered in the second half of February (and often beyond), the green areas have a filled gap in the second half of May, the yellow areas are high mountain areas (presumably) snow covered (at least) until May, the white areas are snow covered at all three dates shown in the RGB image (with a short snow free period in July/August). In the lower left are grey areas, which are permanent data gaps, i.e. lakes, whereas the black areas are valid MERIS fAPAR values (either from MERIS FR or RR data). The pixel at the cross with the metadata listed exhibits snow cover from January until second half of April (band 8), followed by a snow-free period until first half of October (band 19), and two filled data gaps, one in the second half of May (band 10), and the other one in the second half of June (band 12).

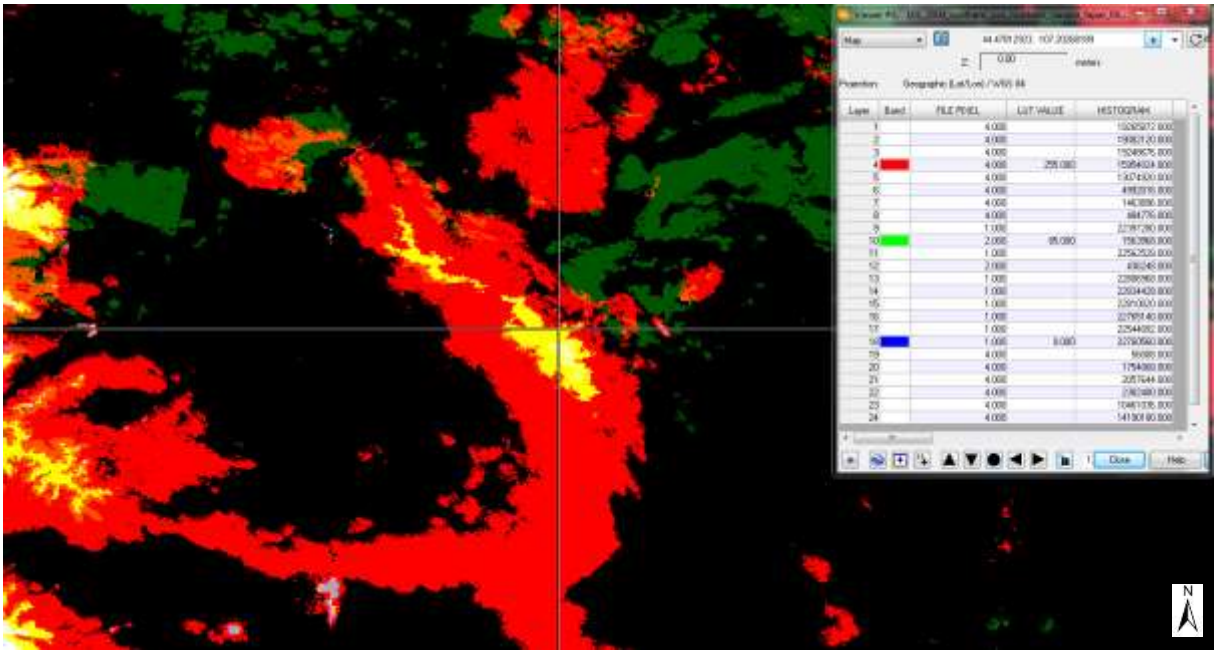

Figure 15: Metadata of part of test site 18. The cross points to mountains in northern Wyoming with a long snow cover

2.4 Formats and projections

All dryland products are raster products in GeoTIFF format.

Pixel size: 300 * 300m²

Projection: Geographic (decimal degrees)

Spheroid: WGS84

Datum: WGS84

All products are thematic products with the same colour schemes as shown in this handbook.

3 Tutorial - How to use the Diversity II products

3.1 Organisation of the dryland products on the ftp server

Before the download information is given in section 3.2, an overview of the product structure of the ftp server is provided. The products are stored as zip files for easy access, and organised in test sites, and for each test site in thematic groups. The zip folders of the products are listed in Table 7 along with a short product description, referring to the product numbers in Thus, a multitude of different products has been generated; however we hope that this guide helps to structure and interpret these products and assist users in an assessment of the dryland processes going on in their region of interest.

Table 6.

A product overview excel sheet is included in each test site folder, where all provided products are listed (e.g., site01_Northern_Central_Mexico_filename_description.xlsx) with a short product description and the respective zip folder name. The product overview sheet looks as shown in Figure 16.

All delivered products are classified products.
The underlying continuous products can be provided on request.
First order status products: green (presented in booklets: dark green)
First order trend/change products: red (presented in booklets: dark red)
Second order products: yellow (all presented in booklets)
Phenology products: blue (all presented in booklets)
Metadata: grey

The colours of the zip folder cells are as follows:
green: fAPAR products
light blue: TRMM RUE products
orange: CCI SMUE products
dark blue: TRMM products
red: CCI SM products
light yellow: second order products
cyan: phenology products
grey: metadata

Product number	Explanation deliverable	01-northern_central_mexico deliverable	ZIP Folder
1	8 bit unsigned TIFF Classified status product Vegetation year average greenness 2003-2010 26 greenness classes Mean of 8 vegetation years average	01_2003-2010_northern_central_mexico_fapar_vegyear_average_mean_classes.tif	site01_Northern_Central_Mexico_101_MERIS_fAPAR_vegetation_year.zip
2	8 bit unsigned TIFF Classified status product Cyclic vegetation greenness 2003-2010 26 greenness classes Mean of 8 cyclic fraction sum values	02_2003-2010_northern_central_mexico_fapar_cycfrac_mean_classes.tif	site01_Northern_Central_Mexico_102_MERIS_fAPAR_cyclic_fraction.zip
3	8 bit unsigned TIFF Classified status product Dry season greenness 2003-2010 26 greenness classes Mean of 8 dry season average values	03_2003-2010_northern_central_mexico_fapar_dry_season_mean_classes.tif	site01_Northern_Central_Mexico_103_MERIS_fAPAR_dry_season.zip
4	8 bit unsigned TIFF Classified status product Vegetation year greenness variability 2003-2010 26 greenness variability classes Variation coefficient of 8 vegetation year average values	04_2003-2010_northern_central_mexico_fapar_vegyear_average_coeffvar_classes.tif	site01_Northern_Central_Mexico_101_MERIS_fAPAR_vegetation_year.zip
5	8 bit unsigned TIFF Classified status product Cyclic vegetation greenness variability 2003-2010 26 greenness variability classes Variation coefficient of 8 cyclic fraction average values	05_2003-2010_northern_central_mexico_fapar_cycfrac_coeffvar_classes.tif	site01_Northern_Central_Mexico_102_MERIS_fAPAR_cyclic_fraction.zip
6	8 bit unsigned TIFF	06_2003-	site01_Northern_Central_Mexico_103_MERIS_fAPAR_dry_season.zip

Figure 16: First part of the product overview excel sheet to be downloaded from the FTP

Table 7: Overview of dryland products on the ftp server for site example Mexico

Dryland product folders on the ftp server	Contents
filename_description_01_northern_central_mexico.pdf	Filename list and short content description
Site01_Northern_Central_Mexico_100_metadata.zip	Metadata per halfmonthly data value. Contains 11 geoTIFF files, covering the period from June 2002 to April 2012
Site01_Northern_Central_Mexico_101_MERIS	01_2003-2010_northern_central_mexico_fapar_vegyear_average_mean_classes.tif

_fAPAR_vegetation_year.zip	04_2003-2010_northern_central_mexico_fapar_vegyear_average_coeffvar_classes.tif 33_2003-2010_northern_central_mexico_fapar_vegyear_mean_trendslope_classes.tif
Site01_Northern_Central_Mexico_102_MERIS_fAPAR_cyclic_fraction.zip	02_2003-2010_northern_central_mexico_fapar_cycfrac_mean_classes.tif 05_2003-2010_northern_central_mexico_fapar_cycfrac_coeffvar_classes.tif 34_2003-2010_northern_central_mexico_fapar_cycfrac_trendslope_classes.tif
Site01_Northern_Central_Mexico_103_MERIS_fAPAR_dry_season.zip	03_2003-2010_northern_central_mexico_fapar_dry_season_mean_classes.tif 06_2003-2010_northern_central_mexico_fapar_dry_season_coeffvar_classes.tif 35_2003-2010_northern_central_mexico_fapar_dry_season_trendslope_classes.tif
Site01_Northern_Central_Mexico_104_TRMM_rainfall_vegetation_year.zip	25_2003-2010_northern_central_mexico_trmm_rainfall_vegyear_average_classes.tif 26_2003-2010_northern_central_mexico_trmm_rainfall_vegyear_coeffvar_classes.tif 42_2003-2010_northern_central_mexico_trmm_rainfall_vegyear_trendslope_classes.tif 46_2003-2010_northern_central_mexico_trmm_rainfall_vegyear_epoch-diff_classes.tif
Site01_Northern_Central_Mexico_105_TRMM_rainfall_cyclic_fraction.zip	27_2003-2010_northern_central_mexico_trmm_rainfall_cycfrac_average_classes.tif 28_2003-2010_northern_central_mexico_trmm_rainfall_cycfrac_coeffvar_classes.tif 43_2003-2010_northern_central_mexico_trmm_rainfall_cycfrac_trendslope_classes.tif 47_2003-2010_northern_central_mexico_trmm_rainfall_cycfrac_epoch-diff_classes.tif
Site01_Northern_Central_Mexico_106_CCI_soil_moisture_vegetation_year.zip	29_2003-2010_northern_central_mexico_sm_vegyear_average_classes.tif 30_2003-2010_northern_central_mexico_sm_vegyear_coeffvar_classes.tif 44_2003-2010_northern_central_mexico_soil_moisture_vegyear_trendslope_classes.tif 48_2003-2010_northern_central_mexico_sm_vegyear_epoch-diff_classes.tif
Site01_Northern_Central_Mexico_107_CCI_soil_moisture_cyclic_fraction.zip	31_2003-2010_northern_central_mexico_sm_cycfrac_average_classes.tif 32_2003-2010_northern_central_mexico_sm_cycfrac_coeffvar_classes.tif 45_2003-2010_northern_central_mexico_soil_moisture_cycfrac_trendslope_classes.tif 49_2003-2010_northern_central_mexico_sm_cycfrac_epoch-diff_classes.tif
Site01_Northern_Central_Mexico_108_TRMM_RUE_vegetation_year.zip	08_2003-2010_northern_central_mexico_fapar_trmm_rue_vegyear_mean_classes.tif 09_2003-2010_northern_central_mexico_fapar_trmm_rue_vegyear_coeffvar_classes.tif 36_2003-2010_northern_central_mexico_fapar_trmm_rue_vegyear_trendslope_classes.tif
Site01_Northern_Central_Mexico_109_TRMM_RUE_cyclic_fraction.zip	10_2003-2010_northern_central_mexico_fapar_trmm_rue_cycfrac_mean_classes.tif 11_2003-2010_northern_central_mexico_fapar_trmm_rue_cycfrac_coeffvar_classes.tif 37_2003-2010_northern_central_mexico_fapar_trmm_rue_cycfrac_trendslopeslope_classes.tif
Site01_Northern_Central_Mexico_110_TRMM_RUE_dry_season.zip	14_2003-2010_northern_central_mexico_fapar_trmm_rue_dry_season_mean_classes.tif 15_2003-2010_northern_central_mexico_fapar_trmm_rue_dry_season_coeffvar_classes.tif 38_2003-2010_northern_central_mexico_fapar_trmm_rue_dry_season_trendslope_classes.tif
Site01_Northern_Central_Mexico_111_CCI_SMUE_vegetation_year.zip	17_2003-2010_northern_central_mexico_fapar_smue_vegyear_mean_classes.tif 18_2003-2010_northern_central_mexico_fapar_smue_vegyear_coeffvar_classes.tif 39_2003-2010_northern_central_mexico_fapar_smue_vegyear_trendslope_classes.tif
Site01_Northern_Central_Mexico_112_CCI_SMUE_cyclic_fraction.zip	20_2003-2010_northern_central_mexico_fapar_smue_cycfrac_mean_classes.tif 21_2003-2010_northern_central_mexico_fapar_smue_cycfrac_coeffvar_classes.tif 40_2003-2010_northern_central_mexico_fapar_smue_cyclic_fraction_trendslope_classes.tif
Site01_Northern_Central_Mexico_113_CCI_SMUE_dry_season.zip	23_2003-2010_northern_central_mexico_fapar_smue_dry_season_mean_classes.tif 24_2003-2010_northern_central_mexico_fapar_smue_dry_season_coeffvar_classes.tif

	41_2003-2010_northern_central_mexico_fapar_smue_dry_season_trendslope_classes.tif
Site01_Northern_Central_Mexico_114_2nd_order_products.zip	50_2003-2010_northern_central_mexico_vegyear-average_pc-cycfrac_relation.tif 51_2003-2010_northern_central_mexico_vegyear-average_pc-cycfrac_relation_change.tif 52_2003-2010_northern_central_mexico_vegyear_trend_cycfrac-dyseason_trend_relation.tif 53_2003-2010_northern_central_mexico_trmm_rainfall_vegyear_trend_relation.tif 54_2003-2010_northern_central_mexico_trmm_rainfall_cycfrac_trend_relation.tif 55_2003-2010_northern_central_mexico_trmm_rainfall_dry_season_trend_relation.tif 56_1981_2002_northern_central_mexico_gpcp_gimms_ndvi_vegyear_trend_relation.tif
Site01_Northern_Central_Mexico_115_phenology_products.zip	57_northern_central_mexico_median_start_of_vegetation_year.tif 58_northern_central_mexico_mean_length_of_vegetation_season.tif 59_northern_central_mexico_mean_start_time_of_vegetation_period.tif

3.2 Download products

Product access information and login credentials are available at: http://www.diversity2.info/products/access/ After receiving username and password, the products can be downloaded either individually from the website, or by browsing the FTP archive.

Single file download (by using a web browser)

1. Open a web browser and go to http://www.diversity2.info/products/
2. Click "Drylands products" in the menu to the left.
3. Click on "Diversity II Products download - Drylands (Map view)"
   or "Diversity II Products download - Drylands (Table view)"
4. Navigate to the site you are interested in.
5. In the list of products, click the desired product
6. Enter username and password
7. Download the product.

Bulk download (by using a FTP client)

1. Open your favourite FTP client.
   (If you don't have one we recommend FileZilla, https://filezilla-project.org)
2. Enter host "ftp.brockmann-consult.de" together with your username and password
3. Navigate to the site(s) you are interested in and download the desired product(s).

3.3 Install software

The Diversity II products are distributed in the widely applied Geotiff format and can be opened in most EO or GIS programs. In this tutorial we will use BEAM, an open-source toolbox and development platform for viewing, analysing and processing of remote sensing raster data.

You can download and install BEAM here:

http://www.brockmann-consult.de/cms/web/beam/releases

Please notice that BEAM functionalities will be continued in SNAP, the common software platform for the three Sentinel Toolboxes which are developed by the European Space Agency (ESA) for the scientific exploitation of the Sentinel-1, Sentinel-2 and Sentinel-3 missions.

3.4 Open products

VISAT is BEAM's visualisation, analysing and processing application. It comes with a clear and intuitive user interface allowing new users to get started quickly.

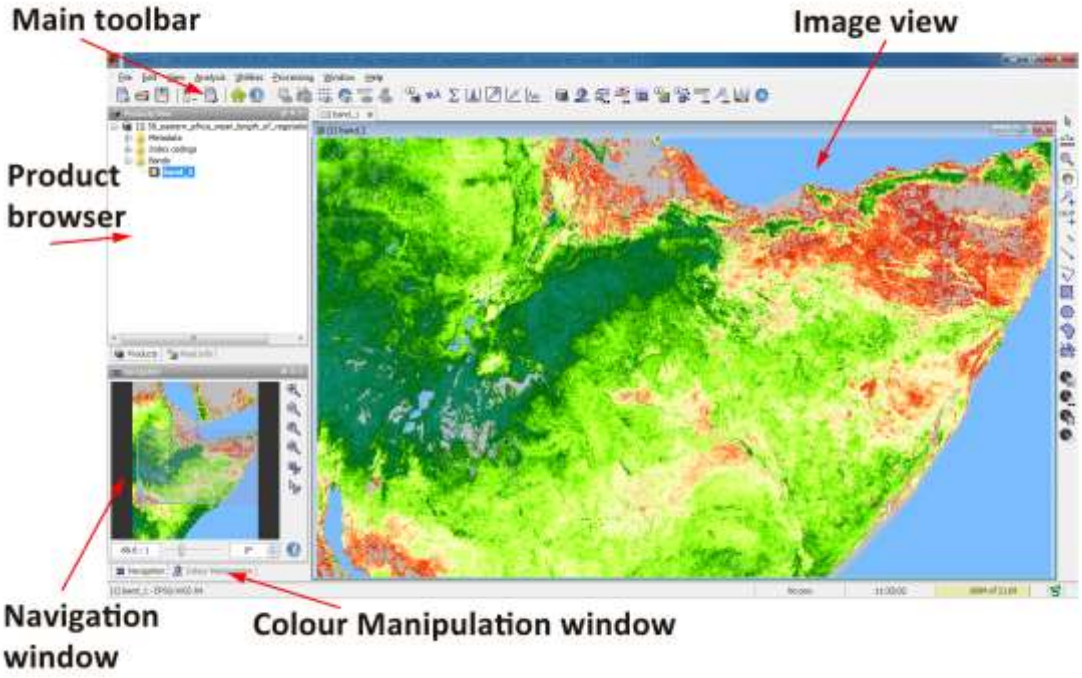

Figure 17: Screenshot of BEAM with some important components highlighted.

VISAT lets you switch between a "Product browser" providing overview over multiple open products within a tree view and a comprehensive pixel information view to display geophysical values, interpolated tie-points and quality flags at the same time.

The tool windows of VISAT provide access to tools, as the name says. These windows can be floating, docked or tabbed. This docking concept allows a tidy work space and you can arrange all tool windows as you like it. All changes you apply to the layout will be saved for the next start of VISAT.

A new "Image view" is simply created by double-clicking on a tie-point grid or spectral/geophysical band. You can open as much images as your computer's memory allows. After you have opened an "Image view" you can inspect the images with the "Navigation window".

After you have opened an Image View you can modify the colours of the image using the "Colour Manipulation window" or overlay an opaque or semi-transparent data mask with the "Mask manager". Both tool windows operate in non-modal mode, which means they float over VISAT's main frame and you can place them somewhere on your desktop.

The following link will guide you through the main components of VISAT's graphical user interface:

http://www.brockmann-consult.de/beam/doc/help/index.html

3.5 Interpretation guide

The information provided in this guide will help users understand the products and show ways how to possibly use them. The guidelines and discussions are structured along the product use cases specified in Table 8, including also interpretation examples of NOAA GIMMS NDVI derived results based on the Diversity II methodology.

Table 8: Overview of use cases presented to assist Diversity II product interpretation

Section	Diversity II product use cases	Usage
3.5.1	Contrasting average phenology with Land Cover	Phenology products can be used to assist regional land cover mapping and assessment.
3.5.2	Longer term phenological trends derived from NOAA GIMMS NDVI data versus in situ trends	Applied to longer history such as the GIMMS NDVI data, the Diversity II methodology can serve to reveal medium term phenological trends, e.g., start of season and length of the growing period.
3.5.3	Relation between fAPAR derived NPP proxies and modelled NPP (BETHY/DLR)	Here the derived vegetation productivity indicators are compared to modelled NPP maps.
3.5.4	Vegetation Productivity and Rainfall / Soil Moisture related First Order Status indicators	First order status indicators provide regional information about the vegetation productivity and the functional composition of the vegetation. The comparisons show how the different status indicators in their combination provide complementary information.
3.5.5	Functional classes compared to Land Cover	The functional classes (P50) serve to assist and assess land cover classifications and mapping of functional ecological units at regional scales.
3.5.6	First order and second order trend products: fAPAR, rainfall, and seasonal trend/change relation	The trend/change products deliver information about the composition of the observed changes and thus potentially to functional biodiversity changes.
3.5.7	First order and second order trend products: RUE and second order trend relation products integrating fAPAR and rainfall trends	With the products based on direct relation between Rainfall and Vegetation Productivity we tried to overcome the limitation and weaknesses of RUE and RESTREND, by showing all vegetation trends along with the potentially related rainfall trends.
0	GIMMS NDVI based second order trend product	The GIMMS NDVI based trend product reveals the story prior to the MERIS period and is as such included in the product suite in order to take a look back beyond the short MERIS period
3.5.9	Relationship between biodiversity and vegetation productivity	Some findings from the literature are presented and a paper pointing to the fact that greening observed with satellite data may not necessarily reveal positive tendencies in terms of biodiversity.
3.5.10	Consistency of trends of different sensors and vegetation indices and derived parameters	The MERIS fAPAR trends of vegetation year averages, cyclic vegetation and dry/cold seasons are contrasted with GIMMS NDVI trends to demonstrate the large consistency between the trends derived with different sensors and trend calculation methods.

3.5.1 Contrasting average phenology with Land Cover

As laid out in section 2.2.1, phenology of the vegetation is the base information for all primary productivity parameters and other products derived in Diversity II. This section illustrates the relationship between major phenological parameters and land cover, comparing CCI land cover[7] data from 2010 to the Diversity II phenological maps.

Figure 18 provides an overview of the three phenological maps and the CCI land cover map for test site 22, Eastern Mediterranean Countries. The brown polygon at the western edge of the region delineates the Akarçay Basin, for which we show detailed comparisons of the start and length of the growing period and land cover in Figure 19. While the overview maps in Figure 18 provides an overview of commonalities of phenological and LC patterns, the detailed views in Figure 19 show that land cover and phenology are closely linked.

The upper part of Figure 19 shows the CCI 2010 LC map for the Akarçay Basin in Turkey, below we see the start of the vegetation year from product P57, and at the bottom the mean length of the growing season (P58) is shown. P57 exhibits basically four groups of vegetation year start periods:

1. The magenta/blueish areas with the first greening in January/February correspond largely to the class “cropland, irrigated or post flooding” of CCI land cover;
2. The blue areas with first greening in March are mapped as deciduous trees;
3. The light blue/cyan coloured (greening from April to June) areas correspond to areas mapped as open vegetation, i.e. grassland or sparse vegetation, predominantly in mountainous areas;
4. The yellow areas, greening from September/October, finally, cover mostly the classes “cropland, rainfed” and “herbaceous cover” of the CCI land cover map.

Areas classified in CCI LC as “cropland, irrigated or post flooding” exhibit the shortest duration of the green season (P58), while part of the areas classified as “herbaceous cover” and “cropland, rainfed”, and “grassland” appear to have the longest vegetation season. Tree covered regions show intermediate values.

Without closer interpretation of this phenological behaviour, a very clear correlation with land cover is obvious and it can be concluded that vice versa phenological parameters are highly suited to support land cover classifications, even at the regional scale of Diversity II. Also for the monitoring of land cover changes phenology would be of great help, however for this purpose EO data with higher spatial resolution would be better suited in order to be able to observe single land cover and vegetation units. For this reason, and especially also because of the short time period observed in this project, we have concentrated on providing average phenology products only.

3.5.2 Longer term phenological trends derived from NOAA GIMMS NDVI data versus in situ trends

Phenological trends are a highly relevant topic from a climate change perspective, therefore we have examined whether the Diversity II methods can potentially contribute to this question. For this purpose, we have analysed longer term GIMMS NDVI data for phenological trends. We compared our results to the findings of Sensoy et al. (2013), who found strong phenological shifts in Turkey related to positive temperature trends in the recent decades. Figure 20 shows a trend map of the growing season length in Turkey compared to NOAA GIMMS based trends of the length of the growing season and to the GIMMS based trends of the start of the vegetation year. Both phenological parameters were derived with the same method as applied to the MERIS fAPAR data.

[7] http://www.esa-landcover-cci.org/

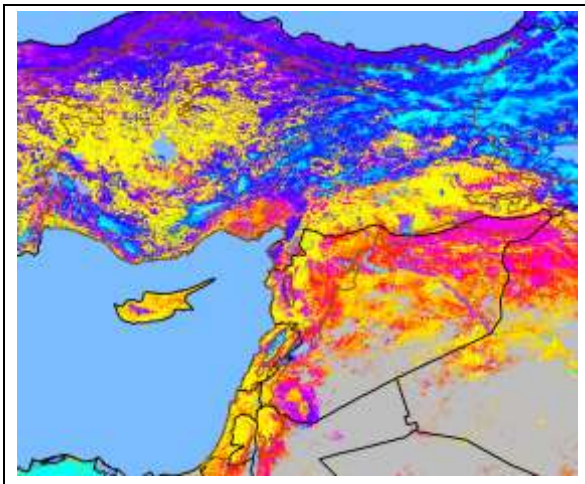

P57 Median start of vegetation year 2003-2010

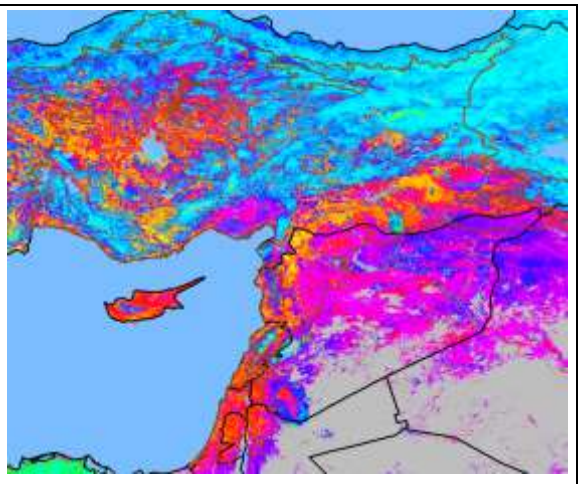

P59 Mean start of vegetation season 2003-2010

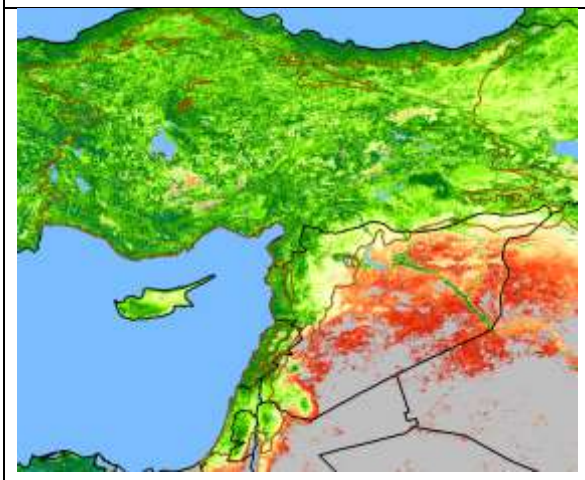

P58 Mean length of the vegetation season 2003-2010

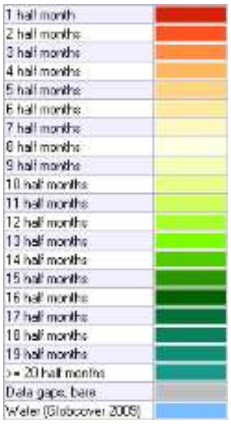

Legend of P58

Legend of P 57, P59

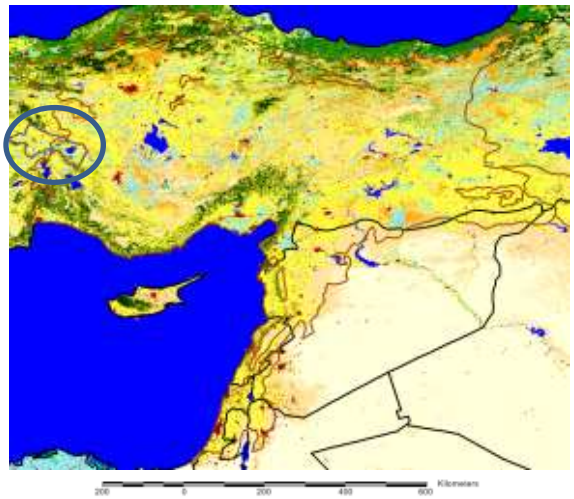

Left: CCI land cover 2010

Highlighted polygon (inside ellipse) in the western part of the CCI LC map:

Location of the Akarçay Basin, Turkey, for which more detailed comparisons of phenology and land cover are presented in Figure 19.

Brown lines: delineation of the Diversity II test site 22, , Eastern Mediterranean Countries

Black lines: country borders

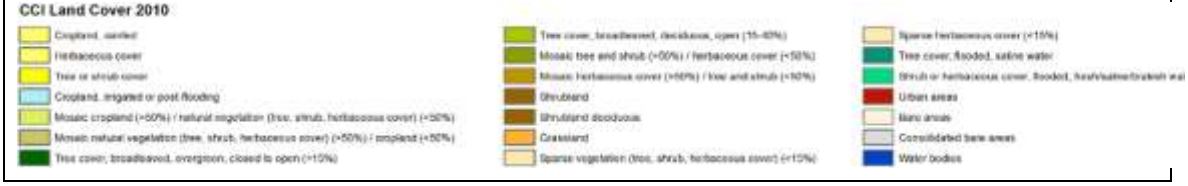

Figure 18: Comparison of phenology and CCI land cover in test site 22, Eastern Mediterranean Countries

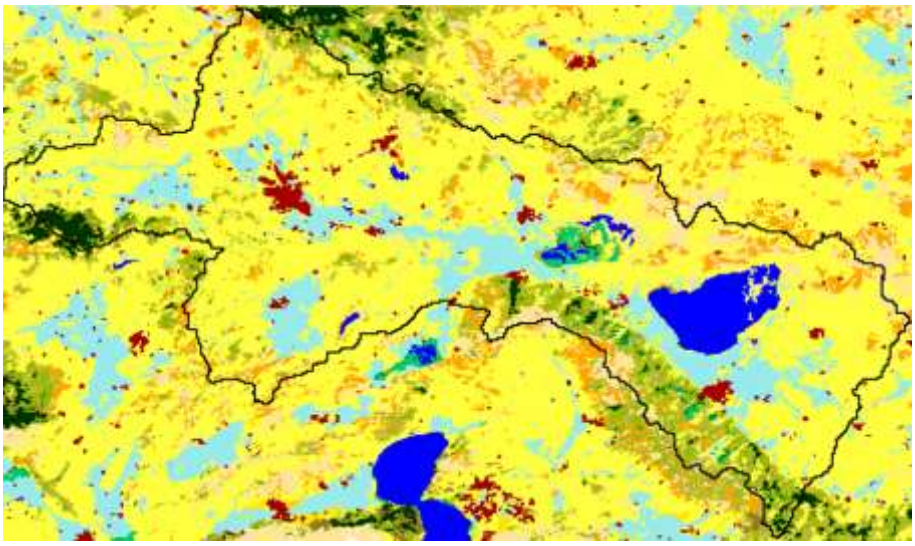

CCI Land Cover 2010

(Legend displayed in Figure 18)

Akarçay Basin in Turkey:

ULX: 30.00277778,

ULY: 39.12993928,

LRX: 31.82500000,

LRY: 38.06111111,

units: decimal degrees.

Location of the Akarçay Basin is shown in Figure 18

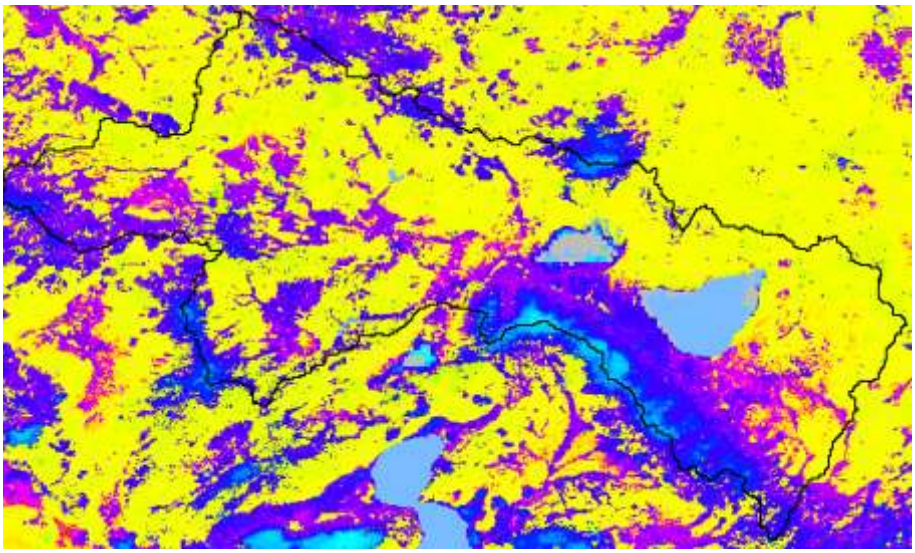

P 57 Mean start of vege-tation year 2003-2010

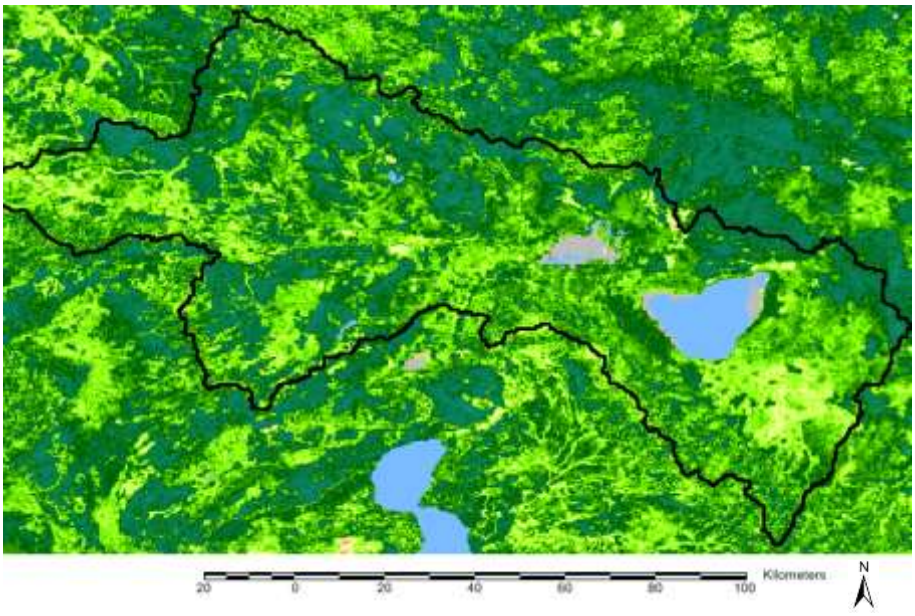

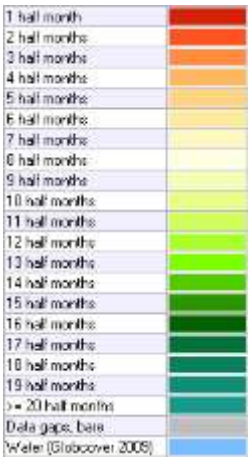

P58: Mean length of the vegetation season 2003-2010

Figure 19: Contrasting Land Cover with phenology in the Akarçay Basin in Turkey, site 22, Eastern Mediterranean Countries

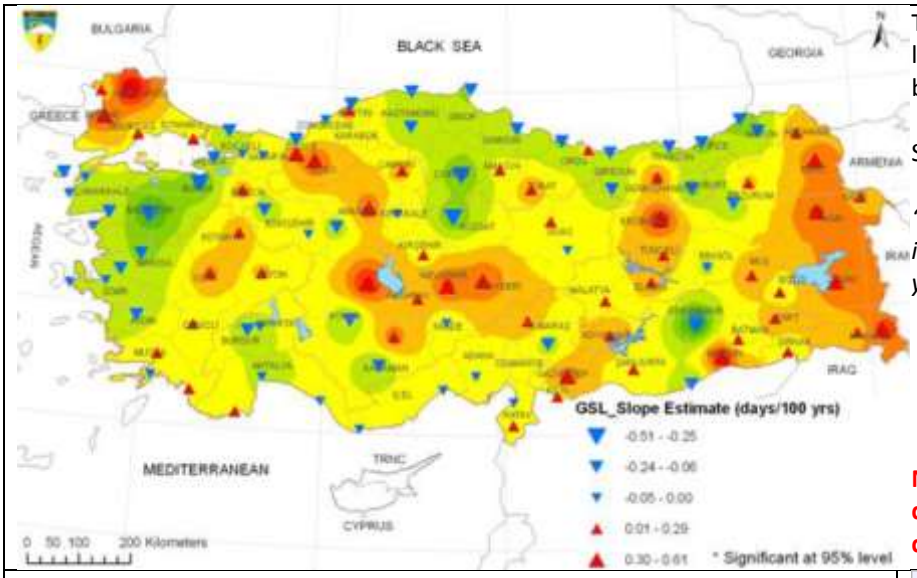

Trend of the growing season length in Turkey 1960-2010 based on in situ observations

Source: Sensoy et al. 2013

"Estimated average increasing is 21 days in 100 years".

Note that increases are depicted in red, and decreases in blue triangles!

Trends of the length of the vegetation season 1982-2010 based on NOAA GIMMS NDVI

yearly decrease	> 3.75	
yearly decrease	3.00 - 3.75	
yearly decrease	2.25 - 3.00	
yearly decrease	1.50 - 2.25	
yearly decrease	0.75 - 1.50	
yearly decrease	< 0.75	
yearly increase	< 0.75	
yearly increase	0.75 - 1.50	
yearly increase	1.50 - 2.25	
yearly increase	2.25 - 3.00	
yearly increase	3.00 - 3.75	
yearly increase	> 3.75	
Insignificant trend		
Water		

Trend classes estimated in days/year (9 0.1)

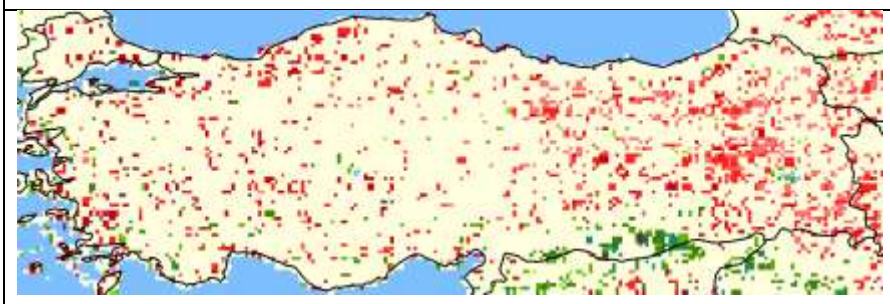

Trends of the start of the vegetation year 1982-2010 based on NOAA GIMMS NDVI. Note that decreases (red) here are related to earlier vegetation growth starts, which can, but do not necessarily lead to longer growing seasons.

yearly decrease	> 2.10	
yearly decrease	1.68 - 2.10	
yearly decrease	1.26 - 1.68	
yearly decrease	0.84 - 1.26	
yearly decrease	0.42 - 0.84	
yearly decrease	< 0.42	
yearly increase	< 0.42	
yearly increase	0.42 - 0.84	
yearly increase	0.84 - 1.26	
yearly increase	1.26 - 1.68	
yearly increase	1.68 - 2.10	
yearly increase	> 2.10	
Insignificant trend		
Water		

Trend classes estimated in days/year (9 0.1)

Figure 20: Trends of the length of the vegetation season based on ground observations (top) and NOAA GIMMS NDVI (mid) in Turkey, as well as GIMMS based trends of the start of the vegetation year (bottom)

The comparison is not quite straightforward, as the colours used in the two trend maps of the growing season length in Figure 20 are opposite and the in situ map has interpolated signatures. The change rates are also not quite comparable, as the rates given by Sensoy et al. are based on longer term observations, while the GIMMS NDVI based trend rates are provided as yearly trend rates for the 29 year observation period 1982-2010.

Nevertheless, areas with increases of the growing periods concentrate in similar regions, and a large part of the decreases are also found in common areas (based on visual comparison).

Thus, it seems that in this area, the long term trends of the growing season length observed in Turkey are more or less reflected in the GIMMS NDI data, though the growing rates in the latter seem to be overestimated (they

are not plausible when extrapolated e.g. to a 100 year period), which should be partly due to the shorter observation period, during which the development has accelerated compared to the longer term trend (see Sensoy et al. 2013).

The GIMMS derived trends of the start of the vegetation years (Figure 20, bottom) largely correspond to the trends of the length of the growing season, i.e. earlier starts of the vegetation growth are overall predominating and concentrate in similar regions as increases of the growing season. However, elongated growing seasons do not necessarily occur along with earlier starts of plant growth, e.g., when considering that the temperature developments leading to earlier growth starts have also led to shorter ripening periods of crops, as found by Sensoy et al. (2013): "*Earliness in the harvest date of cherry, wheat and apple are found as 22, 40 and 25 days/100 years respectively*".

As mentioned above, Sensoy et al. (2013) relate the phenological shifts in Turkey to positive temperature trends: "*Distinct changes in air temperature since 1994 led to clear responses in plant phenology in Turkey in which the phenological phases of the natural vegetation as well as of fruit trees and field crops have advanced clearly in the last decades of the 20th century. The strongest shift in plant development occurred in the very early spring phases. The late spring phases and summer phases reacted also to the increased temperatures*".

To conclude, the Diversity II observation period is too short to capture these phenological trends. However, the methods applied to the derivation of the phenological parameters seem to lead to plausible results when applied to the longer NOAA GIMMS NDVI time series (at least in Turkey). In addition, even the status (average) phenological information derived for the eight vegetation years covered globally with MERIS can serve as valuable supporting information for the mapping or assessment of land cover and functional ecological regions.

3.5.3 Relation between fAPAR derived NPP proxies and modelled NPP (BETHY/DLR)

Below we provide some indication of the relation of the fAPAR-derived NPP proxies to modelled NPP data for two test sites: 04 Northern Kazakhstan and 12 Southern Africa West. For these two sites we used modelled NPP time series data for the period 2003-2011 derived with the most recent version (spring 2015) of BETHY (Biosphere Energy Transfer Hydrology Model, DLR), provided by M. Tum and K. Günther (DLR).

BETHY/DLR is a soil-vegetation-atmosphere-transfer (SVAT) model that was modified to the usage with meteorological and EO based vegetation time series data (Wißkirchen et al. 2013, Tum 2012). The model employs remote sensing products (albedo, LAI, land cover, CO_2 concentration, elevation), partly EO-based meteorological parameters (wind speed, air temperature, precipitation, PAR), climatic zones; and soil data. The LAI (Leave Area Index) data of the provided NPP data came from SPOT VEGETATION, for land cover the GLC 2000 product[10] was used.

The BETHY/DLR NPP data were generated as monthly NPP sums in grams C/m² and 1km² pixel size (at the equator). For comparisons to the MERIS fAPAR derived NPP proxies, they were converted into half-monthly values and 300*300m² pixel size, and then aggregated into sum values per vegetation year, starting from 2003 and ending 2010, exactly like the fAPAR NPP proxies. This way, comparable yearly values were derived, which were used for correlation analysis with the fAPAR status indicators, and for generating the same type of vegetation year – related status and trend indicators as for the fAPAR data. Results are Figure 21 for site 04 Northern Kazakhstan, and in Figure 23 for site 12, Southern Africa West.

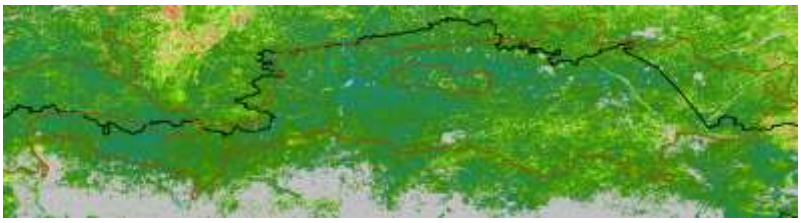

(a) Pearson r between MERIS based vegetation year fAPAR averages and BETHY/DLR vegetation year NPP sums 2003-2010

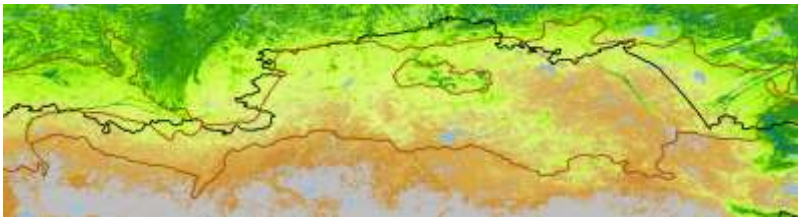

(b) BETHY/DLR average vegetation year sum NPP 2003-2010 [g C/m²]

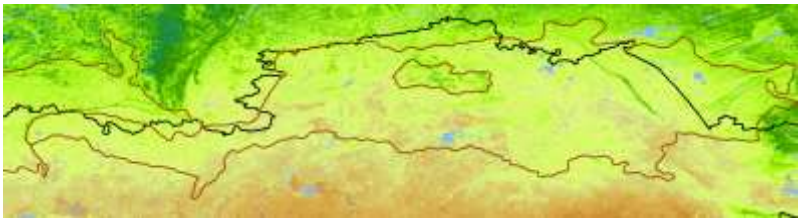

(c) MERIS based average vegetation year fAPAR 2003-2010

(fAPAR data multiplied by 1000)

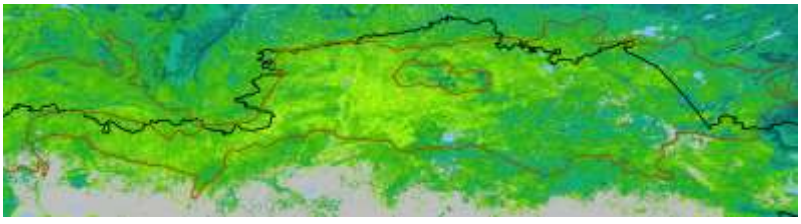

(d) Variation coefficient of BETHY/DLR vegetation year NPP sums 2003-2010 [%]

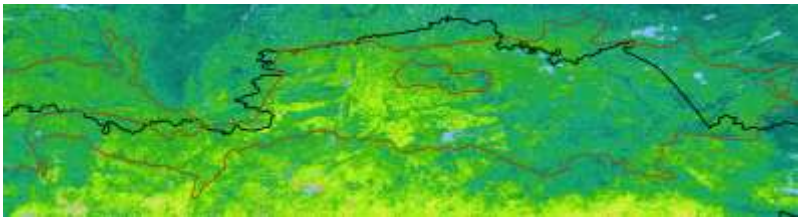

e) Variation coefficient of MERIS fAPAR vegetation year averages 2003-2010 [%]

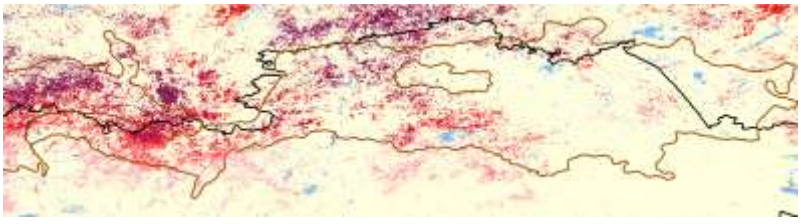

(f) BETHY NPP vegetation year average trends (Theil-Sen, p 0.10) 2003-2010 [g C/m²/year]

(g) MERIS vegetation year average fAPAR trends (Theil-Sen, p 0.10) 2003-2010

(fAPAR data multiplied by 1000)

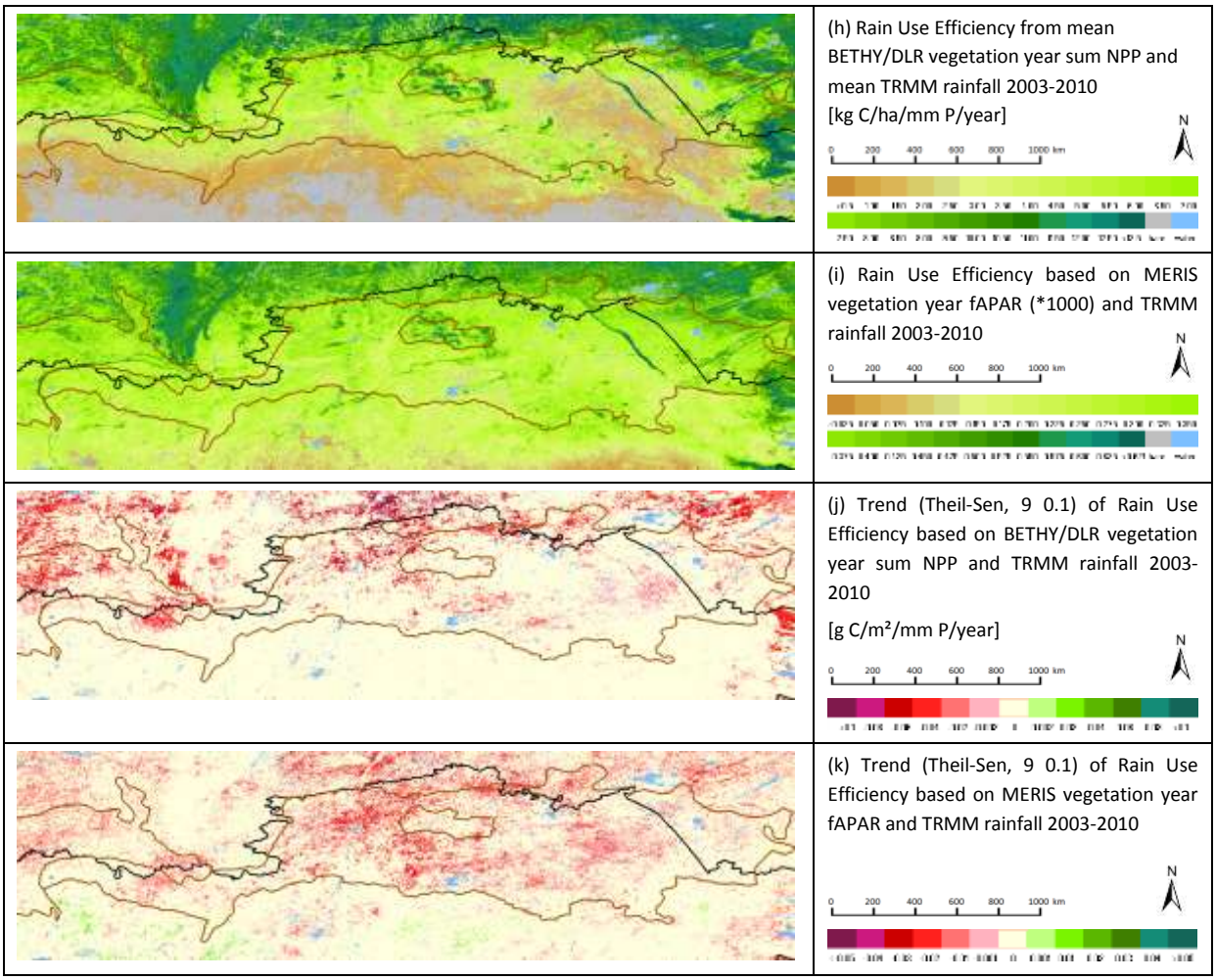

Figure 21: Contrasting MERIS fAPAR derived indicators with BETHY/DLR modelled NPP based indicators in test site 04, Northern Kazakhstan. The black line is the northern country border of Kazakhstan, the brown polygon represents the WWF ecoregion boundary of the actual study site.

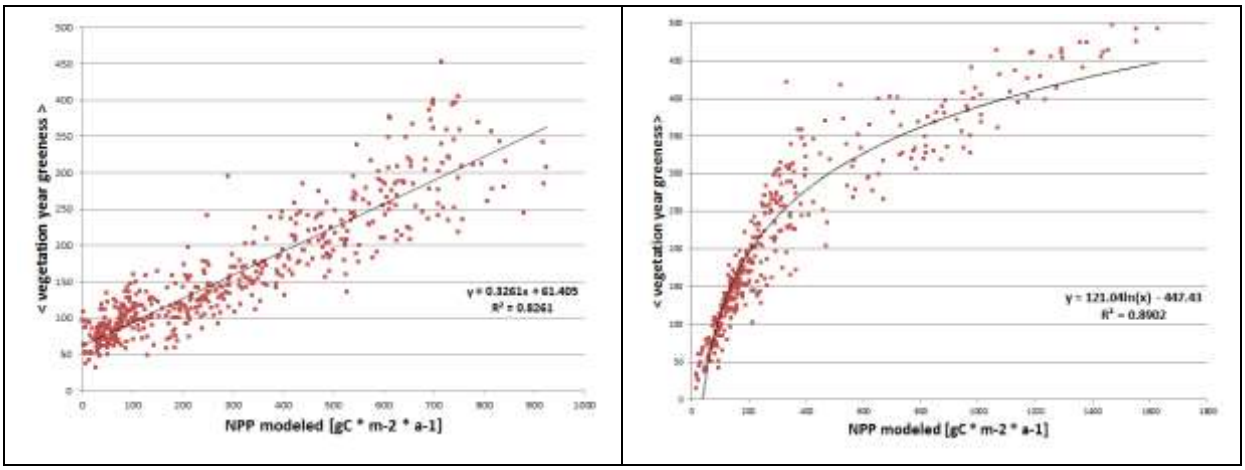

Figure 22: Scatterplot of vegetation year average fAPAR versus modelled NPP (vegetation year sum) in test site 04, Northern Kazakhstan (left) and site 12, Southern Africa (right)

The comparisons show (the reference letters refer to both figures):

- Especially in the dryer parts of the test areas, the pearson correlation coefficients between the vegetation year fAPAR and vegetation year NPP (a) is high to very high ($r > 0.8$) for the eight compared vegetation years 2003-2010.
- In densely vegetated areas the correlation becomes weaker and in some cases even inverse, as can be seen especially in the North of site 12, Southern Africa and to some degree in site 04, Northern Kazakhstan, as well.
- The modelled NPP values follow sharply the underlying land cover data. For instance the bare areas in the NPP map (b) correspond clearly to the bare areas in the GLC LC map (not shown). The fAPAR based maps seem to have more natural transitions to bare areas. Hence, the results of BETHY/DLR will vary among others with the LC data used.
- Regions with low NPP seem to be overestimated by fAPAR, and regions with high NPP underestimated (in Southern Africa), resulting in a logarithmic relationship between fAPAR derived NPP proxies and modelled NPP (b) and (c) in test site 12 (see Figure 22).
- Overall the mean, variability and trend patterns of NPP and RUE are in large parts comparable among the fAPAR based NPP proxies and the modelled NPP based indicators.
- Obvious discrepancies are mainly found in the northern part of Southern Africa, especially with regard to NPP trends and RUE status (Figure 23 (f) vs. (g) and (h) vs. (i)).
- The coefficients of variation (d) and (e) are absolutely in the same order of size and very similar in Northern Kazakhstan, but deviate substantially in the driest parts of Southern Africa.
- The RUE trend maps (j) and (k) fit relatively well in both sites.

We conclude that the fAPAR based NPP and RUE proxies fulfil their function as relative indicators of NPP (plus standing biomass with regard to the vegetation years and the dry season based indicators). However, care must be taken especially with regard to high productivity areas, which seem to be underestimated by the MERIS fAPAR data in test site 12, Southern Africa or overestimated by the NPP data. Areas with low and medium productivity may be overestimated with MERIS fAPAR on the other hand. Part of the discrepancies may also result from the LC data, which are used for the NPP modelling and their parameterization.

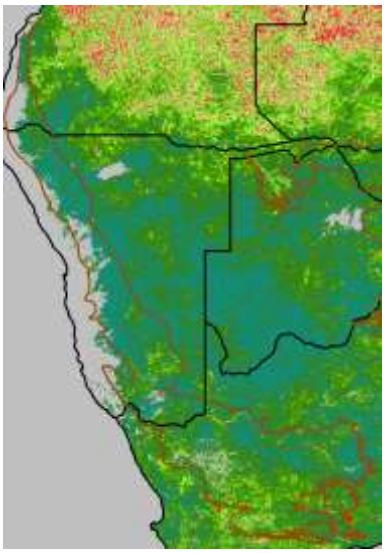

(a) Pearson r between MERIS based vegetation year fAPAR averages and BETHY/DLR vegetation year NPP sums 2003-2010

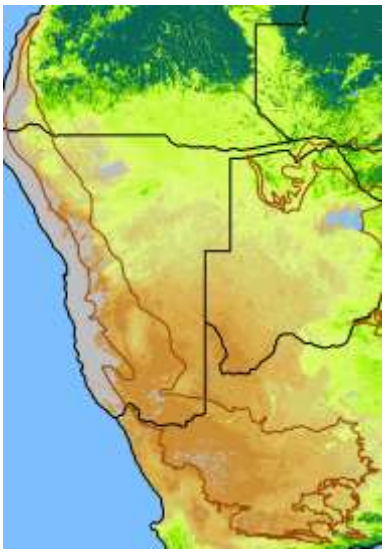

(b) BETHY/DLR average vegetation year sum NPP 2003-2010 [g C/m²]

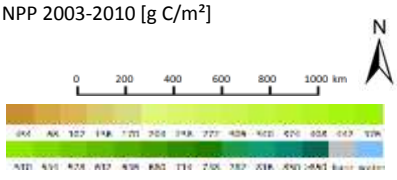

(c) MERIS based average vegetation year fAPAR 2003-2010 (fAPAR data multiplied by 1000)

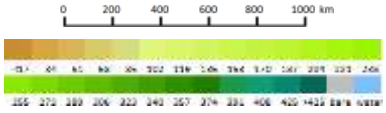

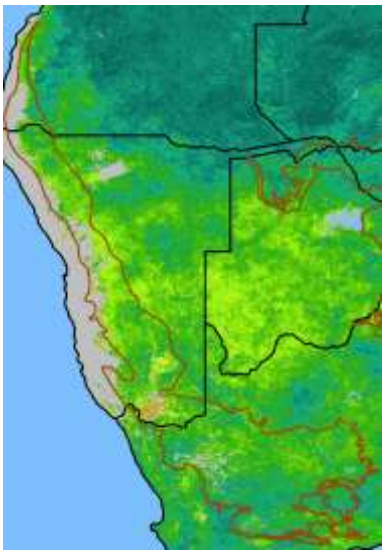

(d) Variation coefficient of BETHY/DLR vegetation year NPP sums 2003-2010 [%]

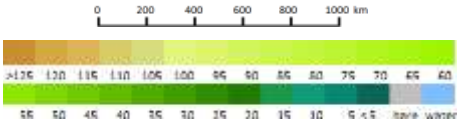

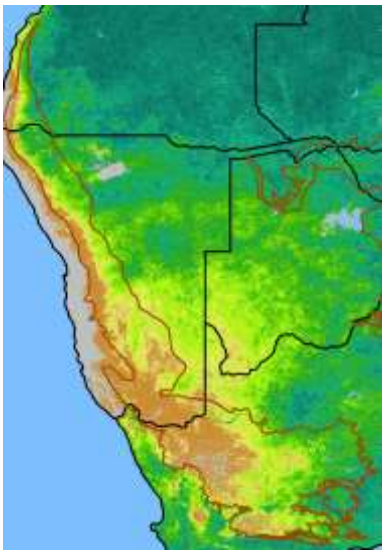

(e) Variation coefficient of MERIS fAPAR vegetation year averages 2003-2010 [%]

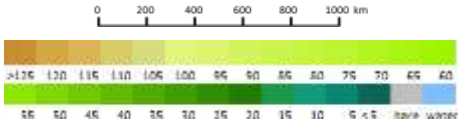

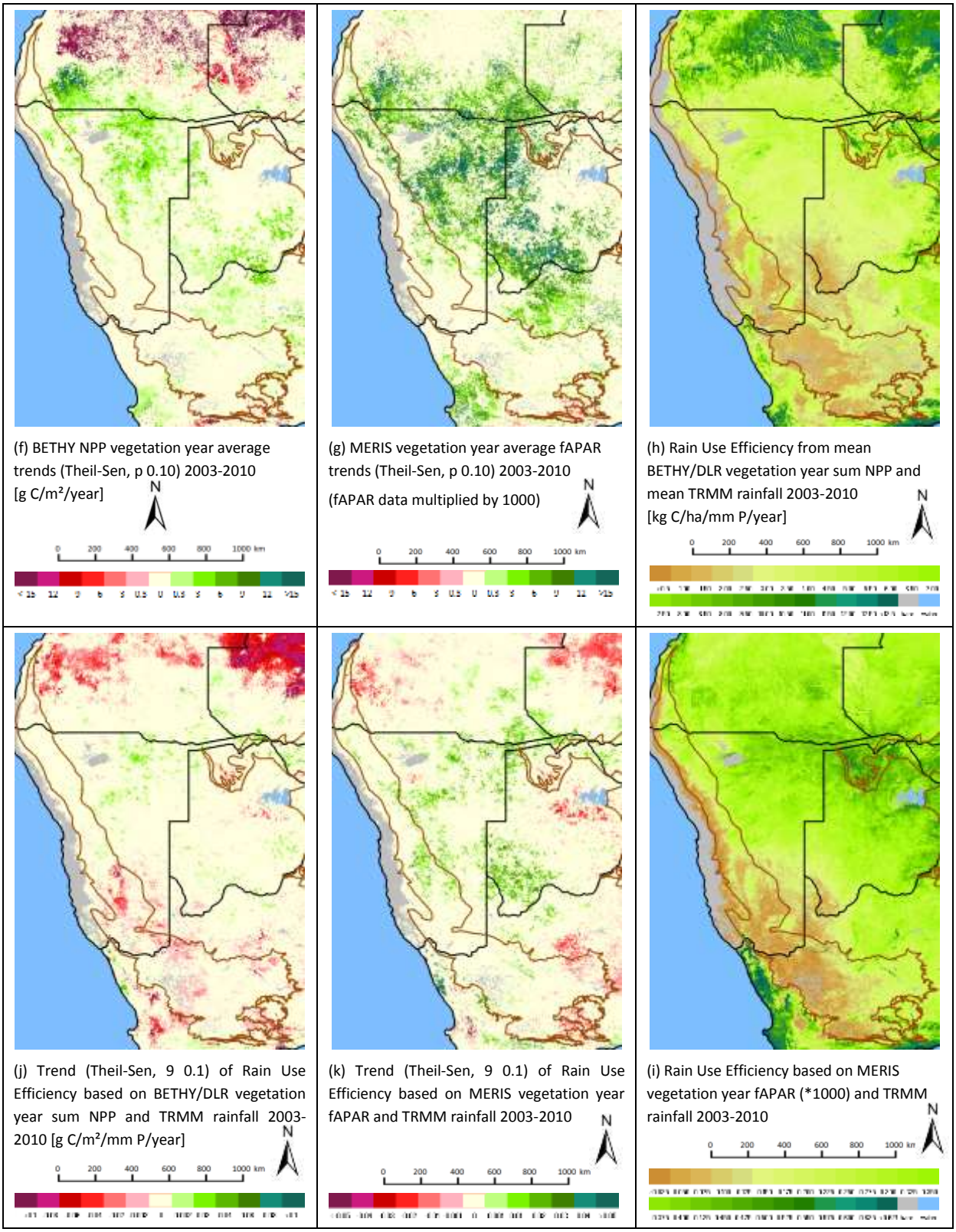

Figure 23: First order rainfall, soil moisture, fAPAR, RUE and SMUE products of site 12, Southern Africa West. The black lines show the country borders, the brown polygon represents the WWF ecoregion boundary of the actual study

3.5.4 First Order Status Indicators of Vegetation Productivity, Rainfall and Soil Moisture

This section provides examples of first order fAPAR status products, i.e., NPP proxies, and describes their relation to rainfall and soil moisture.

The three temporal integration periods of the first order products, i.e. vegetation year, vegetation season and dry season (Figure 3) provide quite different information contents and are not only indicators of the land productivity during these periods. They rather give hints to the functional composition of the vegetation, to land cover, and indirectly also to biodiversity, at least to the functional diversity of the vegetation.

Figure 24 provides an overview of first order status products for site 12, Southern Africa West.

It can be clearly seen that the rainfall (P25, upper left), ranging from virtually zero in the Namib desert along the Namibian coast to over 1000 mm in Angola controls the broad distribution of the vegetation productivity (P01, upper right).

However, apart from the overall pattern, the cyclic vegetation greenenss (P02, second row on the right) and the dry season greenness (P03, third row on the right) exhibit in several regions their own specific patterns. These are related to land cover/use and underlying environmental factors, and differentiate regions with a higher accentuation of seasonal green vegetation (dark (blue-)green areas in P02), and those with woody vegetation cover, such as in central Angola (P03). The much larger no data area (no vegetation signal in dry season, in gray tone) in P03 than in P01 or P02 is typical for P03 products in most test sites.

In this area, CCI Soil Moisture and TRMM rainfall exhibit quite a different average behaviour, but come closer in their spatial distribution of variability. The dark blue-green and green areas have a low variability (opposite colour coding to the quantity itself), the light green areas the highest. However, the variation coefficient of the TRMM rainfall is more than double of that of the soil moisture data and reaches values of up to 80% in the driest areas and frequently 40 to 50% in intermediate areas.

A large area with spring horizons directly south of the Etosha Pan (blue ellipse in P29, top row mid in Figure 24) with numerous surface water ponds exhibits significantly increased soil moisture compared to the surroundings. So this hot spot of faunal biodiversity can be related best or even only to the soil moisture data.

It cannot be concluded vice versa from hotspot in the soil moisture data that these relate to biodiversity hotspots; however along with further information, this data can help retrieve respective areas, if they are large enough to be seen in the soil moisture data with its 0.25° ground resolution.

In the bottom row (left and mid) of Figure 24, P08, Rain Use Efficiency (RUE) and Soil Moisture Use Efficiency (SMUE) of vegetation year average fAPAR 2003-2010, are shown. The different patterns of the underlying rainfall, soil moisture data and fAPAR data, respectively, (top row of Figure 24), obviously lead to quite different patterns of RUE and SMU, where SMUE quite closely resembles the fAPAR patterns (P01) as the soil moisture data variability is relatively low compared to that of rainfall.

Figure 25 presents the three phenology products (P57 – P59) already introduced in section 3.5.1, RUE products for the vegetation year fAPAR (P08), the cyclic vegetation fAPAR (P10) and the dry season fAPAR (P14), and a land degradation reference map from Klintenberg and Seely (2004).

The highest RUE values, in particular in P08 (RUE of mean vegetation year fAPAR) and P10 (RUE of cyclic vegetation) can be found in the South-West of test site 12 in areas with average yearly rainfall below 200mm, while a larger area with a regional maximum of RUE values can be seen in Northern Namibia and north-western Botswana, best developed in P10. There, according to the TRMM data the yearly mean precipitation is in the order of 500mm to 600mm. Further to the north with much higher rainfall and increasing vegetation productivity, RUE decreases. This means that the additional amount of rainfall is not proportionally used for vegetation growth, at least not when the NPP is estimated by EO and therefore limited to surface NPP and measurement from above. This behavior of RUE was already mentioned in 2.2.1, and cannot be interpreted in terms of potential degradation or improvement.

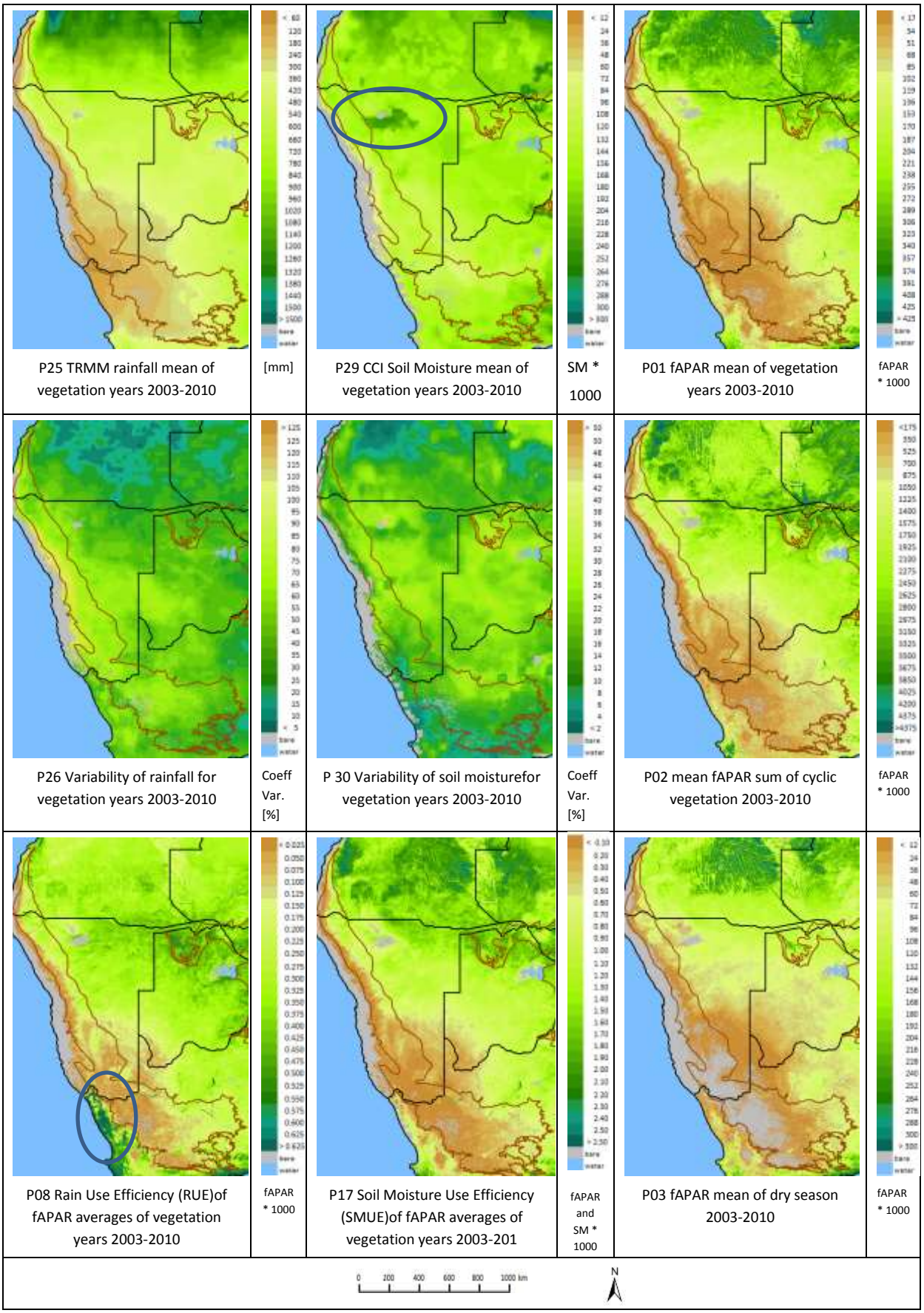

Figure 24: First order rainfall, soil moisture, fAPAR, RUE and SMUE products of site 12, Southern Africa West

Likewise, the general spatial decrease of RUE towards dryer conditions cannot be related to degradation, but may be an expression of the lower usability of the available rainwater due to factors such as higher evapotranspiration, more runoff due to higher rain fall intensity and soil crusting, etc. Nevertheless, spatial RUE patterns can highlight ecosystem conditions, which, when measured with vegetation productivity parameters alone, may not be visible to the same degree.

A very prominent example is the above stated RUE maximum along the coast in the south-west of study area 12: this area with extraordinary high average RUE (see blue ellipse in P08 in Figure 24) contains the Succulent Karoo biome in South Africa ("*The Succulent Karoo is notable for the world's richest flora of succulent plants, and harbours about one-third of the world's approximately 10,000 succulent species*" http://en.wikipedia.org/wiki/Succulent_Karoo). The same area is also characterised by a winter rain regime and an extended length of the green season (see P57 and P58 in Figure 25). Thus, again, phenological maps relate closely to ecosystem conditions and gradients and can help delineate and characterise ecoregions when used together with vegetation productivity parameters.

In the right centre of Figure 25, the land degradation (Klintenberg and Seely, 2004) shows strongly degraded areas in the north of Namibia. The authors developed an assessment scheme of land degradation for Namibia, which they based on the following factors:

- Population pressure
- Total grazing pressure
- Soil erosion
- Rainfall index

The usage of NDVI was considered but then excluded due to issues with bush encroachment. The highlighted area in the lower right map of Figure 25 (showing average RUE of the dry seasons) shows that part of this degraded area has a distinctly lower dry season RUE (not to confuse with the Etosha Pan, which is largely bare area). When comparing the area in the purple ellipse with the RUE maps from the vegetation year and the dry season, it can be seen that the dry season RUE most clearly shows the degradation, while vegetation growth in the rainy period or during the entire vegetation year partially masks the land degradation in this area. However, also the very dry land towards the Namib desert to the west exhibits generally low RUE values, which means that the climatic dependency of RUE (among other factors influencing RUE) must be taken into account when using it for mapping degraded land with diminished vegetation cover (Del Barrio et al. 2010).

Efficiency parameters such as RUE must be used with extra care, and without establishing generic quantitative relations between RUE (or SMUE) and ecosystem characteristics. High RUE values are not only exhibited by certain biodiversity hotspots, but are also seen in intense agricultural land use. An example is highlighted in P10 with a red ellipse (bottom centre of Figure 25). This area contains crop lands with high NPP and RUE, which is also characterised by a shorter duration of the vegetation period (P58 in the centre left of Figure 25), and the often found light blue-green class in P50 (centre right of Figure 25). As demonstrated in section 3.5.5, areas with intense crop cultivation typically exhibit these characteristics, with light tones (high percentage of cyclic vegetation of total) and high and very high productivity classes.

In general, it can be stated that the presented parameters cannot serve as standalone diagnostic features for ecosystem and biodiversity assessments, but should be evaluated in the local/regional context, in combination with each other, and along with reference and in situ information. The presented EO based products can nevertheless give hints and show possible hotspots of biodiversity and land use intensity, as well as ecologically functional classes. The latter are presented in the next section.

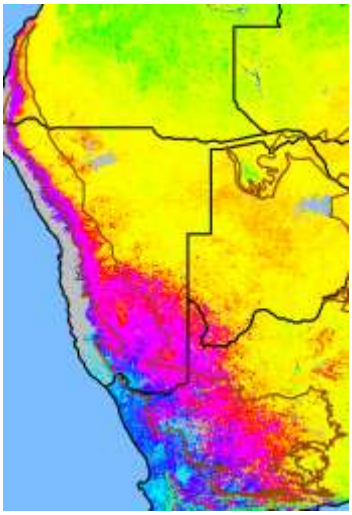

P57 Median start of vegetation year 2003-2010

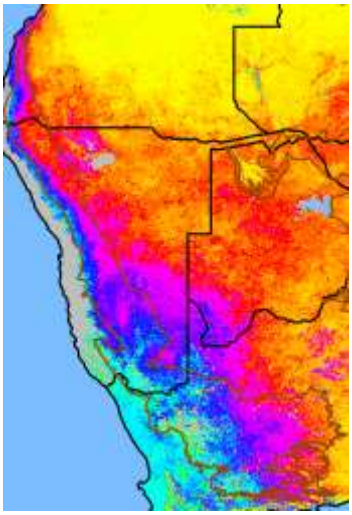

P59 Mean start of vegetation season 2003-2010

Legend for P57 and P59

(the numbers 1 or 2 refer to the first and second half of each month)

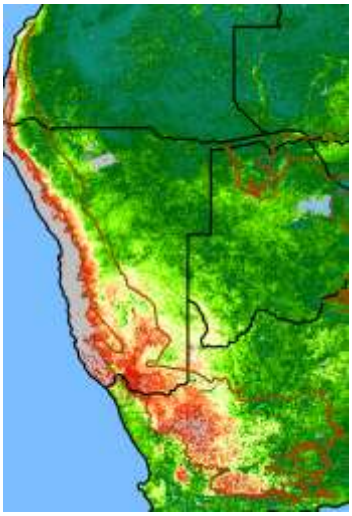

P58 Mean length of vegetation season 2003-2010

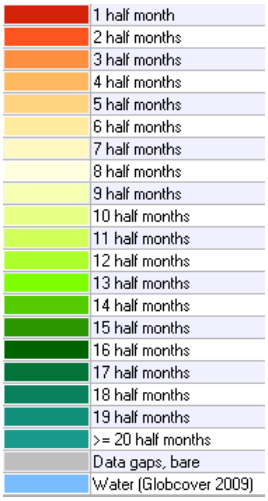

Legend for P58

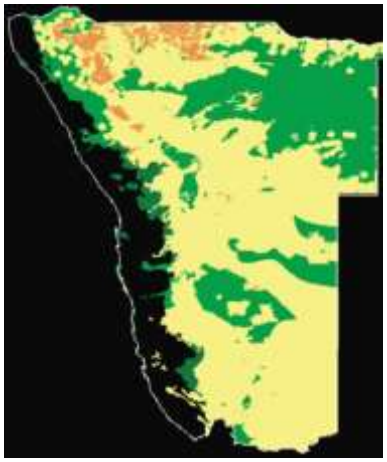

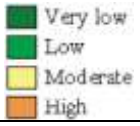

Degredation map of Namibia (from Klintenberg and Seely, 2004)

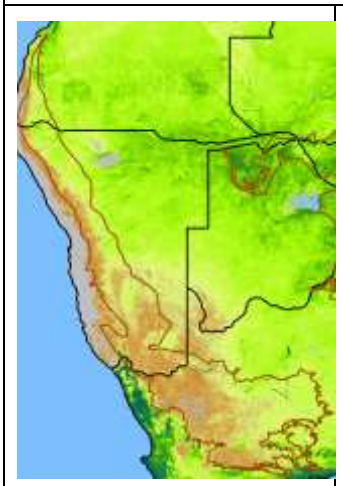

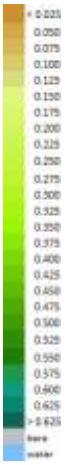

P08 Rain Use Efficiency (RUE) of fAPAR averages of vegetation years 2003-2010

fAPAR * 1000

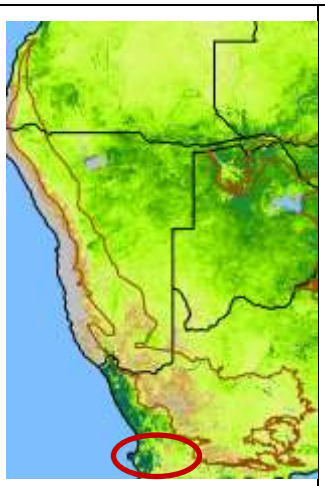

P10 Rain Use Efficiency (RUE) of fAPAR averages of cyclic vegetation 2003-2010

fAPAR * 1000

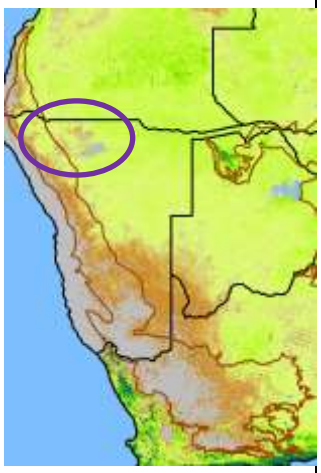

P14 Rain Use Efficiency (RUE) of fAPAR averages of dry seasons 2003-2010

fAPAR * 1000

Figure 25: Phenology products, Functional classes, and RUE products of test site 12, Southern Africa West

3.5.5 Functional classes and Land Cover

Product P50 is a second order product, which combines vegetation productivity classes with the percentage of the cyclic vegetation of the yearly vegetation, where the latter is represented by the sum of the fAPAR values of the vegetation years. The product legend and contents are described in Figure 26.

<table>
<tr><td colspan="3">Legend of P50, Functional Classes
AOI Southern Africa West, Site 12
Country borders
District borders
productivity 1, rel. cyclic fraction 1
productivity 1, rel. cyclic fraction 2
productivity 1, rel. cyclic fraction 3
productivity 1, rel. cyclic fraction 4
productivity 1, rel. cyclic fraction 5
productivity 2, rel. cyclic fraction 1
productivity 2, rel. cyclic fraction 2
productivity 2, rel. cyclic fraction 3
productivity 2, rel. cyclic fraction 4
productivity 2, rel. cyclic fraction 5
productivity 3, rel. cyclic fraction 1
productivity 3, rel. cyclic fraction 2
productivity 3, rel. cyclic fraction 3
productivity 3, rel. cyclic fraction 4
productivity 3, rel. cyclic fraction 5
productivity 4, rel. cyclic fraction 1
productivity 4, rel. cyclic fraction 2
productivity 4, rel. cyclic fraction 3
productivity 4, rel. cyclic fraction 4
productivity 4, rel. cyclic fraction 5
productivity 5, rel. cyclic fraction 1
productivity 5, rel. cyclic fraction 2
productivity 5, rel. cyclic fraction 3
productivity 5, rel. cyclic fraction 4
productivity 5, rel. cyclic fraction 5
sparse vegetation
data gaps (clouds, water, bare)
Water (Globcover 2009)</td><td>Land cover / use classes</td><td>Productivity class</td><td>Percentage of cyclic vegetation</td></tr>
<tr><td rowspan="5">50 Functional classes
The functional classes originate from a combined classification of vegetation productivity and the percentage of cyclic vegetation of the yearly vegetation. The numbers in the legend increase with increasing values of these parameters. The lighter the tone, the higher is the percentage of the cyclic vegetation and the lower the share of evergreen vegetation.
The functional classes cannot be unambiguously assigned to distinct LC classes, but their patterns are related to LC classes. In the table to the right some general class relationsships of LC and functional classes are contained.</td><td>Intensely cultivated cropland, especially irrigated or post-flooding crops</td><td>(3)4 - 5</td><td>4 - 5</td></tr>
<tr><td>Rainfed cropland</td><td>1 – 3(4)</td><td>4 - 5</td></tr>
<tr><td>Grassland depending on the presence of shrubs and trees</td><td>1 - 2</td><td>3 - 5</td></tr>
<tr><td>Shrubland, depending on the share of perennially green parts</td><td>(1)2 - 3</td><td>1 - 3</td></tr>
<tr><td>Sparse vegetation (with hardly any perennially green parts)</td><td>1</td><td>4-5</td></tr>
<tr><td></td><td>Deciduous forest</td><td>4 -5</td><td>3 - 5</td></tr>
<tr><td></td><td>Evergreen forest</td><td>4 - 5</td><td>1 - 2</td></tr>
<tr><td></td><td>Urban areas in general occur in various classes, and can mostly not be well distinguished from their surroundings</td><td>1 - 2</td><td>1 - 3</td></tr>
</table>

Figure 26: Legend and class description of product P50: Functional Classes

P50 cannot be directly used to map land cover / land use, as there is no definite relation between the two (see Figure 26), but it seems that the functional class units are closely related to land cover / land use units and to underlying land capability factors, which control or influence vegetation productivity and composition.

In Figure 27 we contrast the Functional Classes of P50 with CCI (2010) land cover classes in test site 22, Eastern Mediterranean Countries (see Figure 18 for phenology products of this region).

A very prominent figure in northern Turkey is the pink coloured ribbon along the southern coast of the Black Sea in P50 (Figure 27), which is largely composed of deciduous forests with high productivity, whereas in the Nile delta in Egypt the same functional classes are related to intense post-flooding crop cultivation. A differentiation of the two would be possible by using further indices, e.g., P59, Mean start of vegetation season 2003-2010, however LC mapping is not task of Diversity II.

When comparing CCI LC and P50 in the two upper maps of Figure 27, a quite close correspondence between the patterns of the major classes can be seen: e.g.., “cropland, irrigated or post flooding” of CCI LC come out in light green to bluish tones in P50, signalling medium to rather high productivity areas without or small parts of perennial green vegetation. Vice versa, the dark bluish tones in P50 often correspond to evergreen tree cover in CCI LC, while classes with shrubs and trees in CCI LC largely relate to the dark green and dark olive green

areas in P50. In contrast to CCI LC, Diversity II P50 reflects a higher share of perennially active vegetation (or standing green biomass), where CCI LC often shows rainfed agriculture and herbaceous vegetation instead. This may be related to scattered or aligned trees and bushes spread in the landscape, or newly planted trees, which do not change the overall LC class at 300m resolution, but do have an influence on the fAPAR signals. Possibly, the herbaceous vegetation (grasses, herbs) itself does not totally dry off over an extended period on the average, and/or the fAPAR values do not go totally to zero for dried off herbaceous vegetation.

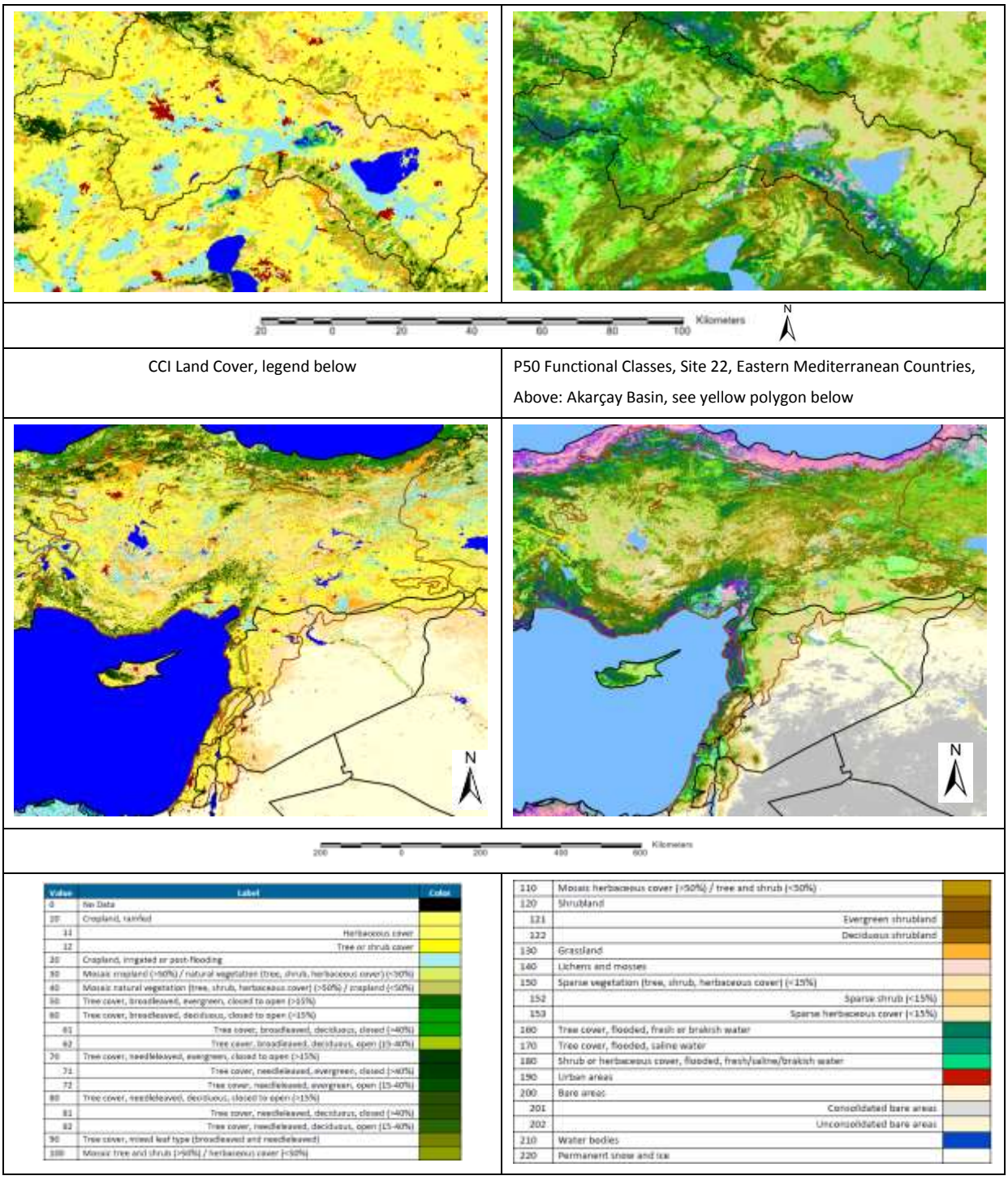

Value	Label	Color
0	No Data	
10	Cropland, rainfed	
11	Herbaceous cover	
12	Tree or shrub cover	
20	Cropland, irrigated or post-flooding	
30	Mosaic cropland (>50%) / natural vegetation (tree, shrub, herbaceous cover) (<50%)	
40	Mosaic natural vegetation (tree, shrub, herbaceous cover) (>50%) / cropland (<50%)	
50	Tree cover, broadleaved, evergreen, closed to open (>15%)	
60	Tree cover, broadleaved, deciduous, closed to open (>15%)	
61	Tree cover, broadleaved, deciduous, closed (>40%)	
62	Tree cover, broadleaved, deciduous, open (15-40%)	
70	Tree cover, needleleaved, evergreen, closed to open (>15%)	
71	Tree cover, needleleaved, evergreen, closed (>40%)	
72	Tree cover, needleleaved, evergreen, open (15-40%)	
80	Tree cover, needleleaved, deciduous, closed to open (>15%)	
81	Tree cover, needleleaved, deciduous, closed (>40%)	
82	Tree cover, needleleaved, deciduous, open (15-40%)	
90	Tree cover, mixed leaf type (broadleaved and needleleaved)	
100	Mosaic tree and shrub (>50%) / herbaceous cover (<50%)	

110	Mosaic herbaceous cover (>50%) / tree and shrub (<50%)	
120	Shrubland	
121	Evergreen shrubland	
122	Deciduous shrubland	
130	Grassland	
140	Lichens and mosses	
150	Sparse vegetation (tree, shrub, herbaceous cover) (<15%)	
152	Sparse shrub (<15%)	
153	Sparse herbaceous cover (<15%)	
160	Tree cover, flooded, fresh or brakish water	
170	Tree cover, flooded, saline water	
180	Shrub or herbaceous cover, flooded, fresh/saline/brakish water	
190	Urban areas	
200	Bare areas	
201	Consolidated bare areas	
202	Unconsolidated bare areas	
210	Water bodies	
220	Permanent snow and ice	

Figure 27: CCI LC and Diversity II P50 functional classes, test site 22, Eastern Med. Countries. Below: CCI LC legend

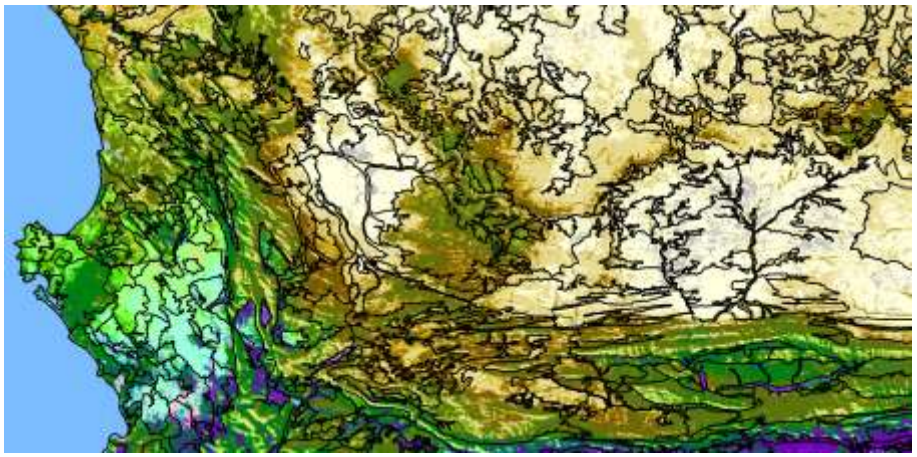

P50 Functional Classes

The overlaid polygons are the boundaries of the SOTER – Soil and Terrain data[8]

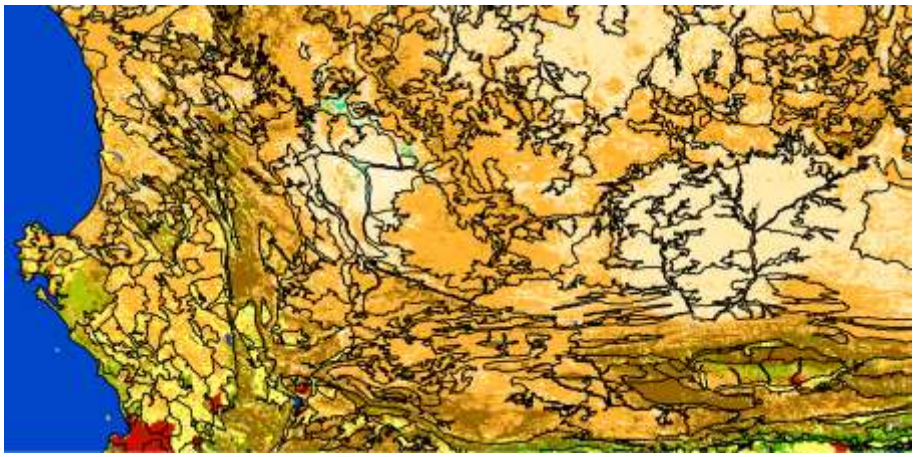

CCI Land Cover 2010,

For legend see Figure 27

The area is mainly composed of grasslands (orange) and shrublands (brown), sparse vegetation (light pink) and some tree cover (green)

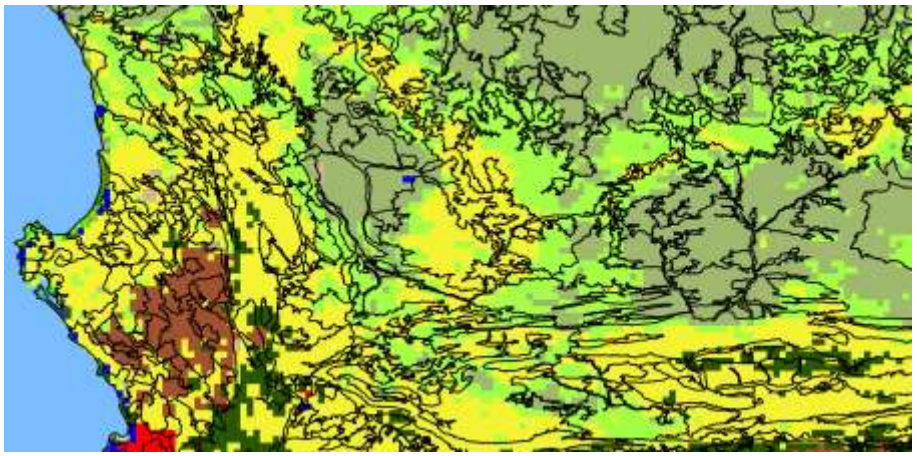

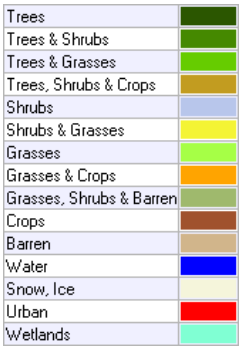

Lifeforms[9] derived from GLC 2000 Land Cover[10]

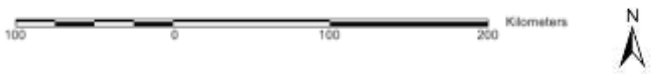

Figure 28: P50, CCI LC and GLC 2000 – derived lifeforms overlaid with SOTER data, test site 12, South Africa West

[8] http://www.isric.org/projects/soil-and-terrain-database-soter-programme

[9] For GLC class aggregation into lifeforms See ESA DUE project "Diversity 2010" http://due.esrin.esa.int/page_project117.php

[10] http://bioval.jrc.ec.europa.eu/products/glc2000/glc2000.php

Figure 28 shows Diversity II P50, Functional Classes, CCI LC data, and GLC 2000 LC data overlaid with SOTER - Soil and Terrain Database (SOTER) data[8]. Quite often, the SOTER data match the boundaries of the Functional Classes and those of CCI LC classes and the GLC lifeform classes, confirming the dependencies of vegetation functional types or LC lasses on underlying soil and terrain conditions mapped in the SOTER data. The CCI LC map shows largely grassland and shrublands, only little croplands in this area. The GLC-derived lifeforms map contains a large cropland area corresponding to the light cyan to green classes of P50 typical for intense cropland, and also the classes Grassland, shrubs & grasses, and Grasses, shrubs &barren can be largely related to the patterns of P50. The GLC lifeforms reflect more strongly the presence of shrubs (with green vegetation signals during the dry season according to the functional classes) than the CCI LC data. Therefore, in this example they correspond more closely to the functional classes with their relatively high greenness values during the dry season. However, it is not known to which degree the dry season values of the fAPAR values are influenced by dried off vegetation and soil reflectance. However, as demonstrated in chapter 4, section 4.4.6, the MERIS based fAPAR should be clearly less influenced by soil reflectance than the NDVI.

The functional classes of P50 may be regarded as valuable additional information to LC data, with classes more directly related to the land properties.

3.5.6 First and second order trend products: fAPAR, rainfall, and seasonal trend/change relation

Trend products are the second major product group of Diversity II. For all first order status products, except variability and the phenology products, trends were derived, supplemented with epochal (two four-year periods) change products for rainfall and soil moisture. In addition, second order trend products have been generated, comprised of combinations of first order trend products.

Even though the observed period is rather short, as it contains only eight yearly observations for each parameter, trends do occur and can be derived with appropriate care. The median-based Theil-Sen trend estimator was applied (Theil 1950, Sen 1968), which is known to be more robust against outliers and therefore more suitable for shorter time series than the commonly applied ordinary least square trend analysis. The trend significance was determined with Mann-Kendall's method (Mann 1945, Kendall 1962). The chosen significance threshold was 0.9 (see also chapter 4, section 4.4.2).

Figure 30 provides an overview about the fAPAR trends for vegetation year fAPAR average (P33), cyclic fraction (P34), and dry season fAPAR average (P35), and contrasts these trends against TRMM rainfall and soil moisture trends as well as epochal changes of rainfall. In addition, rainfall and rainfall variability are shown. The example chosen is test site 2, Southern Australia.

Comparing rainfall trends to vegetation productivity trends shows strong commonalities. The trend patterns of rainfall (P42) and especially the trend of vegetation year average fAPAR (P33) are extremely similar. A "hotspot" of rainfall increase highlighted in P42 (Figure 30) however, is not matched by significant vegetation trends (P33), nor by soil moisture trends (P48). A check of the single year fAPAR and rainfall means however exhibits highly variable vegetation productivity values with positive extremes for vegetation year 2010, when also the rainfall reached its maximum. Exemplary scatterplots are shown below in Figure 29 for a point within the highlighted rainfall trend hotspot. The rather steady and extreme rainfall increase during the observation period is remarkable and would be interesting to be checked with reference station rainfall data[11].

The epochal changes of rainfall and soil moisture show also similar patterns. Where significant rainfall and especially soil moisture trends are missing, the epochal changes show in most cases commonalities with vegetation productivity trends. This confirms that vegetation responses to changes and trends in the rainfall regimes do not only occur on a year by year basis.

[11] Some rainfall values taken from the Australian test site 20 have been compared to station data with positive results reported in the ATBD of Diversity II

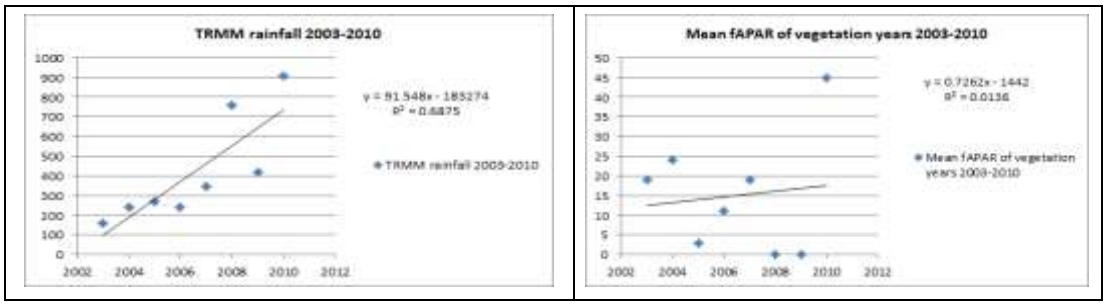

Figure 29: TRMM rainfall trend (aggregated values for vegetation year) versus vegetation year fAPAR at location X, Y: 137.445173, 23.3268028 [dd – decimal degrees]

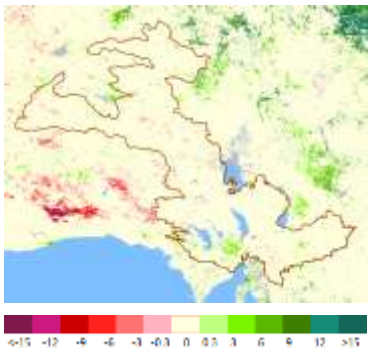

P33: Trend slope of vegetation year mean fAPAR (* 1000) 2003-2010

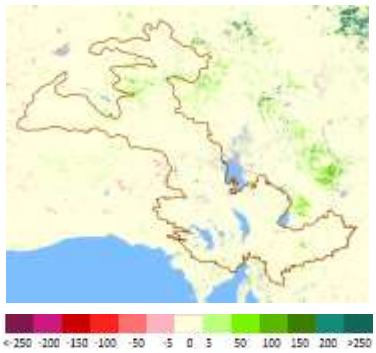

P34: Trend slope of cyclic fraction fAPAR sum (* 1000) 2003-2010

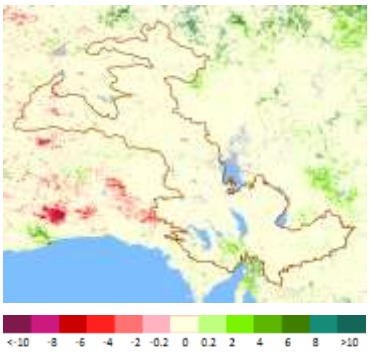

P35: Trend slope of dry season mean fAPAR (* 1000) 2003-2010

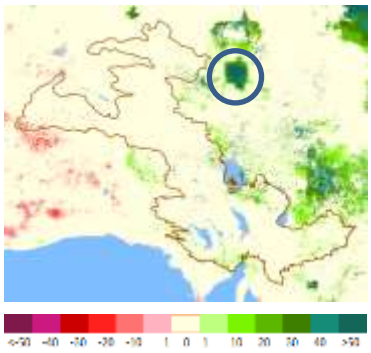

P42: Trend slope of TRMM rainfall aggregated to fAPAR vegetation years [mm]

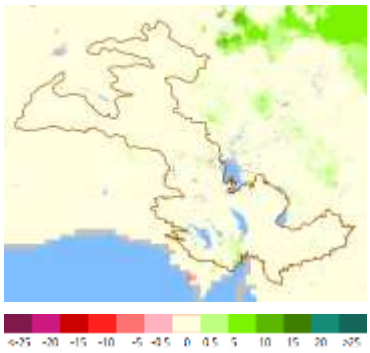

P44: Trend slope of soil moisture [* 1000] aggregated to fAPAR vegetation years

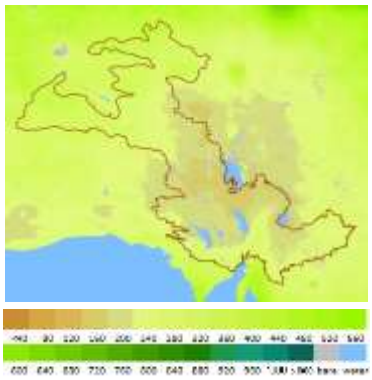

P25: TRMM precipitation average of vegetation years 2003-2010 [mm]

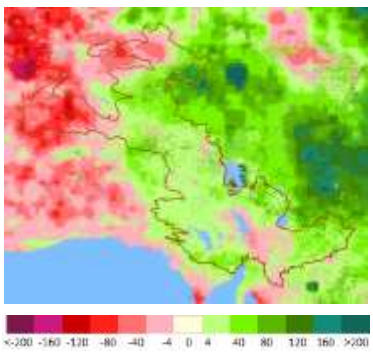

P46: Epochal differences of TRMM rainfall between the two epochs 2003-2006 and 2007-2010 [mm]

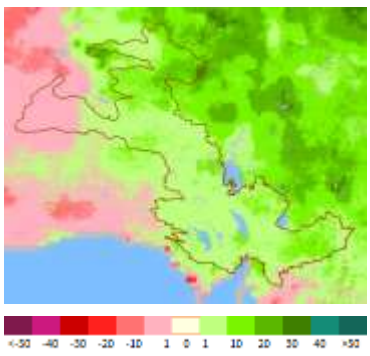

P48: Epochal differences of soil moisture (*1000) between the two epochs 2003-2006 and 2007-2010

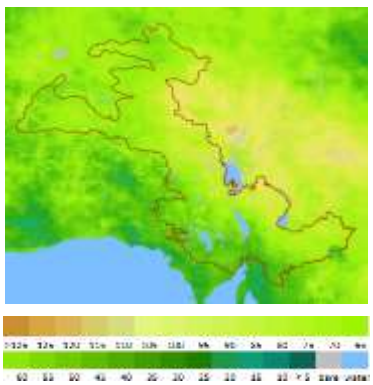

P26: TRMM precipitation coeff. of variation of vegetation years 2003-2010 [%]

Figure 30: fAPAR and rainfall trends, rainfall epochal change, and rainfall status products, site 20, Southern Australia

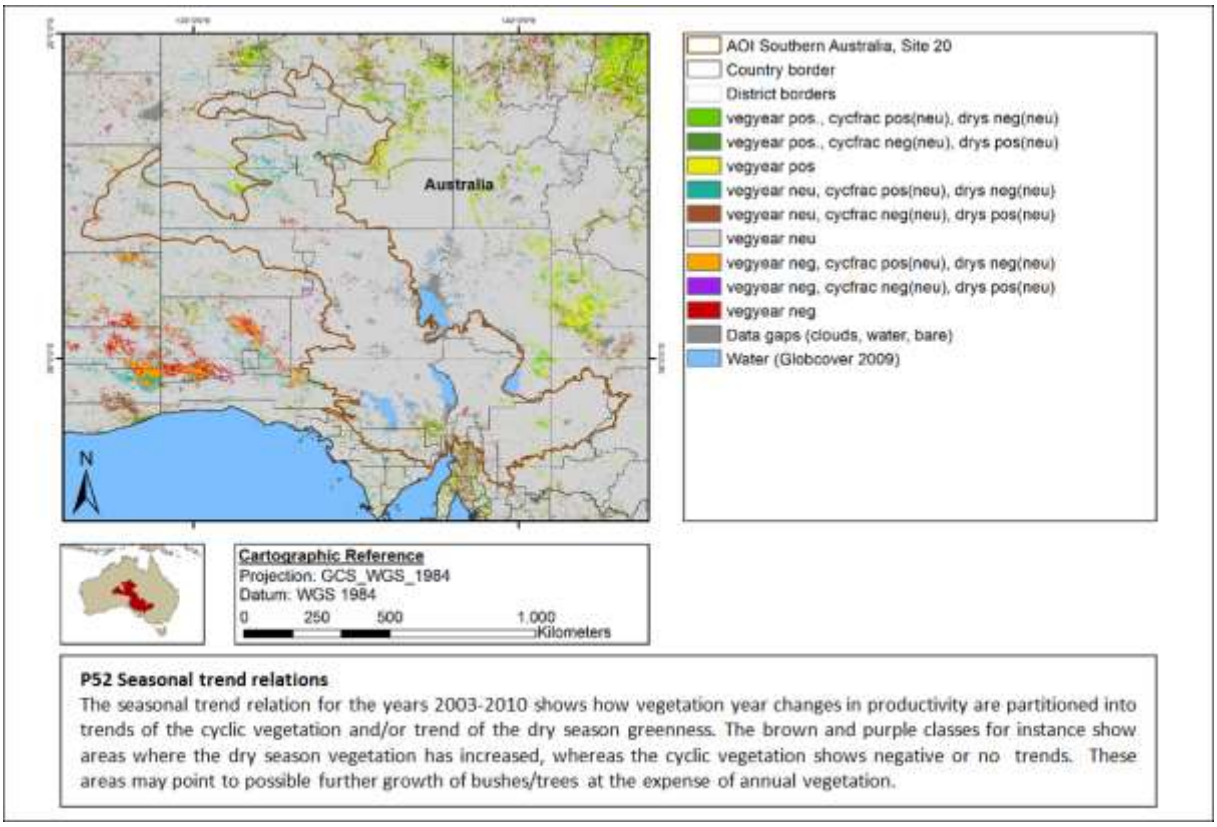

Figure 31: P52 Seasonal trend relations of site 20, Southern Australia

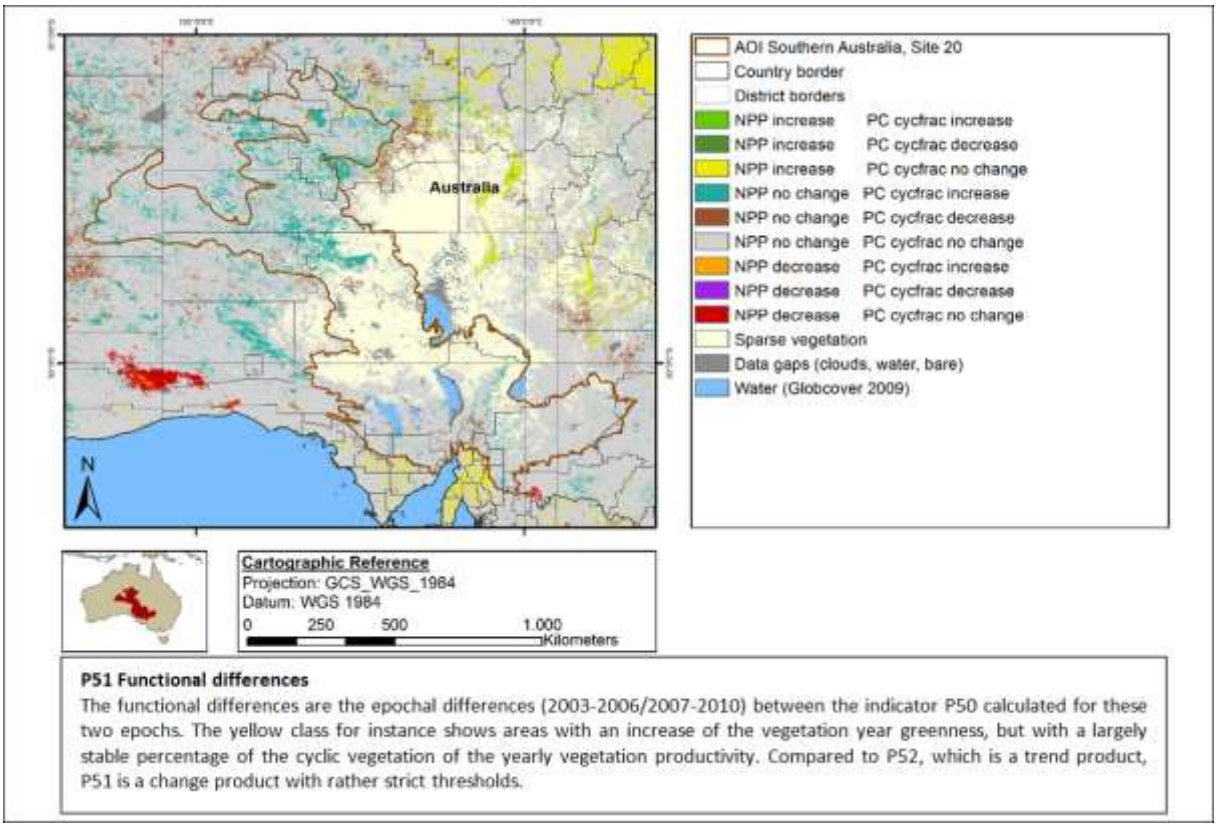

Figure 32: P51 Functional differences of site 20, Southern Australia

The fAPAR trend of the entire vegetation year (P33) resembles more closely the trend of the dry season fAPAR than the trend of the cyclic vegetation in the Southern Australian test site (Figure 30). This seasonal trend differentiation varies from site to site and within the test sites and was defined as a second order product: P52, Seasonal trend relations, shown in Figure 31. This product shows the relationship between the vegetation year fAPAR trends and those of the vegetation season (cyclic fraction), or of the dry season fAPAR, respectively. The orange class "vegyear neg, cycfrac pos(neu), drys neg(neu)" for instance means that the vegetation year fAPAR exhibits a negative trend, which is mainly determined by negative dry season trend. The purple class "vegyear neg, cycfrac neg(neu), drys pos(neu)" has the opposite meaning, here an overall negative vegetation year fAPAR trend is mainly composed of a negative cyclic vegetation trend. Classes without seasonal trend specification in Figure 31, i.e. "vegyear pos" or vegyear neg" do not show seasonal trend concentrations.

Figure 32 shows a second order epochal change product that also relates to the seasonal relation of – in this case – fAPAR changes. This product was directly derived from epochal versions of P50, Functional Classes, and applying strict change thresholds in order to not include changes between adjacent productivity or percent of cyclic vegetation classes. Diversity II product P50, Functional Classes, has been described and interpreted in 3.5.5.

The change product highlights areas with a possible shift of the seasonal vegetation and relates this to the overall epochal vegetation productivity change/no change. The widespread cyan class "NPP no change PC cycfrac increase" in the western part of this Australian test site and especially in the north of the AOI, for instance, contains areas where no substantial overall change of the vegetation year fAPAR was observed, but an increase of the cyclic vegetation, absolute and relative to the yearly fAPAR. However, as seen in P52 (Figure 31), this change class is only to a limited degree matched by corresponding seasonal trend relations.

The trend/change relation products may deliver useful information to the composition of the observed changes and thus potentially to functional biodiversity changes. For instance the widespread phenomenon of bush encroachment (often attributed to overgrazing) may be expected to lead to a relative and/or absolute increase of the dry season fAPAR, depending on the degree of perennial greenness of the bush vegetation, while other vegetation degradation processes and/or other degradation stages may lead to negative responses of the cyclic vegetation only.

3.5.7 First order and second order trend products: RUE, SMUE and second order trend relation products integrating fAPAR and rainfall trends

As already addressed in section 2.2.1, RUE or SMUE indicators need to be generated and interpreted with care. RUE/SMUE trend indicators are provided by Diversity II, but they may actually not fulfill their original purpose of separating man-made changes from rainfall controlled variability of primary productivity. RUE trends are in large parts of the areas correlated with rainfall (both positively and negatively), and thus partly reflect rainfall changes/trends rather than normalizing for rainfall variability (see also Fensholt et al. 2013). The latter would be the prerequisite for RUE trends to indicate human induced land degradation or improvements.

In addition, land use changes, which at least at local scales occur rather abrupt, can hardly be retrieved with RUE trends. Also the RESTREND method (see for instance Wessels 2012), which interprets trends of regression residuals of rainfall and vegetation as human induced vegetation trends (productivity trends that are not explained by rainfall trends), relies on the assumption that rainfall and vegetation productivity are linearly related. While this may hold for shorter periods and certain ecosystems, vegetation has been found to exhibit different correlations with rainfall (at a given location) depending on the type and status of ecosystems and the duration of the observation (Ratzmann 2014).

These findings have led to the development of a group of second order indicators called "Direct relation between Rainfall and Vegetation Productivity", assumed to be a largely assumption-free indicator that directly relates rainfall and vegetation productivity trends to each other. "Largely assumption-free" means that they also must be interpreted with care, as an increase of rainfall amount may not necessarily lead to an increase of vegetation growth at the same place or time. For instance, increased rainfalls may come with higher intensities,

possibly leading to spatial/temporal shifts of the effects via geomorphological and hydrological transportation and transition processes.

Figure 33 displays the above mentioned products for test site 14, Patagonian Steppe in southern Argentina (upper row). TRMM rainfall trends are shown in the lower left for comparison. Notable here is that in particular within the study AOI there are widespread vegetation year fAPAR trends, partly without corresponding rainfall trends, even though the trends of the cyclic vegetation and the dry season are less pronounced. P37, RUE trends of the cyclic vegetation, is shown in the lower centre. The RUE trends partly resemble P54, but exhibit as expected significantly less trends, whereas P54 (and P53 and P55 accordingly) show all vegetation trends, no matter if they are RUE trends or not.

Even though many fAPAR trends seem to be related to rainfall trends, this nevertheless does not mean that all these trend areas, where trends can be explained by rainfall, are safe and stable. Desertification processes may be enhanced by natural fluctuations, and where negative vegetation productivity trends can be observed, there may always be the chance that processes start to get their own dynamics, or that human livelihoods are at risk. Therefore we tried to overcome the restriction to RUE, by showing all vegetation trends in these products along with the potentially related rainfall trends.

In order to provide an overview about the major trends in several testsites, P54: TRMM rainfall versus MERIS fAPAR cyclic fraction greenness trends, and P55: TRMM rainfall versus MERIS fAPAR dry season trends are presented in Figure 34 and Figure 35. The legend to these products can be seen in Figure 33. The general rule for the colour scheme of these products is that the stronger the mismatch between rainfall and fAPAR trend, respectively, the darker either the reddish tone for rainfall/fAPAR decreases or the green tone for increases. The lightest pink or green, respectively show areas without fAPAR trends even though the rainfall data show trends. The light green areas may be interpreted as resilient areas, which did not decrease in productivity in spite of rainfall decreases. The light pink regions, vice versa, may contain areas with missing response to increasing water availability.

P53: TRMM rainfall versus MERIS fAPAR vegetation year greenness trends 2003-2010 (see legend at lower right)

P54: TRMM rainfall versus MERIS fAPAR cyclic fraction greenness trends 2003 - 2010 (see legend at lower right)

P55: TRMM rainfall versus MERIS fAPAR dry season greenness trends 2003 – 2010 (see legend below)

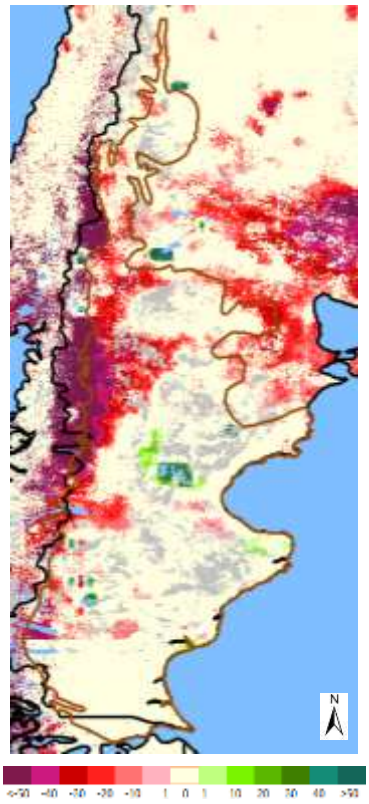

P42: Trend slope of TRMM rainfall aggregated to fAPAR vegetation years [mm]

P37: Rain Use Efficiency trend slopes of cyclic vegetation 2003-2010 (fAPAR * 1000)

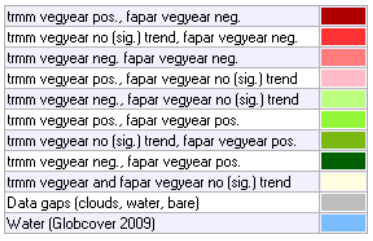

Legend of **P53**

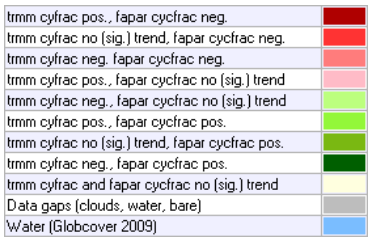

Legend of **P54**

Legend of **P55**

Figure 33: Relation between seasonal vegetation productivity and rainfall, site 14, Patagonian

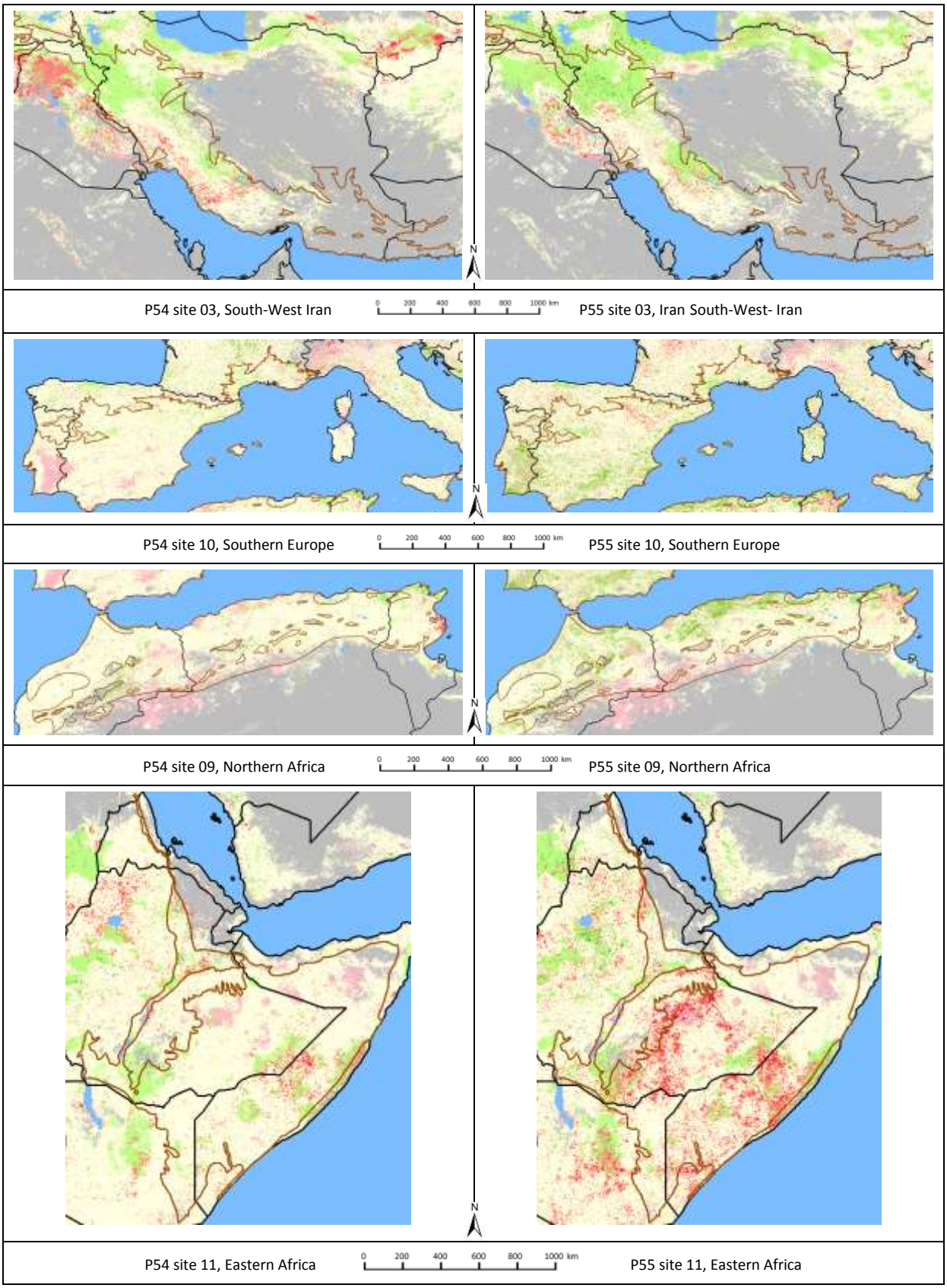

Figure 34: Rainfall versus vegetation productivity trends of the cyclic vegetation (P54) and the dry season fAPAR (P55), site 03, 10, 09, and 11. The legend of these products is shown in Figure 33

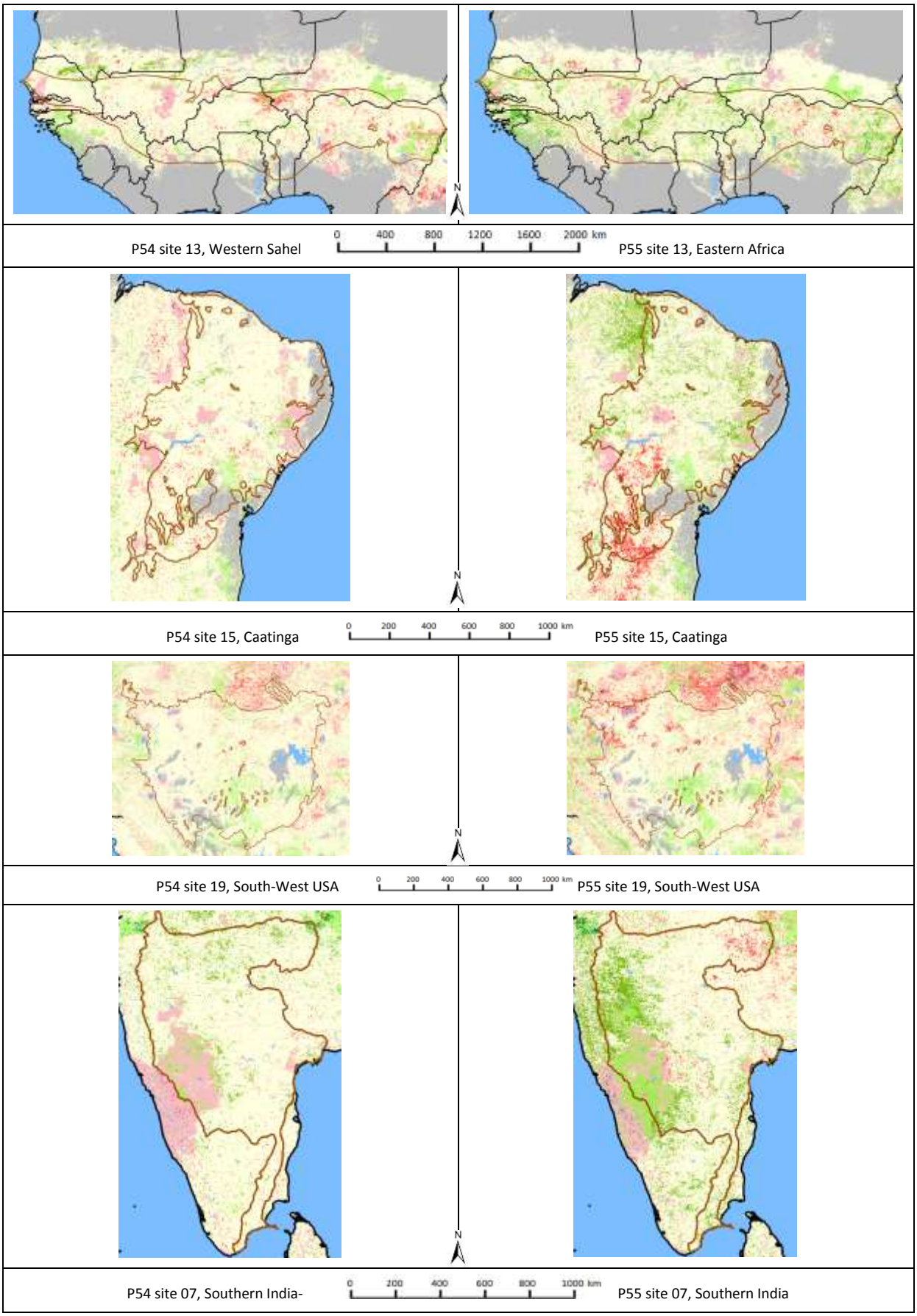

Figure 35: Rainfall versus vegetation productivity trends of the cyclic vegetation (P54) and the dry season fAPAR (P55), site 13, 15, 19 and 07. The legend of these products is shown in Figure 33.

3.5.8 GIMMS NDVI based second order products

NOAA GIMMS NDVI data start 20 years before the MERIS observation period and were combined with GPCP rainfall data of the same period (1982-2002) in product P56: GPCP Rainfall versus GIMMS NDVI vegetation year greenness trend. An example is shown in Figure 36 for test site 13, Western Sahel.

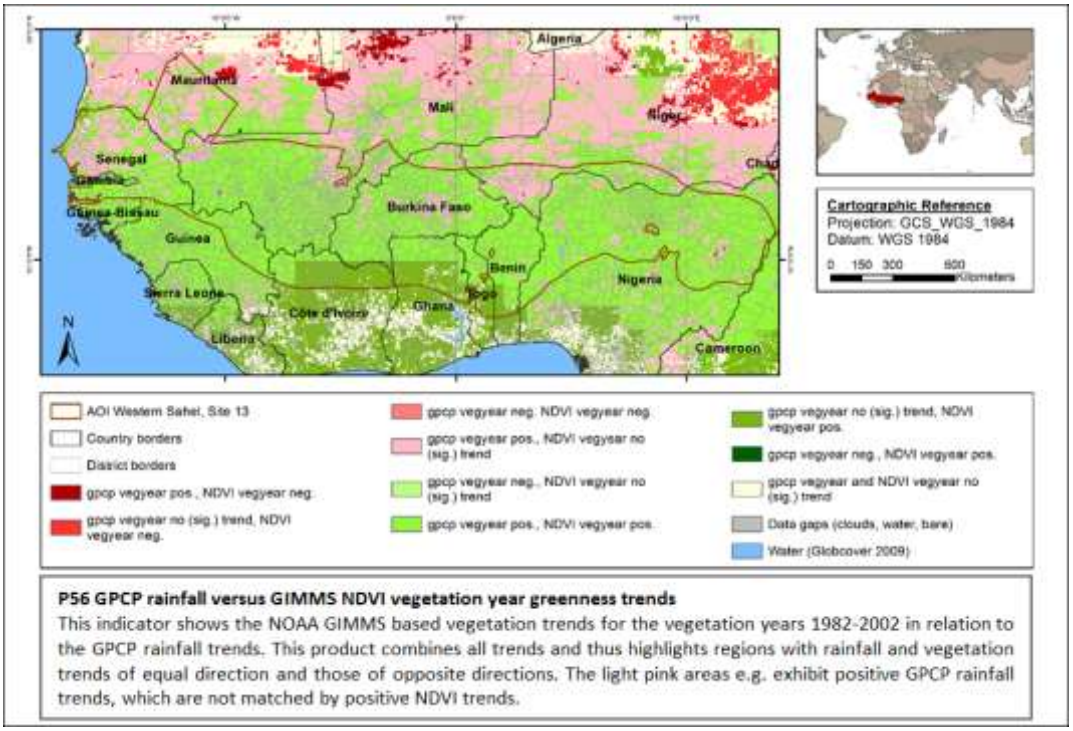

Figure 36: P56 GPCP rainfall versus GIMMS NDVI vegetation year greenness trends

For the Sahel region (the brown polygon delimits the actual ecoregions/test site) the products exhibits a rather uniform picture of a positive rainfall trend along with an overall vegetation greening. This is grading into a light pink coloured zone to the North, where positive (GPCP) rainfall trends are not matched by positive large scale greening trends. North of this, we see some areas with negative vegetation trends in areas with no or positive rainfall trends. Figure 37 shows the global GIMMS NDVI trends 1982-2002 for the vegetation year average greenness (top), below the trend for the cyclic vegetation (the vegetation peak integral of the NDVI time series) and in the third row the dry/cold season vegetation trends. It can be seen that the exhibited negative trends in Figure 36 north of the western Sahel are week vegetation trends only and may as well be artefacts, as these are very dry areas with a presumably low NDVI signal-to-noise ratio (see for instance Fensholt et al. 2009 for an analysis of the temporal consistency of GIMMS NDVI time series data).

The GIMMS NDVI trends 1982-2002 of the cyclic vegetation (in the middle in Figure 37) do not show these negative trends, instead the cyclic vegetation according to this result would have increased in large parts of the Sahara desert. Globally significantly more positive trends can be observed for the average yearly greenness than for the cyclic fraction greenness during the period 1982-2002, i.e. the 20 years prior to the Diversity II observation period. In the case of the Sahel, these positive NDVI trends are clearly matched by positive GPCP rainfall trends (bottom map in Figure 37), also in some other sites, e.g. in southern Africa. Nonetheless, in several sites, especially in southern Europe, in North American sites, Turkey and India, pronounced positive

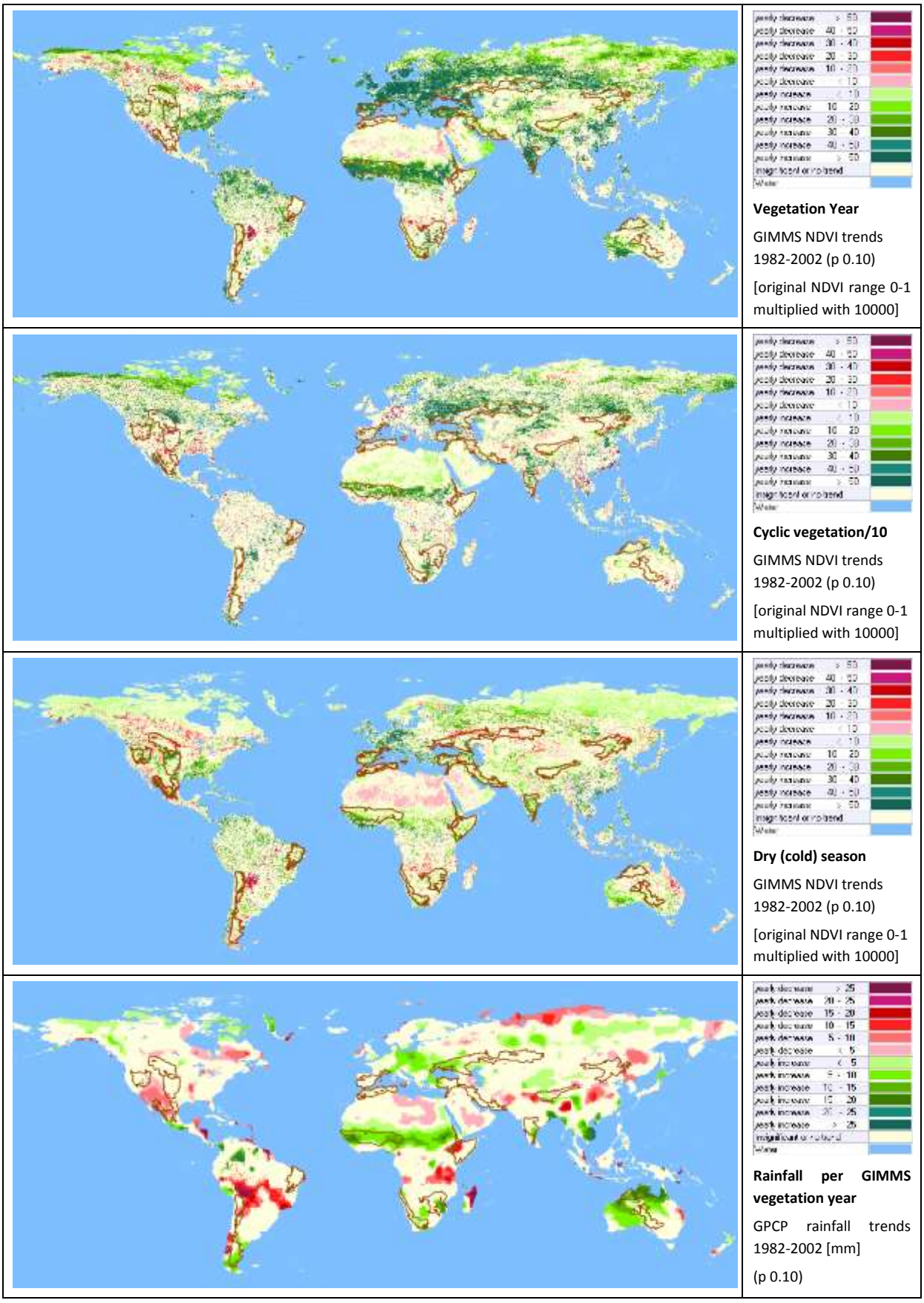

Vegetation Year

GIMMS NDVI trends 1982-2002 (p 0.10)

[original NDVI range 0-1 multiplied with 10000]

Cyclic vegetation/10

GIMMS NDVI trends 1982-2002 (p 0.10)

[original NDVI range 0-1 multiplied with 10000]

Dry (cold) season

GIMMS NDVI trends 1982-2002 (p 0.10)

[original NDVI range 0-1 multiplied with 10000]

Rainfall per GIMMS vegetation year

GPCP rainfall trends 1982-2002 [mm]

(p 0.10)

Figure 37: GIMMS NDVI and GPCP trends 1982-2002 in Diversity II test sites (brown polygons)

vegetation year greenness trends 1982-2002 came at least in large parts of these regions without positive rainfall trends according to the GPCP rainfall data.

Overall, the rainfall trends correspond best to the dry season trends. Further factors controlling these trends, which are not shown, include essentially air temperature and radiation (see 3.6.4), increasing atmospheric CO_2 concentration and land use. Further on, where widespread positive vegetation year and dry (cold) season trends are observed in the absence of cyclic vegetation trends, shifts of the vegetation composition towards more perennially green woody vegetation may play a role, e.g., as observed in Senegal by Herrmann at al. 2013 (see also 3.5.9). With regard to the increasing atmospheric CO_2 concentration, Higgins et al. (2012) show that this will force transitions to vegetation states characterized by higher biomass and/or woody-plant dominance. Possibly, this process was already contributing to the trends shown in Figure 37.

3.5.9 Relationship between biodiversity and vegetation productivity

In chapter 5 of this handbook, results of comparisons between faunal species richness data and various Diversity II dryland products as well as halfmonthly fAPAR time series data are presented and discussed. Plant species richness and vegetation productivity proxies have not been directly contrasted in Diversity II.

When looking at the literature, this issue is debated around some mainstream concepts. Overall, the relationship between vegetation productivity and floral or faunal biodiversity is highly scale dependent and cannot be characterised with generalised linear relationships. The relationship further depends on the type of creatures and species (e.g. plants versus animals, mammals versus birds versus amphibians, etc.), on the range of environmental conditions analysed (e.g., complete spectrum of growing conditions or only arid regions) and on land cover/land use and land management practices.

At very low levels of primary productivity, plant diversity was found to increase with increasing productivity, whereas from intermediate to high productivity levels, decreases have been observed (Oindo et al. 2002). Overall, this relationship is often described as producing a unimodal 'hump-shaped' curve, e.g. by Huston 1979 (cited by Oindo et al. 2002 in a study in Kenya), or by Oba et al. (2001), who analysed grazing areas in arid zones of Kenya. They found that optimum herbaceous species richness in these areas corresponded to a biomass level of 400-500 g/m², and declined when biomass exceeds 500 g/m². Further on, these authors compared open grazing land to grazing exclosures, and observed that "*seasonal grazing exclosures may increase species richness to a certain level, but the decline in species richness with age of exclosures indicates that long-term exclusion of grazing may not necessarily increase species richness in arid-zone grazing lands*". Bhattarai et al. (2004) tested and confirmed the humped-back hypothesis in the arid Trans-Himalayan mountain grassland with a seasonal grazing system and found that species richness was highest at 120 ± 40 g/m². However, these hump-shaped curves of the relationship between primary productivity and plant species richness seem to be observable especially when broad spectra of ecological conditions are analysed.

The hump-shape theory is challenged by several authors, for instance Whittaker 2010, who argues that overall such study results depend among other factors heavily on the scale and sampling design. Further on, as Jenkins (2015) points out, often biomass as the most common proxy for productivity is used for these assessments. According to Jenkins, this may cause error and uncertainty in the resulting relation between NPP and biodiversity due to the fundamental difference between biomass and productivity and variable ratios between the two among and within ecosystems.

Given the spatial variability of relationships found between productivity (or biomass) and plant species richness, it becomes clear that also greening processes observed with satellite data are not necessarily positive with regard to biodiversity per se. Herrmann et al. (2013) investigated the greening of the Sahel since the drought years in the 1970s and 1980s that has been commonly observed with NOAA AVHRR NDVI data and is largely related to increased rainfalls since. They compared the woody vegetation species composition of several test plots in in the Sudanian zone of central Senegal for the years 1983 and 2010 and found: "*While increases in woody vegetation densities could be confirmed at about half of the greening sites, these increases occurred only in the shrub layer. A loss of trees was evident at all greening and control sites. Moreover, our data*

pointed to a loss in species richness and a shift towards more xeric species compositions at almost all sites. Discussions with the local population largely confirmed these observations. Our findings from central Senegal contrast with other findings of increasing field tree densities resulting from farmer managed natural regeneration in other parts of West Africa".

The authors developed the diagram shown in Figure 38, which symbolises possible pathways of greening, where they observed changes in the sense of the blue arrow: greening, but towards a "green desert" made up of less diverse and valuable, but abundant shrub species.

Even in the rather short period of the MERIS data, we could frequently observe positive trends of the dry season greenness levels (without such trends in the cyclic vegetation, i.e. the peak vegetation during the rainy season(s)), which may give hints to the over-proportional thriving of woody vegetation, which in turn might be related to bush encroachment. Detailed studies of these relationships with in situ data would be of high interest.

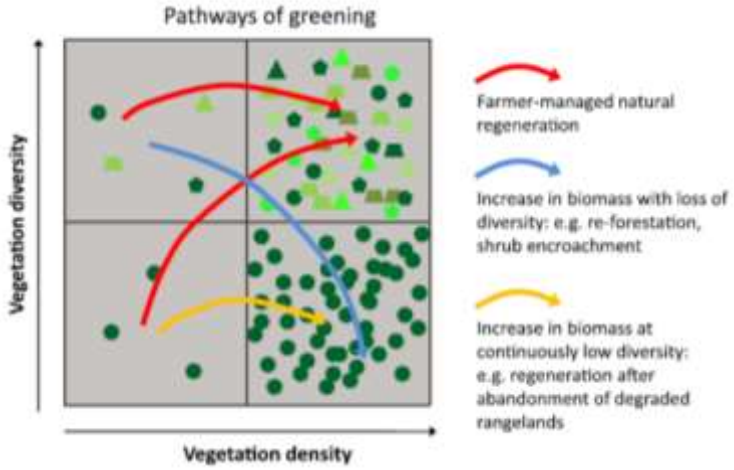

Figure 38: Conceptualized pathways of greening. Point symbols represent different woody species; arrows indicate possible pathways of change towards "greener" conditions. Source: Herrmann et al. 2013

3.5.10 Consistency of trends of different sensors and vegetation indices and derived parameters

In order to "trust" derived EO based trends, it is useful to collect some "convergence of evidence", e.g., by cross-checking with other trend data. We have done this (see section 3.6.1) and demonstrated that the trends derived by Zhou et al. (2015) with GIMMS NDVI are well comparable to the trends computed with the Diversity II methods using also GIMMS NDVI data.

Moreover, we have compared the MERIS fAPAR trends to GIMMS NDVI trends and thus across a big scale difference, and somewhat different trend calculation methods (Theil-Sen (TS) for the fAPAR data versus ordinary least square (OLS) trends for GIMMS, see chapter 4, section 4.4.2). This comparison is of interest as GIMMS NDVI trends are widely analysed in the literature and used for degradation assessments. The results are demonstrated below.

We start with the most controversial case found. Figure 39 contrasts vegetation year based trends for the period 2003-2010 for Diversity II test site 4, Northern Kazakhstan: comparing (b) to (c) shows that the OLS and TS trend calculation methods (see chapter 4, section 4.4.2) deliver quite similar results, though OLS is leading to somewhat more trends at the same level of significance.

However, the GIMMS NDVI trends, while similar in capturing negative trends, deviate quite strongly from the fAPAR trends with regard to their positive trends, which on the other hand correspond to the positive epochal rainfall differences (d) in the east and a thin strip in the north of the site and would hence be plausible. In Figure 40 the trends of the vegetation year, cyclic vegetation, and dry season greenness of this test site can be

compared. While the cyclic vegetation trends are quite comparable, it turns out that the dry season makes the big difference in this site, especially in the western part.

This obvious deviation between MERIS fAPAR and GIMMS NDVI trends is contradicting the much more common cases of similar or comparable trends (in 2003-2010) between the two data sets, as can be seen in Figure 41 to Figure 46. This correspondence of patterns, often of trend intensities and frequently of hotspots, between the trends derived with these different sensors overall confirms that the GIMMS NDVI and MERIS fAPAR data as well as the methods developed and applied in Diversity II are largely consistent. The vegetation productivity parameters, aggregated to vegetation year averages, the cyclic vegetation, and dry season means, are largely comparable even though they were derived for 8km versus 300m data. Hence it can be assumed that these methods can be applied to very different EO vegetation time series.

Nevertheless, there are differences in certain areas, and the general visual impression is partly quite different. Compared to the GIMMS NDVI trends, the MERIS fAPAR trends with 300m * 300m resolution are in many areas less pronounced and are more sparsely distributed. Often, we see large trend areas in the GIMMS data, which are matched by only a few MERIS fAPAR trends pixels. In those areas either the GIMMS NDVI data or derived parameters are more sensitive to vegetation trends, or/and vice versa the fAPAR data or derived parameters are less sensitive, or perhaps more variable due to their much higher spatial resolution and thus “hiding” trends. Also the different and variable contribution of soil reflectance especially of NDVI data is a known issue and can be expected to cause differences of the derived parameters. In chapter 4, section4.4.6 we come back to this issue.

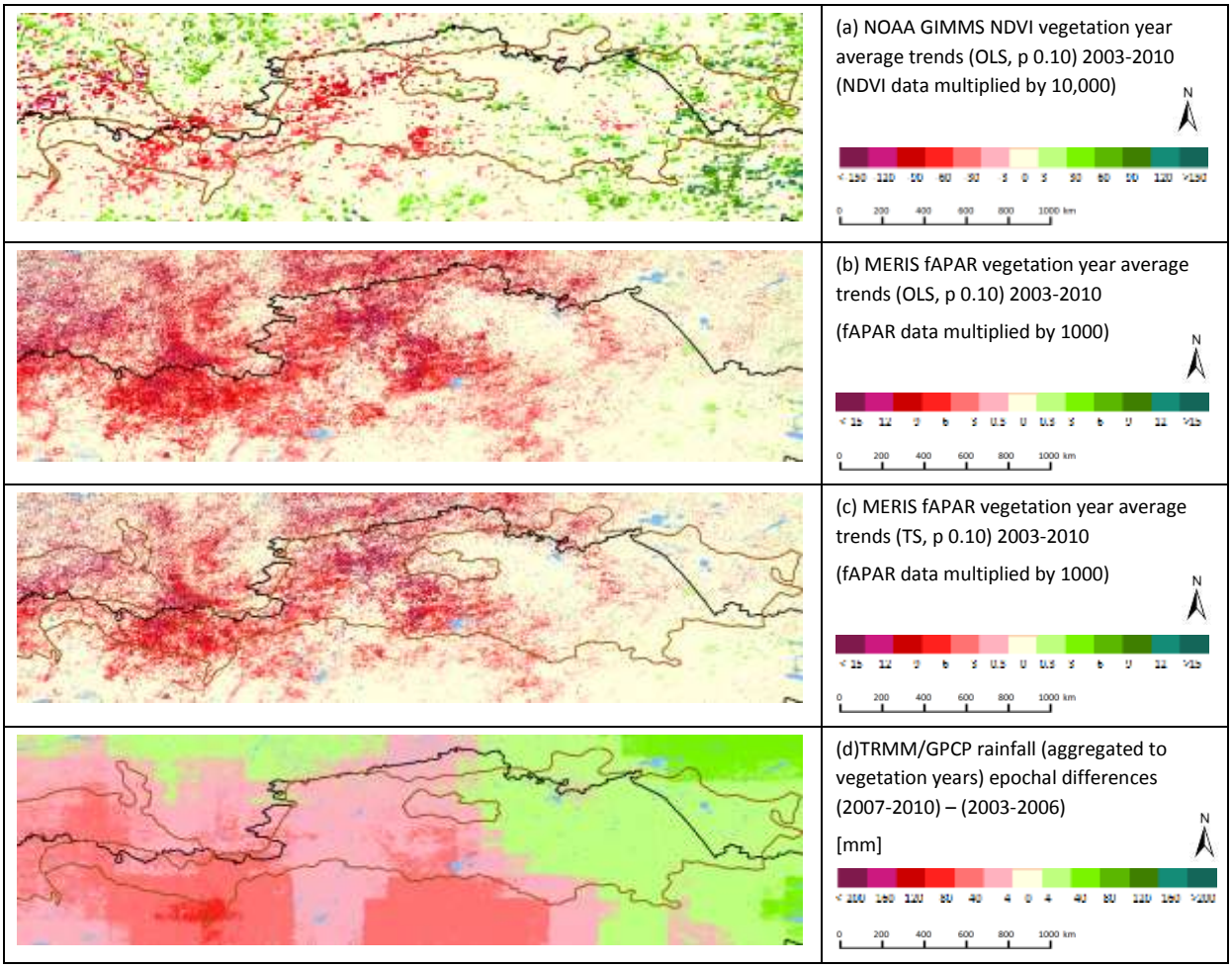

Figure 39: GIMMS NDVI (a) and MERIS fAPAR vegyear average trends (b and c), and epochal differences of rainfall (d) in test site 04: Northern Kazakhstan

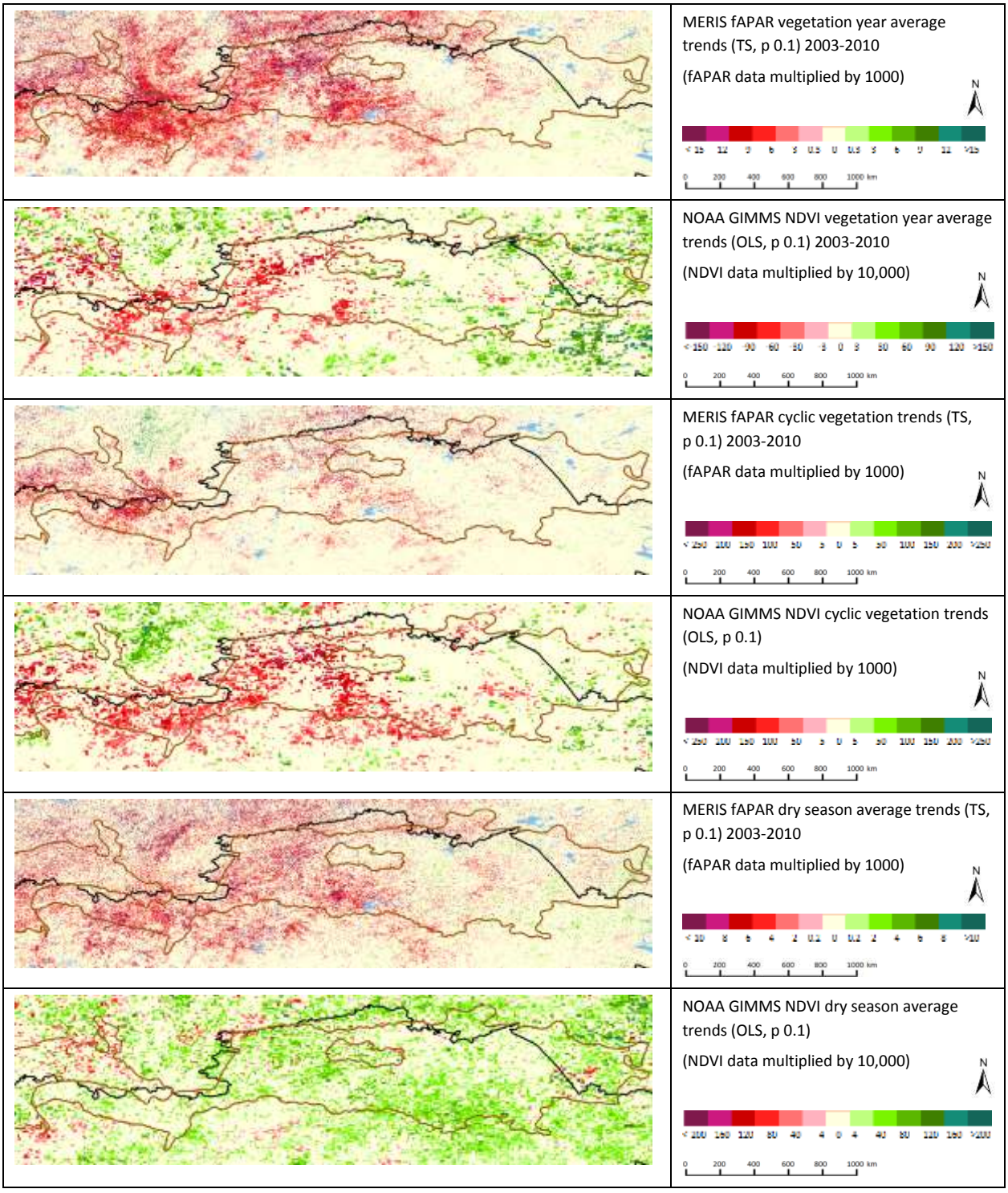

Figure 40: MERIS fAPAR trends versus GIMMS NDVI trends 2003-2010 in test site 04: Northern Kazakhstan

The big differences between the MERIS fAPAR and GIMMS NDVI trends of the vegetation years and the dry season, respectively, are contradicting the much more common cases of similar and comparable trends (in 2003-2010) between the two data sets, as can be seen in Figure 41 to Figure 46. In these figures, the MERIS fAPAR based trends were calculated with the Theil-Sen trend estimator, the NOAA GIMMS NDVI trends with the ordinary least square method. When comparing the fAPAR based vegetation year greenness trend with the NPP trend derived with Bethy/DLR (Figure 21), larger commonalities are exhibited than with the NOAA GIMMS trend in this area.

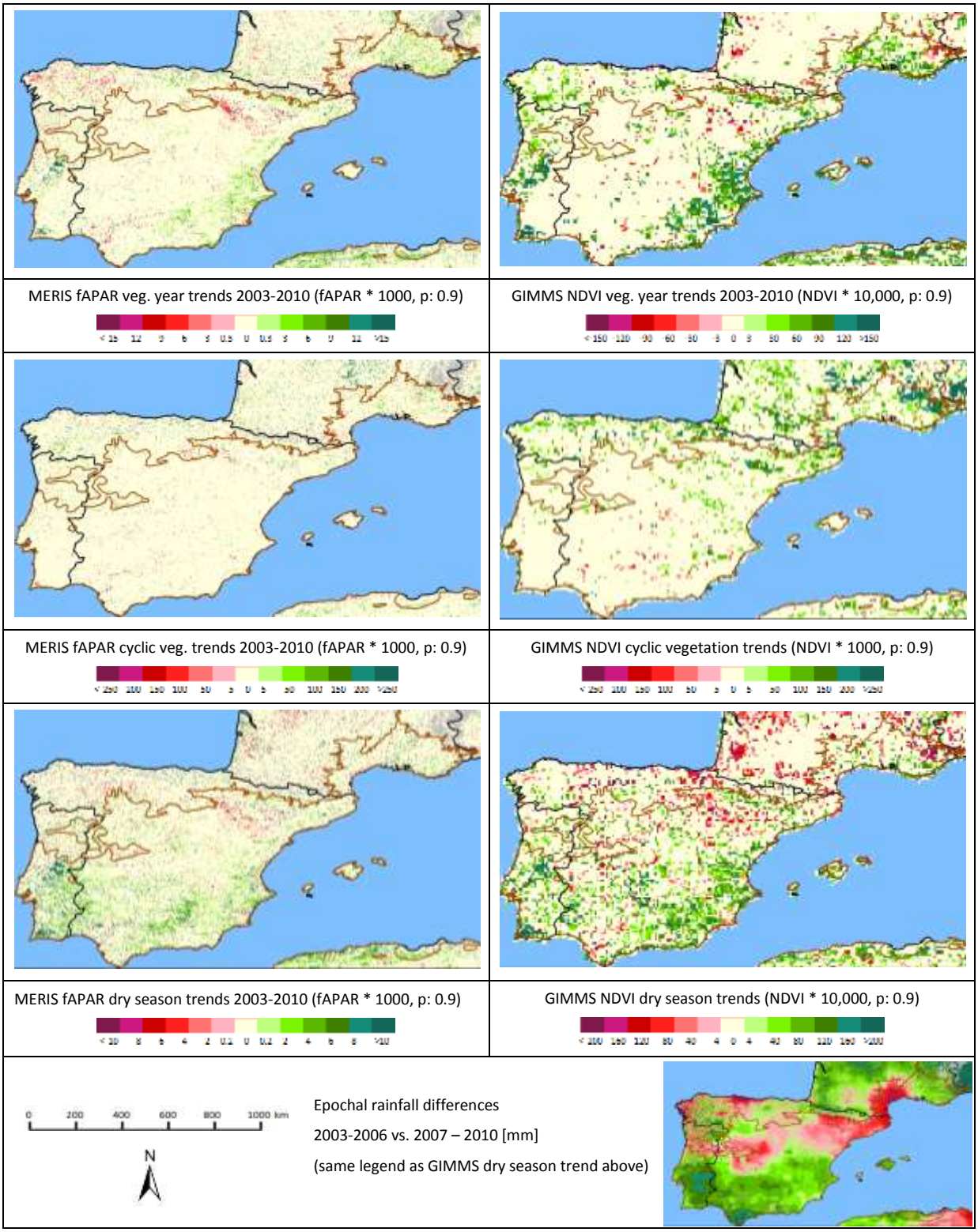

Figure 41: MERIS fAPAR trends versus GIMMS NDVI trends 2003-2010 in test site 10: Southern Europe (western part)

In the southern European site, the parameters derived from both sensors produce a similar mixed pattern: widespread positive dry season trends in the South, also quite frequent negative dry season trends in the northern half, in general less trends of the cyclic vegetation greenness especially in the South with somewhat more negative trends, and positive cyclic vegetation trends in the North. So we see largely a reversed pattern of positive/negative cyclic vegetation and dry season greenness in the northern and southern half of the region. In general the correspondence of trends is quite high between the GIMMS and MERIS based trends.

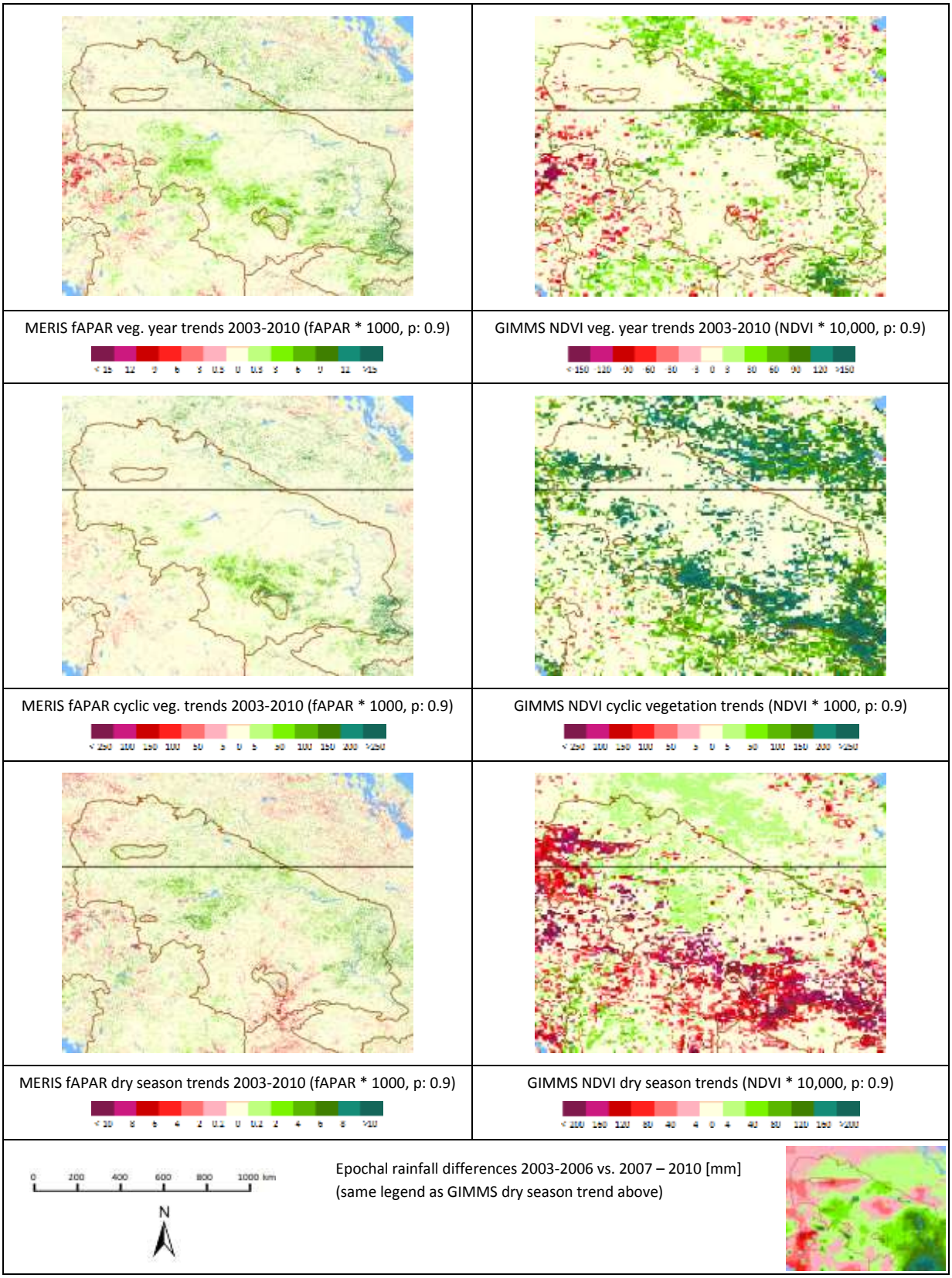

Figure 42: MERIS fAPAR trends versus GIMMS NDVI trends 2003-2010 in test site 18: Northern USA - Southern Canada

In the great plains of northern USA and southern Canada we see also quite similar trends between GIMMS NDVI and MERIS fAPAR parameters building diagonal patterns from NE to SW. The GIMMS trends however are much more pronounced than the MERIS fAPAR based trends.

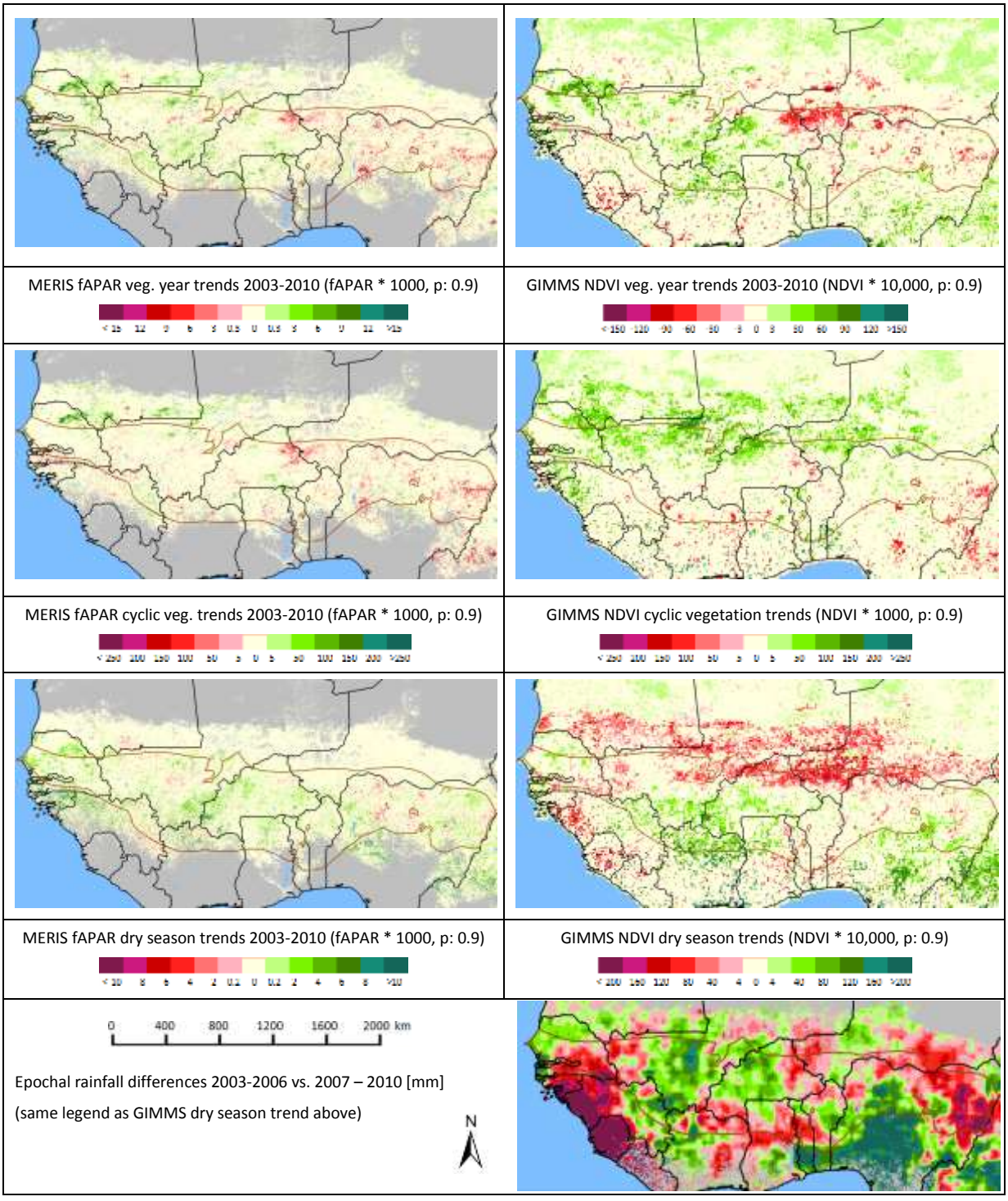

Figure 43: MERIS fAPAR trends versus GIMMS NDVI trends 2003-2010 in test site 13: Western Sahel

While the fAPAR data exhibit virtually no vegetation signals in the Sahara and have too many gaps in the South, we have GIMMS NDVI data all over the test site due to their much more frequent coverages. Trends are well comparable for the vegetation year greenness. For the cyclic vegetation and the dry season greenness, they are similar in the southern half of the area covered with MERIS data. In the northern half, the broad band of positive cyclic vegetation trends and negative dry season trends is only seen in the GIMMS data, and finds only little correspondence in the MERIS fAPAR based trends. These are interesting phenomena in the GIMMS NDVI data and at present it is unclear how they can be explained, if they are not artefacts or due to a higher response of the NDVI to soil background reflectance.

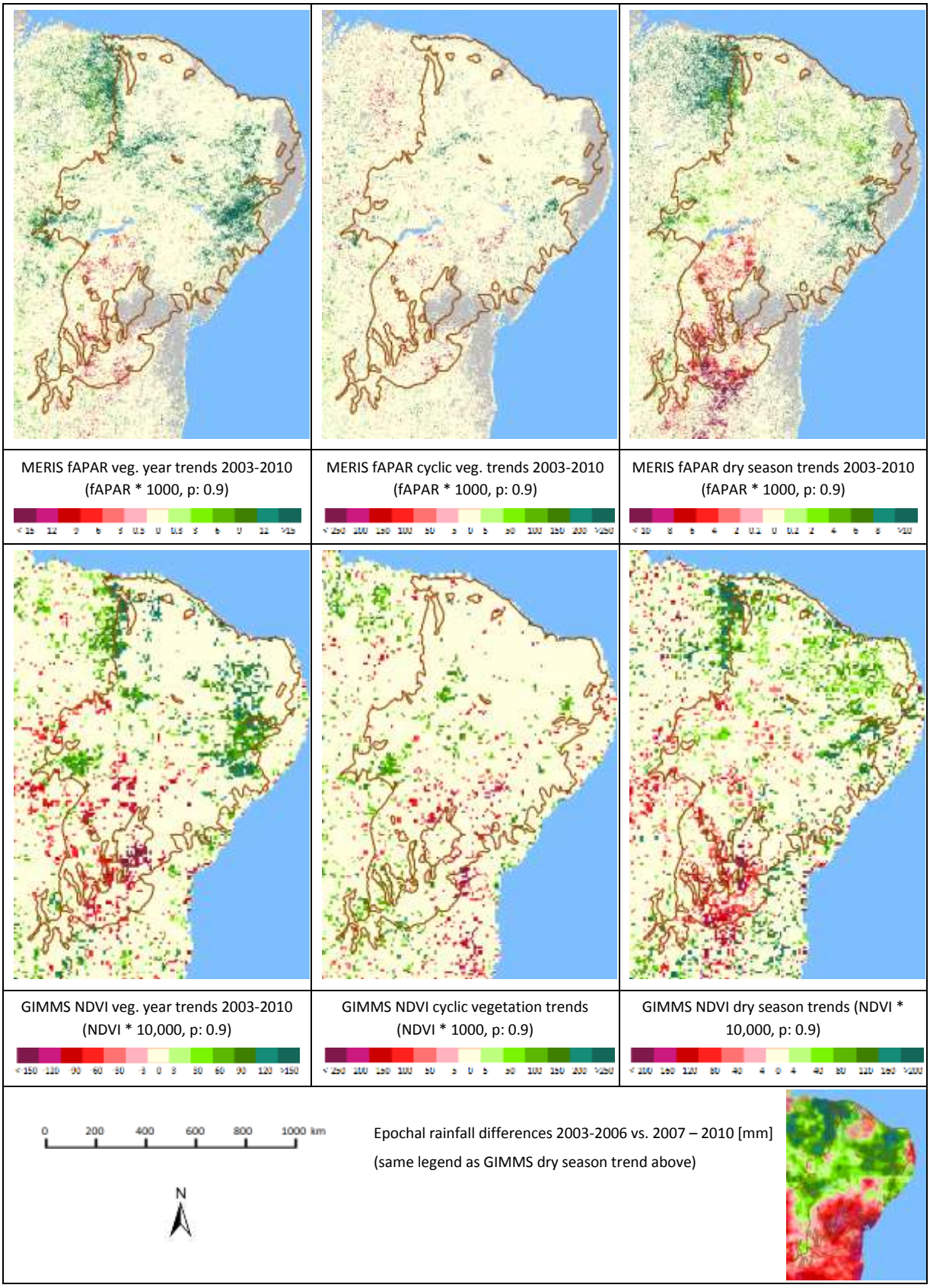

Figure 44: MERIS fAPAR trends versus GIMMS NDVI trends 2003-2010 in test site 15: Caatinga, Brazil

In Caatinga we see a high trend correspondence between MERIS fAPAR and GIMMS NDVI as well, with a hotspot of negative dry season trends exhibited in the South, and predominantly positive trends in the North.

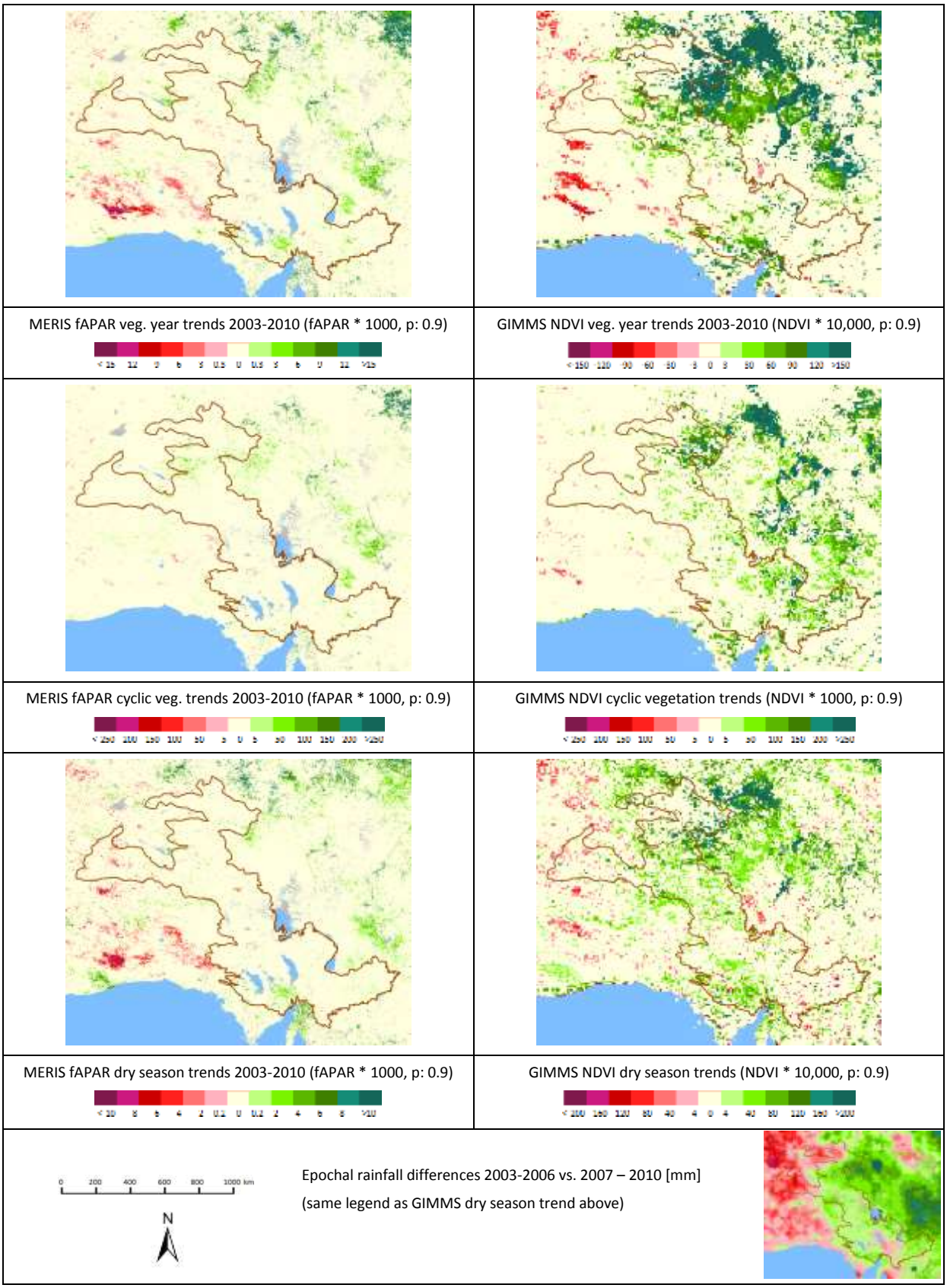

Figure 45 MERIS fAPAR trends versus GIMMS NDVI trends 2003-2010 in test site 20: Southern Australia

Also in South Australia the trends of the GIMMS and MERIS data agree in many regions, with much more pronounced trends in the GIMMS data.

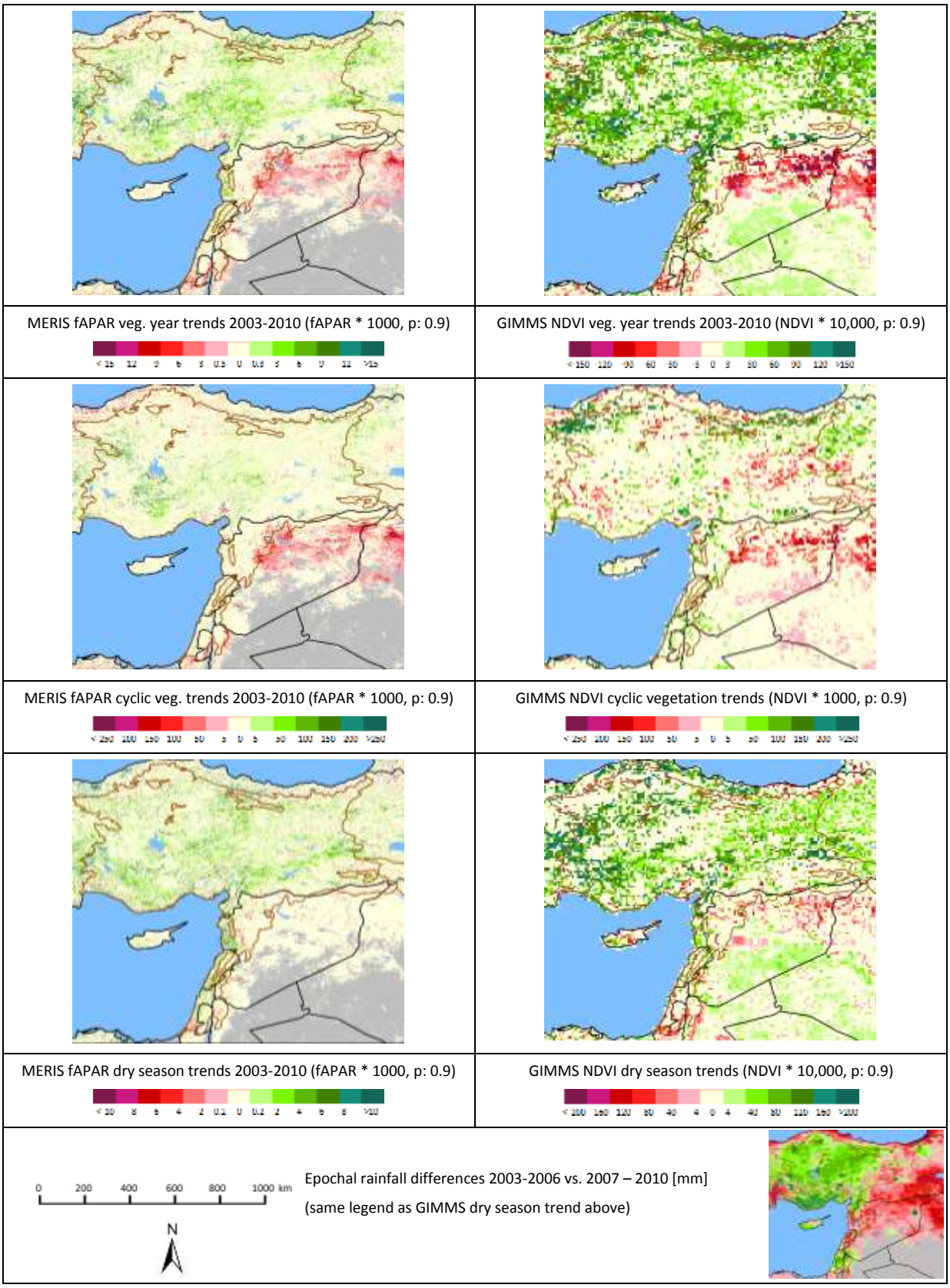

Figure 46: MERIS fAPAR trends versus GIMMS NDVI trends 2003-2010 in test site 22: Eastern Mediterranean Countr.

Again, we see similar trend patterns of GIMMS and MERIS based vegetation parameters. Like in the test sites shown before, the vegetation trends are in general controlled by rainfall variations expressed as epochal differences.

3.6 Known issues and interesting questions

There are several, both project specific and generic issues and interesting questions related to the processing and the products of the Diversity II project, which shall be addressed in the following sections.

3.6.1 Short time series for trend analyses

The variability of rainfalls and subsequently vegetation greenness from year to year is so significant in drylands that it certainly hides trends, which in such a short period (8 vegetation years analysed in Diversity II) may be not very pronounced. There may be more relevant and persistent changes going on than the trend maps for such a short period can show, especially as many changes cannot be expected to exhibit gradual developments and measurable trends. Many of the rainfall trend maps for instance show not many significant trends, while the rainfall change map between the two epochs shows large positive and negative change regions with partly big epochal rainfall differences. Vice versa, due to the short observation period, measured significant trends may not really be part of persistent, longer term development but may already be reversed in the next epoch, or changed if only one additional observation year is added.

In order to demonstrate an example for this issue, GIMMS NDVI trends derived by Zhou et al. (2015) are contrasted with vegetation year trends for the same as well as shorter and longer periods derived in Diversity II using GIMMS NDVI data. Figure 48 shows that the annual GIMMS NDVI trends by Zhou et al. (2015) and the trends derived in Diversity II for vegetation year averages are quite comparable for the periods 1982-1991 and 1992-2011, respectively. Only in the period 1992-2011, some areas, especially east of the Caspian Sea exhibit more negative trends in the Diversity II result than derived by Zhou at al.

When looking at the effects of subdividing or aggregating the trend periods, we see quite different results: The trend map of the period of the heavy negative NDVI trends (1992-2011), when cut into two epochs, shows significantly less trends in each of the partial trend periods and, when looking at the period 2003-2011, even significant positive trends mainly in the eastern part of the area show up. Finally, when elongating the earlier trend period (1982-1991) to the years 1982-2002, a picture of widespread positive GIMMS NDVI trends emerges.

These comparisons show that trends can depend heavily on the exact trend period chosen, especially when the data fluctuate strongly and the time series are short. In such cases single year values can make a big difference, as demonstrated in Figure 47.

Figure 47: Example for GIMMS NDVI vegetation year averages 1982-2011 (northern Kazakhstan): a significant negative trend was only derived for the period 1992-2011 (ordinary least square trend, p 0.05) and not for the partial trend periods 1992-2002 and 2003-2011.

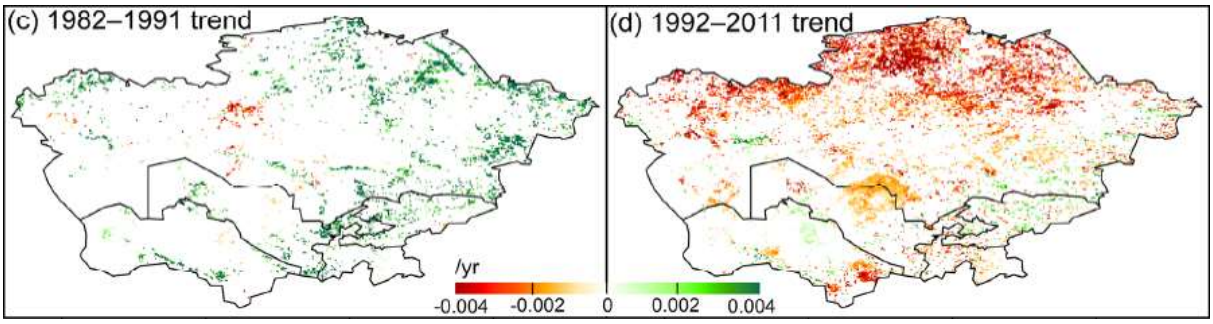

Linear annual GIMMS NDVI trends (p 0.05) for the periods **1982-1991** and **1992-2011**, respectively. **Source: Zhou et al. 2015**

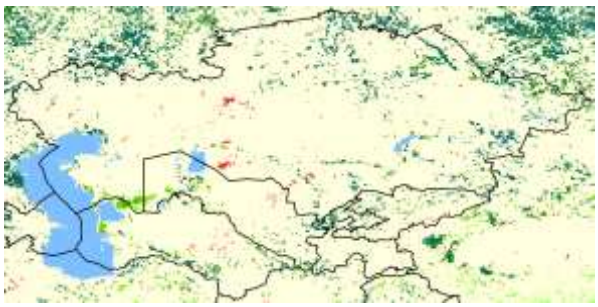

Diversity II: GIMMS NDVI vegetation year trends **1982-1991**

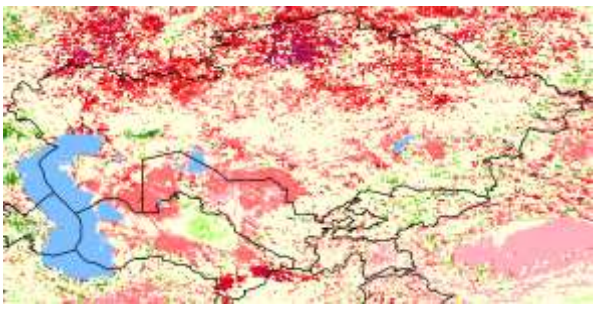

Diversity II: GIMMS NDVI vegetation year trends **1992 - 2011**

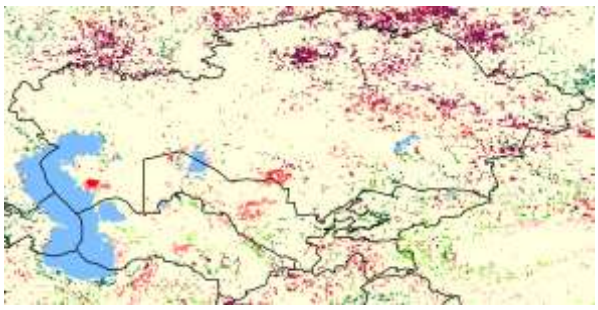

Diversity II: GIMMS NDVI vegetation year trends **1992-2002**

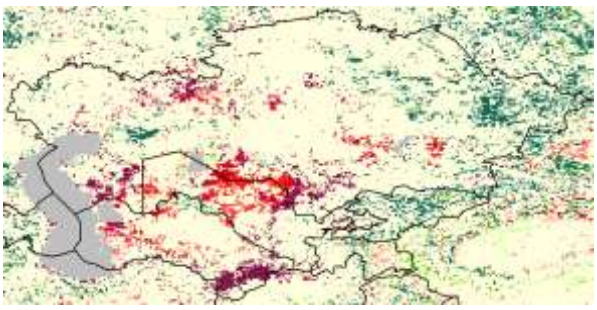

Diversity II: GIMMS NDVI vegetation year trends **2003-2011**

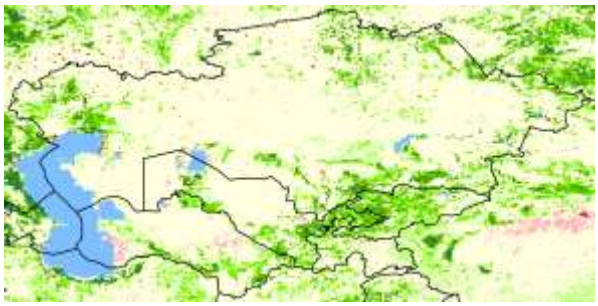

Diversity II: GIMMS NDVI vegetation year trends **1982-2002**

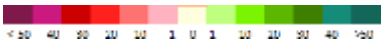

Legend of GIMMS NDVI vegetation year trends (Diversity II)

GIMMS NDVI data have been multiplied by 10.000

The Diversity II trends are based on averages of the vegetation year greennes (p 0.05) versus calendar year trends of Zhou et al. 2015

Figure 48: Yearly GIMMS NDVI trends in Central Asia derived by Zhou et al. (2015) and GIMMS NDVI vegetation year greenness trends derived in Diversity II.

In this context the work of de Jong et al. (2013) is interesting to mention, who propose a season-trend model for detecting major trend shifts in vegetation activity and demonstrate the application to the GIMMS NDVI data. Their proposed model is analogous to the BFAST approach (Verbesselt et al. 2010), but has been optimized (and simplified) for detecting the most influential trend shift in the time series, as opposed to multiple smaller shifts. Figure 49 shows the results. One of the conclusions of the authors is: "*Over time, an increase in the frequency of trend shifts was found. With respect to the 1980s, a four times larger area with changing trends was found in the 2000s. This suggests that relatively stable vegetation regimes have changed*

towards higher turnover rates, implying an increase in the complexity of biospheric alterations and responses to external forces" (Jong et al. (2013), p 1129).

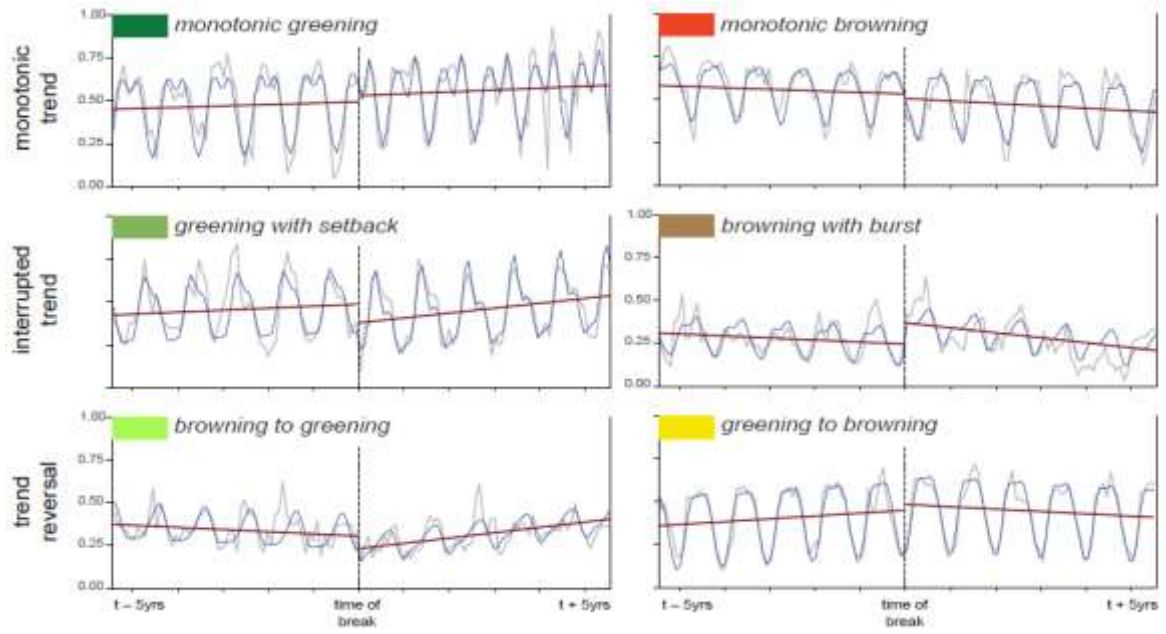

Types of vegetation activity trends (De Jong et al. 2013)

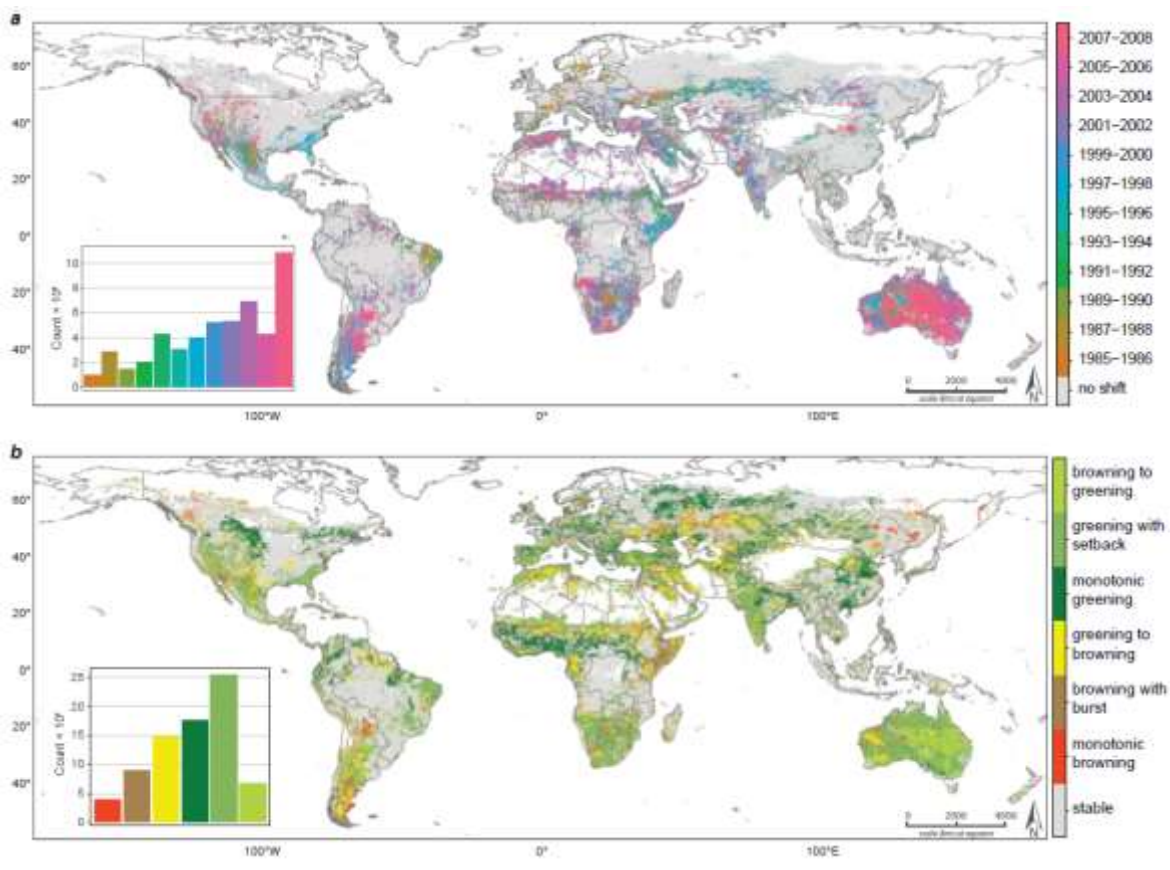

Figure 49: (a) Spatial distribution of the timing of the shifts in the global greening and browning regime. The detected change points were binned into 2-yearly classes. The histogram depicts the number of 0.083_ grid cells per bin; (b) Spatial distribution of types of vegetation activity trends as defined in the upper most diagrams. The histogram depicts the number of 0.083_ cells per trend type. Source: De Jong et al. 2013

3.6.2 Which vegetation parameter to choose for trend analyses?

The choice of the vegetation productivity parameters that are used for trend analysis is of essential importance for the results and their further analyses, hence we have demonstrated this repeatedly in the handbook. Here we discuss the issue once more in the context of the example of Kazakhstan and adjacent central Asian states used in the last section, and focus now on the trend period 1992-2011. For this time span, significant negative annual mean trends of GIMMS NDVI were derived by Zhou et al. (2015) and, largely comparable, also by Diversity II using vegetation year averages (see Figure 48).

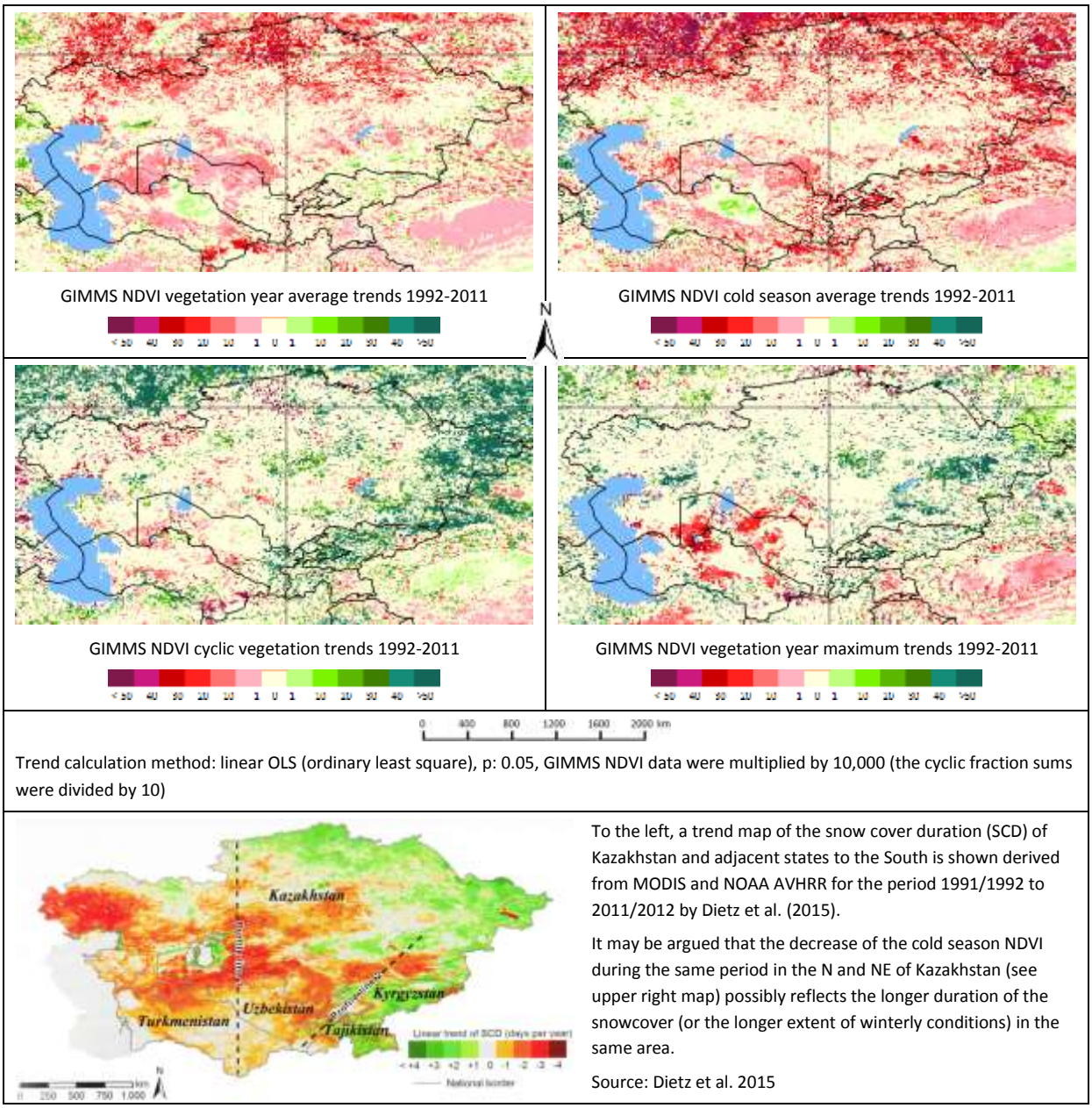

Figure 50: GIMMS NDVI trends 1992-2011 for different vegetation productivity parameters, compared to snow cover duration trends. The cross in the upper four trend maps marks the location of the time series shown in Figure 51

In Figure 50 we compare the vegetation year average NDVI trends (displayed in the upper left) to trends of three other vegetation parameters:

1. Dry season average
2. Cyclic vegetation (integral of the NDVI sums in the vegetation peaks minus base values, see Figure 3)
3. Maximum NDVI of vegetation year (actual NDVI max. value, no base value subtracted)

This comparison shows that the widespread negative yearly average NDVI trends are largely co-occurring with negative dry/cold season trends, while both the cyclic vegetation and the maximum NDVI show clearly less trends in the regions with the strong negative vegetation year and dry season trends. While less frequent, the negative cyclic vegetation trends in Northern Kazakhstan do correspond with the location of the negative vegetation year trends. This supports the findings of Zhou et al. 2015, who state a widespread desiccation during this period partially caused by the warming trend.

On the other hand, we are looking at a region with snow cover and frozen soils in the wintertime, which can last from November to March in these regions. These surface conditions can be expected to interfere with the NDVI signals of the cold season, however to a (to us) unknown extent. In fact, in a recently published study of Dietz et al. (2015) a snow cover duration (SCD) trend map has been derived (copied in Figure 50), which exhibits a positive trend of SCD in the N, E, and SE of Kazakhstan, where pronounced negative dry (cold) season trends of the NDVI can be seen.

Figure 51 (top) shows the NOAA GIMMS time series data for the studied period at the location marked with the cross in the trend images of Figure 50, along with the derived baseline values (see chapter 4, section 4.3.3 for method description). In the bottom the yearly values of the vegetation year mean, the cyclic vegetation sum, the cold season mean and the maximum are plotted. At this location (coordinates shown in the diagram title of Figure 51), for the vegetation year mean and the cold season mean significant negative trends from 1992 to 2011 (p 0.05) were derived, while the cyclic vegetation sum and the maximum do not exhibit significant OLS trends. The baseline separates the cold (and/or dry) season from the cyclic vegetation, whose yearly sum is derived as integral of the values above the baseline, the baseline values being subtracted. The example illustrates the frequently (Figure 50) seen occurrence of the negative cold season trends along with negative vegetation year trends, without significant cyclic vegetation or maximum trends over the entire period.

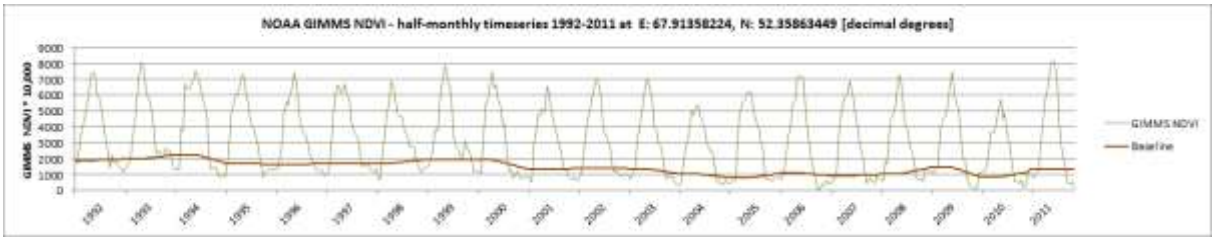

NOAA GIMMS half-monthly time data 1992-2011 along with the calculated baseline that separates cold/dry season values from the cyclic vegetation. The GIMMS data have not been smoothed.

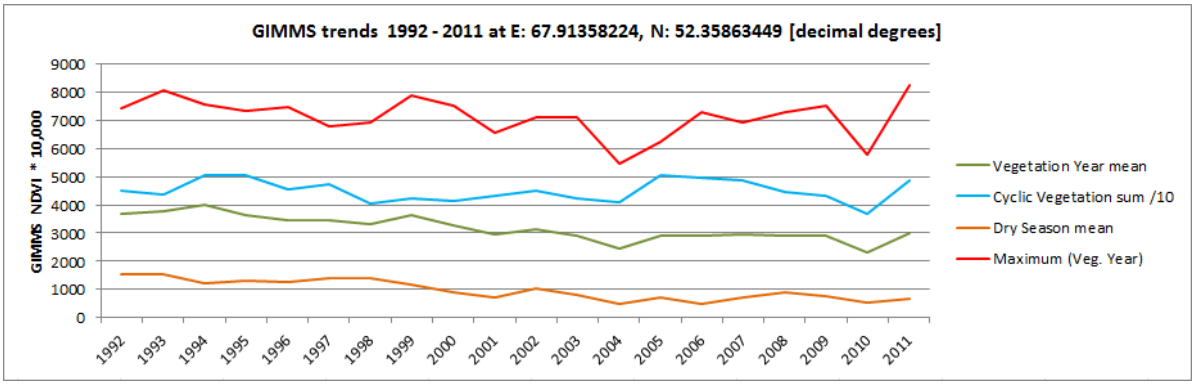

Figure 51: Top: NOAA GIMM time series 1992-2011; Bottom: GIMMS NDVI trends of vegetation year mean, cyclic vegetation, dry season mean, and maximum of vegetation year, derived from the GIMMS values shown in upper diagram

Diversity II provides trends for vegetation years, dry season averages and the cyclic vegetation greenness. These three parameters were considered the most essential and we argue that they need to be studied in combination and if possible with separate investigation of driving factors in order to find out more about the possible nature of observed trends. The trends of the GIMMS maxima have been shown in this section, though they were not included in the Diversity II fAPAR product suite, as they are individual and quite variable values, and often subject to gap filling (cloudy conditions during the rainy periods).

3.6.3 Regional discrepancies between the MERIS fAPAR and the MERIS NDVI based results

Besides MERIS fAPAR, also MERIS NDVI data have been analysed for test sites 04 Northern Kazakhstan and site 12, Southern Africa West, using the same methodology and generating the same products as for the MERIS fAPAR data (see also chapter 4 sections 4.2.2). Some results are presented as follows, contrasting them with the fAPAR products.

In Figure 52 MERIS fAPAR and NDVI values are plotted for three years, taken from a location in Kazakhstan with a rather low productivity. Obviously the two data sets do have somewhat difference responses to the vegetation development, which explains the minor deviations of the start of season. In this test site, a slight delay of the MERIS NDVI based SoS compared to the MERIS fAPAR typically occurs in areas with low productivity, whereas SoS differences the other way around, i.e. an earlier SoS of the NDVI data, are hardly found. Differences between fAPAR and NDVI based SoS of up to three half-months can be observed in the Kazakhstan site.

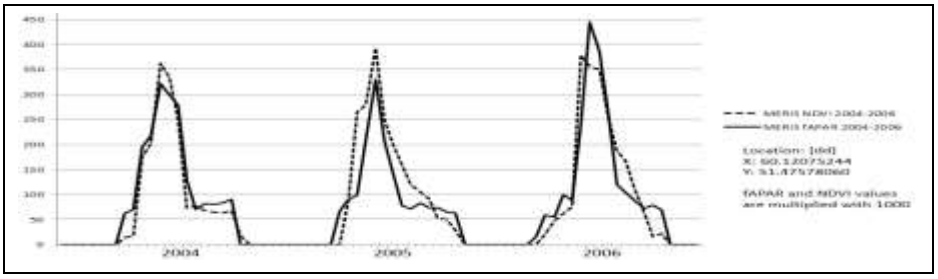

Figure 52: MERIS fAPAR (solid line) versus MERIS NDVI values in test site 04, Northern Kazakhstan

The situation is quite different in test site 12, Southern Africa West, a site with complex phenology and a large local and regional variety of growing conditions. Figure 53 displays the MERIS fAPAR and NDVI time series of a location (see red circle in Figure 54c) in central Namibia. Obviously, the NDVI is more influenced by soil signals than the fAPAR (or the fAPAR less sensitive to small vegetation signals). The NDVI seldom reaches zero values in the dry seasons or in very dry areas as opposed to the fAPAR data. This difference has an influence on the phenology, where in certain regions the NDVI based SoS deviates substantially from the fAPAR SoS. Also the resulting status and trend products reflect these differences.

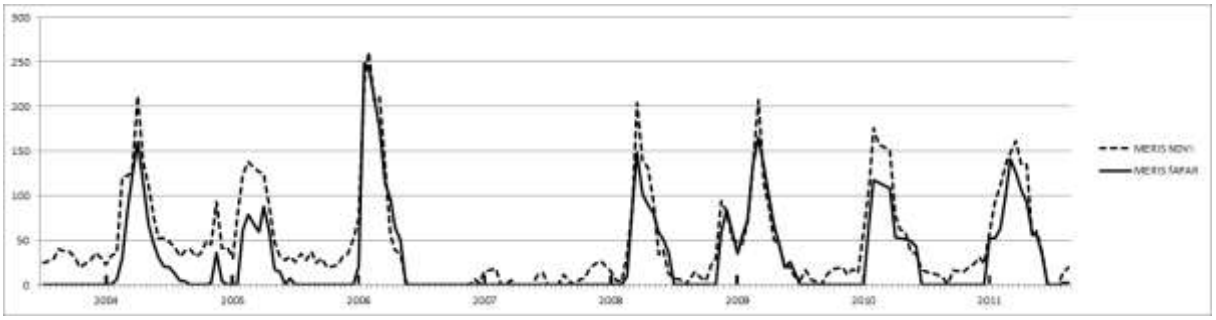

Figure 53: MERIS NDVI and MERIS fAPAR time series in Namibia, at X: 18.65197380, Y: -24.09031143. The years are marked at the start of the calendar years (NDVI and fAPAR multiplied by 1000).

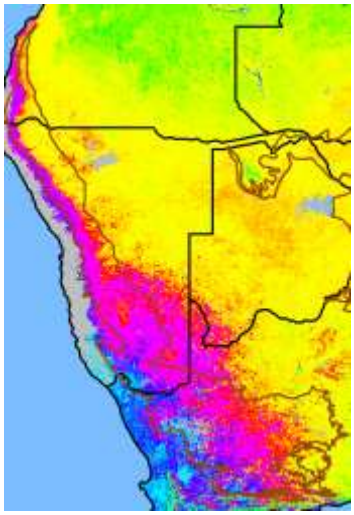

(a) P57 Median start of vegetation year 2003-2010 MERIS fAPAR

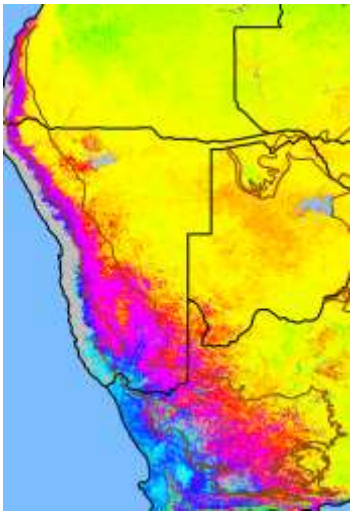

(b) P57 Median start of vegetation year 2003-2010 MERIS NDVI

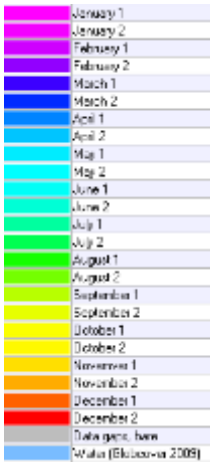

Legend for P57 (a) and (b)

(the numbers 1 or 2 refer to the first and second half of each month)

(c) Diff. between MERIS fAPAR and MERIS NDVI based SoS (rectangle marks location of (d))

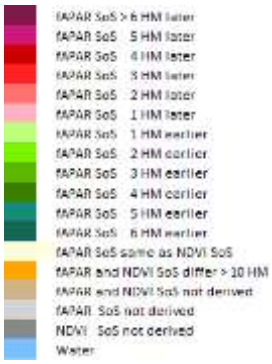

Legend for (c) and (d)

Legend for Pearson r (g)

(d) Detail of (c, blue rectangle) overlaid with SOTER (Soil and Terrain data) polygons

(e) P01 fAPAR mean of vegetation years 2003-2010

fAPAR * 1000

(f) P01 NDVI mean of vegetation years 2003-2010

NDVI * 1000

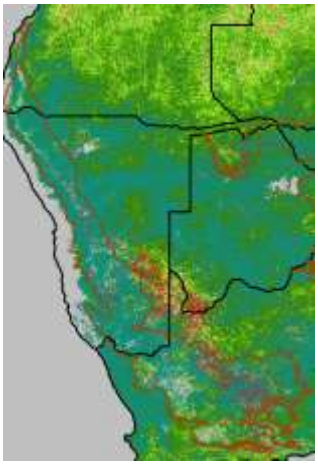

(g) Pearson r of MERIS vegetation year fAPAR and NDVI 2003-2010

Figure 54: Comparison of MERIS fAPAR/NDVI based SoS, and of vegetation year averages of fAPAR and NDVI

The SoS and the vegetation year averages of MERIS fAPAR vs. NDVI are contrasted in Figure 54. Overall, the MERIS fAPAR and NDVI derived SoS are quite similar, but the difference map of the two SoS nevertheless exhibits quite big discrepancies in certain regions. These are related to soil and terrain properties, as the overlay with the SOTER (Soil and terrain data[8]) data (Figure 54d) shows.

The pearson correlation map (Figure 54g) exhibits lower r values between the fAPAR and NDVI based vegetation year averages in the North (Angola) where rainfalls and productivity are higher, and even negative correlation values in the lower centre of site 12, where also the large deviations between the SoS are found.

As already mentioned these results suggest that the fAPAR data are less influenced by soil background reflectance. However they could also mean that the fAPAR data display less sensitivity to low vegetation productivity levels than the NDVI, especially as the differences seem to have a seasonal behaviour. Still the more likely reason might be the first, as the NDVI is known to be more or less strongly influenced by soil reflectance and hence soil properties. Also the regional concentration of the differences may point into this direction.

3.6.4 Vegetation productivity only related to water availability

Precipitation is the most important limiting factor to vegetation growth in drylands, and has as such been used as sole factor to contrast vegetation productivity against, without establishing a relation to the other major climate factors of vegetation productivity, i.e., temperature and solar radiation. Figure 55 shows the weight of these fundamental growth limiting factors at the global scale. Especially in the test sites located in temperate climate zones, temperature and to a lesser degree solar radiation constitute potential constraints to primary production. However, in the regional context the weight of these factors depends on further variables including topography, vegetation types, soil nutrients and other soil properties etc.

As this study does not model NPP (see section 3.5.3) we have related the derived NPP proxies only to precipitation and soil moisture, which can be still regarded as the major growth constraining factors in the analysed test sites.

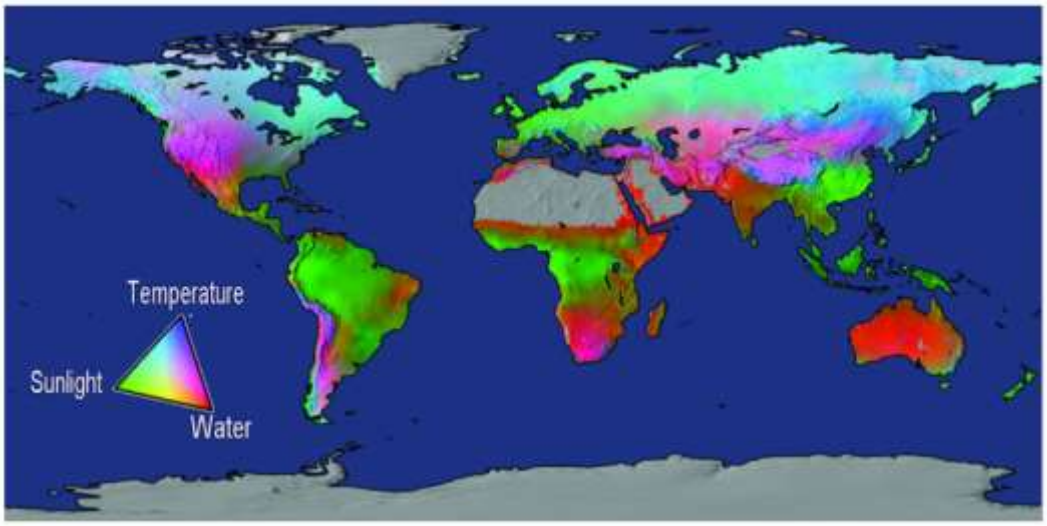

Figure 55: Potential limits to vegetation net primary production based on fundamental physiological limits by solar radiation, water balance, and temperature (from Churkina & Running, 1998; Nemani et al., 2003; Running et al., 2004). Source: http://www.ntsg.umt.edu/project/mod17

Nevertheless, temperature trends during the past decades have been found to influence vegetation activity, for instance in the already introduced recent study by Zhou et al. (2015). They detected a significant warming trend with an increasing rate of 0.052 °C/year in the years 1982-2012 covering over 90% of the vegetated areas in Central Asia (Figure 56), and correlated the temperature trends with vegetation activity trends by means of partial correlation and thus excluding the influence of rainfall trends. They concluded: "*The increasing*

temperature prompted vegetation greening before 1991 for most areas. However, in 1992–2011, this warming trend resulted in desiccation, suppressing the greening trend by increasing evapotranspiration and fire occurrences. The precipitation-controlled area expanded in 1992–2011, compared to 1982–1991" (Zhou et al. 2015).

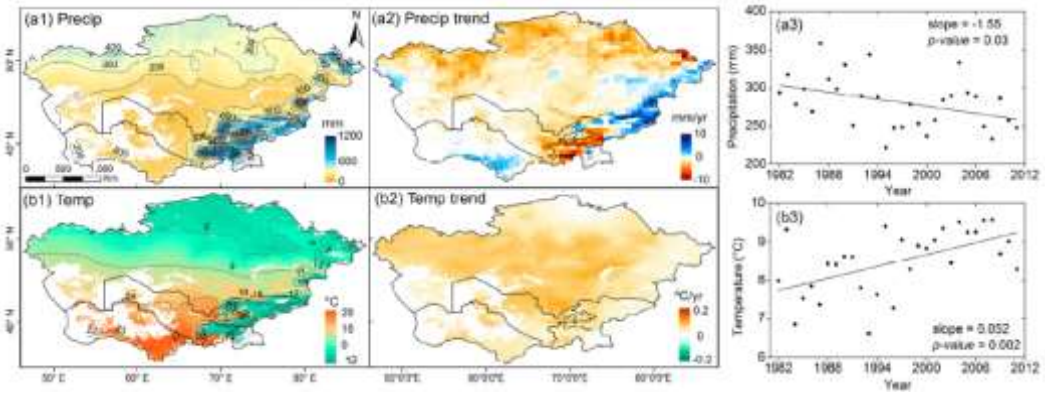

Figure 56: Precipitation and temperature trends 1982-2012 in Central Asia, source: Zhou et al. 2015

Also Sensoy et al. (2013) state, based on temperature trend analyses in Turkey: "*The most interesting feature in this time series is the relatively strong change in air temperature since 1994, which corresponds well to similar trends in many parts of the world* " (Houghton et al. 2001, cited by Sensoy et al. 2013).

3.6.5 Coarse TRMM and CCI SM data

The rainfall and soil moisture data have a relatively coarse spatial resolution (0.25°≈ 25 km² at the equator), especially when compared to the 300m pixel width of the MERIS fAPAR data. Local rainfall and SM differences and transitions may therefore be not well reflected in this data, leading to spatial mismatches of water availability and vegetation productivity. However, as exemplary shown in Figure 24, overall the spatial (also the temporal) distribution of rainfall is clearly correlated with vegetation growth in drylands. Hence, the spatial resolution differences would be more relevant if we looked at single rainfall events or the rainfall of very short periods, which may be expected to be less precisely rendered in the rainfall maps than longer term average rainfall amounts. However with regard to the SM data, their coarseness is more limiting, also the fact that they can only capture soil moisture of the uppermost 2-3 centimetres of the soil. Small scale water availability differences related to geological, soil and hydrological properties (e.g. ephemeral surface waters with higher groundwater tables, or local soils with high water retention) of course cannot be differentiated with such data, but exactly such properties make big differences at the local and regional scale.

3.6.6 Different results with different rainfall data

When looking at different global or continental, EO based datasets of rainfall, it becomes obvious that the results of the products derived from or with the TRMM rainfall data would be more or less different if other rainfall data would have been used. The influence of the rainfall data was examined to some degree in the project, but would need more attention and systematic analysis, including validation results to decide more informed how to deal with this issue. In the absence of systematic comparisons of different EO based rainfall data, we decided to use the TRMM data as an established and globally (up to 50° North and South) available rainfall data set with a – compared to GPCP data with 2.5° * 2.5° - relatively fine resolution of 0.25° * 0.25°, as mentioned above. CMORPH rainfall data with a nominal resolution of 8 * 8 km² were compared to the TRMM data, but often seemed to overestimate rainfall at least relative to the TRMM data, and also the yearly trends of both data sets deviate considerably (see chapter 4, section 4.2.4 for more information on the processing of the rainfall data).

3.6.7 Only look from above at regional scale

Projects such as the presented are intrinsically limited to the perspective from above and the moderate ground resolution of the EO data. Compared to many other projects the spatial resolution of the MERIS is very fine (e.g. compared to 8km NOAA GIMMS data), however when contrasted with local EO analyses and in situ information, the constraints become obvious. The advantage compared to the latter is the frequency of observations, which enables a quasi-continuous monitoring. For comprehensive assessments of dryland conditions, multi-scale approaches have to be applied, combining high and very high resolution imagery and in situ data with time series monitoring. In such a context, results from moderate resolution EO analyses can add valuable information not readily obtained by small scale and in situ studies, or by coarser resolution EO data.

3.6.8 Epochal changes and trends partly influenced by phenology

The rainfall and soil moisture have been tailored to the phenological periods derived with the fAPAR data. This means it may happen that if the start of the vegetation years varies on a small scale due to different land cover or vegetation, deviating rainfall (or soil moisture) periods might be observed, which exert different influences on the resulting trends (or epochal differences in case of the epochal rainfall difference products P46 and P47). With longer observation periods, this issue would be alleviated, but given the globally observed eight vegetation years only and the strong short term rainfall variability in drylands, it might happen that the phenology of the land cover itself is influencing the observed trend.

3.6.9 Validation of input data and final results

Validation is a key to acceptance of the products by the users, and this is the vital to the success of the project. The basic EO parameters, i.e. the MERIS based fAPAR values, have been validated using in-situ measured fAPAR data as well as modelled fAPAR data using the BETHY model developed by DLR. Further on, the TRMM rainfall data were contrasted with ground station values in Australia. All these validation efforts delivered satisfying results described in the ATBD of the Diversity II dryland methodology.

However, a remaining issue in the project is the fact that the final products cannot be quantitatively validated by in situ measurement and comparisons with the conditions on the ground in a comprehensive and systematic way due to the lack of respective reference data covering the same periods, and as this exercise would go much beyond this project.

None the less, we have performed several cross-comparisons and plausibility analyses, and demonstrated these in various sections of chapter 3. Furthermore, comprehensive comparisons of the results with faunal biodiversity are presented in chapter 5.

3.6.10 Diversity II products and land cover change

While it is known that a great part of changes and triggers of degradation in drylands are due to land use and land cover changes, we have not explicitly touched this topic. Urban growth, forest clear cuts, conversion of rangeland into croplands, etc., are all processes that were found to contribute to progressing land degradation and in general losses of biodiversity (see for instance Maitima et al. 2009, who present a detailed analysis of these relationships for eastern Africa), but we have not related or added (from other information sources) such changes to our results. The dryland products of Diversity II may be used to potentially contribute such information to other studies, especially when looking at products P51 or P52, or also when comparing trend products of the cyclic vegetation to those of the dry seasons. Many degradation processes, though, are not involving land cover or land use changes, but consist more of gradual productivity losses, or possibly increases in case of bush encroachment. Such processes are expected to be captured by Diversity II products, if they are not masked by the extreme variability of vegetation productivity during the short observation period.

The recently released CCI LC data (http://www.esa-landcover-cci.org/ may be used for comparisons with Diversity II trend and change products, especially the LC data of nominally 2005 and of 2010, which correspond roughly to the period covered by Diversity II.

We did some visual assessments of the CCI LC data of 2005 and 2010, but found hardly any changes in the dry lands. Therefore we concentrated on comparisons using the CCI LC status map of 2010 only.

3.6.11 Spatial aggregation of the results

Originally it was planned to provide spatially aggregated results in addition to the pixel based information in the indicator products. We had included a respective question in a user questionnaire, asking for the most appropriate criteria for aggregation, such as district boundaries, protected areas, aridity classes, land cover classes, etc. The answers were quite heterogeneous, indicating different priorities for product aggregation. The aggregation will take care of the true proportionality of the pixel size, e.g. by a cosine transformation. In addition, the parameters for aggregation, the method and the kind of presentation of the results have to be defined.

We will look at this issue and possibly provide some Web GIS based solution, but details are yet open.

3.6.12 Summary of possible product applications and major methodological issues

The presented product use cases provide a variety of possible applications of the products, which have been summarized in Table 9. In addition to the big two target topics of Diversity II Drylands, Biodiversity and Land Degradation, we have included various methodological questions, relating to comparisons of the MERIS fAPAR based results to those from other sources such as NOAA GIMMS NDVI. However, as should be stressed, regional vegetation time series products are never standalone solutions for these applications and the possible contributions listed in Table 9 must be understood accordingly.

Table 9: Summary of possible applications of Diversity Dryland products

Application Theme	Topics and questions	How Diversity II products may contribute	Suggested products
Biodiversity	Functional and structural biodiversity (status and trends)	• Land stratification • Trend/change analysis	P50 P57-P59
	Faunal species richness	• Input to species distribution models	1st order status products
	Plant species richness	• Specific analyses of protected areas, enclosures • Correlation with plant diversity data	1st order status products
	Bush encroachment, invasive species	• Seasonal trend differentiation • Investigation with in situ data	1st order trend products
	Land cover and land cover change	• Assist LC and LC change mapping	P50-P52 P57-P59

Land Degradation	Loss or gain of vegetation productivity	• Regional trend maps of vegetation productivity • Longer term trends with GIMMS NDVI • Local scaling approach based on land capability units	1st order trend products
	Interpretation of losses of vegetation productivity	• Derivation of areas were vegetation and rainfall trends are not matching > potential human causes	1st order trend products, P53-P55
	Interpretation of greening trends	• Seasonal trend differentiation • Investigation with in situ data	1st order trend products, P51, P52
	Land cover and land cover change	• Assist LC and LC change mapping	P50-P52 P57-P59
Methodological questions	Relationship between fARAP derived NPP proxies and NPP data	• Relation of MERIS fAPAR based products to modelled NPP data • Spatial variability of the relation	1st order status products
	Consistency of fAPAR and other biophysical variables / vegetation indicators	• Comparison of MERIS fAPAR based and MERIS NDVI based indicators • Spatial variability of comparison results	All products
	How similar are the MERIS fAPAR based trends to the widely used NOAA GIMMS NDVI trends?	• Trend comparison of MERIS fAPAR with NOAA GIMMS NDVI based trends	P33-P35

4 Overview of Algorithms and Processing

4.1 Overall processing scheme of the Diversity Dryland Products

The software to generate the Diversity II Products is complex and has to work on very large amounts of data efficiently. The processing chain includes steps from child product generation, cloud screening, atmospheric correction, bio-optical inversions, indices calculation, spatial and temporal integration, trend and change detection, indicator calculation, up to the final map generation. The production involves processing of more than 100 terabytes of input data. New algorithms have been developed largely using the ESA BEAM toolbox, for fAPAR generation and the pre-processing of all ancillary data.

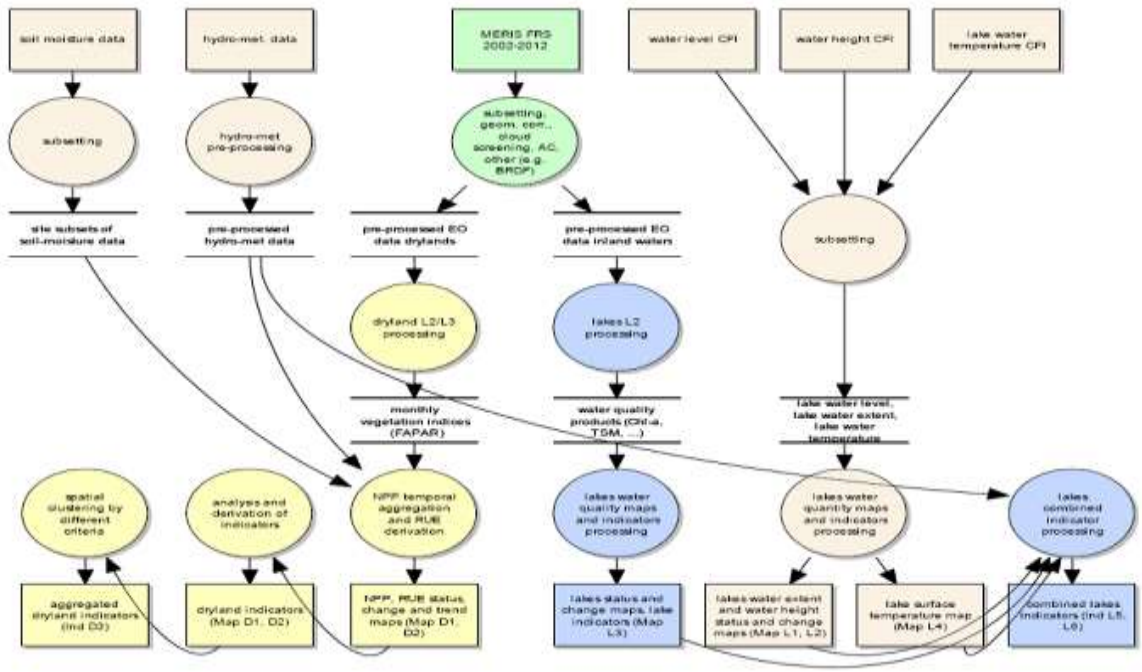

Figure 57: Overall processing overview of the Diversity II drylands and inland water products

The actual processing and generation of the dryland products was performed with ERDAS IMAGINE models, which have all been specifically developed for this purpose.

In the following section, an overview of the ERDAS based processing of the fAPAR and ancillary time series data is provided.

4.2 Pre-processing of fAPAR and ancillary data

The MERIS based input data were generated and the ancillary data were procured and pre-processed by Brockmann Consult with BEAM (except for the modelled NPP data). Utilised input data include:

1. MERIS full and reduced resolution (FR and RR) fAPAR data (all Diversity II sites)

2. MERIS full and reduced resolution (FR and RR) NDVI data (for test sites 04 Northern Kazakhstan and site 12, Southern Africa West for testing and comparing to fAPAR)

3. Modelled NPP data generated by DLR with the BETHY/DLR model (for test sites 04 Northern Kazakhstan and site 12, Southern Africa West for testing and comparing to fAPAR)

3. TRMM and GPCP rainfall data (GPCP only used from 50° N and S)

4. CCI Soil Moisture (SM) data

5. NOAA GIMMS NDVI data

6. Globcover (2009) and CCI (2010) land cover data

All ancillary data sets were output analogue to the NOAA GIMMS NDVI data grid with a grid spacing of 0.07272727 degrees (8 km), and geographic coordinates, WGS84.

4.2.1 MERIS full and reduced resolution (FR and RR) fAPAR data

The centrepiece of the analyses is MERIS based fAPAR data that have been generated with the algorithm of Gobron (2011), described in this Algorithm Theoretical Basis document (ATBD, Gobron 2011) and therefore not further specified in this document: "*The ATBD describes the Joint Research Center (JRC)- procedure used to retrieve information of absorbed photosynthetical radiation by the vegetated terrestrial surfaces from an analysis of the Top Of Atmosphere (TOA) data acquired by Medium Resolution Imaging Spectrometer (MERIS) on board ENVISAT*".

Temporal compositing of the single fAPAR values was performed using the maximum value within the halfmonthly time intervals for the generated time series data.

The acquisition frequency of MERIS RR (1200m * 1200m) data was higher than that of FR (300m *300m) data, and the latter had sometimes gaps where still RR data were available. These gaps were filled with RR fAPAR data where possible. Figure 2 shows the global availability of MERIS FR data, where it can be seen that especially in South America the FR coverage is reduced, but also to some degree in parts of Australia and southern Africa, and in general in 2003 and 2002. Further gap filling was performed using a linear approach applied in two iterations (see section 4.3.1). Metadata for all halfmonthly data sets are made available indicating the filled and remaining gaps. The MERIS fAPAR data and all further input data were used as half-monthly time series data without smoothing.

4.2.2 MERIS full and reduced resolution (FR and RR) NDVI data

NDVI data were derived based on the method of Günther at al. (1999), who proposed a band weighting approach in order to make the MERIS NDVI as compatible as possible with the NOAA GIMMS NDVI. The method is described in the ATBD by Günther at al. (1999). Temporal compositing was also performed with the maximum method for halfmonthly time steps, and all further pre-processing steps were the same as those applied to the fAPAR data.

As the MERIS fAPAR data were used as the main source for the Diversity II products, the MERIS NDVI data were only processed for two exemplary sites. These were site 04 Northern Kazakhstan and site 12, Southern Africa West. The results were compared to the fAPAR based results. Examples are shown in section 4.4.6.

4.2.3 Modelled NPP data based on BETHY/DLR

Also for test sites 04 Northern Kazakhstan and 12, Southern Africa West modelled NPP time series data have been processed and compared to the MERIS based indicators. The NPP data were derived with the most recent version (spring 2015) of BETHY/DLR (Biosphere Energy Transfer Hydrology Model, DLR), and provided by M. Tum and K. Günther (DLR).

As already described in chapter 3 (section 3.5.3) BETHY/DLR is a soil-vegetation-atmosphere-transfer (SVAT) model that was modified to the usage with meteorological and EO based vegetation time series data (Wißkirchen et al. 2013, Tum 2012). BETHY/DLR has been tested for several regions in the world. It is used at DLR to estimate sustainable bioenergy potentials. It employs remote sensing products (Albedo, LAI, Landcover, CO_2 concentration, elevation), meteorological parameters (Wind speed, Temperature, Precipitation, PAR), climatic zones, and static data, i.e., soil types. Figure 58 provides an overview of the input data used. BETHY/DLR is currently assessed at continental to country scales.

The BETHY NPP data were generated as monthly NPP sums in grams C/m² and 1km² pixel size (at the equator). For comparisons to the MERIS fAPAR derived NPP proxies, they were converted into half-monthly values and

300m*300m pixel size, and then aggregated into sum values per vegetation year, starting from 2003 and ending 2010, exactly like the MERIS fAPAR based NPP proxies.

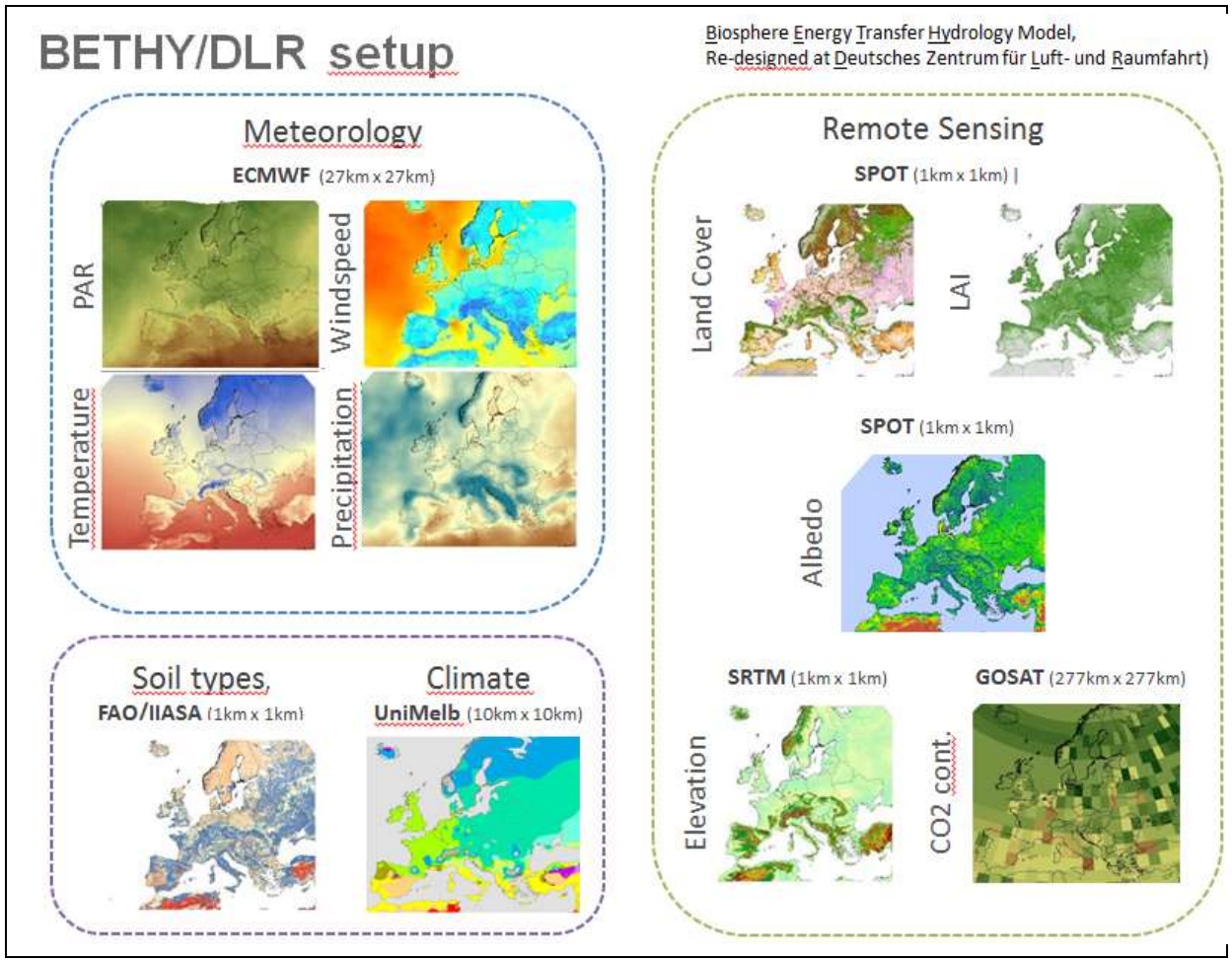

Figure 58: Input data used for BETHY/DLR, overview provided by M. Tum, DLR

4.2.4 Rainfall data

TRMM rainfall data[12] with an original grid spacing of 0.25° were the main source of precipitation estimates used in Diversity II. TRMM 3B42 data were summed to halfmonthly values and the small number of remaining gaps was filled with TRMM 3B43 data. Beyond 50° N and S, GPCP v2 data[13] (original grid spacing of 2.5°) were mosaicked with the TRMM data after breaking down these monthly data to halfmonthly values. Thus in the respective test sites mixed rainfall data are being used, as it was preferred to exploit the TRMM data with their significantly better resolution to the maximum extent. As mentioned earlier, also CMORPH[14] rainfall data were checked, as they have a relatively high spatial resolution (a grid spacing of 8km at the equator[15]). However they

[12] http://pmm.nasa.gov/trmm

[13] http://precip.gsfc.nasa.gov/

[14] http://www.cpc.ncep.noaa.gov/products/janowiak/cmorph.shtml

[15] *"With regard to spatial resolution, although the preciptation estimates are available on a grid with a spacing of 8 km (at the equator), the resolution of the individual satellite-derived estimates is coarser than that - more on the order of 12 x 15 km or so" (http://www.cpc.ncep.noaa.gov/products/janowiak/cmorph_description.html)*

were derived exclusively from satellite data, and were found to deviate substantially and inconsistently from the TRMM data, while TRMM and GPCP data deliver more comparable rainfall estimations. Hence, CMORPH data were not used for the generation of the Diversity II products.

TRMM/GPCP rainfall data served for deriving Rain Use Efficiency (RUE) indices, i.e. first order status and trend indicators.

4.2.5 CCI Soil Moisture data

CCI soil moisture v2.0 data[16] (see also Dorigo et al., 2012) was used for all test sites as an alternative data set for the availability of water. Halfmonthly time series were derived from the originally daily SM data by averaging valid daily values. The data were transformed from an original spatial resolution of 0.25° in the 0.07272727° cell size grid of the GIMMS NDVI data.

The soil moisture data were used in an analogue way to the rainfall data in order to relate vegetation development to soil moisture, derive "Soil Moisture Use Efficiency" (SMUE) status and trend indicators and compare the results to the RUE products.

4.2.6 NOAA GIMMS3g NDVI data

NOAA GIMMS NDVI data[17] (Tucker et al. 2004) version 3g were quite extensively used in the project for several reasons and purposes:

- This data has been investigated in a large number of studies, which provide useful reference information to this project
- Vegetation trends of NOAA GIMMS derived in Diversity II have been compared to the MERIS fAPAR based trends (see 3.5.10) to check the consistency of the applied methods
- For demonstrating past trends prior to the period with MERIS data and comparison of the developments within the MERIS periods to the preceding 20 years.

4.2.7 Globcover (2009) and CCI (2010) land cover data

Globcover land cover data from 2009[18] were used for masking water areas in the Diversity II products. Further on, CCI LC data[19] from 2010 (based on EO data from 2008-2012) have been visually contrasted with Diversity II products in several test sites.

4.3 Drylands algorithms and processing

The dryland algorithms were developed with the ERDAS Model Maker of the ERDAS versions 2013 to 2015. In the course of the project, the models were translated in the newer ERDAS Spatial Model Editor. Implementation of the final processing chains with batch routines was performed with model scripts in ERDAS 2014 and 2015. Figure 59 shows a flow diagram of the production chain.

As opposed to the common notion of doy (day of year), the Diversity derived temporal parameters refer to half-monthly periods.

The yellow box in the flowchart highlights the phenological parameterisation of the time series data, which was stressed throughout this document as the fundamental approach to deriving the Diversity II indicators. All products are based on these parameters. Beyond the actual phenological parameters used for the product

[16] http://www.esa-soilmoisture-cci.org/

[17] http://glcf.umd.edu/data/gimms/

[18] http://www.esa.int/Our_Activities/Observing_the_Earth/Envisat/ESA_unveils_latest_map_of_world_s_land_cover

[19] http://www.esa-landcover-cci.org/

generation, additional parameters were generated, which served mainly for internal analyses. They can be potentially used for further investigations and the generation of additional indicators, and can be made available to interested users on request. These additional parameters are listed in Table 11.

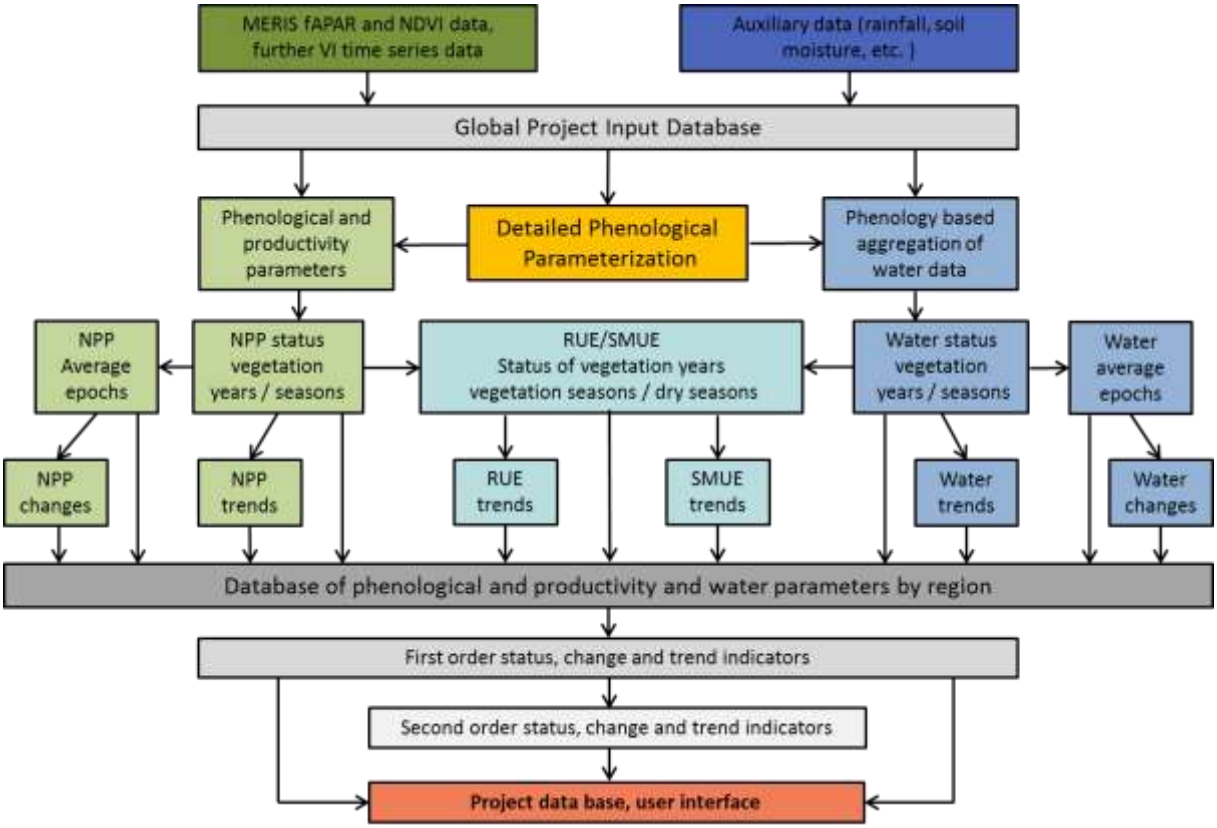

Figure 59: Simplified processing scheme of the Diversity II dryland products. Water status/change refers to rainfall and soil moisture as parameters for water availability, RUE/SMUE refers to Rain Use - and Soil Moisture Use Efficiency.

4.3.1 Gap filling of fAPAR data

After the initial filling of MERIS FR fAPAR with MERIS RR fAPAR data, remaining data gaps were filled using a two-sided weighted linear trend extrapolation approach. This means, the gradients on both sides of data gaps (> one halfmonth) were extrapolated toward the outer values of the gap. On both sides, i.e., before and after a gap, the two adjacent gradients were used and differently weighted in order to derive weighted mean gradients. Two iterations were applied (filling the first and the last gap of a longer gap series each). Prior to, in between and after these two iterations, gaps of single halfmonths were filled by linear interpolation. This way, gaps of up to five halfmonths have been filled (with ERDAS, i.e. without the necessity to transform the data in order to use other gap filling tools), which was sufficient for all but one test site, i.e. site 15, Caatinga in Brazil.

Timesat software, a freeware of the University of Lund (see manual by Eklundh and Jönsson 2012), was tested and applied in this site for filling remaining gaps with the Savitzky–Golay filter after application of the above procedure. When directly applying the Savitzky–Golay filter to the data, the data gaps were too large and frequent in this particular test site to be properly filled with the Savitzky–Golay filter.

Pixels that had remaining data gaps after the gap filling procedure were discarded from the results and as no data values in the indicator maps.

The metadata provide exact information for each single fAPAR (and MERIS NDVI) data value, whether it is an original (FR or RR) value, or has been gap filled.

4.3.2 Special processing of test sites with data gaps due to snow

Snow cover or other winter conditions without measured fAPAR was observed and specially treated in 13 out of 22 test sites during the local winter time (see Table 10).

Table 10: Test sites with and without (or neglected) snow cover

Test sites with snow cover	Test sites without snow cover
03 South West Iran	01: Northern - Central Mexico
04 Northern Kazakhstan	02: Northern Australia
05 E Mongolia W Manchuria	07 Southern India
06 Central Tibetan Plateau	11 Eastern Africa
08 Pontic Steppe	12 Southern Africa West
09 Northern Africa	13 Western Sahel
10 Southern Europe	15 Caatinga, Brazil
14 Southern Argentina	20 Southern Australia
16 Western South America	21 Southern Africa East
17 Southern Central USA	
18 Northern USA Southern Canada	
19 South West USA	
22 Eastern Mediterranean Countries	

When generating the fAPAR data, snow and clouds resulted in undifferentiated no-data values, i.e. data gaps. While the data gaps related to clouds and rainfall during the growing season could be closed with the above described procedure for the most parts, it was neither appropriate nor possible to close the data gaps related to snow cover or other winter related conditions without plant growth. In parts of the regions with snow cover in the winter time the snowy periods (including winter clouds and frozen soils) caused data gaps extending through several months. These data gaps had to be identified as “winter gaps” in order to treat them properly and to use the remaining valid data and not discard these pixels due to extensive data gaps.

fAPAR data gaps with potential snow cover and/or clouds (during the winter season) were derived by labelling respective data gaps as snow based on the following assumptions:

- Continuous data gaps starting at the begin of the calendar years on the northern hemisphere, or starting in July on the southern hemisphere, were classified as snow
- Any data gaps occurring during the first seven and last five halfmonths, i.e. on the northern hemisphere from January to mid April, and from mid October to end of December (in the South shifted by half a year), were classified as snow.

These temporal limits were derived by checking the data gaps in the respective test sites and studying meteorological information about the test sites. Prior to the next step, i.e. the derivation of the Start of Season, the data gaps classified as snow were set to zeroes. For the later calculation of the vegetation productivity, the snow values were assigned the estimated dry (cold) season mean values of the respective vegetation years, in order to not overestimate the fAPAR averages of the vegetation years (relative to pixels not concerned by snow cover) by calculating the means only for the valid values during the vegetation season, or to underestimate the averages by counting the snow gaps as zero values.

4.3.3 Derivation of the Start of Season of Vegetation Years and estimation of the baseline

For the description of the methods for deriving vegetation phenology and productivity parameters, in Figure 60 the scheme already shown in Figure 3 is displayed again.

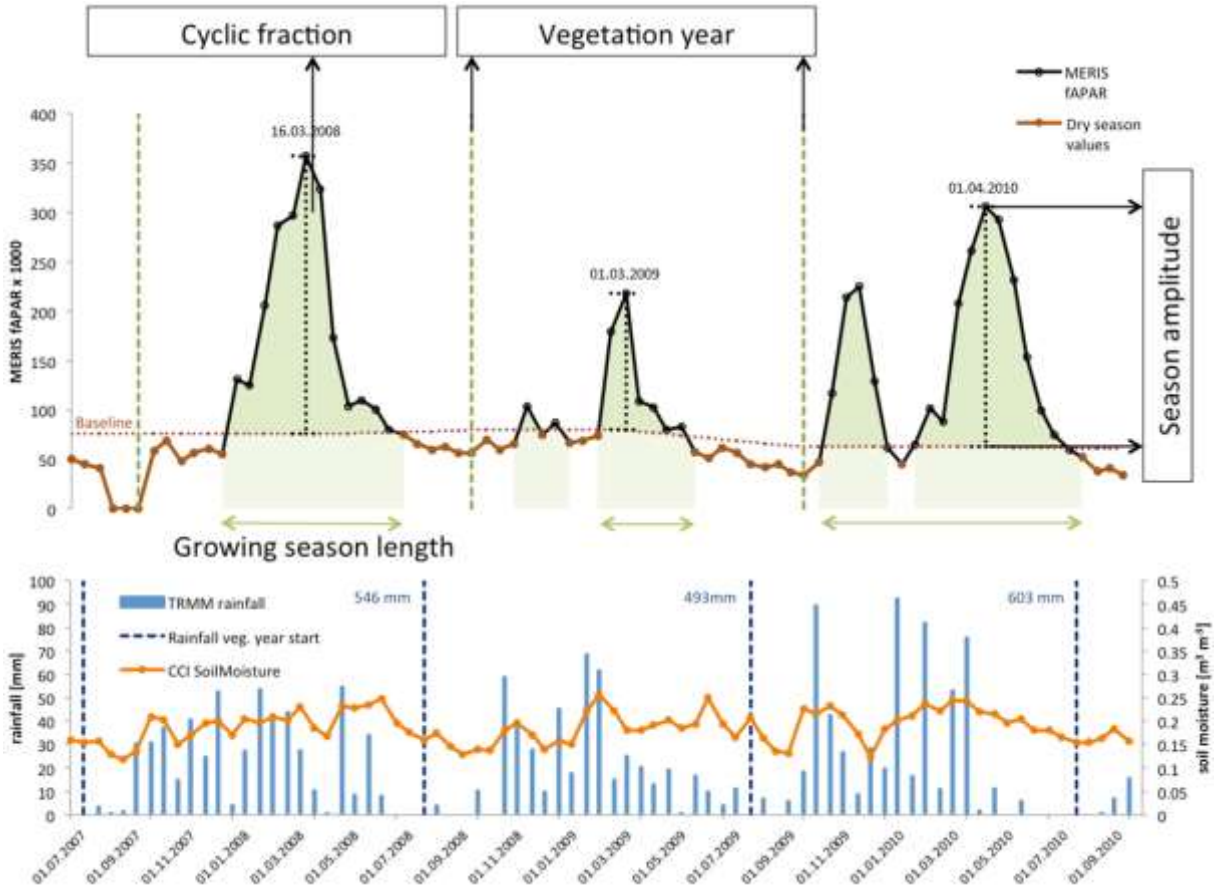

Figure 60: Scheme of the extracted phenological descriptors and periods, and corresponding rainfall and soil moisture data. Location: South Africa, Y: -29.896337, X: 25.7373764 (same as figure 3)

Start of the Season

The Start of the Season (SoS) is the key phenological parameter, which provides access to many further phenological properties and data of a location. Yet it is differently defined and calculated by different authors with consequently deviating results, as demonstrated by White et al. (2009) for various approaches.

Within the Diversity II test sites, a large variety of phenological conditions was met both in spatial and temporal respects. Hence, the method for deriving the start of the vegetation season had to cope with a wide range of SoS conditions, including sharp to weak increases of the vegetation signal, big to very small and hardly recognisable vegetation peaks, unimodal vegetation curves and multiple SoS per year, and all combinations of the above. The commonly applied “Timesat” software (Eklundh and Jönsson, 2012) would have required a great deal of individual, test site (and possibly sub-site) specific parameter tuning and was therefore not used.

Another approach for calculating phenological and productivity parameters is described by Ivits et al. (2013), who developed the “Phenolo” software at the EC Joint Research Centre. Phenolo derives a full range of phenology and productivity parameters and is globally applicable without regional adaptations. The basic principle of the SoS derivation of Phenolo is a time lagged moving average filter and the extraction of the intersection points of the filtered time series with the actual time series, which mark the turning points (start and end of season) of the trends. The length of the required filter window is spatially and temporally variable (even within years) and is automatically determined on a yearly basis by Phenolo (Ivits et al. 2013). Consequently, the adaptive length of the moving window is the key factor of this approach. Phenolo uses smoothed time series data (Savitzky–Golay filter with 4th polynomial degrees) and interpolates the data to daily values.

In Diversity II, as said before, half-monthly, unsmoothed time series data were used and processed with specifically developed ERDAS IMAGINE models. Only for the derivation of the SoS, a slight smoothing was applied by linearly interpolating low outliers (values lower than their neighbours by more than 5% of the amplitude of the underlying fAPAR values within the time period considered, i.e. three years). In order to automatically cope with all global conditions, we developed a method that is very sensitive to any increases in the vegetation curve in order to minimise the number of missed SoS. At the same time, vegetation peaks considered too small or of too short duration could be discarded by respective fine-tuning of the method. Basically, a three-step procedure was applied:

1. First, for each year, the timing of all potential SoS was derived based on the cumulative gradients of the fAPAR or NDVI time series. The moving sum values of six consecutive increments were derived, which create peaks, whose temporal position and size were used to determine the SoS. By means of further fine-tuning, the SoS was defined to occur right at the start of the respective vegetation increase period. This led to a 24 layer raster file per calendar (one layer per halfmonth) year indicating for every halfmonthly value if there was a SoS or not. It was derived for the years from 2003 to 2011, for which full MERIS coverages were available.
2. In the second step, the temporal ranges of the most frequent SoS accumulations during these nine years were determined. The starts of season within these ranges were taken as the “dominant” SoS group, which constitutes the local start of the vegetation year. In cases where no SoS had been derived for a given year or several years within the defined range, the mean SoS of the other years was used for substitution. This way, singular SoS (not occurring in temporal clusters) could be discarded, and missing SoS in extremely dry years substituted. In regions with two (or more) growing seasons per year, in many cases not all of their SoS were detected in all years. Consequently, within one of the resulting temporal SoS ranges, the number of SoS derived was higher than in the other(s). This SoS group constituted the dominating SoS group. If two SoS groups were detected in the same number of years, the first within the calendar year was taken as the dominant SoS.
3. In the third step, the single year SoS were smoothed in the following way: the mean of the SoS of the previous and following years was derived for each SoS, and the SoS of a particular year was replaced by the mean of its “neighbours” if the mean was earlier than the actually determined SoS. This way, an overly varying length of the vegetation years from year to year could be avoided. This is relevant for the calculation of the average fAPAR (NDVI) per vegetation year. Without the smoothing, the greenness of vegetation years with a late SoS followed by a vegetation year with an early SoS (this fluctuation was found to be typical) would be overestimated, as it would include a much shorter dry season.

Calculation of the baseline

Besides the SoS, the “baseline” is a crucial parameter in the presented concept of vegetation phenology and productivity, as it separates dry (or cold) season values from the cyclic vegetation and determines the amount of the “cyclic vegetation”, as well as the size of the “amplitude”.

The probably most commonly applied and very straight forward approach for deriving the baseline is realised in the Timesat software package (Eklundh et al. 2010). It defines the baseline as (user adjustable) threshold in percent of the amplitude given by the minimum level and the vegetation peak maximum, e.g., typically using 20% or 25% of the amplitude as threshold. I.e. when the vegetation curve reaches this level, the growing season would start. The cyclic vegetation is calculated as integral of the time series curve above this baseline (called “small integral” in the Timesat software). We have first taken a similar approach, and compared the outputs to Timesat derived outputs (for the cyclic vegetation alias “small integral”), resulting in pearson $r^2 > 0.9$ in most cases.

However it turned out that the resulting baseline may vary quite strongly from year to year and did sometimes not well reflect the upper dry season boundary, which we felt would represent the baseline. Thus, for using the

dry season average values as explicit parameter (the Timesat concept does not explicitly consider the dry season level as a parameter), some other determination of the baseline appeared more appropriate.

We developed an approach based on an estimation of the mean amplitude of two consecutive vegetation years and its relation to the estimated mean value of the smallest values in between these maxima. This relation, expressed in a linear regression equation, determines the upper threshold of low values that are included in the estimation of the baseline. The average and the standard deviation of the included low values were derived (taking the threshold itself as a low value for cases with only zeroes as low values). The baseline was then determined by adding the standard deviation, multiplied by 1.5, to the average value. The base values of consecutive years were interpolated to obtain a smooth baseline, which should represent the approximate upper boundary of the low season values with smooth transitions from one vegetation year to the next. Only if the maxima of the two consecutive years differed very strongly, such that the second year's maximum was less than half or more than double the preceding year's maximum, a separate base value for the second year was determined. Hence, in most cases the transitions of the baseline from one vegetation year to the next have smooth gradients, aimed at building an appropriate upper boundary for the dry season values included.

4.3.4 Definition of phenological and productivity parameters

The "vegetation year" constitutes a statistical SoS based time frame, used for temporally referencing all further phenological parameters derived from the vegetation times series data. The vertical green dashed lines in Figure 60 mark the starts of the vegetation year in the shown example. As mentioned earlier, the Diversity derived temporal parameters are expressed in half-monthly values.

A wealth of phenological and productivity parameters was extracted (see Table 11), which all relate to the temporal frame of the local vegetation years. However, only the highlighted parameters have been actually used for generating the Diversity II products, as they were regarded as the most important parameters, and in order to avoid an overload of products.

All parameters are stored as raster data and were derived for:

- MERIS based fAPAR data for the 22 globally distributed Diversity II test sites (Figure 1) covering the period from 2002/June to 2012/April
- MERIS based NDVI data for Diversity II test sites 04 Northern Kazakhstan and site 12, Southern Africa West covering the period from 2002/June to 2012/April
- NPP data provided by DLR, using the BETHY/DLR model 2003-2010, test site 04 Northern Kazakhstan and site 12, Southern Africa West, and
- NOAA GIMMS NDVI data (globally, 1982-2011)

Table 11: Major phenological and productivity parameters derived for each pixel (highlighted parameters are directly used in the Diversity II products)

No.	Phenological and productivity parameters	Description
1	Start of Season (SoS)	Turning points at the start of vegetation peaks with a defined minimum length (see section 4.3.3)
2	Dominant start of vegetation year	The average timing of the most frequently occurring SoS group, derived from (1)
3	Yearly start of the vegetation year	The specific SoS of single years within the dominant SoS group. If in a particular year no SoS was derived during the time period of the dominant SoS group, the average (2) is taken (see section 4.3.3)
4	Vegetation year average greenness	Average yearly fAPAR (NDVI): proxy for the annual vegetation productivity within the period between two yearly SoS (3). This

		parameter interferes with biomass estimation to an unknown degree, depending on the structure of the vegetation canopy and the activity throughout the year. In test sites with fAPAR (NDVI) data gaps due to winter conditions (snow, frozen ground, clouds), the estimated average cold season level of the fAPAR values were filled in the gaps in order to make the yearly averages of those pixels better comparable to pixels where no winter-gaps were present. Otherwise the average greenness of the vegetation year may be underestimated (if the "winter gaps" are included in the average), or overestimated, if they are not included.
5	Baseline	Threshold line separating the growing season from the dry or cold season base values. It is defined based on the amplitude and the average dry (cold) season values (see 4.3.3) and delineates approximately the upper limit of the dry (cold) season values.
6	Start of growing season	Time when the baseline is surpassed on the way from the dry (cold) season to the (first if more than one) peak
7	End of growing season	Time when the curve falls the last time within the vegetation year under the baseline
8	Overall cyclic vegetation	Sum of all values above the baseline; from every value the baseline is subtracted
9	Length of overall cyclic vegetation	Number of half-months from the first value above the baseline to the last value above the baseline
10	Start of growing season excluding very small and short peaks	Time when the baseline is surpassed on the way from the dry (cold) season to the (first if more than one) peak, not considering very small and short peaks (see (14) for definition of "small" and "short" peaks)
11	End of growing season excluding very small and short peaks	Time when the curve falls the last time within the vegetation year under the baseline not considering very small and short peaks (see (14) for definition of "small" and "short" peaks)
12	Cyclic vegetation from start of growing season to maximum	Sum of all values above the baseline prior and including the maximum value; from every value the baseline is subtracted
13	Cyclic vegetation from maximum to and of growing season	Sum of all values above the baseline after the maximum value; from every value the baseline is subtracted
14	Cyclic vegetation without very small and short peaks	Sum of all values above the baseline excluding very small and short peaks; from every value the baseline is subtracted. Small is defined as peaks including not more than five percent of the overall cyclic fraction sum; short is defined as peaks no longer than 2 half-months.
15	Length of cyclic vegetation without very small and short peaks	Same as (9) minus the number of half-months with very small or short peaks.
16	Dry season average	Average of all values after the end of the growing season
17	Dry season average including very small and short peaks	Same as (16) including values of very small or short peaks (see (14) for definition of "small" and "short" peaks)
18	Time of Maximum	Number of half-month with the highest value within the vegetation year relative to the start of the vegetation year

19	Maximum value	Highest value of the vegetation year; if there are two or more equal maximum values, the earliest is taken
20	Amplitude	Difference between maximum and baseline value at the time of maximum
21	Number of peaks	Number of peaks within the vegetation year; a peak is defined as a maximum within 11 halfmonths that is larger than (or equals) the minimum value of the vegetation year plus 25% of the amplitude
22	Time of peaks	The numbers of half-months with defined peaks (19) relative to the start of the vegetation year
23	Percent of cyclic vegetation sum of vegetation year sum values	This percentage reflects the share of annual vegetation of the overall greenness of the vegetation years and has, along with (4) been used for the derivation of second order indicator P50: Functional Classes

The parameters not directly used for the product generation are potentially useful for further analyses and were stored in the project outputs accordingly.

4.3.5 Temporal aggregation of rainfall and soil moisture data

The rainfall and soil moisture data were aggregated based on the phenology of the vegetation index time series data they were used for. Thus for relating rainfall and soil moisture to the MERIS fAPAR based NPP proxies, the MERIS fAPAR derived parameters were used, whereas for MERIS NDVI the phenological parameters generated with the MERIS NDVI were used, and for the GIMMS NDVI data the GIMMS based phenology parameters, respectively. Only for the modelled NPP data the phenology parameters of the vegetation time series data the NPP data were contrasted with were used, in order to cover the same periods for the comparison.

Rainfall and soil moisture data were aggregated into two periods:

1. The vegetation year, where sum values for the rainfall data were derived, and average values for soil moisture. The time for the aggregation of the rainfall data was shifted back by two month prior to the start of the vegetation year, the period for the soil moisture data was shifted back by one month. Both temporal shifts were defined based on visual comparisons of the time series data and on various experiences with such time lags (see also Figure 60).
2. The second aggregation period starts at the same time as that of the vegetation year, but ends at the end of the growing season. The rainfall sums and soil moisture averages of this period were compared to the cyclic vegetation.

4.4 Dryland product generation

The dryland products have been generated as classified products with globally consistent classes and colour schemes. Also between the different products consistency was maintained in colour schemes and the number of classes. The products contain averages, trend slopes, epochal changes and phenological parameters calculated for the eight vegetation years worldwide covered by the MERIS data. The start of the vegetation years ranges globally from January 2003 until December 2010, depending locally on the average timing of the dominant SoS group and the individual yearly (smoothed) SoS within this SoS range.

The original fAPAR (and NDVI) values have been multiplied by 1000, and these values are the ones contained in the legends of the products. Thus the product class legends do not refer to the original data values, as these would often have been very small and therefore not easily readable.

Table 3 provides an overview of the organisation of the first order products, in Table 4 the second order products are summarised, Table 5 lists the phenology products, and Table 6 contains all generated products.

4.4.1 First order status indicators

The first order status products indicate the average and the variability of the respective parameters through the eight vegetation years (n=8). All parameters are classified into 26 classes each. For variability, coefficients of variation were calculated in percent, i.e. the standard deviation is put in relation to the mean. The variability classes derived for every parameter were given the same colours as the averages, but in the opposite sequence. This reflects the fact that in drylands rainfall variability and thus essentially also the variability of primary productivity largely increases with decreasing mean annual rainfall. Examples can be seen e.g. in Figure 24 and Figure 25.

4.4.2 First order trend indicators

The trends were calculated with the Theil-Sen trend (TS) median slope trend analysis, which calculates the median slope of all pairwise combinations over time. The Theil-Sen method was chosen because of its resistance against outliers which makes it especially suited for trend estimations in short and noisy time series (Fensholt et al. 2013). Statistical trend significance was tested with a Mann-Kendall significance test generating z scores, which are thresholded to only include trend slopes above or below a selected minimum significance. The chosen confidence level was 90%, resulting in a z-sore of +/- 1.645 for a two-tailed test. I.e. for the trend to be significant at p=0.90, z-scores had to be larger than + 1.645 (positive trends) or smaller than – 1.645 for negative trends. The Mann-Kendall significance test as a non-linear trend indicator measures the significance (z-scores) of a monotonic trend but is commonly used as a trend test for the (linear) Theil-Sen trend slope estimator (Fensholt et al. 2013).

The outputs of the trend analyses are trend slope images (raster files), where the slope values indicates the average absolute yearly trend. These continuous slope figures were classified into six positive and six negative trend slope classes each. One tenth of the trend slope class interval was taken as lower threshold for displaying trends. Examples of trend slope maps are provided for instance in Figure 30.

All trends of the MERIS fAPAR, MERIS NDVI and the modelled NPP data were calculated this way, whereas the NOAA GIMMS NDVI trends were derived with the ordinary least square (OLS) regression method. Results of both methods are contrasted in Figure 39 using on MERIS fAPAR data, while Figure 40 to Figure 46 compare MERIS fAPAR trends (TS) to NOAA GIMMS NDVI trends (OLS) for various test sites.

The yearly rainfall sums and those for the growing season were slightly smoothed prior to the indicator calculation: every yearly value was replaced by a weighted average of the prior value (*0.5) and the current (*1) value. This was done in order to account to some degree for the known “memory effect” of ecosystems, i.e. to react on rainfall amounts of the previous year(s) in addition to the rainfall of the current year. This memory effect was studied for instance by Zhou (2013) or Martiny at al. (2005).

4.4.3 First order epochal change indicators

Epochal difference products were derived for rainfall and soil moisture only. As already mentioned, trends in vegetation productivity are often co-occurring with epochal rainfall (and soil moisture) changes, and not just linked to steady trends of water availability. The epochal change products of the water parameters thus often better reflect the relation of vegetation trends to changing water budgets than year-by year water trends alone. The above mentioned “memory effect” of ecosystems is an expression of the relation between vegetation productivity and water availability beyond the current year.

For the epochal change products, the eight vegetation years were divided into two epochs, the first from 2003 to 2006, and the second from 2007 to 2010. The average amounts of rainfall and the average soil moisture of the two epochs were calculated and the resulting mean values of the first epoch were subtracted from the mean values of the second epoch. The resulting difference values were like the trend slopes classified into six positive and six negative difference classes each. They express the difference of the average rainfall/soil moisture between the two epochs. The class intervals are, as mentioned above, globally standardized and

exhibit substantial epochal differences worldwide, the biggest reaching over 200 mm epochal decrease or increase of rainfall per year. Examples can be seen in Figure 30, as well as in Figure 41 to Figure 46 along with vegetation trends.

4.4.4 Second order status, trend and change indicators

For the second order indicators, with one exception (P52) no more than two first order indicators were combined per indicator to keep them simple. The kind of combinations have been described in chapter 2, section 2.2.3 with an overview table (Table 4).

Only one second order status indicator was defined: P50 Functional Classes, constituting a combination of first order status indicator P01 Vegetation year average greenness 2003-2010, and the mean percent of cyclic vegetation of vegetation year greenness (sum) 2003-2010 (parameters (4) and (23) in Table 11).

This indicator product was presented and compared to the CCI land cover map 2010 and to SOTER data in chapter 3, section 3.5.5. The indicator was derived by dividing the two inputs into class intervals and combining the derived classes. The class intervals used are listed in Table 12. The Functional classes 1 to 5 for example include average vegetation year fAPAR values from 17 to 85 each (fAPAR * 1000), and are further subdivided into percentage classes of the cyclic vegetation of the yearly fAPAR sum ranging from ≤ 30 to > 60. The intervals of these percentages are somewhat lowered in the higher productivity classes 16 to 25.

The indicated class intervals were equally applied to all test sites. As this product is derived with a simple thresholding approach, it can be easily modified and is fully reproducible. For these reasons the second order products were all conceived as simple first order product combinations.

P50 was called “Functional Classes”, as it integrates the two major characteristics of vegetation productivity: amount and seasonal distribution. The results resemble to a high degree LC class patterns and may be used for land cover and ecosystems classifications.

All other second order products are change or trend products (P51 – P56). P51 is an epochal change indicator of the above specified second order status product P50. This means, the inputs for P50 were calculated for the two epochs 2003-2006 and 2007-2010, respectively, and the resulting classes of the two epochs were subtracted from each other. The derived epochal differences were put in relation to each other only considering the direction of the change combinations (and not the size of the changes). An example of product P51 is shown in Figure 32, where it is contrasted with P52, which exhibits the seasonal trend relation.

The latter, like all remaining second order MERIS based products (P52 – P55) is a trend relation product, where the trend directions (not considering the slopes) of two (only P52: three) variables are combined. Hence, the calculation method is also straight forward and fully repeatable with other data or for other periods.

While in P52 vegetation year average trends are combined with cyclic vegetation and dry season trends, in products P53-P55 rainfall trends are combined with yearly and seasonal NPP proxy trends.

Product examples for P53-P55 are shown and commented in chapter 3, section 3.5.7, containing Figure 33 to Figure 35. As a short background, these products were developed in order to integrate vegetation productivity trends and rainfall trends, and to highlight trend areas where rainfall and NPP proxy trends diverge. Consequently this type of products is a synoptic trend product combining the major driver of NPP trends in drylands, i.e. water, with NPP proxy trends. Negative NPP proxy tends which are not coinciding with negative rainfall trends (or areas with positive rainfall trends and missing positive or even negative NPP proxy trends) may point to potentially degraded areas, analogue to RUE, but showing separately the developments of each single parameter.

The problems of RUE and also of the RESTREND method (Wessels et al. 2012) are shortly discussed in section 3.5.7 and in chapter 7, as they build the rationale for the developed rainfall/NPP proxy trend relation products.

Table 12: Aggregations of input parameters for second order product P50: Functional classes

Functional classes	Average vegetation year greenness (= product P01)	Average percent of cyclic vegtation of yearly fAPAR sum
26	< 17 sparse vegetation	
1	17-85	< = 30
2		30 - 40
3		40 - 50
4		50 - 60
5		> 60
6	85-153	< = 30
7		30 - 40
8		40 - 50
9		50 - 60
10		> 60
11	153-221	< = 30
12		30 - 40
13		40 - 50
14		50 - 60
15		> 60
16	221-289	< = 25
17		25 - 35
18		35 - 45
19		45 - 55
20		> 55
21	> 289	< = 20
22		20 - 30
23		30 - 40
24		40 - 50
25		> 50

4.4.5 Phenology indicators

Products P57, P58, and P59 are phenology products, whose content was explained in chapter 2, section 2.2.4. They show average conditions of the SoS (start of the vegetation year, P57), the length of the growing period (P59) and the start of the growing season (P58). These parameters are explained in Table 11. For P57, the median of all SoS was taken, while for P57 and P58 rounded average values were derived.

4.4.6 MERIS based NDVI products

For two test sites, 04 Northern Kazakhstan and site 12, Southern Africa West, respectively, the entire product suite was generated with MERIS NDVI data in addition to the fAPAR data. Short background information about the MERIS NDVI is given in section 4.2.2, and in chapter 3, section 3.6.3 some MERIS NDVI based results are contrasted with the fAPAR outcomes.

4.4.7 GIMMS NDVI based products

With P56 one GIMMS NDVI product was added to the MERIS based product suite of Diversity II. P56 is a second order trend relation product, combining GPCP rainfall trends with NDVI trends 1982-2002, i.e. in the period prior to the MERIS epoch. P56 enables trend comparisons between the MERIS epoch (P53 trend relation of the vegetation year greenness and rainfall based on MERIS fAPAR 2003-2010) and the 20 years before. An example for P56 is shown in Figure 36.

As stated by de Jong et al. (2013) and illustrated in Figure 49, at and after the turn of the millennium worldwide many trend breaks of the vegetation productivity can be observed. Indeed, when comparing P53 and P56 in the various test sites, the differences between these two trend periods are in most cases quite obvious.

In Figure 61 P56 and P53 are contrasted for test site 21, Southern Africa East to demonstrate an example using trends of vegetation year average values. It can be seen that the two trend periods exhibit predominantly different yearly trends of both rainfall and vegetation productivity. Especially the border region between Botswana, Zambia and Angola had strong negative vegetation trends (without corresponding rainfall trends) over the 20 years prior to MERIS, which are not continued during MERIS. Note that the light green and light pink classes are not actual NPP proxy trends, but contain areas with negative or positive rainfall trends that are not matched by NPP proxy trends in the same direction.

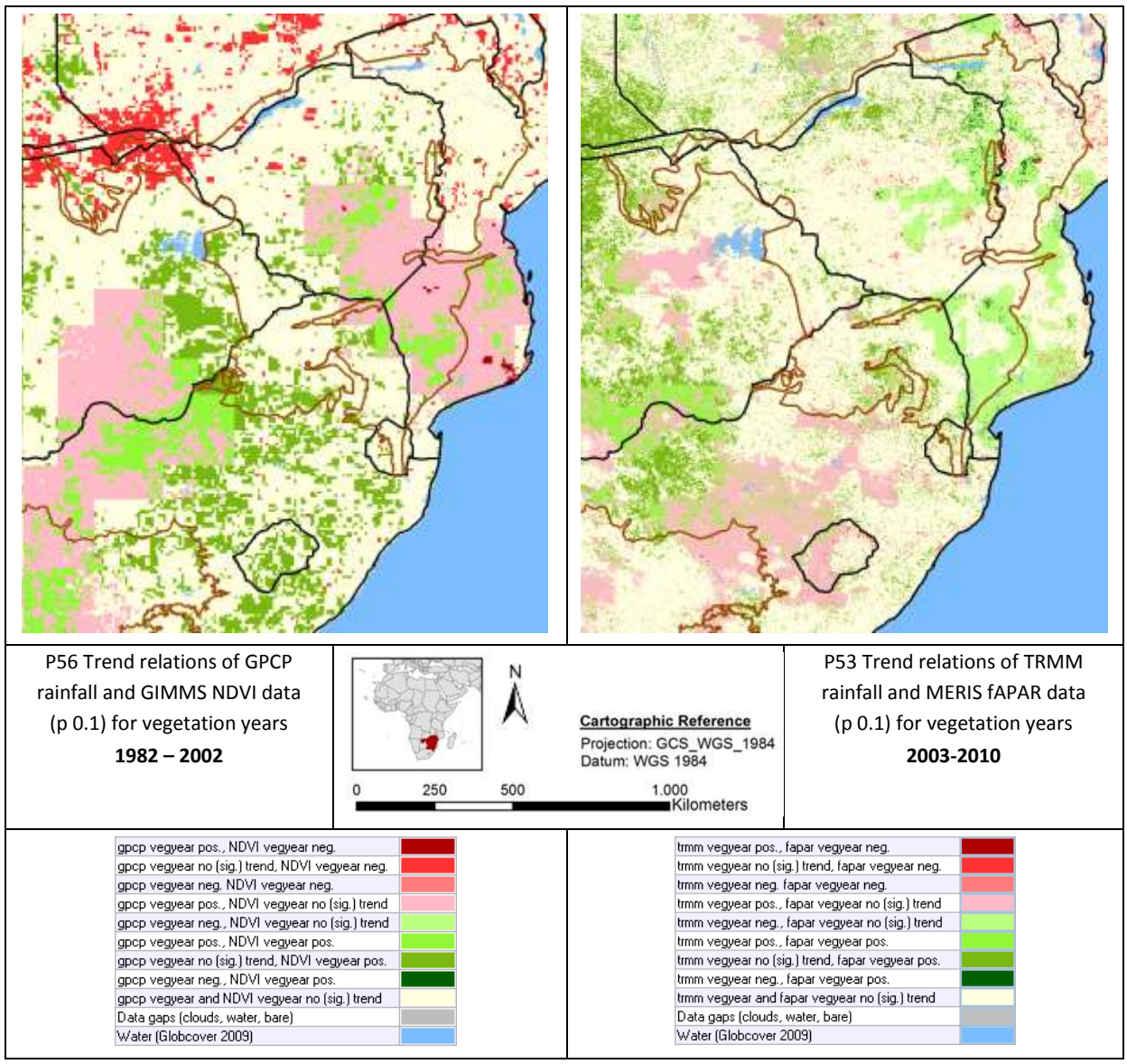

Figure 61: Trend relations of rainfall and NPP proxies (per vegetation year) for the two trend periods 1982-2002 and 2003-2010, respectively. Test site 21, Southern Africa East

5 Comparison of the results with faunal species richness

In the five validation sites (site number 10, 12, 13, 15, and 20), the final products were contrasted with faunal species abundance data derived from models and partly from in situ investigations. Their spatial distribution patterns and temporal variability were compared to the derived NPP proxies, to check if the expected commonalities can be seen. The results are presented in this chapter.

Biodiversity distribution data is a fundamental aspect of the validation process of DIVERSITY II products. Such distribution data are essential to determine the accuracy and usefulness of derived biodiversity indicators produced within the scope of the project. As such, distribution data were collected from multiple sources that include: GBIF, Global Biodiversity Facility Information (www.gbif.org); Distribution Atlases of biodiversity at national or continental level; and unpublished data available at CIBIO/UP from particular regions (e.g., S-Europe or West Sudanian savannah).

The following chapters give a brief description, for both status and trend analyses, of the available data sources, methodologies used and results.

5.1 Contrasting Status Indicators against Modelled Faunal Species Distribution

In the context of the DIVERSITY II project, species distribution models (SDMs) were used to determine suitable areas for the occurrence of selected vertebrates in the dryland test-sites, which were used to derive potential species richness per grid cell. Maps of species richness were then related to DIVERSITY II indicators to evaluate relationships between species richness and indicators.

5.1.1 Biodiversity Data

Distribution data for drylands comprises observations of terrestrial non-volant vertebrates: amphibians, reptiles and mammals. These groups are known to exhibit strong relationships with the indicators to be estimated during the project (Lomolino et al. 2010).

Biodiversity distribution data at 1x1 km of resolution were obtained from GBIF (www.gbif.org) and complemented in some test-sites with unpublished data available at CIBIO/UP (e.g., Southern Europe or Western Sahel). Nearly 400,000 presence records from 1,670 species were collected and stored as ArcGIS shapefiles.

5.1.2 Environmental Data

Three sets of environmental factors, or ecogeographical variables (hereafter EGV), were used for building SDMs. These sets included: 1) one topographical grid (USGS, 2006) that was used to derive the variable Slope; 2) six grids representing averages, extremes and seasonality in precipitation and temperature levels (BIO1, BIO5, BIO6, BIO12, BIO13 and BIO14) (Hijmans et al., 2005); and 3) a land-cover grid, globcover from the year 2009 (ESA 2010). Finally, two sets of EGVs were created: 1) a continental set of EGVS at 10x10km; and 2) a regional set of EGVs at 1x1km corresponding to each test sites. All EGVs were resampled from the original to 10x10km and 1x1km, respectively.

5.1.3 Species Distribution Models and Species Richness

The SDMs were built at a 10x10km resolution using the continental set of EGVs and then projected to the test sites at 1x1km. All SDMs were performed on Biomod2 package (Thuiller et al. 2009, Thuiller et al. 2012). Four modelling algorithms (GLM, ANN, GBM and MaxEnt) were chosen as they had high performances for all datasets. All SDMs were produced using default Biomod2 parameters whenever possible (Thuiller et al. 2009). The number of pseudo-absences for each species was chosen to have the same weight than presence data (species observations) in the calibration process of the models (i.e., prevalence=0.5) (Barbet-Massin et al.

2012). 80% of presence data were randomly assigned to model training with the remaining 20% for model testing. Individual models were evaluated using the true skill statistics (TSS). Only models with TSS>0.70 were kept for subsequent analyses, with the exception of the Caatinga test site, for which the value was decreased to 0.5. The values were chosen after analyses of models output and resulted from a compromise between performance and replicates per species (Martínez-Freiría et al. 2013). Individual model replicates were projected to the test sites (regional EGVs at 1x1km).

To obtain species richness maps for each test site, the consensus species-individual probabilities of occurrence were converted to a binary value of predicted species presence/absence using optimized thresholds automatically selected by Biomod2. Species richness was estimated by adding the individual predictions of species presence/absence in each grid cell (Araújo and Williams 2000, Cumming 2000, Soares and Brito 2007, Benito et al 2013).

5.1.4 Correlating Biodiversity Indicators with Species Richness

Vegetation productivity indicators derived by DIVERSITY II were contrasted against predicted species richness. A total of 27 indicators were used (including mean and variation): 1) fAPAR cyclic fraction, dry season and vegetation year; 2) Rainfall cyclic fraction and vegetation year 3) Rain Use Efficiency (RUE) cyclic fraction, dry season and vegetation year; 4) Soil Moisture cyclic fraction and vegetation year; 5) Soil Moisture Use Efficiency (SMUE) cyclic fraction, dry season and vegetation year; and 6) Length of Vegetation Season.

Correlation coefficients between biodiversity indicators and species richness were then calculated using the "Band Collection Statistics" tool in ArcGIS 10.1. Significant correlations (r>0.50, absolute value) should provide evidence of consistencies between derived products and biodiversity distribution across diverse environmental backgrounds.

5.1.5 Results

Correlation analysis between vegetation productivity indicators and species richness partly reached statistically significant relationships (above 0.5 absolute value), with most of the coefficients varying considerably between -0.5 and 0.5. Even though the majority of coefficients are below 0.5 (absolute value), the analysis of Figure 62 and Figure 63 allow observing a fair match between areas of greater species richness and greater primary productivity (and also regions where the length of the vegetation season is longer). These are particularly clear in the South African and Australien test sites, as well in some parts of the Caatinga.

The significant results suggest in almost all cases positive relationships between species richness and primary productivity (mean values of each indicator), and negative relationship with variation of those same indicators (only one reported example of a positive correlation between variation of an indicator and biodiversity). Thus, high values of species richness apparently are related with areas of high and stable primary productivity. These results are comparable with macro-scale biogeographical patterns of global distribution of species richness, in which high species richness is mostly found in climatically more stable regions (Lomolino et al. 2010).

Regarding the South African test site, the two strongest correlations (one positive and one negative) are displayed in Figure 64. Mammal diversity seems to be higher in areas where vegetation is more stable through time, in more inland regions further away from the influence of the Namibian desert. The opposite occurs in the more arid areas where vegetation is more seasonal, and so species richness decreases.

The Southern Australian test site was the one exhibiting the strongest patterns, with 37 significant correlations. Figure 65 illustrates the best examples with Amphibian richness. Both the most northern and southern areas of the test site present the highest values of biodiversity, as well as primary productivity and environmental stability.

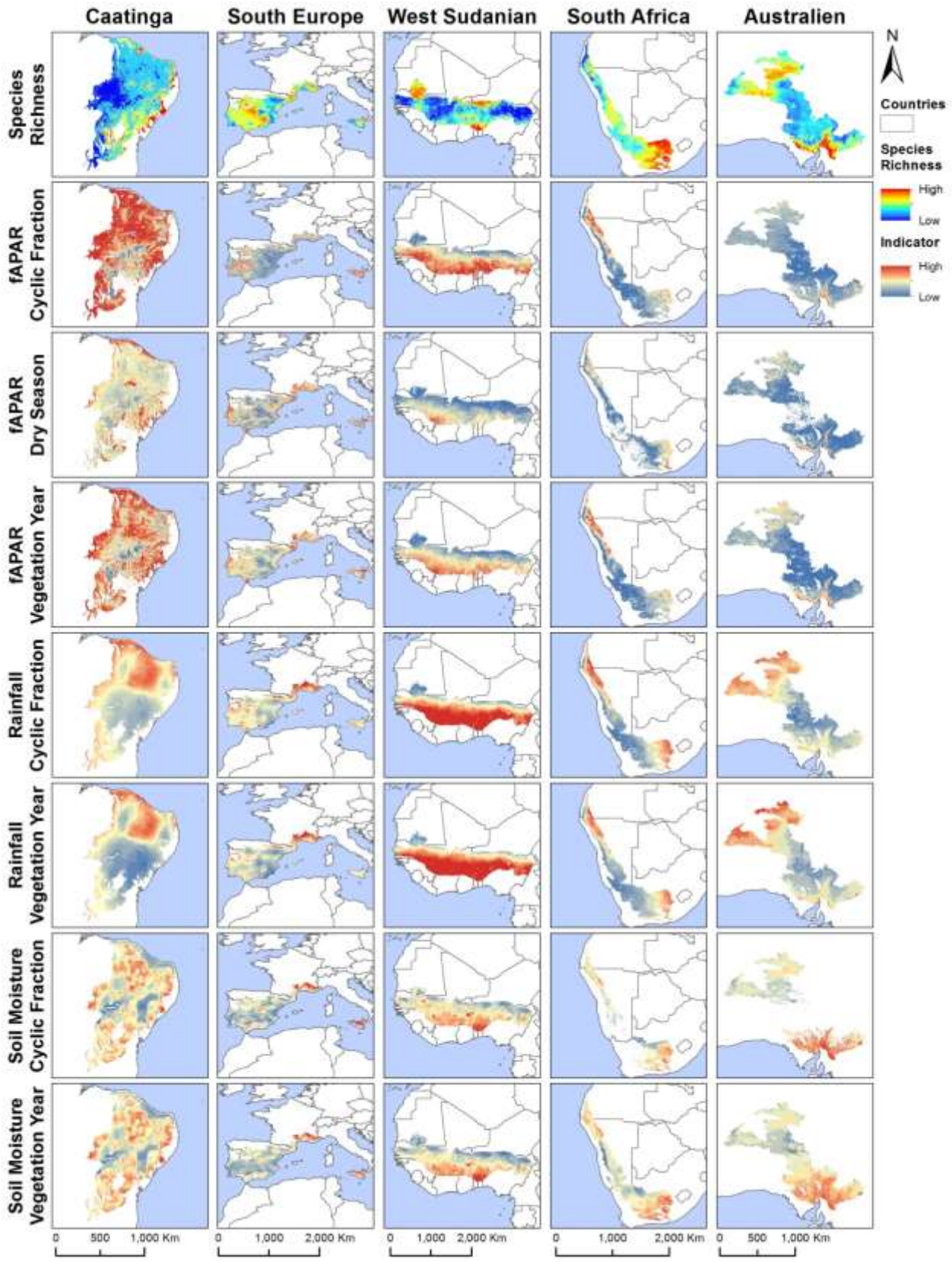

Figure 62: Geographic distribution of mean values of NPP indicators and species richness for each dryland test site. From left to right: Caatinga - reptiles; South Europe - amphibians; West Sudanian savannah - reptiles; South African - mammals; Australien - reptiles.

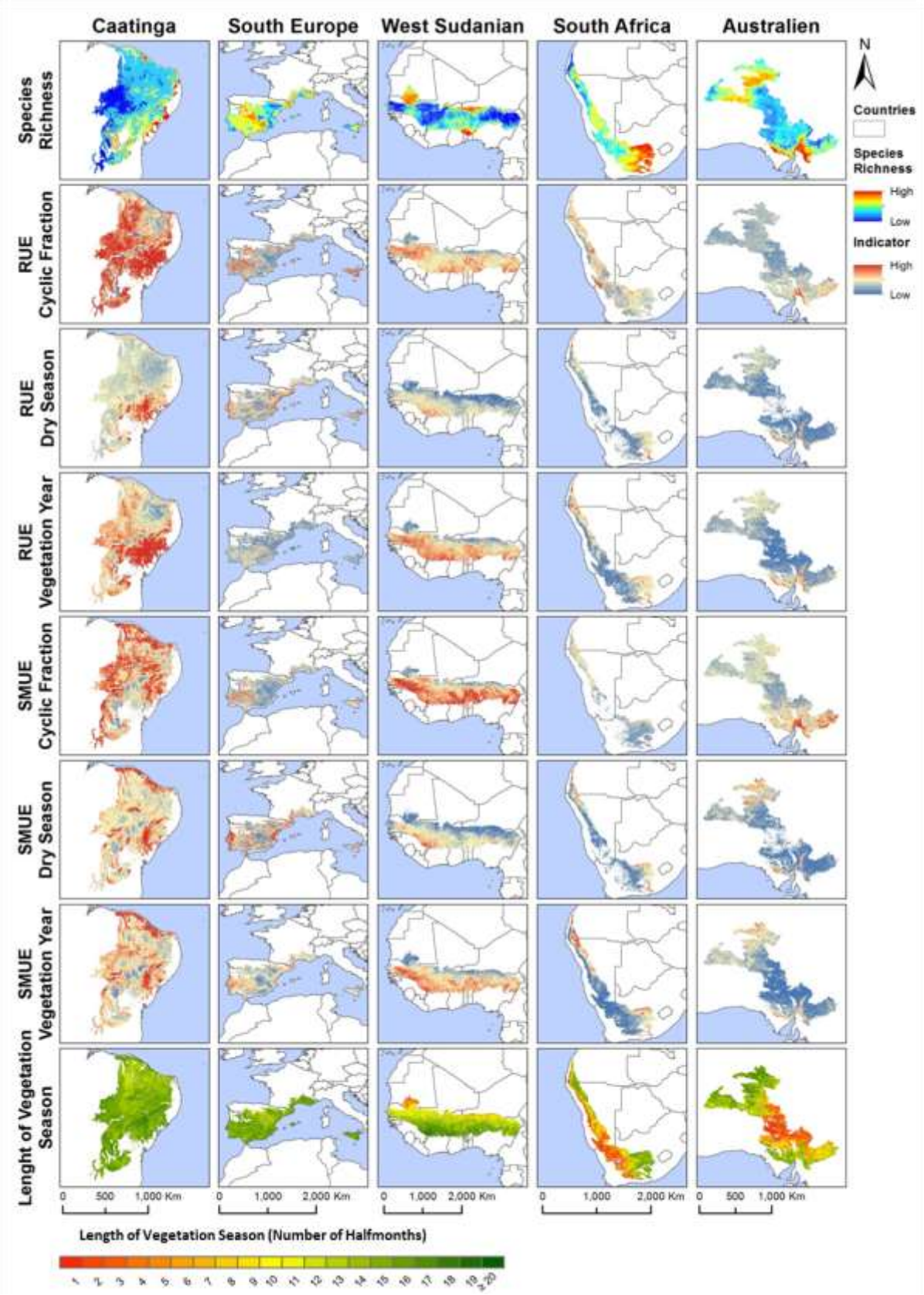

Figure 63: Geographic distribution of mean values of NPP indicators and species richness for each dryland test site. From left to right: Caatinga - reptiles; South Europe - amphibians; West Sudanian savannah - reptiles; South African - mammals; Australien - reptiles.

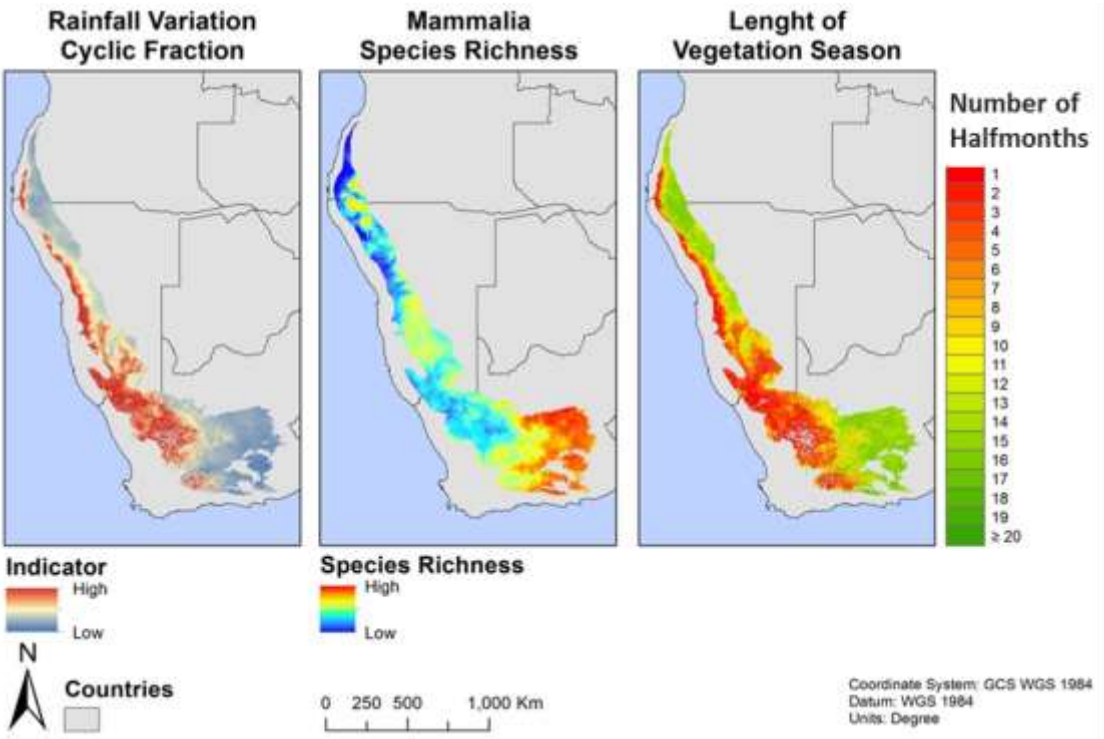

Figure 64: From left to right, Rainfall Variation Cyclic Fraction, Mammalian species richness and Length of Vegetation Season for the South African dryland test site.

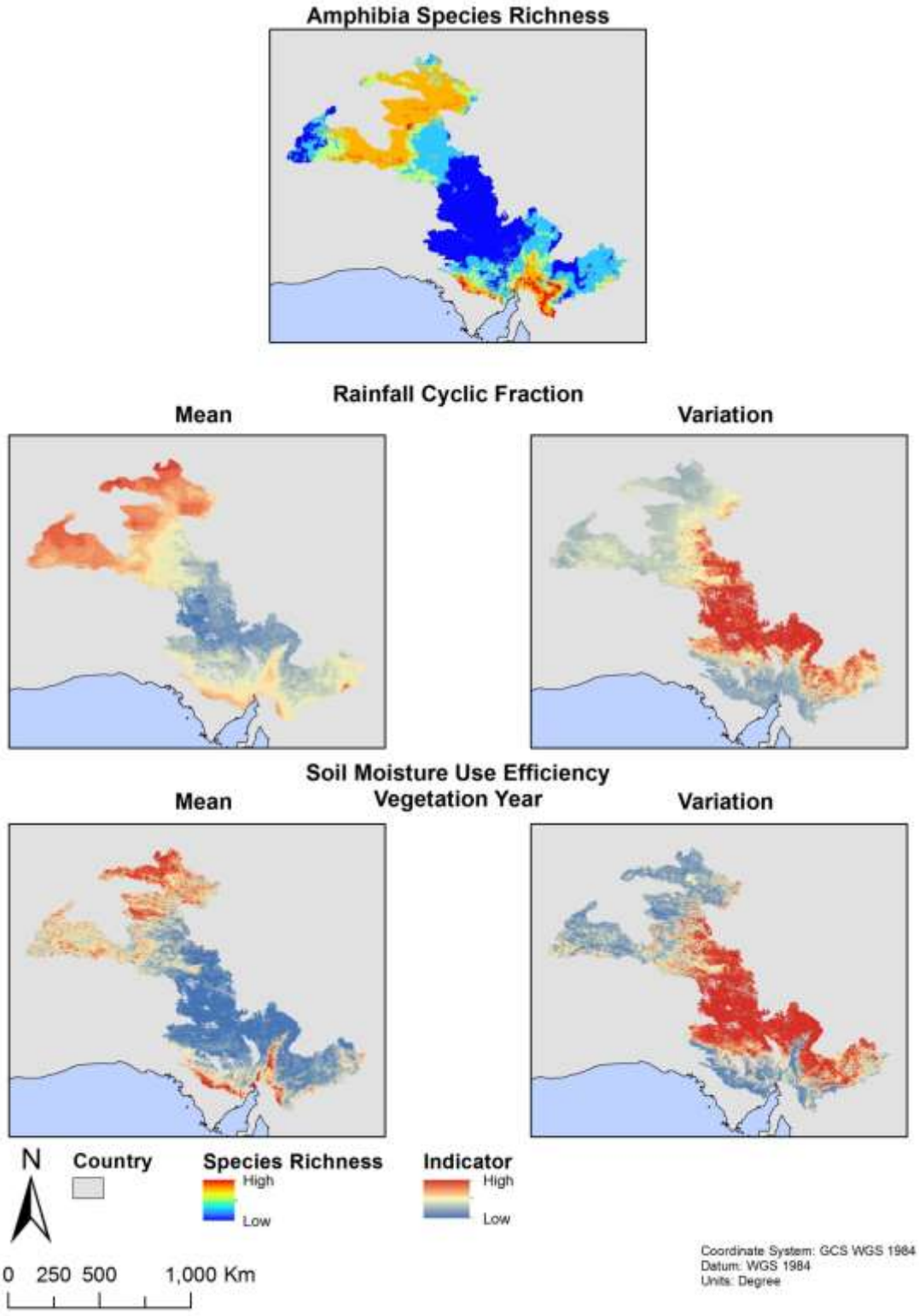

Figure 65: Amphibia species richness, Rainfall Cyclic Fraction (Mean and variation) and SMUE Vegetation Year (Mean and variation) for the Australian dryland test site.

5.2 Contrasting NPP Trend Indicators against Faunal Species Distribution

For the Southern Europe and South Africa dryland test sites, the NPP proxy trends and faunal presences/abundances could be correlated, with some example results been given below.

5.2.1 Southern Europe

For the Southern-Europe dryland test site, biodiversity trend data was kindly provided by Mário Ferreira and Dr. Pedro Beja, from CIBIO/UP. This data was collected in the coastal plateau of southwest Portugal, within the "Sudoeste Alentejano e Costa Vicentina" National Park. The dataset comprised information on presence and abundance of amphibians in temporary ponds, measured as the average number of larvae by 30 second dip-netting, and collected in 2002, 2006 and between 2009 and 2011 (Ferreira & Beja, 2013).

While amphibian data in test ponds was retrieved by days, indicator (fAPAR) values were averaged by fortnight (15 days). As such, the correlations between biodiversity and indicators were essayed using several aggregation schemes as illustrated in Figure 66**.**

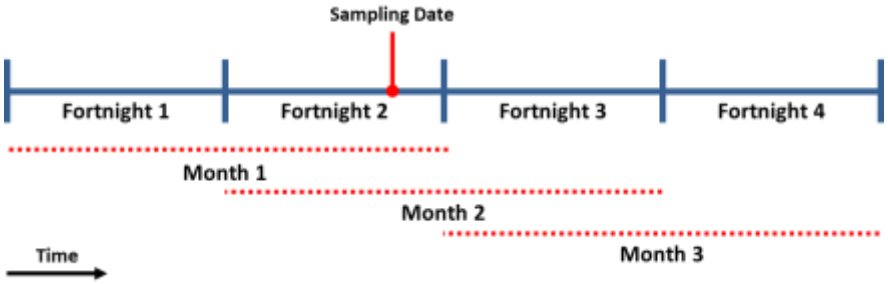

Figure 66: Aggregation schemes of fAPAR values to correlate with biodiversity data

Spearman's rank order correlation analyses were used to access significance of relationships between biodiversity and indicators. Significance of results were tested by their probability values (p), considering a confidence level of $p<0.05$.

Correlation analysis of trend data for Southern Europe retrieved positive relationships between the biodiversity indicator fAPAR (taken from various time frames) and amphibian abundance in ponds. The best example is illustrated in Figure 67**.**

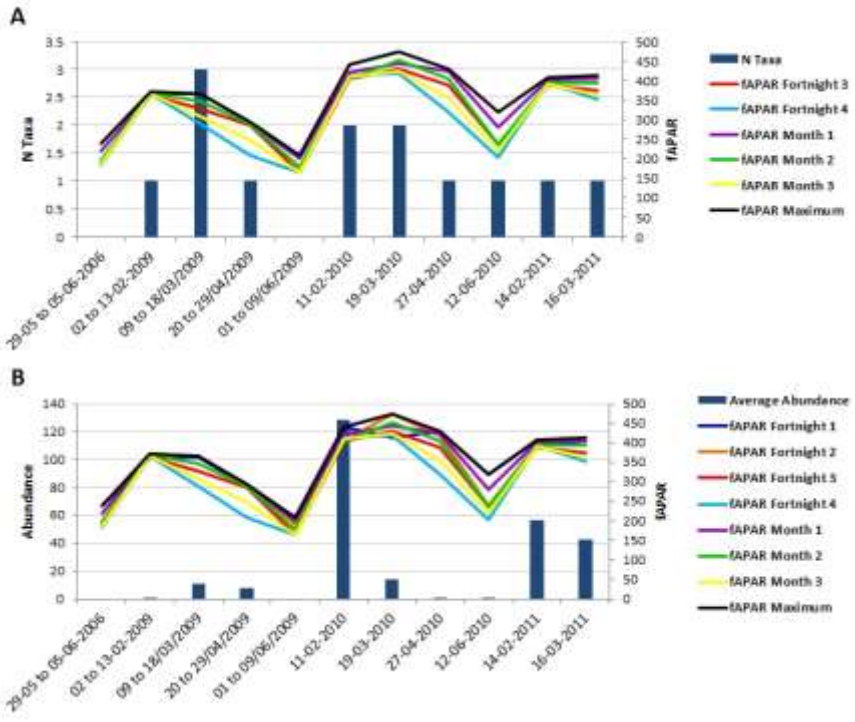

Figure 67: Correlation analysis for test pond A10 based on Spearman's r. Charts depict biodiversity measure (left Y axis) and indicator (right Y axis), per sampling date (X axis): A – Number of amphibian taxa (N Taxa) and fAPAR values; B – Number of amphibian larvae (Abundance) and fAPAR values

5.2.2 South Africa

For the South-Africa dryland test site, biodiversity trend data was kindly provided by Dr. Rita Covas, from CIBIO/UP, and comprises various parameters on the life cycle of the sociable weaver (Philetairus socius). The species is known to live in colonies and in general the reproductive season occurs between September and February, in which two breeding events can occur, a first beginning in September/October and a second one starting December/January, since it takes more or less one month to a chick to develop (from the time the egg is laid to when it finally leaves the nest) (Covas et al. 2008). The data was obtained at the Benfontein Game Farm in the Northern Cape Province, South Africa, during 2010 and 2012.

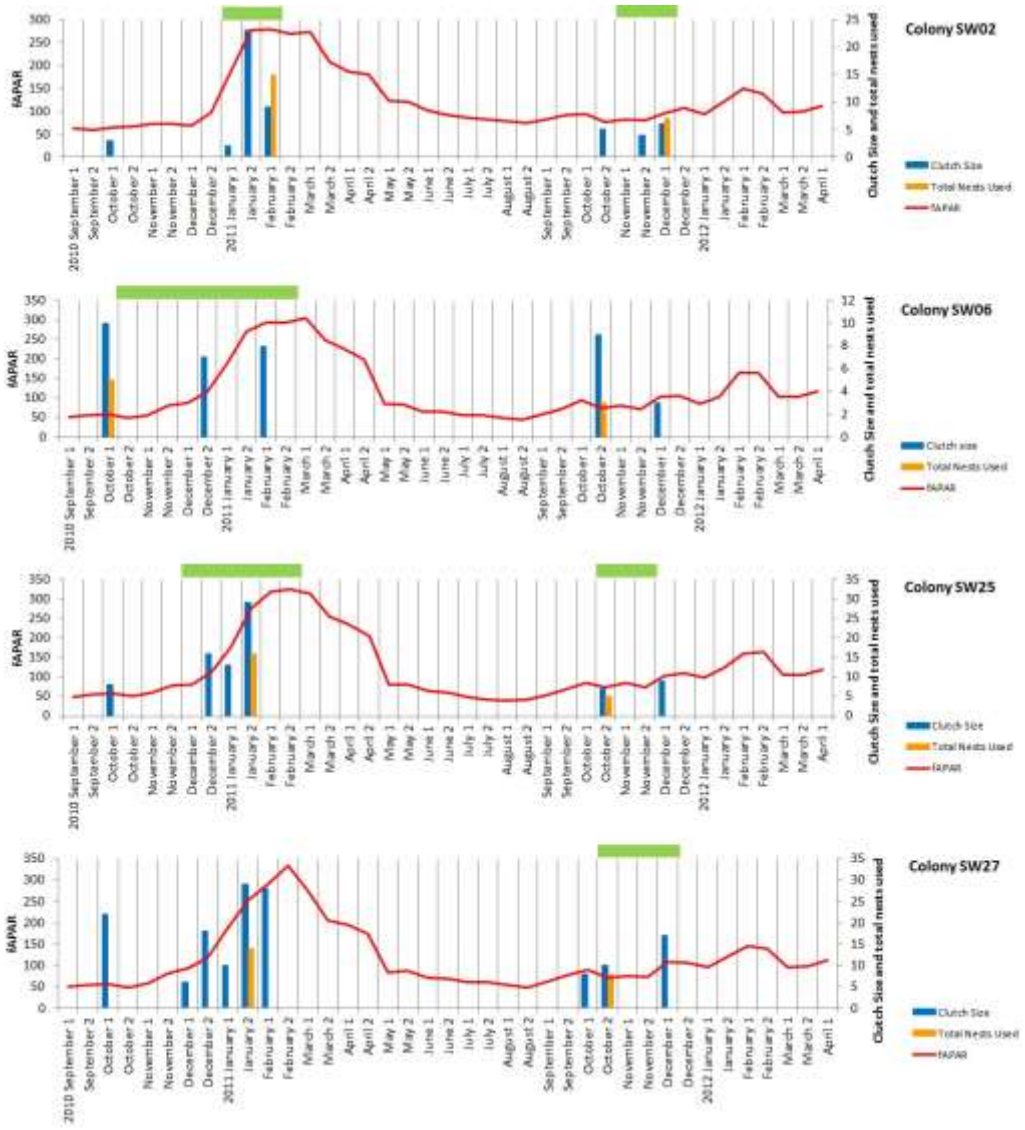

In

Figure 68 it is observable that clutch sizes are larger and egg laying events are more frequent during the second fortnight of December and the first fortnight of February, which matches the highest peak of fAPAR. Also, comparing between the 2010 and 2011 reproductive seasons, it is very clear that the number of eggs, the frequency at which they were laid and the number of nests used were much higher in 2010 than in 2011. In terms of fAPAR, the increased peak of productivity observed in January-February of 2011 is not noticeable during the same time period in 2012. Hence it seems that the primary productivity of the surrounding environment has a positive relationship with breading success of social weavers.

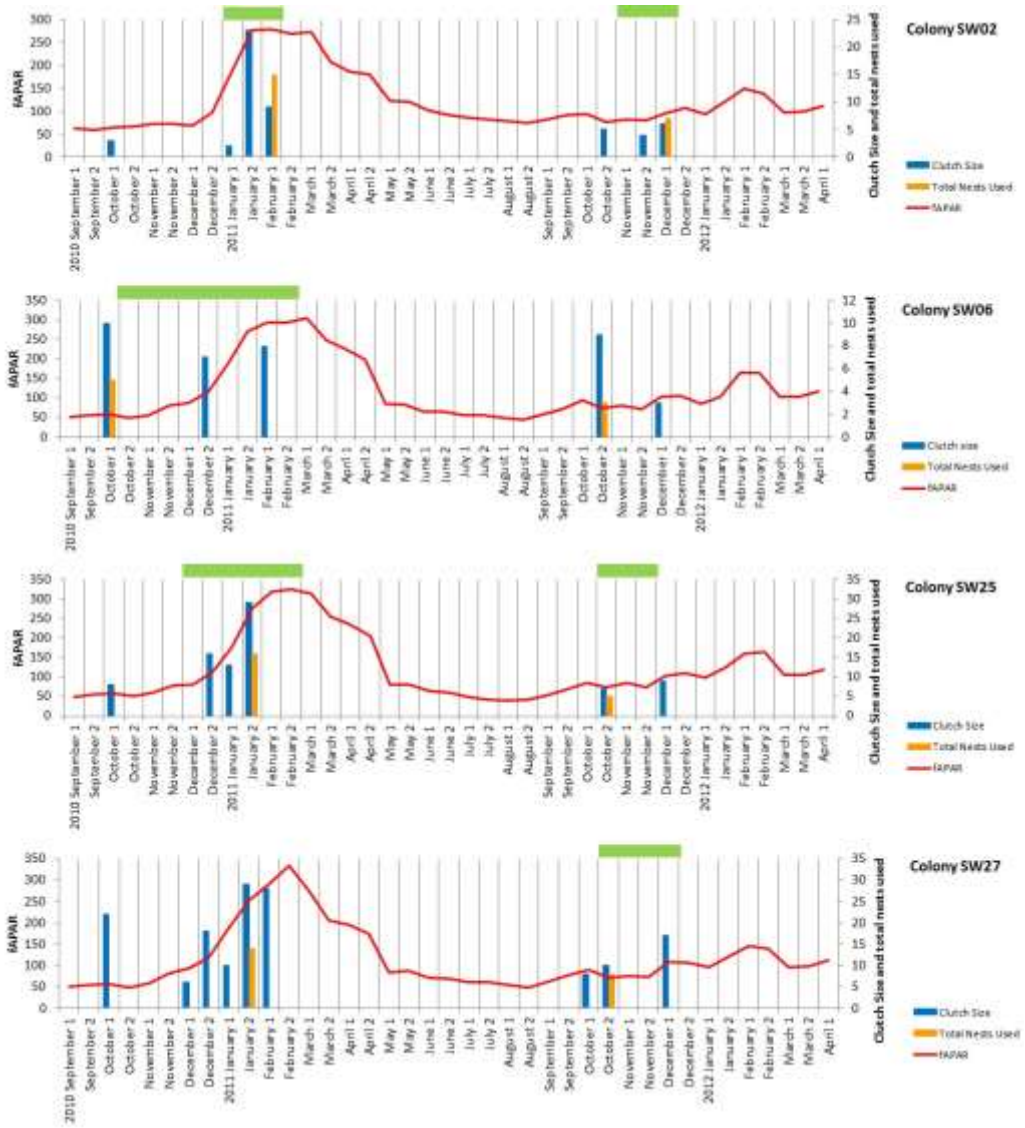

Figure 68: Fortnight fAPAR values (left Y-axis, red line) along with clutch size (right Y-axis, blue vertical bars), total nests used (right Y-axis, orange vertical bars) and breeding season length (green horizontal bars), for the first four colonies out of the eight selected. Time period from September 2010 to April 2012

5.3 Known Issues

During the validation process of DIVERSITY II products, including data extraction, analyses and interpretation of results, several precautions had to be taken into account in order to draw the maximum input from the derived RS indicators. In this chapter, encountered known issues are reported, recommendations for avoiding them or minimizing their impact are presented, and possible solutions for the users are suggested.

5.3.1 Status Products

5.3.1.1 Biodiversity Data

For the validation process the main source of biodiversity distribution data was the Global Biodiversity Information Facility (GBIF). The advantage of GBIF is that is freely accessible and it comprises worldwide data submitted by Natural History museums and other institutions. Despite the huge amounts of data available, there are some concerns about accuracy and quality of the geographic, temporal, and taxonomic coverage, suggesting that GBIF records should be used only after a first careful inspection (Guralnick et al 2007, Beck et

al. 2013, Costello et al 2013). Depending on the type of analysis, the user should take into account the following topics:

- **Time-period** – species distribution data should be collected in a time-period as similar as possible to the period of DIVERSITY II products (June 2002 to April 2012). Old distribution data may not be well suited for analysis since the landscape may have changed. We recommend the usage of most recently obtained data as possible.
- **Taxonomic revision** – many taxa names (species, sub-species, even genus) are outdated and may skew the number of records for the user's target taxa or group of taxa. We recommend checking certified biodiversity database, such as the IUCN Red List of Species (www.iucnredlist.org), or available literature, for synonyms and taxonomic updates.
- **Geographic range** – many taxa are incorrectly assigned to certain geographic areas, as consequence of local extinction or presently being considered as exotic or invasive species. Depending on the user's intended investigation, we recommend to check for the most recent distribution ranges of the target taxa.
- **Data duplication** – many taxa have duplicated observations in the same pixel, which may influence analyses. Depending on the pixel size, we recommend to confirm if there is only one taxa record per pixel.

To use the DIVERSITY II products in full, the user should ideally have obtained locally high precision distribution data (coordinates collected in the field with a GPS), which can then be complemented with GBIF records, if needed.

5.3.1.2 Data pre-processing and analyses

Biodiversity distribution data can be compared and contrasted against DIVERSITY II products using a variety of GIS software, such as BEAM, ArcGIS, Quantum GIS, among others. Before any analyses, a preliminary data assessment should be made. Depending on the type of investigation, the user may take into account the following topics:

- **Confirm pixel size** – the user's variables need to have the same pixel size. The resolution of the DIVERSITY II products is 300x300m².
- **Confirm layer extent** – errors can occur if the GIS layers (raster images, shapefiles, etc.) being analysed do not have exactly the same extent (the entire geographic frame including surrounding no data pixels, and not only the area of interest). Check with the highest detail possible if the extents match.
- **Remove unnecessary data** – DIVERSITY II products come with data gaps and information on water cover. For most studies these pixels should be removed. The same pixels should also be excluded from the biodiversity data.

DIVERSITY II products file sizes are considerably large due to their high resolution. When combining biodiversity data (or other environmental variables), the user may end up with very large volumes of data. This can become very difficult to handle, both in terms of practicality and computer power.

In terms of analyses feasibility (but also data extraction and processing), it may become less time consuming if the user has some knowledge on programming languages, such as Python (useful with BEAM and ArcGIS), R (statistical analyses for example), Pearl, among others. The use of scripts, macros (for Excel) and batched processes (same task performed for various files) allow users to perform their analyses automatically and less time-consuming.

5.3.2 Trend Products

An issue that may be encountered during the validation process of trend data is the mismatch between biodiversity data and DIVERSITY II products, whether it was in terms of spatial or temporal coverage (or even both at the same time). When the users' research involves investigating data through time, the following topics should be taken into consideration:

- **Sampling date** – DIVERSITY II dryland trend indicator (fAPAR) is provided at 15 day intervals (two integration periods per month) from June 2002 to April 2012. The exact date of when biodiversity data is obtained in the field should be known in order to associate the correct half-month it corresponds to.
- **Sampling effort** – Given the high temporal resolution of the DIVERSITY II product, user's biodiversity data should be collected systematically at equal intervals throughout the considered time frame (ideally at least with 15-day intervals).
- **Temporal frame** – fAPAR is a proxy of primary productivity and species (especially fauna) may react to changes with a certain time delay. Also, many species are highly influenced by specific time periods (reproductive seasons for example). All of these factors differ from taxa to taxa. The user should test different fAPAR averaging schemes (see the Southern Europe example given above). Depending on the user's objectives, time frames could go from the half-month corresponding to the sampling date, to an average during spring or Rainy Seasons (peaks of productivity) or even annual averages.
- **Geographical extent** - DIVERSITY II products' resolution is 300x300m², but fAPAR data can be extracted for a larger area, depending on the user's target taxa. While for some species it may be interesting to use pin-point measures of productivity (low dispersal organisms or highly associated with certain habitats), in other cases it may be better to extract data for a wide area covering various environments (high dispersal, generalist organisms).
- **Data gaps** – DIVERSITY II products come with data gaps (related for example with cloud cover) throughout the time series, so users should be aware of this when performing their research.

To summarize, for users to take full advantage of the DIVERSITY II products, optimized biodiversity data should have been collected, with spatial and temporal high resolutions.

6 Booklets

Besides this Product User Handbook, dryland site specific booklets have been prepared. The booklets compile and summarize important outcomes per test site, and thus constitute regional complements to the project reports and the Product User Handbook, which provide in depth and complete project documentation without highlighting every test site.

Interested users, for instance those who will not look at the map files themselves, will find some major results presented in the booklet, as well as a short description of the methodology and of the individual products shown.

The booklets can be downloaded at http://www.diversity2.info/products/ .

A total of 22 booklets have been prepared, displaying 23 map products each. Every booklet has a short introduction to the regions, and a so called "dryland story", where two of the booklets have received stories from local experts of the regions (Bob Scholes and Graham v. Maltitz). In addition, the booklets contain the faunal species richness maps, where these have been generated (site 10, 12, 13, 15, and 20), and more detailed description of the biodiversity of these five sites.

7 Conclusions

The ESA DUE project Diversity II generated both a large quantity and variety of map products for 22 globally distributed drylands. They include status, trend and change indicators of vegetation productivity (NPP proxies) and their relation to water availability, originating mainly from MERIS fAPAR and ancillary data. Figure 69 (top) provides an overview of the covered drylands by overlaying the yearly mean fAPAR trends on a map with the UNEP aridity zones[20]. It shows that a substantial part of the global drylands is mapped with the MERIS products. Temporal coverage of the MERIS data reaches from 2002 to 2012, where worldwide eight "vegetation years" starting in 2003(2002) and ending in 2011(2012) have been covered. The "vegetation year" was defined to begin (end end) with the local start of the dominant vegetation season. To our knowledge, the derivation and usage of the vegetation year is a novel approach (even though already suggested by Le Houérou, 1984, who called it *biological year*) and goes beyond the parameterization of the growing season only. It includes also the dry (cold) season(s), for which explicitly vegetation greenness/productivity values are derived.

The provided products include so-called first and second order indicators, where the first order indicators relate to phenology, vegetation productivity, rainfall, soil moisture, as well as Rain Use – and Soil Moisture use efficiency (RUE and SMUE). The second order indicators are composed of mostly two, in one case three first order indicators. All indicators have been listed and described in this document, and most indicators have been illustrated with various examples from different test sites.

A further novelty compared to other studies is the usage of soil moisture data in analogue form to rainfall data. Some of the respective soil moisture and rainfall derived indicators were compared in section 3.5.4. Theoretically soil moisture indicates more directly the available water for vegetation growth than rainfall, which is subject to runoff, interception, evaporation, etc. On the other hand, the soil moisture data used refer to surface soil moisture of the upper few centimeters of the topsoil only, measured once a day, and may also be subject to evaporation. From these first comparisons it can be concluded that soil moisture is in general positively correlated with rainfall, but often behaves differently and it will be interesting to further examine these differences.

The products were conceived towards the information needs of the two UN conventions CBD and the UNCCD, which are shortly summarised in chapter 1. Consequently, the user handbook is geared in these directions, which have in common the need for assessing the status and trends/changes of vegetation productivity and of land cover. Land cover was not explicitly addressed in this project, though many indicators are related to land cover and one of our aims in this handbook was to demonstrate this close relationship. Product P50, Functional Classes, is most obviously related to land cover as has been shown in section 3.5.5).

Literature findings as to the relation of NPP and plant species richness have been shortly reviewed in section 3.5.9. Such relations have been studied in various environments with different results, which are site specific and depend on the scale and the range of conditions studied. For example it was found that from very dry conditions on, increasing humidity will lead to an increase of the number of species, but this culminates at a certain, spatially varying NPP level and with further increasing vegetation productivity diversity may decrease. Instances of (known) plant biodiversity hotspots could be recognized in diverse NPP/RUE/SMUE proxies; however it remains open whether regions with a high floral diversity could be systematically narrowed down with such data (and further geo-data, such as DEM, etc.). We believe that there would be potential and that it would be worth to study in detail.

In the faunal domain, systematic relations between environmental variables and faunal diversity are used in large scale (continental to global) models, which predict faunal diversity. NPP, and thus the NPP/RUE/SMUE proxies by expressing combined environmental characteristics consequently also exhibit relations to faunal

[20] http://www.unep.org/geo/gdoutlook/016.asp

biodiversity. The relations depend on the taxa studied and their habitat requirements. These relations have been examined in five Diversity II test sites and are reported in chapter 5. Biodiversity trend or change data are harder to find than status assessment. Nevertheless, some temporal studies of the NPP-faunal species richness relation could be presented as well.

Relating NPP/RUE/SMUE proxy trends to biodiversity of plants was only possible in a generic way, based on the literature and reported developments observed in drylands. In particular reference was made to bush encroachment, a global phenomenon that in some regions is proceeding since decades, e.g., Namibia. The widespread observed greening of dryland during the last decades has been partially connected with bush encroachment and related issues such as invasive species expansion and impoverishment of indigenous species, often connected with tremendous economic losses. Without in situ knowledge, however, such forms of land degradation cannot directly be identified from space. However, with our approach to develop seasonal NPP/RUE/SMUE indicators not only for the growing season and yearly (vegetation year) NPP, but also explicitly for the dry seasons, we tried to advance such indicators towards this direction.

As addressed in chapter 3, section 3.6.1, the time span covered by the MERIS data is rather short for trend analyses; they do not indicate whether the trends are longer term developments, and vice versa due to the high rainfall and productivity variability between years not all trends may be recognized. For this reason we have looked beyond the MERIS period into longer term data sources, i.e. NOAA GIMMS NDVI data and the literature to get a “bigger” picture of the major vegetation productivity developments, and have referred to these repeatedly throughout the document. In addition, it seemed to be of interest to compare results derived with the widespread used GIMMS NDVI data to the MERIS derived results to check if derived trends during the same periods are consistent. Likewise, we contrasted the MERIS fAPAR based indicators with modelled NPP (BETHY/DLR) and MERIS NDVI derived indicators. In Table 8 an overview of these approaches is provided, comparison results with MERIS NDVI are described in section 3.6.3.

At and after the turn of the millennium, when MERIS started in 2002, worldwide many trend breaks of the vegetation productivity were observed (De Jong et al. 2013, see Figure 49). For this reason it is not surprising that in most cases the trends of 1982-2002 (GIMMS NDVI, presented in Product P56) and the MERIS trends (2003-2010, P53) are different (see Figure 61 for an example). Since the early 1990s, stronger rising trends of the air temperature were observed in many regions worldwide (see chapter 3, section 3.6.4), which are for instance made partially responsible for the desiccation trends in the Central Asian regions (e.g. Zhou at al. 2015).

This and other developments are reflected in the map of worldwide NPP trends in the first decade of the 2000s by Zhao and Running 2010 (Figure 69 lower right). When compared to the GIMMS NDVI based trend map derived in this project in the lower left of Figure 69, it becomes obvious that NPP proxy (GIMMS NDVI) and (modelled) NPP trends are not everywhere going in the same direction, especially not in the southern hemisphere. Increasing air temperature can lead to heavy NPP losses due to increased autotrophic respiration, what according to Zhao and Running (2010) happened in the Amazon rainforest, enhanced by a severe drought in 2005. Zhao and Running state a major drying tendency with decreasing NPP from 2000 to 2009 for the entire southern hemisphere, whereas for example in southern Africa the yearly GIMMS NDVI trends (vegetation years 2000-2009) exhibit clearly less negative and more positive trends, and the fAPAR vegetation year trends 2003-2010 even show widespread positive trends. (However, the shift between these two trend periods (2000-2009 vs. 2003-2010) may partly cause these differences, if not the different data themselves.)

Obviously, we cannot directly infer NPP increases or losses from greening or browning trends observed with fAPAR or other NPP proxies without NPP modelling, and thereby taking into account temperature and many more environmental variables, including “*environmental stresses and plant autotrophic respiration”* according to Zhao and Running (2010). On the other hand, NPP modelling results are still subject to large variations depending on the underlying assumptions, parameters considered, and data used. Critiques of the study of Zhao and Running suggest that the apparent overall decline in global NPP after 2000 could be a result of an overly strong temperature sensitivity of the NPP model used, resulting in an overestimation of plant respiration

(Medlyn 2011 and Samanta et al. 2011, cited by Ahlström et al. 2012). Oijen et al. (2010) argue, confirming the outcome of many other studies, (however with a mathematical approach based on the law of conservation of mass) that on the longer run (weeks and longer), the ratio of respiration and photosynthesis is constrained to a narrow range of about 0.4-0.5, as the long term ratio of (carbon) storage to photosynthesis cannot be negative. According to Oijen at al. the uncoupled modeling of photosynthesis and respiration may lead to extreme responses of modelled NPP to environmental changes, such as "*model predictions that much of the Amazonian rainforest may disappear this century because of global warming*".

Supported by the overall promising comparison results between the modelled (BETHY/DLR) NPP data (or derived indicators) and the fAPAR derived products (section 3.5.3) we assume that the fAPAR based NPP indicators are valid indicators for the status and trends of vegetation activity and degradation. However, having developed and analyzed a variety of different indicators in their combinations, we argue that dryland condition, functional biodiversity and major developments of drylands towards degradation or land improvement cannot be expressed in single indicators. Rather, we recommend the combination of seasonal productivity indicators, including what we called the "vegetation year", plus the cyclic vegetation and the dry season. This way we aim to capture areas with perennially green vegetation, the widespread phenomenon of bush encroachment, or areas with short vegetation cycles.

From the first order indicators, combined "second order" products have been derived, such as Diversity II product P50 "Functional Classes", which are related to functional ecosystem types and were shown to correspond also closely to land cover patterns. In addition, phenology products were generated, i.e., the start and length of the growing season, which are provided by Diversity II as status indicators (mean values). Phenological trends of these parameters were not studied with the MERIS data due to the short observation period, but examples for phenology trends and relations to in situ data are demonstrated in section 3.5.2., derived with long term GIMMS NDVI data and the Diversity II methodology.

For characterizing the relationship of NPP proxies and water availability the approach of Rain Use Efficiency - RUE was applied, which has been introduced by Le Houérou (1984). RUE was supplemented with Soil Moisture Use Efficiency (SMUE), which is based on soil moisture data instead of rainfall data. For RUE and SMUE, status and trend indicators were derived for the vegetation year, the growing season, and the dry season, respectively. RUE and respectively SMUE show how much vegetation grows in relation to the available water, but as – especially at smaller scales, many other factors influence vegetation productivity as well besides water (e.g., nutrients), the interpretation of RUE and SMUE status and trend is not straight forward. In particular, RUE is correlated (in different ways depending on soils, aridity, etc., see Le Houérou, 1984) with rainfall, for which it is often claimed to normalize vegetation productivity. This assumption led to the use of RUE as indicator for land degradation, which is potentially man-made as it is supposed to be de-coupled from rainfall, but this straight forward usage of RUE has been challenged. To summarize, the relation between vegetation productivity and rainfall depends on factors such as

- whether the spatial or temporal domain is studied,
- the amount, temporal and spatial distribution of rainfall and runoff,
- other climatic conditions, especially, temperature and evapotranspiration,
- soil properties, hydrology, terrain, land cover, land use,
- changes of these variables and climatic systems through time, or
- the current conditions of the ecosystems with regard to environmental changes (e.g. , time elapsed since the last drought, see Miehe et al. 2010 or Ratzmann 2014).

Due to these influences many areas do not fulfill the basic assumption of RUE, i.e. a linear or even proportional relation between rainfall and NPP through time (see for instance Fensholt et al. 2013 and Ratzmann 2014). Approaches such as "2dRUE", developed by Del Barrio et al. (2010) and applied to the Iberian Peninsula take into account the influence of aridity on RUE, but would require detailed reference data for regional and local fine-tuning also with regard to the other important variables that determine NPP.

Further on, RUE or SMUE as a lumped indicator is not revealing whether negative trends for instance are related to increasing rainfall and/or to decreasing vegetation productivity. In addition, RUE depends on how vegetation productivity is measured, or the type of EO based NPP proxy data used, as can be seen for instance in Figure 23, where NPP (modelled by BETHY/DLR) based and MERIS fAPAR based RUE average maps are contrasted.

Against this background and the short observation period, we stress again that the derived RUE indicators should only serve as qualitative indicators of potentially worsening or improving areas, and not strictly to infer land condition or man-made land condition trends. RUE status maps nevertheless seem to provide information about functional ecosystem properties, especially when using all seasonal RUE maps in combination.

Looking at RUE status as indicator for land condition, it seems that the dry season RUE may have the highest potential to provide such information (see section 3.5.4): it shows where the perennial vegetation cover is reduced relative to rainfall, and may consequently be understood as potential indicator for soil erosion risk, as areas with larger portions of bare soil during the dry season are more prone to soil erosion. Of course, care must be taken for the interpretation of dry season RUE (status), as it depends on various factors, and bears the risk of confusing extreme aridity (where dry season is RUE is generally low) with bad land condition. Also crop land that is harvested and then bare has low dry season RUE values, which may not necessarily be related to land degradation (however, as crop lands are often prone to soil erosion dry season RUE/SMUE may also provide useful information in this respect). Finally, RUE status information must be based on averages of several years (here: eight vegetation years) in order to deliver valid assessments of land conditions, given the high climatic variability in drylands.

The RESTREND method is an alternative way to study degradation trends, by determining the trends of residuals of linear regression analysis between NPP (proxies) and rainfall, assuming a linear relationship between NPP and rainfall during the observation period. A decreasing trend of the regression residuals would point to a potential degradation. Based on a comprehensive study of the RESTREND method including simulations of trend input variables in South Africa, Wessels et al. 2012 came to the conclusion that "*Unless a confirmed non-degraded reference period is available to establish the expected ΣNDVI–rainfall relationship for an area, the RESTREND method will suffer from this inherent limitation. Correcting for rainfall trends and variability therefore remains one of the biggest challenges when monitoring land degradation*". Obviously the RESTREND approach is only applicable for trend estimations, and not (directly) for status assessment.

As an alternative to the derived RUE trends, we created a second order indicator ("trend relation") that exhibits both vegetation greenness AND rainfall trends separately, but synoptically in one indicator. It comes in three products, i.e., P53 (vegetation year), P54 (cyclic vegetation, and P55 (dry season), which have been presented for several regions in Figure 34 and Figure 35. Figure 61 displays the same type of indicator for the period 1982-2002 (derived from GIMMS NDVI) in comparison to the analogue MERIS based indicator for 2003-2010. In order to not overload the indicator with information, the strength of the trends is not differentiated, but it could be, or minimum trend thresholds may be applied.

Table 9 presents a summary of the application themes and related topics and questions that were found being of interest to users and that have been addressed by Diversity II.

Validation was addressed as an issue that could not be solved in the project with systematic reference data of degraded land. However, the performed cross-comparisons with results derived from other sensors such as NOAA GIMMS NDVI data, results from the literature, and especially with the modelled NPP data derived with BETHY/DLR confirm a high degree of consistency of the Diversity II products with other state of the art data and assessments. Also the performed comparisons with faunal species richness contribute to the convergence of evidence at least on large scales.

Finally, we would like to encourage users to return comments, make suggestions, or share relevant data or know how with us, or vice versa request more detailed data. All feedback and exchange is welcome and will be highly appreciated.

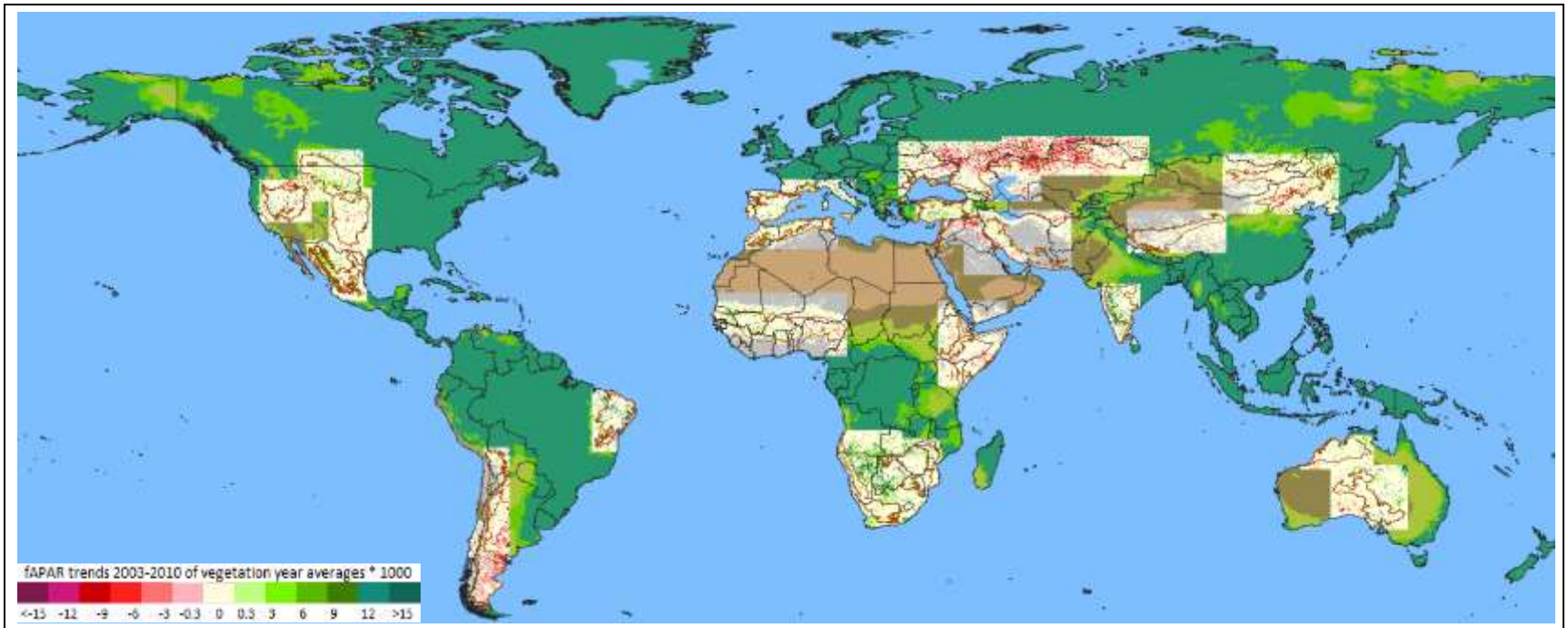

2003–2010 trends of the vegetation year mean fAPAR (*1000) and Aridity zones (UNEP), where the beige to green areas are (hyper)arid to dry sub-humid and the blue-green areas humid regions

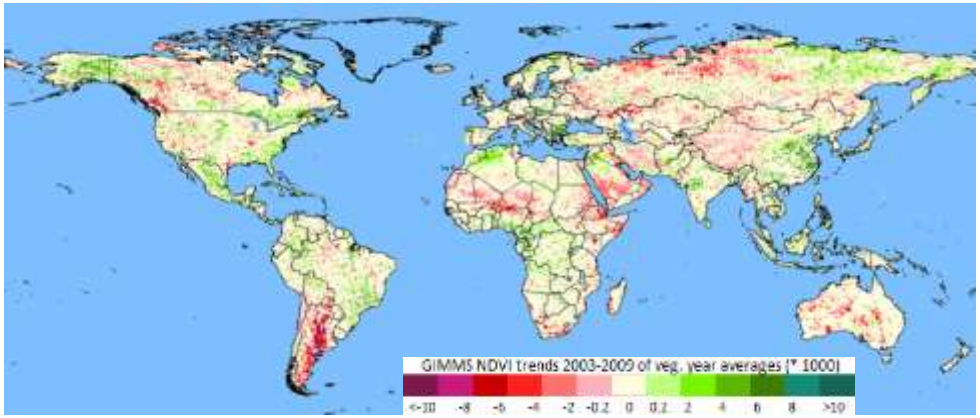

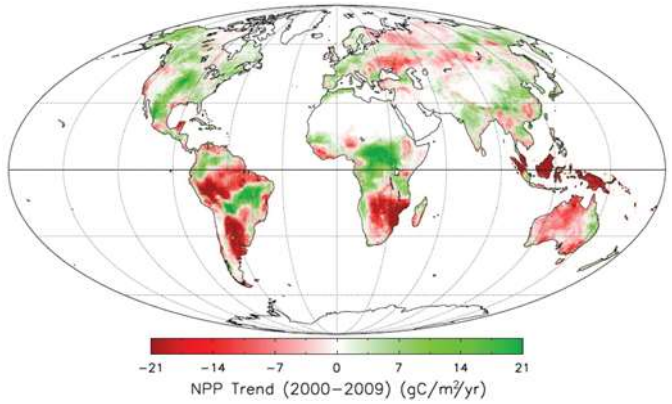

Figure 69: Top: Vegetation year fAPAR trend 2003-2010 in the 22 test sites (TS, p 0.1); lower left: GIMMS NDVI trend 2000-2009 (OLS, p 0.05); lower right: NPP trend 2000-2009 (Zhao and Running 2010)

8 References

Ahlström, A., Miller, P.A., Smith, B. (2012), Too early to infer a global NPP decline since 2000, Geophysical Research Letters, 39, L15403.

Araújo, M.B., Williams, P.H. (2000), Selecting areas for species persistence using occurrence data. Biological Conservation, 96, 331-345.

Barbet-Massin, M., Jiguet, F., Albert, C.H., Thuiller, W. (2012), Selecting pseudo–absences for species distribution models: how, where and how many? Methods in Ecology and Evolution, 3, 327–338.

Beck, J., Böller, M., Erhardt, A., Schwanghart, W. (2013), Spatial bias in the GBIF database and its effect on modelling species' geographic distributions. Ecological Informatics, doi: 10.1016/j.ecoinf.2013.11.002.

Benito, B.M., Cayuela, L., Albuquerque, F.S. (2013), The impact of modelling choices in the predictive performance of richness maps derived from species-distribution models: guidelines to build better diversity models. Methods in Ecology and Evolution, 4, 327-335.

Churkina G., Running, S.W. (1998), Contrasting climatic controls on the estimated productivity of different biomes. Ecosystems 1, 206–215.

Costello, M., Michener, W.K., Gahegan, M. Zhang, Z-Q., Bourne, P.E. (2013), Biodiversity data should be published, cited, and peer reviewed. Trends in Ecology & Evolution, 28(8), 454-461.

Covas, R., du Plessis, M.A., Doutrelant, C. (2008), Helpers in a colonial cooperatively breeding bird help to counteract the effects of adverse breeding conditions. Behavioral Ecology and Sociobiology, 63, 103-112.

Cumming, G.S. (2000), Using habitat models to map diversity: pan-African species richness of ticks (Acari: Ixodida). Journal of Biogeography, 27, 425-440.

De Jong, R., Verbesselt, J., Zeileis, A., Schaepman, M.E. (2013), Shifts in Global Vegetation Activity Trends. Remote Sens. 5, 1117-1133.

Del Barrio, G., Puigdefabregas, J., Sanjuan, M.E., Stellmes, M., Ruiz, A. (2010), Assessment and monitoring of land condition in the Iberian Peninsula, 1989-2000, Remote Sensing of Environment, 114, 8, 1817-1832.

Dietz, A.J., Kuenzer, C., Dech, S. (2015), Analysis of Snow Cover Time Series – Opportunities and Techniques. In: Kuenzer, C., Dech, S., Wagner, W. (ed.), Remote Sensing Time Series, Revealing Land Surface Dynamics. Remote Sensing and Digital Image Processing, 22, Springer Int. Publishing AG Switzerland.

Dorigo, W., de Jeu, R., Chung, D., Parinussa, R., Liu, Y., Wagner, W., and Fernández-Prieto, D. (2012), Evaluating global trends (1988–2010) in harmonized multi-satellite surface soil moisture. Geophys. Res. Lett. *39*, L18405.

Eisfelder, C., Klein, I., Niklaus, M., Kuenzer, C. (2014), Net primary productivity in Kazakhstan, its spatio-temporal patterns and relation to meteorological variables. Journal of Arid Environments, 103, 17-30.

Eklundh, L., Jönsson, P. (2012), Timesat 3.1 Software Manual.

ESA, (2010), GlobCover 2009 (Global Land Cover Map). Retrieved from: Http://due.esrin.esa.int/globcover/

Fensholt, R., Rasmussen, K., Nielsen, T. T., Mbow, C. (2009), Evaluation of earth observation based long term vegetation trends — Intercomparing NDVI time series trend analysis consistency of Sahel from AVHRR GIMMS, Terra MODIS and SPOT VGT data. Remote Sensing of Environment, 113, 1886−1898.

Fensholt, R., Rasmussen, K., Kaspersen, P., Huber, S., Horion, S., Swinnen, E. (2013), Assessing Land Degradation/Recovery in the African Sahel from Long-Term Earth Observation Based Primary Productivity and Precipitation Relationships. Remote Sensing, 5, 664-686.

Ferreira, M., Beja, P. (2013), Mediterranean amphibians and the loss of temporary ponds: are there alternative breeding habitats? Biological Conservation, 165, 179-186.

GEO BON (2011), Adequacy of Biodiversity Observation Systems to support the CBD 2020 Targets. A report prepared by the Group on Earth Observations Biodiversity Observation Network (GEO BON), for the Convention on Biological Diversity.

Gobron, N. (2011), Envisat's Medium Resolution Imaging Spectrometer (MERIS) Algorithm Theoretical Basis Document: FAPAR and Rectifed Channels over Terrestrial Surfaces. JRC Scientific and Technical Reports.

Günther, K.P., Maier, S. (1999), AVHRR compatible NDVI ATBD. DLR document ID: MAPP-ATBD-NDVI.

Guralnick, R.P., Hill, A.W., Lane, M. (2007), Towards a collaborative, global infrastructure for biodiversity assessment. Ecology Letters, 10, 663-672.

Higgins, S.I., Scheiter,S. (2012), Atmospheric CO2 forces abrupt vegetation shifts locally, but not globally. Nature Volume: 488, Pages: 209–212.

Hijmans, R.J., Cameron, S.E., Parra, J.L., Jones, P.G., Jarvis, A. (2005), Very high resolution interpolated climate surfaces for global land areas. International Journal of Climatology, 25, 1965-1978.

Houghton, J.T., Ding, Y., Griggs, D.J., Noguer, M., van der Linden, P.J., Xiaosu, D. (2001), Climate Change 2001. The Scientific Basic. Contribution of Working Groupe I to the Third Assessment Report of the Intergovernmental Panel on Climate Change.

Huston, M., (1979), A general hypothesis of species diversity. The American Naturalist, 113, 1, 81-101.

Ivits, E., Cherlet, M., Mehl, W., Sommer, S. (2013), Ecosystem functional units characterized by satellite observed phenology and productivity gradients: A case study for Europe. Ecological Indicators 27, 17–28.

Jenkins, D.G. (2015), Estimating ecological production from biomass. Ecosphere 6(4):49, 31p.

Kendall, M.G. (1962), Rank Correlation Methods, Charles Griffin and Company, London.

Klintenberg, P., Seely, M. (2004), Land Degradation Monitoring in Namibia: A First Approximation. Environmental Monitoring and Assessment, 99, 5-21.

Knorr, W. (1997), Satellite remote sensing and modelling of the global CO^2 exchange of land vegetation: A Synthesis Study. PhD Thesis, Hamburg, Max-Planck-Institut für Meteorologie.

Le Houérou, H.N. (1984), Rain use efficiency: a unifying concept in arid-land ecology. Journal of Arid Environments, 7, 213-247.

Lomolino, M.V., Riddle, B.R., Whittaker, R.J., Brown, J.H. (2010), Biogeography (4th ed.). Sinauer Associates Inc., 560 pp.

Mann, H.B. (1945), Non-parametric tests against trend. Econometrica, 13, 163-171.

Martínez-Freiría, F., Argaz, H., Fahd, S., Brito, J.C. (2013), Climate change is predicted to negatively influence Moroccan endemic reptile richness. Implications for conservation in protected areas. Naturwissenschaften, doi: 10.1007/s00114-013-1088-4.

Martiny, N., Richard, Y., Camberlin, P. (2005), Interannual persistence effects in vegetation dynamics of semi-arid Africa. Geophysical research letters, 32(24).

Medlyn, B. E. (2011), Comment on "Drought-induced reduction in global terrestrial net primary production from 2000 through 2009," Science, 333(6046), 1093.

Miehe, S. , Kluge, J., v. Wehrden, H., Retzer, V. (2010), Long-term degradation of Sahelian rangeland detected by 27 years of field study in Senegal. Journal of Applied Ecology, 47, 692–700.

Nemani, R.R., Keeling, C.D., Hashimoto, H., Jolly, W.M., Piper, S.C., Tucker, C.J., Myneni, R.B., Running, S.W. (2003), Climate-driven increases in global terrestrial net primary production from 1982 to 1999. Science 300, 1560–1563.

Oba, G., Vetaas, O. R., Stenseth, N. C. (2001), Relationships between biomass and plant species richness in arid-zone grazing lands. Journal of Applied Ecology, 38, 836-845.

Oijen, M.V., Schapendonk, A., Höglind, M. (2010), On the relative magnitudes of photosynthesis, respiration, growth and carbon storage in vegetation. Annals of Botany 105, 793-797.

Oindo, B.O., Skidmore, A.K., de By, R.A. (2000), Interannual variability of NDVI and species richness in Kenya. Int. Archives of Photogrammetry and Remote Sensing, 23, Part B7, 1402-1409.

Ratajczak, Z., Nippert, J.B. and Scott, L. (2011), The effects of woody encroachment on plant diversity in global grasslands and savannas: a meta-analysis. http://media.wix.com/ugd/d270f9_013ee3e8ed68377da3047468fb523488.pdf.

Ratzmann, G., (2014), EO-based Relationships BetweenVegetation and Rainfall in Drylands. Towards better understanding of eco-hydrological patterns and dynamics. Master's thesis at the Faculty of Science, University of Copenhagen.

Running, S.W., Nemini, R.R., Heinsch, F.A., Zhao, M., Reeves, M., Hashimoto, H. (2004), A Continuous Satellite-Derived Measure of Global Terrestrial Primary Production. BioScience 54, 6, 547-560.

Samanta, A., M., Costa, M.H., Nunes, E.L., Vieira, S.A., Xu, L., and Myneni, R.B. (2011), Comment on "Drought-induced reduction in global terrestrial net primary production from 2000 through 2009," Science, 333(6046), 1093.

Sen, P. K. (1968), Estimates of regression coefficients based on Kendall's tau. J. Amer. Statist. Assoc. 63, 1379–1389.

Şensoy, S., Türkoğlu, N., Çiçek, I., Yücel, G. (2013), Climate changes and trends in phenology of fruit tree and field crop in Turkey, 1971-2012.

Soares, C., Brito, J.C. (2007), Environmental correlates for species richness among amphibians and reptiles in a climate transition area. Biodiversity and Conservation, 16, 1087-1102.

Theil, H. (1950), A rank-invariant method of linear and polynomial regression analysis I, II and III, Nederl. Akad. Wetensch. Proc., 53, 386–392, 521–525, 1397–1412.

Thuiller, W., Lafourcade, B., Engler, R., Araujo, M.B. (2009), BIOMOD - a platform for ensemble forecasting of species distributions. Ecography, 32, 369-373.

Thuiller, W., Georges, D., Engler, R. (2012), Package "biomod 2" version 3.1-18. Available at http://cran.r-project.org/web/packages/biomod2/biomod2.pdf.

Tucker, C.J., Pinzon, J.E., Brown, M.E. (2004), Global Inventory Modeling and Mapping Studies. NA94apr15b.n11-VIg, 2.0, Global Land Cover Facility, University of Maryland, College Park, Maryland, 04/15/1994.

Tum, M., Buchhorn, M., Günther, K.P., Haller, B.C. (2011), Validation of modelled forest biomass in Germany using BETHY/DLR. Geosci. Model Dev., 4, 1019–1034.

Tum, M. (2012), Modelling and validation of agricultural and forest biomass potentials for Germany and Austria. Dissertation, Georg-August-Universität Göttingen.

USGS (2006), Shuttle Radar Topography Mission (SRTM): Mapping the World in 3 Dimensions. United States Geological Survey. Retrieved from: http://srtm.usgs.gov/index.html.

Verbesselt, J., Hyndman, R., Newnham, G., Culvenor, D. (2010), Detecting trend and seasonal changes in satellite image time series. Remote Sens. Environ. 114, 106–115.

Wessels, K.J., Van den Bergh, F., Scholes, R.J. (2012), Limits to detectability of land degradation by trend analysis of vegetation index data. Remote Sensing of Environment, 125, 10–22.

White, M.A., De Beurs, K.M., Didan, K., Inouye, D.W., Richardson, A.D., Jensen, O.P., O'Keefe, J., Zhang, G., Nemani, R.R., Van Leeuwen, W.J.D., Brown, J.F., De Wit, A., Schaepman, M., Lin, X., Dettinger, M., Bailey, A.S., Kimball, J., Schwartz, M.D., Baldocchi, D.D., Lee, J.T., Lauenroth, W.K. (2009), Intercomparison, interpretation, and assessment of spring phenology in North America estimated from remote sensing for 1982–2006. Global Change Biology (2009), 15,10, 2335-2359.

Whittaker, R.J. (2010), Meta-analyses and mega-mistakes: calling time on meta-analysis of the species richness–productivity relationship. Ecology 91, 2522–2533.

Wißkirchen, K., Tum, M., Günther, K.P., Niklaus, M., Eisfelder, C., Knorr, W. (2013), Quantifying the carbon uptake by vegetation for Europe on a 1 km² resolution using a remote sensing driven vegetation model. Geosci. Model Dev., 6, 1623–1640.

Zhao, M., Running, S. (2010), Drought-Induced Reduction in Global Terrestrial Net Primary Production from 2000 through 2009. Science 329, p. 940-943.

Zhou, Y.(2013), Inter-annual memory effects between Soil Moisture and NDVI in the Sahel. Master's Thesis at the Department of Physical Geography and Ecosystem Science of Lund University.

Zhou, Y., Fensholt, R., Wang, K., Vitkovskaya, I., Tian, F. (2015), Climate Contributions to Vegetation Variations in Central Asian Drylands: Pre- and Post-USSR Collapse. Remote Sensing 2015, 7, 2449-2470.